Characterisation of KEAP1 as a novel factor in DNA base damage repair and investigation of its relationship with PARPs

Jagoda Janina Rokicka
Jesus College
University of Oxford

Thesis submitted for the award of DPhil

38,980 words

Abstract

Genomes are constantly subjected to various genotoxic stresses that can cause DNA damage, which, if unrepaired, can lead to cancer or cell death. To counteract this threat, cells have evolved a network of pathways that resolve DNA damage, termed DNA damage response (DDR). These crucial pathways and the interactions between them are regulated by post-translational modifications, including poly(ADP-ribosyl)ation, which is carried out by poly(ADP-ribose) polymerases (PARPs). PARP1 and PARP2 play important roles in the regulation of base damage repair. BER, one of the key base damage repair pathways, has been extensively studied, however, its regulation and crosstalk with alternative pathways resolving DNA base lesions is not fully understood. This work aims to identify novel factors contributing to base damage repair and assess their relationship with PARPs.

Using a genome-wide CRISPR-Cas9 screen, we identified KEAP1 as a potential novel factor in alkylation base damage repair. KEAP1 acts as a substrate adaptor for the KEAP1-CUL3-RBX1 E3 ubiquitin ligase complex and had not been previously implicated in base damage repair. To validate the screen, we generated KEAP1-deficient cell lines using genome editing. We found that loss of KEAP1 increases cellular sensitivity to the alkylating agent MMS. We determined that all of the KEAP1 domains necessary for its function in the E3 ubiquitin ligase complex are also required for it to convey tolerance to MMS-induced damage. Disruption of KEAP1 is not epistatic with inhibition of repair through BER or direct repair, suggesting that KEAP1 acts in an alternative base damage repair pathway. Following damage, KEAP1

is recruited to chromatin in a PARP1-dependent manner. Interestingly, loss of KEAP1 results in chromatin enrichment of PARP1 and PARP2 when exposed to MMS. We also identify a novel synthetic lethal interaction between KEAP1-deficiency and PARP inhibition, which could have therapeutic potential in the treatment of KEAP1-deficient tumours.

Acknowledgements

I am grateful to my supervisor, Professor Nicholas Lakin, for his guidance during my project. I would like to thank the members of the Lakin lab for their companionship during my research journey. I owe special thanks to George Ronson and Khairul Ramlee for their readiness to help and advise, especially during the early days of the journey. I would like to say a separate thank you to Julien Brustel, who not only always found the time to discuss any research issues, but who also let me understand the privilege of working daily alongside a really good friend.

I feel lucky to have met some wonderful friends in the neighbouring Cohn lab and I shall miss our gelato trips during evening incubation times. I could always find comfort in the camaraderie I shared with Colette Lipp and Kelvin Yaprianto. You are both dear friends and you have made this journey so much easier. I am already missing chats with Colette and Kelvin's infectious laughter resounding in the (almost) empty laboratory past midnight.

I would like to thank Gabriela Pavarini for her constant support in all my endeavours and for motivating me to keep going. A friend like you is a treasure and I was so lucky that you overheard my yoga chat in the common room during my first week in Oxford. I feel very lucky to also have had wonderful friends and fellow DPhil students as neighbours – Marie Wong and Derek Xu, our socially-distanced picnics and baked goods exchanges were a lifeline during the pandemic for both Eugene and me.

I feel very thankful to Chris Maddison and Piero Stallo for always making me feel at home when I visit. It is truly a blessing to meet such warm and welcoming people by a chance encounter, but even more so to have them become friends of whom you think as family. You guys have no idea how much it has meant for me, especially during the times when I could not travel to be with my immediate family.

I would like to thank my parents Wiesława and Piotr, who always believe in me and who have always let me choose my own path. I am grateful to my wonderful aunt Mirka, whose kindness, warmth and understanding never cease to astonish me. I would not have made it this far without your support. I am thankful for the support and encouragement from my brother Tomasz and my sister Małgorzata, who cheer me on despite the geographical distance. I would also like to thank my parents-in-law, Anna and Pavel, who have been making so many accommodations, big and small, to make writing easier for me.

Finally, I would like to thank my husband Eugene Leypunskiy. I could not have dreamed of a more supportive, understanding and loving partner. Thank you for your patience when experiments got in the way of our plans and for always seeing the glass half-full and motivating me to keep going.

I dedicate this thesis to Janina and Feliks, my wonderful niece and nephew, who are just the most curious and thirsty of knowledge kids out there. The way you look up to me makes me feel honoured, but it is also binding. I hope you can feel proud of your aunt.

Abbreviations

APE1 – apurinic/apyrimidinic endonuclease 1

BER – base excision repair

BRCA1 – breast cancer type 1 susceptibility protein

BRCA2 – breast cancer type 2 susceptibility protein

BRCT – BRCA1 C-terminus

CRISPR – clustered regularly-interspaced short palindromic repeats

CUL3 – Cullin 3

DDR – DNA damage response

D-loop – displacement loop

dNTP – deoxynucleoside triphosphate

DSB – double strand break

gRNA – guide RNA

HD – helical subdomain

HR – homologous recombination

KEAP1 – Kelch-like ECH-associated protein 1

MAR – mono(ADP-ribose)

MGMT – O^6-methylguanine-DNA methyltransferase

MMS – methyl methanesulfonate

MPG – N-methylpurine DNA glycosylase

NAD^+ - nicotinamide adenine dinucleotide

NEIL1/2 – Nei-like DNA glycosylase 1/2

NHEJ – non-homologous end joining

NRF2 – nuclear factor erythroid 2-related factor 2

NTHL1 – Nth-like DNA glycosylase 1

OFP – Okazaki fragment processing

PAR – poly(ADP-ribose)

PARG – poly(ADP-ribose) glycohydrolase

PARP – poly(ADP-ribose) polymerase

PARPi – PARP inhibitor

PCR – polymerase chain reaction

PTM – post-translational modification

ROS – reactive oxygen species

RPA – replication protein A

siRNA – short interfering RNA

SSB – single strand break

SSBR – single strand break repair

TLS – translesion synthesis

TMZ – temozolomide

UNG1 – Uracil-DNA glycosylase 1

XRCC1 – X-ray repair cross complementing protein 1

Table of Contents

1. Introduction

1.1 DNA damage repair

Cells are constantly exposed to environmental and endogenous stress factors causing DNA damage. To counteract these genotoxic stresses, cells have developed a multitude of pathways that repair various types of DNA damage, which together constitute a network of DNA damage response (DDR). Cooperation and partial redundancies between these pathways in the resolution of lesions are key factors in the successful maintenance of genome integrity. DNA damage can be caused endogenously, for example triggered by hydrolytic reactions of DNA with water or oxidative reactions with reactive oxygen species (ROS), or it can be induced by exogenous factors, such as UV and ionising radiation, and chemical agents (Chatterjee and Walker, 2017). Both endogenous and environmental factors can give rise to a variety of DNA damage types. The main focus of this thesis will be alkylation DNA base damage.

1.2 Alkylation damage repair

1.2.1 Sources of alkylation damage

Base damage is the most commonly occurring DNA lesion and results from a chemical modification, such as hydrolysis, oxidation, deamination or alkylation of the nucleotide base, or from formation of a bulky base adduct (Bauer et al., 2015).

Although alkylation is not the most common among the different types of DNA base damage, it can be highly mutagenic (Drabløs et al., 2004). Methyl groups can be transferred from the electrophilic donor to the ring nitrogen or exocyclic oxygen atoms of the DNA bases and have the potential to generate 12 different lesions (Fu et al., 2012; Wyatt and Pittman, 2006).

Alkylation damage can have endogenous or exogenous causes. Endogenous alkylation damage derives from the activity of metabolic enzymes (Nay and O'Connor, 2013). In particular, the family of S-adenosyl methionine (SAM) methyltransferase enzymes, which serve as a methyl donor in over 40 metabolic reactions, may play a significant role, but the detailed mechanisms are not thoroughly characterised (Cantoni, 1953; Soll et al., 2017). Exogenous alkylation agents are present environmentally as nitrosoureas producing mostly *O*-alkylation, or as methanesulfonates resulting mainly in *N*-alkylation (Nay and O'Connor, 2013). Another group of exogenous alkylating agents are chemotherapeutic drugs. Alkylating drugs were used in clinic as the first class of cancer therapy and are still important in the treatment of some cancers (Drabløs et al., 2004). Most of them are monofunctional methylating agents, bifunctional alkylating agents or chloroethylating agents (Kondo et al., 2010). Methyl methanesulfonate (MMS) has been used in research for many years to study the effects of alkylation DNA damage in cells (Lundin, 2005).

1.2.2 DNA damage induced by MMS and mechanisms of repair

MMS is a monofunctional alkylating agent which displays high affinity to nitrogen in purines and pyrimidines, inducing a range of methyl base adducts, with N7-methylguanine contributing to 84% of the mutations, followed by N3-methyladenine (8.5%) and N3-methylguanine (1.2%) (Nikolova et al., 2010). Unlike N3-methyladenine and N3-methylguanine, N7-methylguanine does not block replication, but also leads to a potentially mutagenic apurinic (AP) site (Nikolova et al., 2010). O6-methylguanine constitutes only a small share (0.3%) of MMS-induced mutations and is resolved through O^6-methylguanine-DNA methyltransferase (MGMT) (Kondo et al., 2010). Although *O*-alkylation is more mutagenic than *N*-alkylation, both types of modification are cytotoxic and genotoxic (Nay and O'Connor, 2013). Alkylated purines tend to be highly unstable, which results in a spontaneous depurination (Izumi and Mellon, 2021).

MMS has also been implicated in the formation of double strand breaks (DSBs), which are normally resolved through homologous recombination (HR) repair (Nikolova et al., 2010). Despite the reports that the observed DSBs are in fact artefacts attributed to the instability of methylated DNA when exposed to heat (Lundin, 2005), substantial evidence has been gathered from multiple other studies, including from our group, that supports the emergence of DSBs as an indirect effect of MMS treatment (Ensminger et al., 2014; Nikolova et al., 2010; Ronson et al., 2018). These DSBs are caused by collision of progressing replication forks with an unresolved single strand break (SSB) intermediate of BER (Ensminger et al., 2014;

Shiu et al., 2020). Accumulation of the DSB marker γH2AX foci in S-phase cells after MMS treatment is inhibited in the case of early BER disruption or DNA synthesis prevention, demonstrating the γH2AX foci are not directly induced by the alkylated bases and proving a requirement for active replication to generate DSBs from BER intermediates after alkylation damage (Ronson et al., 2018).

Base damage induced by MMS and other alkylating agents can be resolved by several DNA damage repair pathways. The specific route of repair can be preferentially chosen depending on the type of base modification, but often these pathways are partially redundant, providing alternative lesion resolution scenarios to prevent mutagenesis. Below we will review the main pathways of alkylation base damage repair.

1.2.2.1 MGMT-mediated direct lesion repair

Direct lesion repair removes alkylation damage from the DNA base without the requirement for a nucleotide template and it does not cleave the DNA backbone (Nay and O'Connor, 2013). Methylguanine DNA methyltransferase (MGMT) facilitates the removal O^6-methylguanine (O^6-meG) and O^4-methylthymine (O^6-meT) in a single step reaction by accepting the alkyl adduct from the base oxygen onto its cysteine residue (Figure 1.1; Verbeek et al., 2008; Yu et al., 2020). Being able to facilitate only one methyltransferase reaction, MGMT acts as a 'suicide' enzyme and after accepting the alkyl group, it is ubiquitylated and targeted for proteasomal

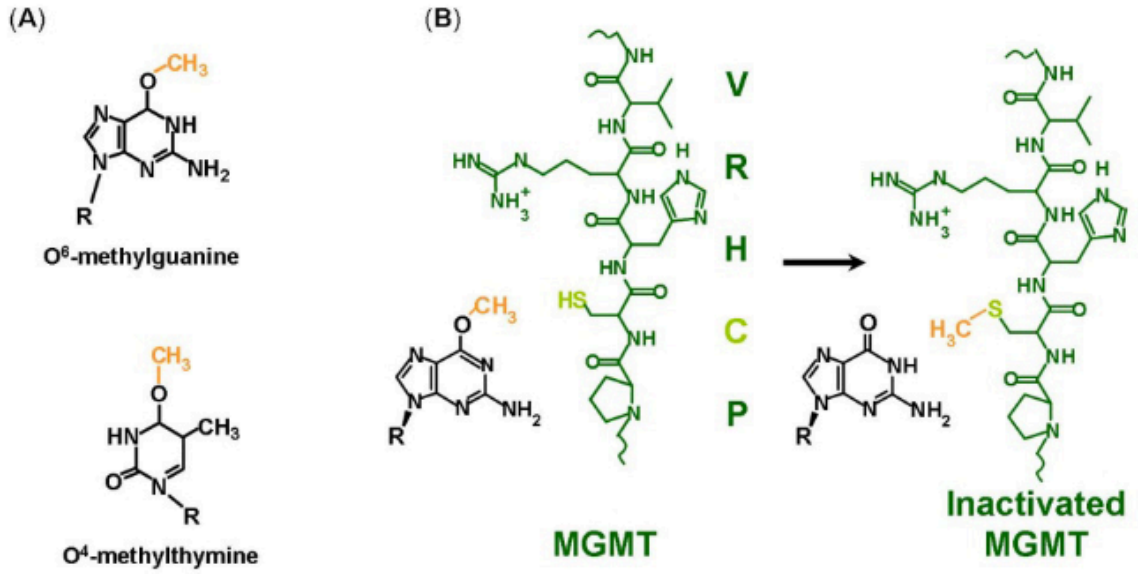

Figure 1.1 Schematic demonstrating the activity of MGMT in direct repair of alkylation base damage. MGMT facilitates the transfer of the methyl group from *O*^{6}-meG and *O*^{6}-meT onto its reactive Cys145, here marked in lime green. Reprinted from Nay and O'Connor, 2013.

degradation (Mitra, 2007; Srivenugopal et al., 1996). MGMT can bind to both double-stranded and single-stranded DNA though its DNA binding channel and helix-turn-helix (HTH) DNA binding motif (Nay and O'Connor, 2013). This C-terminal region also contains the active site with its cysteine motif (-PCHR-) and residues that facilitate the alkyl group transfer to Cys145 (Crone and Pegg, 1993; Nay and O'Connor, 2013).

Although the O^6-meG adducts are generally stable when not removed by MGMT, they are extremely mutagenic, as they can lead to G:C to A:T mutations (Soll et al., 2017). Therefore, targeting the MGMT activity provides an attractive opportunity to potentiate the effect of alkylating drugs on cancer cells. The expression status of MGMT is an important consideration in choosing cancer treatments, as the activity of this enzyme contributes to chemoresistance to alkylating drugs (Yu et al., 2020). In particular, hypermethylation of the CpG islands within the *MGMT* promoter decreases the expression level of the protein, which correlates with longer survival of glioblastoma patients treated with a combination of radiotherapy and the alkylating drug temozolomide (Hegi et al., 2005). Glioblastoma tumours with unmethylated *MGMT* promoter display resistance to temozolomide (TMZ), resulting from the active removal of methyl adducts from the DNA bases by MGMT (Rivera et al., 2010). Although the epigenetic status of *MGMT* can serve as a predictor of the TMZ response, a reversal of methylation of the *MGMT* promoter and acquisition of drug resistance upon initial TMZ treatment has been observed in some patients, leading to tumour recurrence (Park et al., 2012). This highlights the need to develop fail-safe strategies to control the MGMT activity in clinical setting. Clinical studies

involving O^6-benzylguanine (O6BG) and O^6-(4-bromothenyl) guanine (O6BTG), the two O^6-meG analogues that act as pseudosubstrates for MGMT and thereby inhibit its activity, have shown promising results in sensitising cells to treatment with TMZ (Quinn et al., 2005; Ranson et al., 2006). However, later clinical studies determined that treatment with the O^6-meG analogues increases the risk of cerebrospinal fluid leak, brain infection and leads to myelosuppression, which prevented the approval of these drugs for use in clinic (Quinn et al., 2009; Ranson et al., 2006).

1.2.2.2 ALKBH-mediated direct lesion reversal

The mammalian alpha-ketoglutarate-dependent dioxygenase alkB homolog (ALKBH) family includes nine proteins, three of which (ALKB1-3) can remove alkyl adducts from DNA bases (Gutierrez and O'Connor, 2021). ALKBH1 is a mitochondrial protein, but ALKBH2 and ALKBH3 are localised to the nucleus, where they can facilitate the repair of dsDNA and ssDNA, mostly removing 1-methyladenine (1-meA) and 3-methylcytosine (3-meC) adducts (Falnes, 2004; Westbye et al., 2008). The 1-meA and 3-meC adducts can pose a hindrance for replication and transcription progression, as well as lead to A:T transversions and C:T transitions, it is therefore important to repair these lesions in a timely manner (Gutierrez and O'Connor, 2021).

The human ALKBH proteins are characterised by highly conserved secondary structure. They also possess a catalytic core comprised of the double-stranded β-helix (DSBH), the nucleotide recognition lid (NRL) and the N-terminal extension (NTE) (Nay and O'Connor, 2013). Additionally to the conserved catalytic region, three

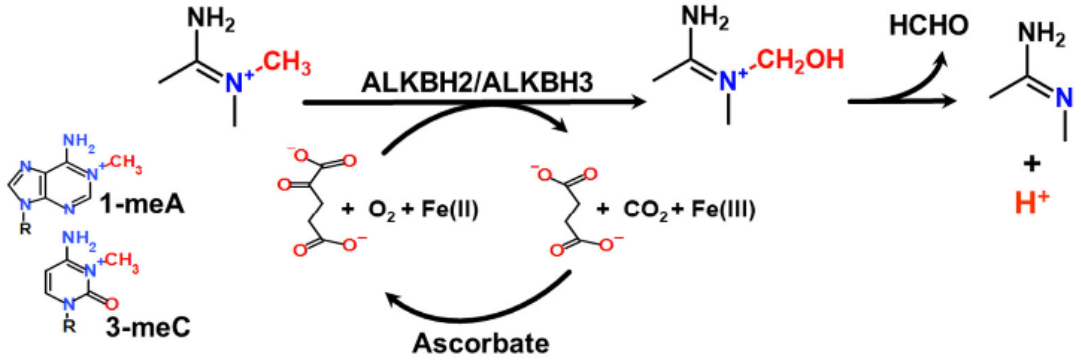

Figure 1.2 ALKBH-mediated repair of 1-meA and 3-meC adducts. The repair mediated by ALKBH2/3 is a reaction consisting of several steps. The conversion of α-ketoglutarate to succinate, and requires oxygen and Fe(II), releasing CO_2. The repair to normal base releases formaldehyde. Reprinted from Gutierrez and O'Connor, 2021.

distinctive motifs localised on ALKBH2 are responsible for increasing the binding to both DNA strands, enabling efficient repair on dsDNA (Yang et al., 2008). To facilitate binding to ssDNA, ALKBH3 domain organisation that allows for higher degree of DNA backbone manipulation (Nay and O'Connor, 2013).

Contrary to MGMT, the ALKBH family proteins are not 'suicide' enzymes and each molecule can perform numerous repair rounds. However, the repair of 1-meA or 3-meC is a multistep reaction (Figure 1.2; Gutierrez and O'Connor, 2021). It involves the conversion of α-ketoglutarate to succinate, and restoration to undamaged base, releasing formaldehyde (Begley and Samson, 2003).

1.2.2.3 Base excision repair

Base excision repair (BER) is the main pathway through which a wide range of base damage is repaired. BER is a multistep pathway that can resolve small, non-bulky lesions, such as oxidation, deamination and methylation of the DNA bases and is mostly active during the G1 phase (Krokan and Bjoras, 2013). The repair is initiated by one of the 11 lesion-specific glycosylases which recognises and removes the damaged base (Chatterjee and Walker, 2017). The DNA glycosylases can be either monofunctional, such as UNG1 and the methyl purine glycosylase (MPG), which recognises alkylation damage, or bifunctional with an additional β-lyase activity, like NTHL1 and NEIL1/2 (Krokan and Bjoras, 2013). Depending on whether the abasic site was created by a monofunctional or a bifunctional glycosylase, it is channeled to be processed either by the short-patch BER or the long-patch BER, respectively (Figure 1.3; Dianov and Hübscher, 2013).

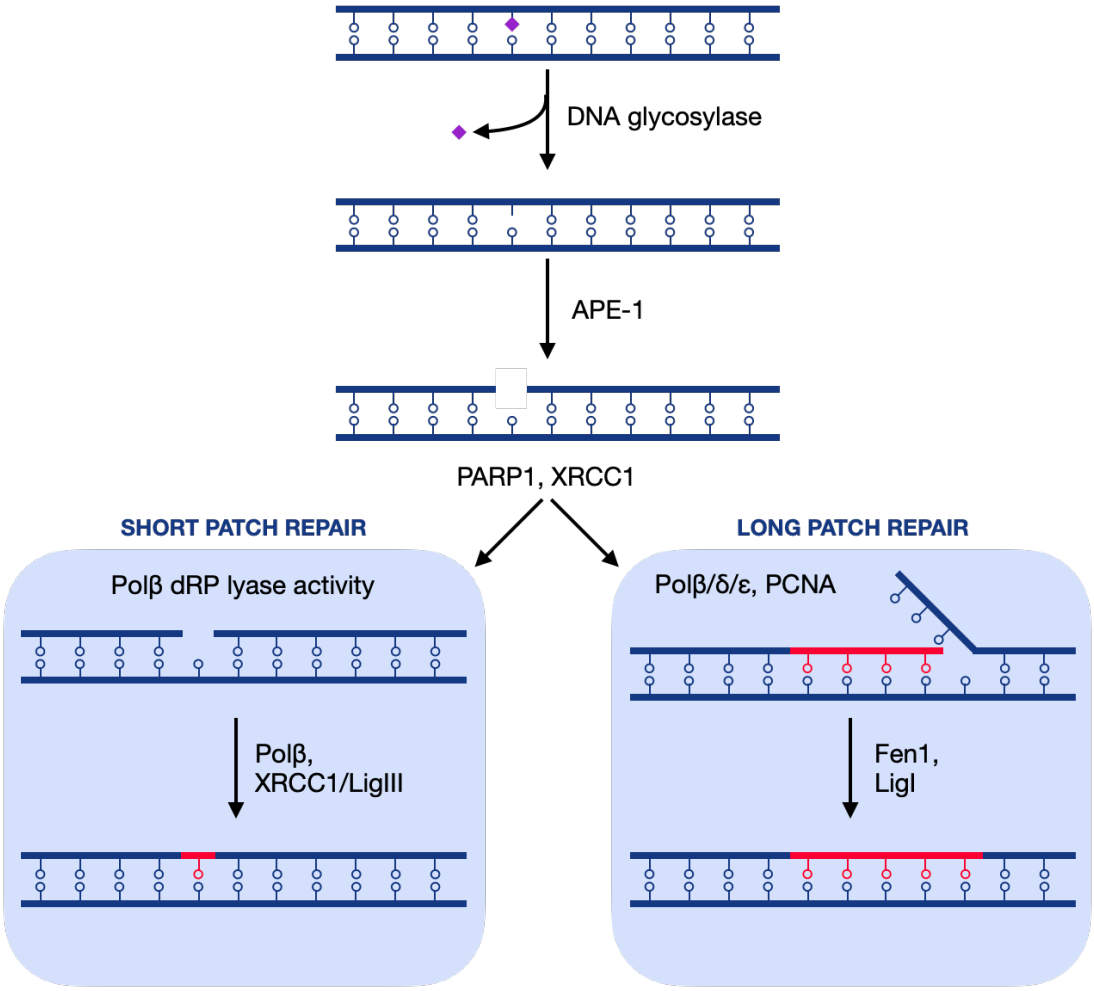

Figure 1.3 Simplified schematic of base excision repair through short-patch and long-patch pathway. DNA glycosylase detects the base damage and removes the base. The resulting abasic site is recognized by APE1, which cleaves the DNA backbone, generating a single nucleotide gap. This gives rise to a SSB, which is detected by PARP1, the major sensor of SSBs. PARP1 activation and subsequent PARylation recruits other repair factors to the lesion, such as XRCC1. The SSB can be resolved through a short-patch or a long-patch repair pathway. Adapted from Caldecott, 2008.

Monofunctional glycosylases remove the damaged base, producing an abasic (AP) site, which requires further processing by the apurinic/apyrimidinic endonuclease 1 (APE1) that cleaves the DNA backbone generating a deoxyribose phosphate (dRP) 5' end. The bifunctional glycosylases remove the base and incise the DNA backbone through their lyase activity, producing a 3' phosphate or a 3' α,β-unsaturated aldehyde end (Figure 1.4). The single strand break following phosphodiester bond cleavage is detected by the SSB sensor PARP1. Upon binding to the SSB, PARP1 becomes activated and synthesizes poly(ADP-ribose) chains (PAR), modifying itself and other DDR proteins at the lesion. This modification facilitates recruitment of downstream PAR-binding repair factors, such as the scaffolding factor X-ray repair cross complementing protein 1 (XRCC1) and polymerase β (Polβ) (Caldecott et al., 1996). Polβ then tailors the 5'-dRP end produced by the APE1 endonuclease through its 5'-dRP lyase activity and fills the single nucleotide gap. The short-patch repair is completed through ligation of DNA by a complex of DNA ligase 3 (LIG3) and XRCC1 (Almeida and Sobol, 2007). However, the DNA ends resulting from the lyase activity of bifunctional glycosylases are converted to 3'-OH by APE1 in the case of 3'phosphate, or by polynucleotide kinase 3'-phosphatase (PNKP) for the 3'α,β-unsaturated aldehyde (Coquelle et al., 2011; McNeill et al., 2020). In the long-patch repair pathway Polβ synthesizes a DNA polymer, which then displaces the strand, creating a flap (Akbari et al., 2008). In the final step of the long-patch repair, the flap endonuclease 1 (FEN1) in a complex with proliferating cell nuclear antigen (PCNA) removes the flap and the ligation is completed by LIG1 (Craggs et al., 2014).

DNA glycosylase	Mode of function	Substrate specificity
UNG1	monofunctional	U, 5-FU
UNG2	monofunctional	U, 5-FU
SMUG1	monofunctional	U, 5-HMU, 5-FU
MBD4	monofunctional	U or T opposite G, 5-HMU in CpG, 5-FU in dsDNA
TDG	monofunctional	U or T opposite G, 5-HMU in dsDNA, 5-FU
MPG	monofunctional	3meA, 3meG, 7meG, Hx
OGG1	mono-/**bifunctional**	8-oxoG opposite C, Fapy opposite C
MUTYH	monofunctional	A opposite 8-oxoG/C/G
NTHL1	bifunctional	thymine glycol, FapyG, 5-HC, 5-HU
NEIL1	bifunctional	thymine glycol, FapyA, FapyG, 5-HU, 8-oxoG, Sp and Gh in both ssDNa and dsDNA
NEIL2	bifunctional	thymine glycol, FapyA, FapyG, 5-HU, 8-oxoG, Sp and Gh in both ssDNa and dsDNA
NEIL3	**mono**-/bifunctional	FapyA, FapyG, Sp and Gh in ssDNA

Figure 1.4 Known human DNA glycosylases and their substrates. DNA glycosylases can be either monofunctional and catalyse the excision of the base, or bifunctional with an additional AP lyse activity that allows for the DNA backbone cleavage leading to a single strand break. When a glycosylase can act either as mono- or bifunctional, the most common mode of function was marked in bold. A – adenine, C – cytosine, T – thymine, G – guanine, 5-FU - 5-fluorouracil, 5-HMU - 5-hydroxymethyluracil, 3meA - 3-methyladenine, 3meG - 3-methylguanine, 7meG - 7-methylguanine, Hx – hypoxanthine, 8-oxoG - 8-oxoguanine, Fapy – formamidopyrimidine, 5-HC -5-hydroxycytosine, 5-HU -5-hydroxyuracil, Sp – spirominodihydantoin, Gh – guaninohydantoin. Adapted from Krokan and Bjoras, 2013.

1.2.2.4 Replication-coupled DNA base damage repair

Unresolved DNA damage can act as an obstacle for the replisome. Replication-coupled repair mechanisms help cells overcome these challenges and ensure replication forks progression. Although most base damage does not prevent the progression of the replicative CMG helicase, it can pause the polymerases, leading to replisome uncoupling (Cortez, 2019). Base methylation, base oxidation and abasic sites constitute some of the most frequent replisome obstacles among the various kinds of DNA base damage, even though they are not bulky adducts which are also well-known to hinder replication (Brickner et al., 2019; Cortez, 2019).

Lesions that are not repaired in a timely manner, and therefore collide with replication forks, induce different replication-coupled repair mechanisms depending on the DNA strand where the damage is located (Figure 1.5). Base damage on the lagging strand can induce the stalling of primase Polα and Polδ, but efficient Polα repriming prevents the stalling of replication forks (Bainbridge et al., 2021; Quinet and Vindigni, 2018). The resulting ssDNA gaps are thought to be filled by translesion bypass polymerases after the completion of replication.

In contrast to lesions on the lagging strand, those on the leading strand present greater potential for replisome blocking and lead to the uncoupling of replication forks (Cortez, 2019). However, cells have developed several strategies to either bypass or repair DNA damage encountered by replication forks on the leading strand. Repriming DNA synthesis on the leading strand with a specialised PrimPol is

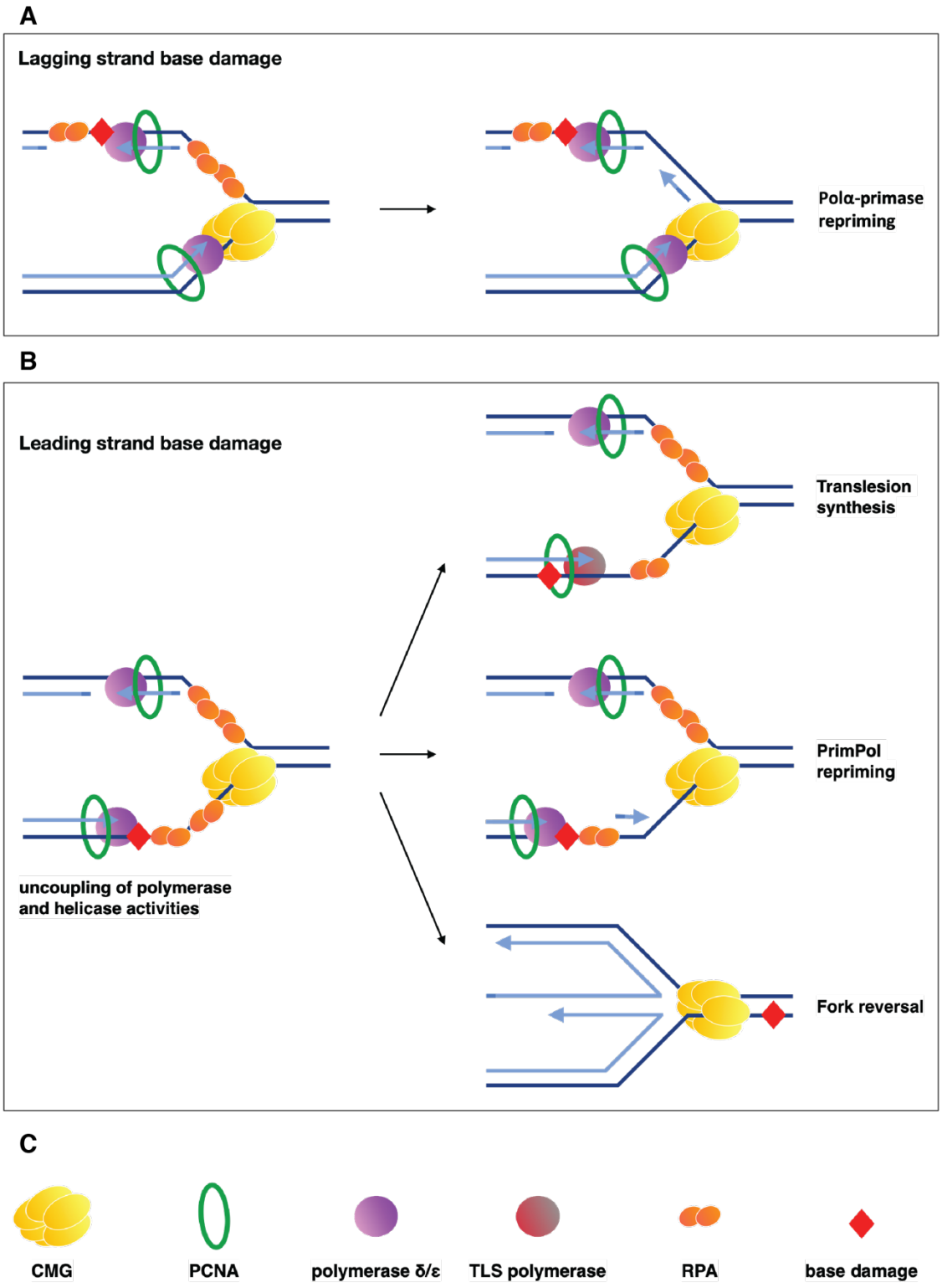

Figure 1.5 Schematic demonstrating the different response of replication-coupled repair mechanisms to base damage in the lagging strand and in the leading strand. A. Base damage on the lagging strand usually escapes replication stalling due to the activity of primase Polα. **B.** Base lesions in the leading strand cause the uncoupling of replisome and is repaired or tolerated by employing translesion synthesis, repriming by PrimPol or fork reversal. **C.** Legend of graphic symbols. Adapted from Cortez, 2019.

possible following the uncoupling of the CMG helicase and the polymerase, allowing lesion skipping (Mourón et al., 2013). The resulting single-strand DNA (ssDNA) gap can be further resolved through an error-prone or an error-free mechanism. The ssDNA gap could be filled by the low-fidelity bypass polymerases in translesion DNA synthesis (TLS) using the damaged DNA strand as a template, and potentially leading to a mutation (Cortez, 2019; Sale et al., 2012). The lesion could also be resolved in an error-free mode through template switching (TS). Template switching uses the nascent sister DNA strand to extend the newly synthesised strand (Ashour and Mosammaparast, 2021a). Replication forks stalled by a lesion on the leading strand can also migrate backward to create the so called 'chicken foot' structure (Berti and Vindigni, 2016). This three-way forks junction reanneals the two newly synthesised strands, protecting the ssDNA and providing more time for repair pathways to resolve the lesion ahead of it (Ashour and Mosammaparast, 2021a).

As discussed above, alkylation base damage can be resolved through multiple pathways – for example, direct repair, base excision repair, and replication-coupled repair – which provide cells with several resolution scenarios depending on the type of lesion and the cell cycle context. The regulation of these partially redundant pathways and the crosstalk between them remains to be better understood.

1.3 PARPs and alkylation DNA damage repair

1.3.1 ADP-ribosylation in DNA damage response

The DNA damage response (DDR) constitutes a network of pathways that enable smooth and efficient repair of DNA lesions. In transcriptionally silent chromatin, DNA is densely packaged around nucleosomes and organised into 'beads on a string' fibres, then into higher levels of fibres and fractal globules, which then form chromosomes (Hübner et al., 2013). In order to be able to resolve the lesion, the DDR factors require physical access to the site of damage, made possible by local chromatin decondensation. Moreover, successful repair of DNA damage requires a high degree of spatiotemporal organisation of the DDR factors involved. Proteins involved in the DNA damage repair need to not only be able to access the site of lesion, but to do so at the right time. Importantly, the localisation to the site of damage is transient and the DDR proteins disassociate from chromatin after having fulfilled their role, which facilitates the recruitment of downstream factors and the repair pathway progression (Adamson et al., 2012; Li and Yu, 2015). To a large extent, these processes are mediated and regulated by post-translational modifications (PTMs), such as phosphorylation, ubiquitylation, sumoylation and ADP-ribosylation. ADP-ribosylation plays a significant role in base damage resolution and is required for an efficient lesion repair. Therefore, this section will focus on the mechanism and the roles of ADP-ribosylation in DDR.

ADP-ribosylation is carried out by ADP-ribosyl transferases, which are also known as poly(ADP-ribose) polymerases (PARPs). PARPs have the ability to transfer the ADP-ribose moiety from bound nicotinamide adenine nucleotide (NAD^+) to a target protein (Hoch and Polo, 2020). ADP-ribosylation can involve the modification of the target molecule either with a single mono(ADP-ribose) unit (MARylation), or with a linear or branched chain of poly(ADP-ribose), called PARylation. PARylation plays a crucial role in sensing DNA damage, activating DDR pathways and facilitating repair (Li and Yu, 2015).

PARylation of proteins associated with chromatin can induce chromatin decondensation, facilitating repair (Ciccarone et al., 2017). PARP1 has been shown to induce uncoiling of nucleosomal DNA after binding to a double-strand break in close proximity to a nucleosome, an effect which was reversed upon auto-PARylation of PARP1 (Sultanov et al., 2017). The negative charge of the PAR modification induces disassembly of nucleosomes and relaxation of chromatin (Messner and Hottiger, 2011). The PARylation of histones is a crucial step in the DDR, as it causes the initial chromatin decondensation, which is then enhanced by recruitment of additional PAR-dependent chromatin remodellers (Andronikou and Rottenberg, 2021).

Moreover, PARylation plays a prominent role in orchestrating the process of protein recruitment to the lesion (Brown and Jackson, 2015; Gunn et al., 2016). Activated PARP1 auto-PARylates itself and the resulting poly(ADP-ribose) modifications are recognised by proteins containing a PAR-recognition domain (Ray Chaudhuri and Nussenzweig, 2017). Such target proteins bind noncovalently to the PAR chains and

as a result they are recruited to the site of damage (Krietsch et al., 2013). Several classes of PAR-binding domains have been identified, including the PAR-binding zinc finger (PBZ) domain, the PAR-binding motif (PBM), the WWE domain, the Macrodomain, the BRCT domain and the forkhead-associated (FHA) domain (Wei and Yu, 2016). Various PAR-recognising domains display different interaction modes with PAR. For example, the PBZ domain binds to two consecutive ADP-ribose moieties, while the WWE domain binds to iso-ADP-ribose and the Macrodomain recognises the terminal ADP-ribose (Ahel et al., 2009; Isogai et al., 2010; Teloni and Altmeyer, 2016; Wang et al., 2012). The scaffolding protein XRCC1 is a core factor in SSB repair and it is recruited to the single-strand break by PARP1 or PARP2 in a PAR-dependent manner (Hanzlikova et al., 2017). The binding of XRCC1 to PAR is mediated by the BRCT domain of XRCC1, which is also responsible for binding to DNA, and both of these interactions are necessary for efficient SSB repair (Polo et al., 2019). Another important factor recruited to the PAR moieties on activated PARP1 is the chromatin remodeller ALC1, which binds PAR through its C-terminal Macrodomain and catalyses nucleosome sliding (Ahel et al., 2009; Andronikou and Rottenberg, 2021). The PBZ domain, which is less frequently found in mammalian proteins, enables the DNA-repair histone chaperone APLF to recognise and bind PAR (Mehrotra et al., 2011). While numerous DDR proteins with PARP-dependent chromatin recruitment pattern have been identified, others likely remain to be uncovered.

1.3.2 DNA-dependant PARPs

Poly(ADP-ribose) polymerases (PARPs) constitute a superfamily of 17 proteins which can catalyse the transfer of the ADP-ribose, which derives from NAD^+, onto itself or other proteins (Liu et al., 2017). Despite the name of the superfamily, most PARPs are mono(ADP-ribosyl) transferases and can modify their targets with a single unit of ADP-ribose. Only PARP1, PARP2, PARP4 and PARP5 have the ability to synthesise poly(ADP-ribose) chains (PAR), which can be either linear or branched, depending on the enzyme (Kamaletdinova et al., 2019; Zarkovic et al., 2018). However, the superfamily is defined by a sequence homology within the C-terminal catalytic domain (Hottiger et al., 2010). The founding member of the family, PARP1, was discovered in 1963 in Paul Mandel's laboratory following the observation of rapid NAD^+ consumption and synthesis of a new polyadenylic acid after the exposure of cells to alkylation agents (Chambon et al., 1963; Drew, 2015). For many years PARP1 was assumed to be a protein with unique abilities to sense and signal DNA damage, solely responsible for cellular ADP-ribosylation. However, the observation of retained ability to synthesise poly(ADP-ribose) chains in PARP1-deficient mouse embryonic fibroblasts, together with the identification of two PARP1-homologues in *Arabidopsis thaliana,* suggested an additional PARP factor might be present in mammals (Lepiniec et al., 1995; Shieh et al., 1998). This eventually led to the discovery of murine and human PARP2 through a search based on the similarity with the catalytic domain of the *A. thaliana* poly(ADP-ribose) polymerase, APP (Amé et al., 1999). Shortly after that, an expressed sequence tag (EST) library screen based

on the similarity to the catalytic domain of human PARP1 revealed another member of the family, PARP3 (Johansson, 1999).

PARP1, together with PARP2 and PARP3, form a subclass of DNA-dependent PARPs which require the binding to specific DNA structures to become activated. An estimated 90% of PARylation is conducted by PARP1, with PARP2 being the second dominant PARylating factor (Beck et al., 2014). PARP3 cannot synthesise PAR chains, but modifies its target via the addition of a mono(ADP-ribose) unit (Zarkovic et al., 2018).

PARP1 binds to specific DNA damage sites, such as SSBs, DSBs, overhangs or hairpins, through zinc finger domains ZFI and ZFII, both located in the N-terminal domain. ZFII also plays an important role in the activation of PARP1 after binding to DNA (Figure 1.6, Kamaletdinova et al., 2019). PARP1 also possesses an automodification domain with subdomain BRCT and flanking regions, a WGR domain, and a highly conserved C-terminal catalytic domain (CAT) comprised of a helical subdomain (HD) and ADP-ribosyl transferase (ART) subdomain (van Beek et al., 2021). The BRCT domain is crucial for protein-protein interactions and WGR plays an important role in DNA-dependent activation (Kamaletdinova et al., 2019). The ART domain contains the NAD^+ acceptor site and the HD allosterically controls the binding capabilities of the ART domain (van Beek et al., 2021). Although PARP2 and PARP3 do not possess the N-terminal zinc finger domain, they can bind to 5'phosphorylated DNA breaks through the WGR domain (van Beek et al., 2021; Zarkovic et al., 2018). It has been demonstrated using information derived from crystal structures of PARP1 at a

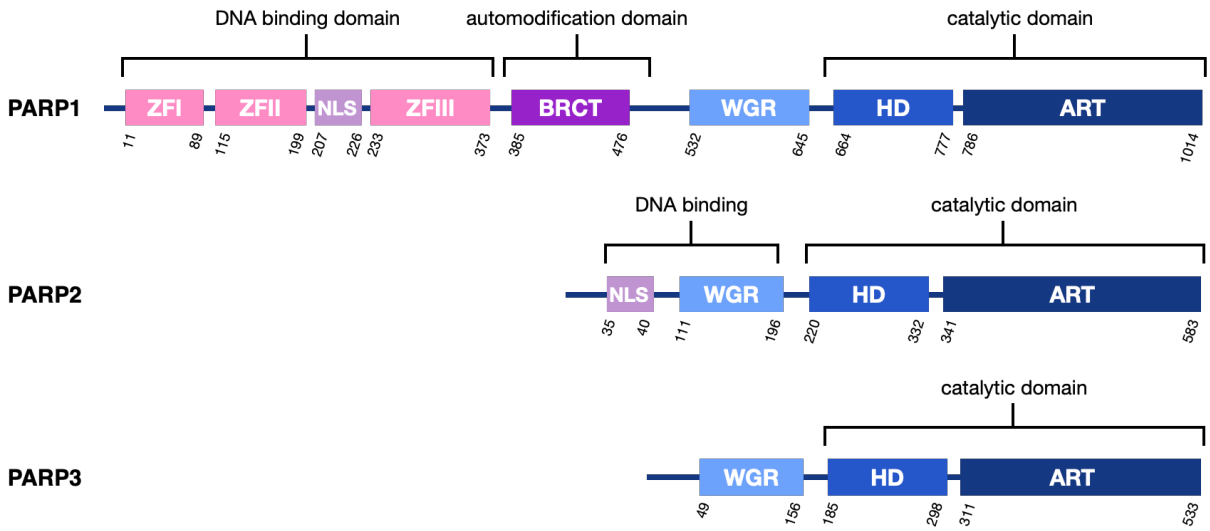

Figure 1.6 Schematic comparison of the domain organization of the DNA-dependent PARPs. ZFI - zinc finger I, ZFII - zinc finger II, ZFIII - zinc finger III, NLS - nuclear localization signal, BRCT - BRCA1 C-terminal. The catalytic domain contains the NAD^+ acceptor site and residues important for PAR synthesis. Adapted from Kamaletdinova et al., 2019.

double strand break, that upon binding to the DNA damage site by ZFI and ZFII, the ZFIII and WGR interact with the minor groove of the DSB, facilitating contact between domains (Langelier et al., 2012). This interaction induces conformational changes in the HD, triggering the catalytic activation of PARP1 (Langelier et al., 2012). This allosteric regulation mechanism is partly shared with PARP2 and PARP3 as well, where the destabilisation of HD results from the binding of WGR domain to DNA (Langelier et al., 2014). Subsequently, catalytically activated PARP1 and PARP2 synthesise PAR chains that can be long and branched and are covalently bound to the target proteins (Ray Chaudhuri and Nussenzweig, 2017). The targets of this modification can be PARP itself, other DDR proteins or histones. PARP1 and PARP2 have the ability modify their targets by PARylation, as well as by MARylation, and they both preferentially modify their own aspartate and glutamate residues (Rudolph et al., 2021b). However, interaction of PARP1/2 with HPF1 (histone PARylation factor 1) redirects the target residue specificity to serine and promotes transPARylation of histones over autoPARylation (Bonfiglio et al., 2017; Gibbs-Seymour et al., 2016; Suskiewicz et al., 2020). The ADP-ribosylation of serine residues strictly requires HPF1 and constitutes the majority of DNA damage-induced ADP-ribosylation occurring in mammalian cells (Bonfiglio et al., 2017; Palazzo et al., 2018). As mentioned previously, PARP3 can only transfer mono(ADP-ribose) units onto its targets, potentially due to an absent D-loop in its donor site (van Beek et al., 2021).

PARylation is a rapid process, occurring within seconds of DNA damage (Ray Chaudhuri and Nussenzweig, 2017). After the DNA lesion is resolved, the PAR chains

are promptly removed from the modified proteins by (ADP-ribosyl)hydrolases. Removal of the PAR chains is a crucial final step of the signalling cascade, which prevents the trapping of the proteins bound to PAR at the site of DNA damage (Kassab et al., 2020). Because of the heterogeneous nature of bonds within the PAR chains, dePARylation involves the degradation of the linear linkage between two ADPr units, as well as the hydrolysis of the branch point between two ADPr units, and the cleavage of the terminal amino acyl-ADP-ribosyl bond (Rack et al., 2021). The two main hydrolases participating in the degradation of ADP-ribosylation modifications of serine, which is the primary acceptor of ADPr in DDR, are poly(ADP-ribose)glycohydrolase (PARG) and (ADP-ribosyl)hydrolase 3 (ARH3) (Rack et al., 2020). While PARG can degrade both the linear and the branched linkages in the PAR chain, it is unable to remove the terminal ADP-ribose unit bound to the serine of the modified protein (Slade et al., 2011). However, this seryl-ADP-ribosyl linkage can be cleaved by ARH3, which is the only known enzyme with the ability to remove MARylation of serines (Fontana et al., 2017; Rack et al., 2021). Removal of the proximal ADP-ribose moiety from aspartate or glutamate of the acceptor protein requires the activity of other hydrolases, such as TARG1 or MacroD1/2 (Kassab et al., 2020). The cooperation of appropriate hydrolases is necessary for effective DNA damage repair and any mutations leading to accumulation of PAR can be catastrophic to cell survival (Ray Chaudhuri and Nussenzweig, 2017; Zhou et al., 2010).

1.3.3 PARPs and BER

PARP1 is a sensor of single strand breaks (SSBs), both those originating directly, for example as a result of exposure to UV, gamma-irradiation, or reactive oxygen species (ROS), and those arising during BER as a result of endonuclease activity (Caldecott, 2008; Lankinen et al., 1996; Pogozelski and Tullius, 1998). However, the important role of PARP1 in BER was not immediately clear in the early studies in this field. Although PARP1-deficient murine cells exhibited high sensitivity to treatment with an alkylating agent *N*-methyl-*N*-nitrosourea, another study reported that mouse embryonic fibroblasts efficiently repair base damage in the absence of PARP1 (de Murcia et al., 1997; Vodenicharov et al., 2000). Reports of the lack of requirement for PARP to reconstitute BER *in vitro* also seemed to support the thesis that PARP1 is dispensable for that pathway (Pascucci et al., 2002).

A possible explanation of these observations was offered by the discovery that cells derived from PARP1-/- mice synthesised poly(ADP-ribose) chains identical to those synthesised by PARP1 when exposed to an alkylating agent (Shieh et al., 1998). This indicated another factor must be present that carries out PARylation in response to base damage in the absence of PARP1. The subsequent discovery of PARP2 and its similarities with the PARylation abilities of PARP1 prompted a hypothesis of redundancy between the two proteins in alkylation DNA damage repair (Amé et al., 1999). Moreover, combined deficiency in PARP1 and PARP2 resulted in embryonic lethality in mice, indicating redundancy of these two proteins (Menissier de Murcia, 2003). In contrast to *parp1*Δ and *parp2*Δ cells, *parp1/2*Δ cells exposed to MMS

displayed a significant rise in SSB levels compared to wild-type cells, indicating redundancy in resolution of SSBs resulting from BER processing (Ronson et al., 2018).

PARP1 and PARP2 act redundantly in facilitating the progression of BER by recruiting the scaffolding protein XRCC1 to the SSBs (El-Khamisy, 2003). XRCC1 recognises and non-covalently binds to PAR through its BRCT motif (Polo et al., 2019). XRCC1 is recruited to chromatin in the absence of either PARP1 or PARP2 following H_2O_2 exposure, but no XRRC1 recruitment was observed were neither of the PARP proteins were present (Hanzlikova et al., 2017). PARylation by either PARP1 or PARP2 also induces the localisation to chromatin of the chromatin remodeller ALC1 containing a Macrodomain (Lehmann et al., 2017). ALC1 promotes chromatin decondensation, providing access to the lesion for other repair factors (Ooi et al., 2021). Chromatin relaxation induced by modification of histones can further facilitate the binding of BER factors to the site of damage, such as reported PARylation of histones by PARP1 or PARP2 requiring an interaction with histone PARylation factor 1 (HPF1) (Rudolph et al., 2021a).

1.3.4 PARPs and replication fork reversal in alkylation damage repair

PARP1 also plays a role in regulation of fork reversal, one of the replication-coupled repair mechanisms that can contribute to resolution of alkylation base damage (Ray Chaudhuri et al., 2012). PARylation by PARP1 has an inhibitory effect on the RECQ1 helicase activity (Berti et al., 2013). PARylation of RECQ1 prevents untimely fork

restart and stabilises the forks in the reversed state, allowing for the repair to be carried out and avoiding replication run-off that can result in DSBs (Berti and Vindigni, 2016). The activity of PARP1 at the reversed replication fork can be inhibited by the E3 ubiquitin ligase MDM2. Ubiquitylation by MDM2 targets PARP1 for proteasomal degradation, which in turn results in replication fork progression (Giansanti et al., 2022).

1.4 PARP inhibitors

Given the important role of PARPs in DNA damage repair, it is not surprising that they are active targets of therapeutics. Poly(ADP-ribose) polymerase inhibitors (PARPi) are nicotinamide analogues competing with NAD^+ in binding the active site of PARP, thereby suppressing its catalytic activity (Yi et al., 2019). PARP inhibition was first observed as an effect of nicotinamide and thymidine treatment over five decades ago (Preiss et al., 1971). Although a number of PARP inhibitors were identified in the following years, it was not until 2014 that olaparib became the first of these drugs to be approved for use in clinic (Kaufman et al., 2015; Terada et al., 1979). Since then, several more PARPi have been developed and approved for cancer treatments. Olaparib has been approved for the treatment of ovarian, breast, pancreatic and prostate cancers (Kindler et al., 2022; Mateo et al., 2020; Tutt et al., 2021). Rucaparib has been approved for use in patients with ovarian and prostate cancers (Abida et al., 2020; Ledermann et al., 2020). Talazoparib has been approved for treatment of breast cancer and niraparib for maintenance of ovarian, fallopian tube and peritoneal cancers (González-Martín et al., 2019; Litton et al., 2018). There

are ongoing clinical trials involving the use of PARPi, also in combination with other drugs, to treat numerous other types of cancer (Topatana et al., 2020).

1.4.1 Synthetic lethality

The term synthetic lethality describes an event in which a concurrent functional loss of two genes leads to cell death, while the loss of just one of the genes is tolerated by the cell and allows its viability (Yi et al., 2019). The idea of synthetic lethality was first developed based on the outcome of simultaneous mutations in two genes in *Drosophila* in 1922 and later extensively studied in yeast (Bridges, 1922; Nijman, 2011). At the beginning of the 21st century, uncovering synthetic lethal interactions involving known cancer mutations became a focus of interest (Kaelin, 2005). Identifying such relationships was attractive as it would provide a possible pharmacological target for specific mutation-tailored cancer therapies. The discovery of synthetic lethal interaction between BRCA1/2 deficiency and PARP inhibition in 2005 by two independent groups presented new opportunities in designing treatment strategies that would kill specifically BRCA1- or BRCA2-deficient tumours (Bryant et al., 2005; Farmer et al., 2005). These reports laid the foundation for developing the first PARP inhibitor, olaparib, to be used in clinic, as well as the later approved for patient treatment rucaparib (Drew, 2015). Two more PARPi, niraparib and talazoparib, were approved for clinical use in 2017 and 2018, respectively (Rose et al., 2020).

The drug-gene synthetic lethality induced by PARP inhibitors in BRCA1/2-deficient cells relies on the presence of mutations causing impaired homologous recombination repair (HR). While the tumour suppressor genes *BRCA1* and *BRCA2* are essential for HR, a concept of BRCAness has been developed, which is defined as a defect in HR that mimics BRCA1/2 deficiency in sensitivity to PARPi (Byrum et al., 2019). Therefore, other factors that regulate BRCA1/2 expression or their function in HR may lead to synthetic lethality with PARPi. Recently, the definition of BRCAness has been expanded to include defects in replication fork protection, as well as DNA damage checkpoint proteins and kinases, such as CDK12, which promote BRCA1/2 function in HR (Byrum et al., 2019). Such a revised understanding of BRCAness may broaden the range of possible gene deficiencies that could be exploited by therapeutic strategies involving PARP inhibition.

1.4.2 Possible mechanisms driving the cytotoxicity of PARP inhibition

Despite extensive research involving PARP inhibitors, the exact mechanism responsible for their synthetic lethality with certain cancer mutations has not yet been established. The first reports of synthetic lethality between PARPi and BRCA1/2 deficiency proposed that the observed cytotoxicity of this relationship stems from accumulation of DNA single strand breaks due to PARP inhibition (Bryant et al., 2005; Farmer et al., 2005). During DNA synthesis, replication forks encountering these SSBs would stall and collapse, giving rise to double strand breaks. Without functional HR, DSBs would be repaired via non-homologous end joining (NHEJ), which is more

error-prone and more likely to result in genomic instability (Patel et al., 2011). This model was questioned by a later study, which demonstrated PARP inhibition did not lead to an increase in the level of SSBs in HR-defective cells (Gottipati et al., 2010; Rose et al., 2020). Additionally, depletion of XRCC1, which is an important SSB repair factor, did not result in increased sensitivity to PARP1 depletion (Nazarkina et al., 2007; Patel et al., 2011).

The observation that PARP inhibition is more cytotoxic than PARP depletion indicated that an additional mechanism might contribute to the synthetic lethal interaction of PARP inhibitors with HR (Murai et al., 2012). It was proposed that after having bound the inhibitors to the NAD^+-binding domain, PARPs' ability to auto-PARylate is lost and they become trapped on the DNA (Figure 1.7; Rose et al., 2020; Shen et al., 2013). However, the trapping is not directly caused by the inhibition of the PARylation activity of PARP. Through binding to its helical domain, specific PARPi have different effect on the allostery of PARP1, and can either promote allosteric retention, be allosterically neutral, or promote allosteric release (Zandarashvili et al., 2020). Interestingly, olaparib and talazoparib were found to be allosterically neutral, while other data indicate that talazoparib has the highest trapping potential among the clinically-approved PARPi, followed in its trapping potency by niraparib, olaparib and rucaparib, and lastly, the low-trapping veliparib (Blessing et al., 2020; Pommier et al., 2016; Zandarashvili et al., 2020). This could suggest that the PARP trapping abilities of these inhibitors are driven mostly by inhibition of the auto-PARylation-dependent release mechanism. PARPs trapped at the site of DNA damage provide obstacles which cannot be bypassed by replication forks, resulting in the rise of

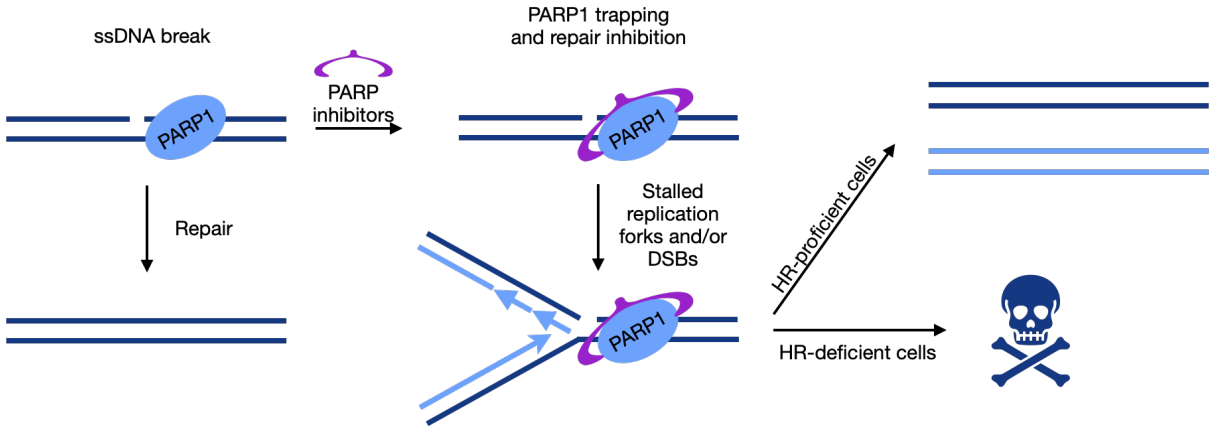

Figure 1.7 Schematic demonstrating the PARP-trapping model of synthetic lethality between PARPi and HR deficiency. After binding to the inhibitor, PARP loses its ability to autoPARylate and becomes trapped on the DNA. Trapped PARP becomes an obstacle for the replication forks, leading to rise in DSBs, which can be resolved by HR in HR-proficient cells, or by error-prone NHEJ in HR-deficient cells., often resulting in genomic instability.

DSBs, which in HR-deficient cells reliant on NHEJ leads to genomic instability (Farmer et al., 2005; Murai et al., 2012). Although the cytotoxic effect of PARP trapping at the site of damage is well documented, it is still unclear how much it contributes to the synthetic lethality with HR (Adamowicz et al., 2021; Juhász et al., 2020). Several PARPi are successfully used in treatments against BRCA-mutated ovarian and breast cancer, among other (Topatana et al., 2020). However, PARP trapping by PARPi has a cytotoxic effect both on cancer and on healthy bone marrow cells, calling into question the therapeutic application of inhibitors with high trapping potency (Hopkins et al., 2019).

Another mechanism that might contribute to the cytotoxicity of PARP inhibition is the stalling of replication forks. PARP1 is required at stalled replication forks to promote MRE11-mediated restart (Berti et al., 2013; Bryant et al., 2009). Furthermore, PARP1 stabilises the replication forks at BER intermediates to prevent nucleolytic resection, acting redundantly with PARP2 (Ronson et al., 2018). PARP1 and PARP2 are also redundant in directly promoting BER through signalling DNA damage and recruiting DDR factors to the lesion (Ronson et al., 2018). Despite these redundancies between PARP1 and PARP2, this relationship does not apply to synthetic lethality with HR, which depends largely on the loss of PARP1 (Ronson et al., 2018). The absence of catalytically active PARP prevents replication forks restart and leads to uncontrolled nucleolytic resection at the stalled forks. If replication forks are unable to restart and are not stabilised, they collapse, which can result in the formation of DSBs (Cortez, 2015). DSBs can also arise from the collision of

replication forks with an unresolved SSB (Berti and Vindigni, 2016). The resulting DSBs cannot be repaired in an error-free manner without functional HR, which can explain the synthetic lethality of PARP inhibition in HR-deficient cells (Rose et al., 2020). Moreover, this effect is further exacerbated by the inhibitor-induced trapping of PARPs at the lesion, which provides an obstacle for the replication machinery, leading to forks collapse and emergence of DSBs (Murai et al., 2012).

Additionally, upregulation of NHEJ in cells with defective HR might play a part in the synthetic lethality between PARP inhibition and BRCA-deficiency. DSBs can be repaired either by an error-free HR pathway using an intact homologous DNA template, or through an error-prone NHEJ. When the repair of DSBs through HR is not possible, cells become overly reliant on NHEJ, which can lead to an increased mutational burden and by itself is sufficient to cause cell death (Scully et al., 2019). PARP inhibition promotes the requirement for NHEJ phosphorylation of DNA-PK targets, which results in NHEJ upregulation (Patel et al., 2011). Moreover, depletion of Ku80, which is required for NHEJ, alleviated the cytotoxicity of PARPi in BRCA2 deficient cells (Patel et al., 2011). Although these are appealing arguments for the role of NHEJ upregulation in the synthetic lethality of PARPi with HR deficiency, opposing conclusions can be drawn from the reports of additive cytotoxic effect of combined DNA-PK and PARP inhibition in HR-deficient cells (Fok et al., 2019; Rose et al., 2020).

However, the recently proposed model of replication gaps driving PARPi cytotoxicity challenges the validity of the previously considered mechanisms. A recent study

demonstrated that instead of slowing down or stalling DNA replication, PARP inhibition resulted in acceleration of the replication fork progression by 40% (Maya-Mendoza et al., 2018). The initial interpretation of this finding suggested that catalytically inactive PARP1 fails to promote fork reversal, leading to a replication runoff of the unrestrained forks and, subsequently, to the rise of DSBs (Maya-Mendoza et al., 2018; Quinet and Vindigni, 2018). Alternatively, Cong *et al.* hypothesised that the PARPi-induced high speed replication results in the accumulation of replication-associated ssDNA gaps, which is synthetic lethal in BRCA1/2-deficient cells due to the role BRCA proteins play in preventing replication-associated gaps, and to the PARP1 participation in Okazaki fragment processing (Cong et al., 2019). Indeed, an accumulation of ssDNA gaps was observed in BRCA1-RAD51-deficient cells exposed to PARPi, leading to synthetic lethal interaction caused by the combination of defects in Okazaki fragment processing (OFP) and in replication gap suppression (Cong et al., 2021). This model is further supported by the sensitivity of BRCA1-deficient cells to inhibition of OFP and ssDNA binding by RPA, resulting in exposed gaps, and this sensitivity can be rescued by the loss of 53BP1 which restores OFP (Cong et al., 2021). Moreover, the resistance to PARP inhibition correlates with gap suppression (Cong et al., 2021). This newly proposed model of replication-associated gaps- driven PARPi cytotoxicity provides an opportunity to explore potential strategies for overcoming PARPi resistance emerging in some cancer cells. It could also lead to expansion of the potential tumour targets for PARPi therapy beyond those exhibiting a defect in HR.

Despite the fact that PARPi are safely and effectively used in cancer treatment, what drives the synthetic lethality with HR remains to be determined. Possibly, more than one of the described mechanisms is a contributing factor. Further investigation into the foundation of this synthetic lethal relationship is needed and has the potential to reduce the side effects experienced by patients treated with PARPi and possibly expand the patient population that might benefit from PARPi therapy. Similarly, identification of other factors that work together with PARPs in DDR and may exhibit synthetic lethal phenotypes may also offer therapeutic potential.

1.5 KEAP1

1.5.1 KEAP1 functions as a substrate adaptor for E3 ubiquitin ligase regulating the activity of NRF2

KEAP1 (Kelch-like ECH-associated protein 1) was discovered in 1999 by Yamamoto and colleagues as the negative regulator of the transcription factor NRF2 (Itoh et al., 1999). It is a highly conserved, 624-amino-acid-long protein rich in cysteines (Figure 1.8; Dayalan Naidu and Dinkova-Kostova, 2020). KEAP1 is a sensor for endogenous and exogenous oxidants and electrophiles, which inhibit its activity and cause NRF2 accumulation (Itoh et al., 1999). NRF2 then translocates to the nucleus, where it upregulates the transcription of cytoprotective genes by binding to antioxidant responsive elements (AREs) or electrophilic responsive elements (EpREs) (Reddy, 2008).

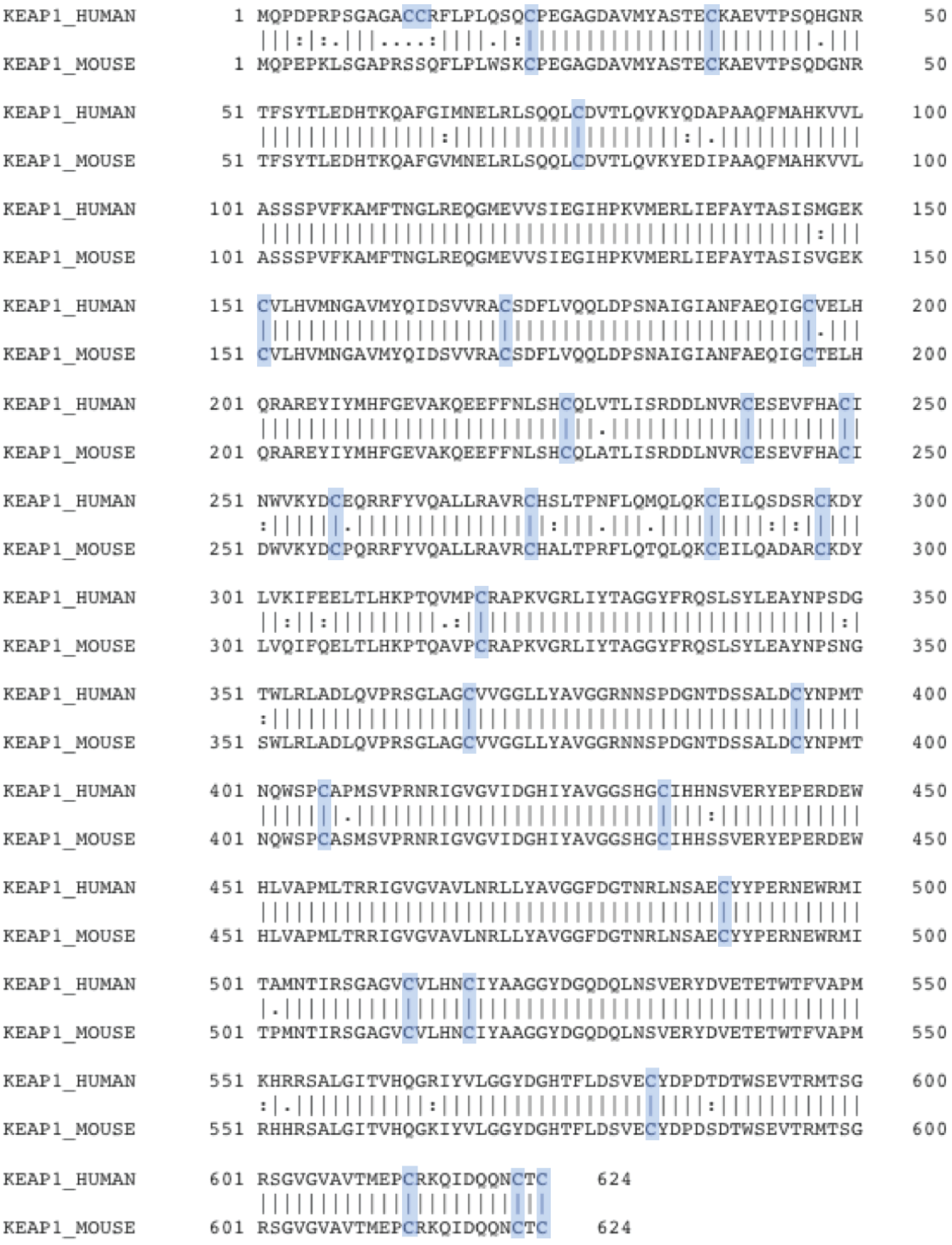

Figure 1.8 KEAP1 is a highly conserved, cysteine-rich protein. Pairwise sequence alignment of human and murine KEAP1 using EMBOSS Needle indicates 94.1 % identity and 97.3 % similarity between amino acid residues. A period (.) indicates conservation between amino acid groups exhibiting weakly similar properties. A colon (:) indicates conservation between amino acid groups exhibiting strongly similar properties. A vertical slash (|) indicates identical amino acids.

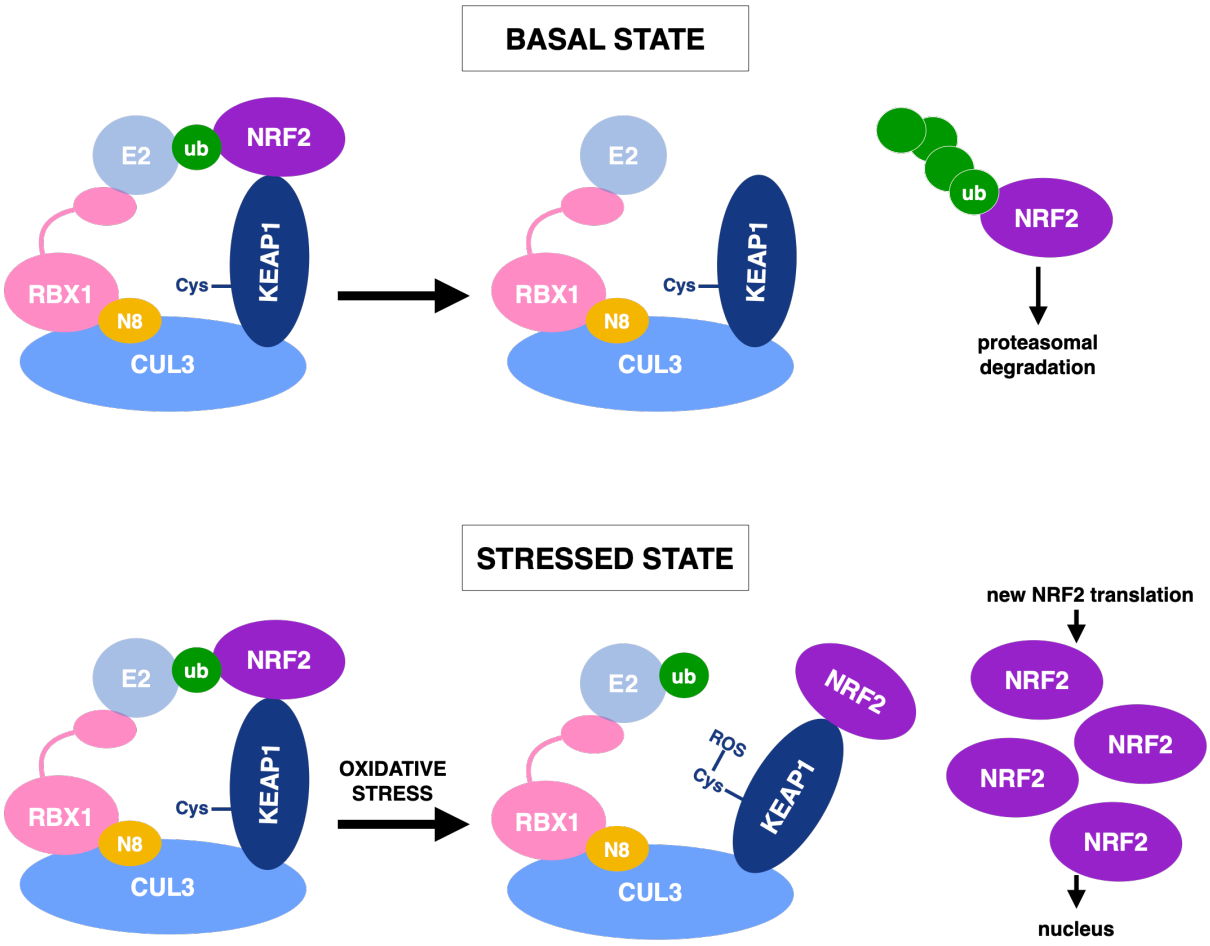

Figure 1.9 Schematic representation of the KEAP1-CUL3-RBX1 complex (depicted as a monomer) and its interactions with NRF2 both in basal and in stressed state. In the basal state NRF2 is ubiquitinated by the E3 ligase and degraded by the proteasome. In the presence of oxidative stress, the NRF2 ubiquitination is inhibited and the trapped NRF2 saturates the KEAP1 binding sites. This allows for newly translated NRF2 to escape the KEAP1-dependent ubiquitination and proteasomal degradation. NRF2 translocates to the nucleus, where it upregulates ARE-dependent cytoprotective gene expression. N8 depicts neddylation by NEDD8. Adapted from Baird and Yamamoto, 2020.

KEAP1 is a component of a multimeric Cullin-RING ubiquitin ligase (CRL). It forms a complex with Cullin3 (CUL3) and the RING protein RBX1, where KEAP1 combines the roles of both the substrate recognition and the adapter protein (Dinkova-Kostova et al., 2017). RBX1 facilitates the ubiquitin transfer from an E2-ubiquitin conjugating enzyme to the E3 ubiquitin ligase complex, while CUL3 serves as a scaffold connecting KEAP1 and RBX1 (Baird and Yamamoto, 2020). Under normal conditions Figure 1.9), the complex positions the NRF2-bound KEAP1 and the E2-bound RBX1 in a configuration that enables the ubiquitylation of NRF2 (Baird and Yamamoto, 2020). Repetitive rounds of ubiquitination and attachment of polyubiquitin chain of at least four ubiquitins linked through their Lys48 residues targets NRF2 for degradation by the 26S proteasome (Pierce et al., 2009).

1.5.2 Structural organisation of the KEAP1 protein

KEAP1 belongs to the BTB-Kelch protein family characterised by the presence of the BTB domain and the Kelch domain (Kopacz et al., 2020). Structurally, the KEAP1 protein is comprised of five different regions (Figure 1.10), namely the N-terminal region (residues 1-49), the BTB domain (residues 50-179), the intervening region (IVR, residues 180-314), the Kelch domain (residues 327-611) and the C-terminal region (residues 612-624) (Dinkova-Kostova et al., 2017).

The BTB domain is an evolutionary conserved region named after the *Drosophila melanogaster* proteins Broad-Complex, Tramtrack and Bric a brac, where it was first discovered, and since identified in the proteins of various organisms, such as

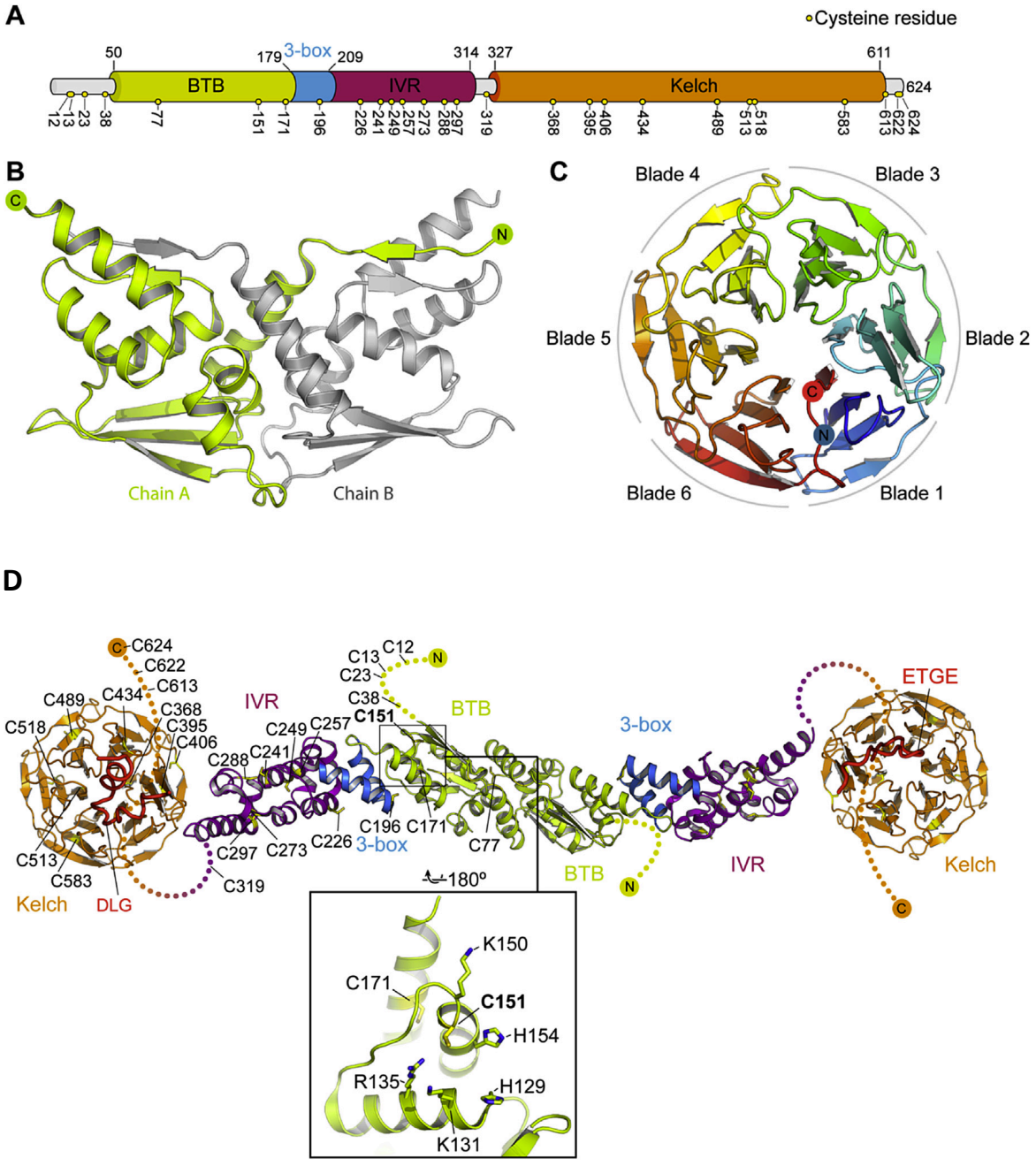

Figure 1.10 A. Organisation of domains within human KEAP1 with indicated locations of its cysteine residues. **B. The crystal structure of the BTB domains (PDB ID: 4CXI) of the KEAP1 molecules forming a dimer.** Each of the two monomers is marked with a different colour. **C. The crystal structure of the Kelch domain of KEAP1** (PDB ID: 2FLU), showing the six propeller blades. **D. Model of the predicted complete KEAP1 homodimer structure.** The structure of the KLHL11 BTB and BACK domains (PDB ID: 313N) was used to model the BTB and IVR domains of KEAP1. The Kelch domain of KEAP1 is shown in complex with either the ETGE motif (PDB ID: 2FLU) or the DLG motif (PDB ID: 3WN7). The cysteine residues of the human KEAP1 have been modelled onto the KLHL11 structure. The inset shows the highly reactive Cys151 (PDB ID: 4CXI) surrounded by basic residues. Reprinted from Dinkova-Kostova et al., 2017.

poxvirus, zebra fish, mouse and human (Chaharbakhshi and Jemc, 2016). Structurally, the BTB domain of KEAP1 consists of six α-helices organized in α-helical hairpins and of three β-strands organized in a β-sheet (Cleasby et al., 2014). The BTB domain is a protein-protein interaction motif, facilitating homo- and heterodimerization and multimerization (Bardwell and Treisman, 1994). In KEAP1 specifically, the BTB domain is responsible for its homodimerization (Zipper and Mulcahy, 2002). The BTB domain in KEAP1 is also necessary for its binding to CUL3 (Furukawa and Xiong, 2005).

The structure of the IVR in KEAP1, also known as the BACK domain, has not been solved to date. However, the known structures of the BACK domains of KLHL3 and KLHL11 exhibit an extended helical organization, which is thought to play a role in the correct positioning of the Kelch domain (Canning et al., 2013; Dinkova-Kostova et al., 2017; Ji and Privé, 2013). The AI-based protein structure prediction with Alphafold proposes a model (PDB ID: Q14145 and PDB ID: A0A024R7C0) of the IVR as six α-helices loosely organized in α-helical hairpins (Jumper et al., 2021; Varadi et al., 2022). A “3-box” motif at the N-terminus of the IVR creates a hydrophobic groove and, together with BTB domain, is critical for CUL3 binding (Yamamoto et al., 2018).

The C-terminal Kelch domain of KEAP1 contains six repeats of the Kelch motif, forming a six-bladed β-propeller (Dinkova-Kostova et al., 2017). While the regions of Kelch domain maintaining its structural organization are highly conserved, the sequences of Kelch repeats vary between different KLHL proteins belonging to BTB-Kelch family, and it is thought that those differences are responsible for substrate

specificity (Dhanoa et al., 2013; Kopacz et al., 2020). The Kelch domain is required for KEAP1 interaction with all its known substrates, such as NRF2, PALB2 or Marburgvirus' VP24 (Itoh et al., 1999; Orthwein et al., 2015; Page et al., 2014). The Kelch domain shows a high affinity to the ETGE motif and a lower affinity to the DLG motif, both of which are found in the Neh2 domain of NRF2 (Yamamoto et al., 2018).

Like all CRLs based around CUL3, the KEAP1-CUL3-RBX1 ubiquitin ligase functions as a homodimer, which is a feature unique among the superfamily of CRLs and crucial for its mode of action (Dinkova-Kostova et al., 2017; McMahon et al., 2006; Tong et al., 2006). The assembly of the complex is dependent on the homodimerization between the BTB domains of two KEAP1 molecules (Choo and Hagen, 2012). This interaction is necessary and sufficient for the dimerization of the two KEAP1-bound CUL3 proteins through their WH-B domains (Choo and Hagen, 2012). Although the structure of the KEAP1-CUL3-RBX1 complex has not been solved to date, this model of structural interactions within the complex is supported by single particle electron microscopy imaging of a mouse KEAP1 dimer, which demonstrated a structure of two spheres (Kelch domains and IVR) joined together by stems (BTB domains) in a cherry-like fashion (Canning et al., 2015; Ogura et al., 2010). Analysis of the CryoEM data revealed that the distance between the two Kelch domains of the homodimer matches the length of the ETGE- and DLG-containing Neh2 domain of NRF2, suggesting that KEAP1 homodimer binds to the two motifs of a single NRF2 molecule (Canning et al., 2015). Solving the structures of the KEAP1 BTB domain and Kelch domain – either with a truncated NRF2 peptide or without the ligand – further elucidated the nature of the protein interactions within the complex (Cleasby et al.,

2014; Li et al., 2004; Lo et al., 2006). Moreover, biochemical data demonstrates that the KEAP1 homodimer interacts with two distinct binding sites of a single NRF2 molecule (Genschik et al., 2013; McMahon et al., 2006). These findings gave the foundation for developing the model of 'hinge-and-latch' mechanism of binding NRF2 by KEAP1 (Tong et al., 2007). This model proposes that in order for NRF2 to become positioned in a way that enables its ubiquitination, the KEAP1 dimer must bind both to its ETGE motif ('hinge') and to its DLG motif ('latch') displaying a 200-fold lower affinity than ETGE (Dinkova-Kostova et al., 2017). Finally, neddylation of CUL3 reconfigures the KEAP1-CUL3-RBX1 complex so that the associated E2 complex is positioned in spatial proximity of NRF2, which facilitates the transfer of ubiquitin onto NRF2 (Dinkova-Kostova et al., 2017).

1.5.3 KEAP1 in HR

The relationship with NRF2 is the most thoroughly studied of KEAP1 interactions. However, KEAP1 has been reported to interact with over 20 other proteins, in many cases recognising a variation of the ETGE or, less frequently, the DLG motif of its target (Kopacz et al., 2020). Its functions extend beyond targeting substrates for proteasomal degradation and it has been implicated in regulating various cellular processes, such as S-nitrosylation or actin cytoskeleton organisation (Kopacz et al., 2019; Velichkova et al., 2002). Notably, KEAP1 plays a role in suppression of homologous recombination in G1 cells by inhibiting the PALB2-BRCA1 interaction (Orthwein et al., 2015). BRCA1 promotes the DNA resection at the DSB, which results in ssDNA and enables strand invasion (Densham and Morris, 2019). Through the interaction with PALB2, BRCA1 recruits BRCA2 and RAD51 to DSBs and allows the

repair through homologous recombination (Orthwein et al., 2015; Zhang et al., 2009). Through its Kelch domain, KEAP1 binds to the ETGE motif on PALB2 (Ma et al., 2012). PALB2 competes with NRF2 for binding to KEAP1, therefore promoting NRF2 accumulation and leading to a decrease in the level of the reactive oxygen species (Ma et al., 2012). KEAP1-CUL3-RBX1 E3 ligase ubiquitinates BRCA2-bound PALB2, which prevents it from interacting with BRCA1 and hinders homologous recombination (Orthwein et al., 2015). The PALB2-KEAP1 interaction is not cell cycle dependent, but the KEAP1-mediated ubiquitination of PALB2 is counteracted by USP11, a deubiquitylase regulated by cell cycle (Orthwein et al., 2015; Schoenfeld et al., 2004). A rapid turnover of USP11 in G1 allows efficient PALB2 ubiquitination by KEAP1 and results in HR suppression during G1 (Orthwein et al., 2015).

1.5.4 KEAP1 is a cysteine-based stress sensor

Although KEAP1 was identified as the negative regulator of NRF2 in 1999, its existence had been predicted over a decade earlier by Paul Talalay, who hypothesised that a protein with reactive cysteines would act as a sensor for small-molecule inducers of the phase 2 response (Talalay et al., 1988). Soon after the discovery of KEAP1 and its role in NRF2 regulation, researchers' attention was drawn to the cysteine residues of KEAP1 and the protein quickly became the ideal candidate for the inducer sensor (Dinkova-Kostova et al., 2017; Sekhar et al., 2010). The 27 cysteines contained in human KEAP1 make up 4.33 % of all its amino acids, which is nearly twice the ratio observed in an average human protein (2.26 %) (Kopacz et al., 2020; Miseta and Csutora, 2000). Ten of these cysteines are surrounded by basic amino acids, which lowers the *pKa* of the cysteine and increases

its reactivity (Dayalan Naidu and Dinkova-Kostova, 2020). Arguably the most reactive of cysteines in KEAP1, Cys151, is surrounded by five basic amino acids (His129, Lys131, Arg135, Lys150 and His154), which are positioned in its structural proximity (McMahon et al., 2006). A triple mutation of these residues to Lys131Met, Arg135Met and Lys150Met resulted in the inability of Cys151 to sense the electrophiles it normally recognises (McMahon et al., 2010).

The cysteine residues of KEAP1 are targeted by oxidants and electrophiles, which can lead to a multitude of different modifications. The variety of inducers and redundancy between the cysteines in response to them makes it challenging to decipher the intricacies of the cysteine code of stress-sensing in KEAP1. The discrepancy in conclusions due to differences in human and murine KEAP1 cysteine sensor adds to the confusion (Sekhar et al., 2010). However, four different cysteine sensors recognising a wide range of inducers have been identified in KEAP1 (Baird and Yamamoto, 2020). There have been efforts to classify the inducers based on their cysteine preference (Figure 1.11). Cys151 is the target of class I inducers, such as bardoxolone, the isothiocyanate sulforaphane (SFN), the alkylating agent iodocetamide (IAA), tetr-butyl hydroquinone (tBHQ) and diethylmateate (DEM) and more (Baird and Yamamoto, 2020; Dayalan Naidu and Dinkova-Kostova, 2020). Prostaglandin 15d-PGJ_2 exclusively modifies Cys288 and is currently the only known class II inducer (Saito et al., 2016). Class III inducers target either Cys151, Cys273 or Cys288 and include 4-hydroxynonenal (4-HNE), nitro-oleic acid and arsenite (Saito et al., 2016). Class IV inducers, such as cadmium or zinc chloride and H_2O_2, are recognised by a fail-safe sensor comprised of Cys226, Cys613 and Cys622/Cys624

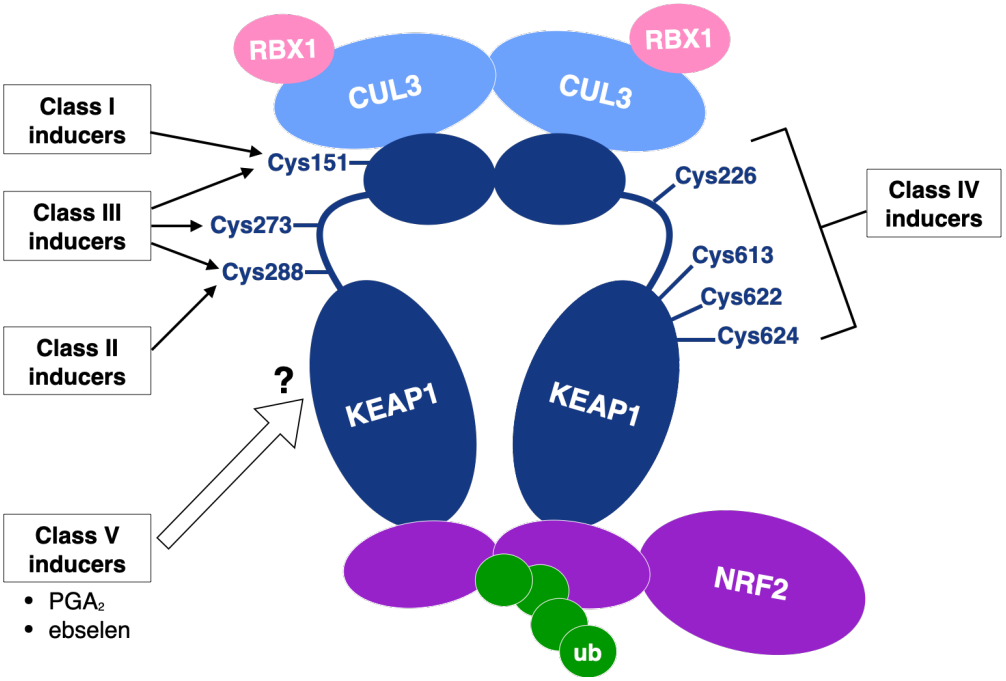

Figure 1.11 Schematic of different classes of NRF2 inducers. Classification is based on the preference for interacting with specific cysteine stress sensors within KEAP1. Adapted from Baird and Yamamoto, 2020.

(Baird and Yamamoto, 2020; Suzuki et al., 2019). Study in an 11-cysteine mutant of murine KEAP1 suggests the existence of another, yet unidentified, cysteine sensor targeted by PGA_2 (Suzuki et al., 2019).

Upon modification by a cysteine-reactive inducer, KEAP1 becomes inactive, which results in NRF2 escaping ubiquitination and degradation. There has been speculation about the mechanism of this inhibition, some proposing that KEAP1 thiol-group modifications lead to disassociation of CUL3 (Cleasby et al., 2014). This model of KEAP1 inhibition was supported by the observation that Cys151Trp mutation disrupts CUL3 binding and results in constitutive NRF2 activation, and assumed that inducer binding leads to the same outcome (Cleasby et al., 2014). However, the disassociation of CUL3 and KEAP1 is a process happening on the scale of hours, while NRF2 becomes activated within 15 minutes after KEAP1 modification by inducers (Baird and Yamamoto, 2020; McMahon et al., 2003). Moreover, the crystal structure of BTB domain of KEAP1 does not place Cys151 in the vicinity of the CUL3 binding site (PDB ID 5NLB). Together, these data suggest that cysteine modifications by the inducers do not lead to the disassociation of NRF2 from KEAP1, but instead inhibit the E3 ligase activity of the KEAP1-CUL3-RBX1 complex with bound NRF2 (Eggler et al., 2005). Subsequently, NRF2 becomes 'trapped' by KEAP1, as it is neither ubiquitinated nor released, and acts as a suicide substrate saturating the binding sites of cysteine-modified KEAP1 (Baird and Yamamoto, 2020). When KEAP1 becomes saturated, freshly translated NRF2 can freely translocate to the nucleus, where it drives the upregulation of ARE-dependant gene expression (Baird and Yamamoto, 2020; Kwak et al., 2002).

Several models describing the fate of KEAP1 post-cysteine-modification have been proposed (Dinkova-Kostova et al., 2017). Observed KEAP1 polyubiquitination coinciding with NRF2 activation and accumulation prompted a model in which cysteine residues modification induces a shift of CUL3-dependent ubiquitination from NRF2 to KEAP1 (Hong et al., 2005). Alternatively, it has been suggested that KEAP1 is degraded through p62-dependent autophagy in a process that aids the recovery of KEAP1 after the modifications introduced by the inducers (Dinkova-Kostova et al., 2017; Taguchi et al., 2012). However, more research is needed to gain insight into this process.

1.5.5 KEAP1 in cancer

Large scale genomic sequencing of cancer samples have identified KEAP1 alterations in 3.43 % of all cancers, with missense mutations being the most common (AACR Project GENIE Consortium, 2017). The highest prevalence of *KEAP1* mutation was observed in non-small cell lung cancer (NSCLC) at 13.48 %, followed by cholangiocarcinoma (5.56 %), hepatobiliary cancer (4.92 %), head and neck cancer (4.08 %) and endometrial cancer (3.83 %) (Figure 1.12; Weinstein et al., 2013). The mutation of *KEAP1* in NSCLC was first reported in 2006, followed two years later by the report of *NRF2* mutation (Padmanabhan et al., 2006; Shibata et al., 2008). While nonsynonymous mutations, abolishing the function of the KEAP-CUL3-RBX1 complex, were identified throughout the coding region of *KEAP1,* mutations of *NRF2* were largely constrained to the regions encoding the KEAP1-binding ETGE and DLG

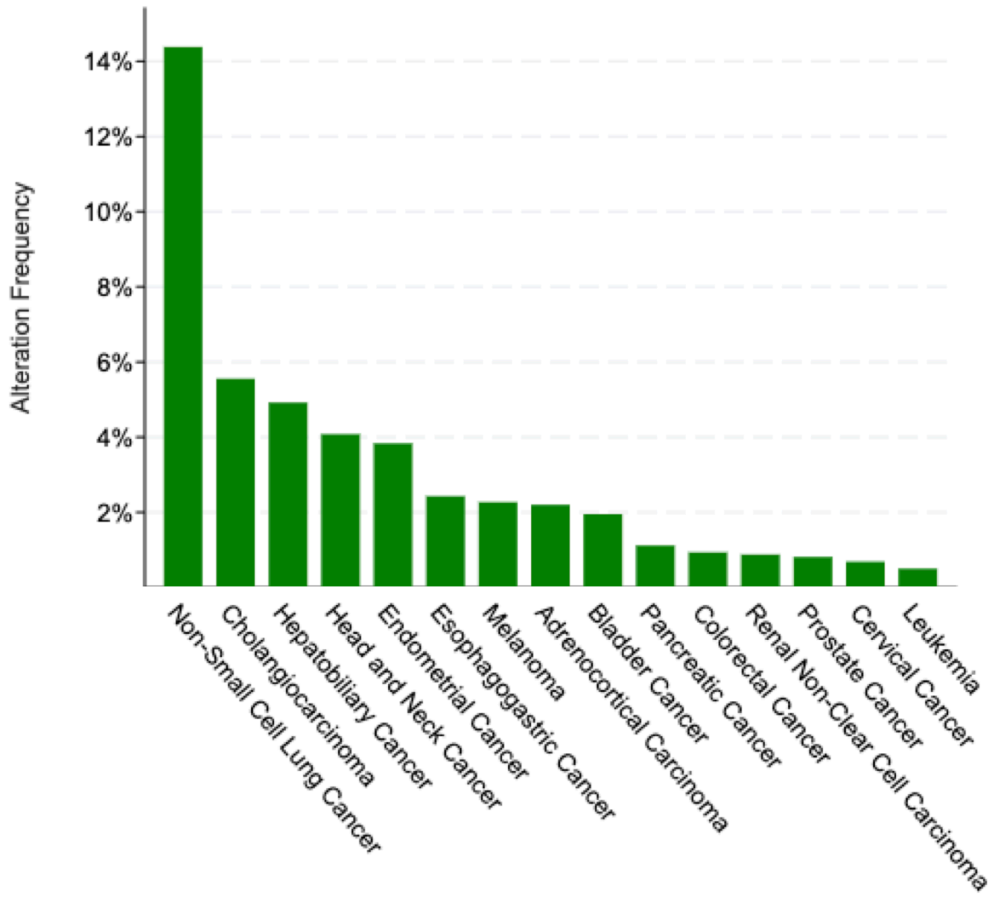

Figure 1.12 Nonsynonymous mutations in *KEAP1* are prevalent in a number of cancers. Data from The Pan-Cancer Atlas demonstrate the frequency of KEAP1 genetic alterations in different cancers. The results shown in the figire are in whole based upon the data generated by the TCGA Research Network: www.cancer.gov/tcga.

motifs (Yamamoto et al., 2018). Therefore, observed cancer mutations in the KEAP1-NRF2 system prevent NRF2 degradation and lead to constitutive activation of NRF2 signalling. Subsequent NRF2-induced transcription of cytoprotective genes provides cancer cells exposed to anticancer drugs with a survival advantage, with persistent NRF2 activation driving drug resistance and malignancy (Taguchi et al., 2011). KEAP1-deficiency confers resistance to topoisomerase II poisons used widely as chemotherapeutics, such as doxorubicin and etoposide (Wijdeven et al., 2015). *KEAP1* mutations were also found to be a negative prognostic for outcomes of treatment with immune checkpoint inhibitors (ICIs) used as anticancer drugs (Chen et al., 2020; Cordeiro de Lima et al., 2022; Di Federico et al., 2021). It has recently been shown that the resistance to ICI treatment in lung cancers can be caused by suppression of type I interferon signalling in KEAP1-deficient cells, leading to immune evasion (Marzio et al., 2022). Profiling tumours for *KEAP1* mutations can prevent patients from undergoing ineffective treatment and help choose therapeutic strategies to which they might be more responsive (Wijdeven et al., 2015). However, *KEAP1* mutations have a negative prognostic value for survival of cancer patients (Chen et al., 2020).

Given the prevalence and consequences of *KEAP1* mutations in cancer, there has been a focus on developing novel therapeutic approaches. Recent report identifies a synthetic lethal interaction between KEAP1-deficiency and inhibition of the ATM (Ataxia-telangiectasia mutated) kinase inhibition both *in vitro* and *in vivo* (Li et al., 2023). Moreover, transcript levels of KEAP1 and ATM correlated inversely across the TCGA PanCancer dataset of tumours (Li et al., 2023). This novel synthetic lethal

relationship provides an opportunity to exploit the KEAP1-deficiency of the tumour by targeted therapy with ATM inhibitors. Currently, three ATM inhibitors are undergoing phase I of clinical trials in cancer patients and if successful, could potentially be employed in the future to treat KEAP1-deficient tumours (Li et al., 2023). Possibly, more synthetic lethal relationships remain to be uncovered and can strengthen the efforts to develop targeted therapies for cancer patients with *KEAP1* mutations.

1.6 Aims

Although the major repair pathways resolving DNA base damage have been extensively studied, much remains to be uncovered. Base damage repair pathways display some redundancies; however, it is not fully understood how the specific pathway to resolve the lesion is determined. Moreover, within the one pathway there can be different routes that the lesion can be processed through, involving different enzymes, as in the case of short-patch and long-patch BER. Post-translational modifications play a crucial role in the regulation of cellular processes, including DDR, where PARylation is a prominent factor in coordinating repair. Numerous repair proteins that are recruited to the lesion through binding PAR, or are PARylated themselves to modulate their function, have been identified. However, there are likely still unknown factors that interact with PARPs and might contribute to regulation of base damage repair.

We were therefore motivated to identify any novel factors that participate in the repair of DNA base damage caused by alkylation. Secondly, we aimed to characterise the mechanism of action of this newly identified repair factor. Thirdly, we wished to determine in which repair pathway it is involved. Lastly, our goal was to explore the relationship of the novel repair factor with PARPs.

2. Materials and methods

2.1 Materials

2.1.1 Buffers

Phosphate Buffered Saline (PBS)

10 mM phosphate buffer

2.7 mM KCl

137 mM NaCl

DNA loading dye

0.25 % bromophenol blue

40 % sucrose

TBS-T

2.48 mM Tris-Cl

137 mM NaCl

(pH 7.4)

0.2 % Tween-20

SDS Loading Buffer

25 mM Tris-Cl (pH 6.8)

10 % glycerol

0.125 % bromophenol blue

2 % SDS

80 mM DTT

SDS-PAGE Running Buffer

25 mM Tris-Cl

192 mM glycine

0.1 % SDS

SDS-PAGE Transfer Buffer

25 mM Tris-Cl

192 mM glycine

20 % methanol

DNA Extraction Buffer

10 mM Tris-Cl (pH 8.0)

25 mM NaCl

1 mM EDTA

200 μg/ml proteinase K

TAE

40 mM Tris-Cl

20 mM acetic acid

1 mM EDTA

(pH 8.2)

Chromatin Extraction Buffer 1

10 mM Tris-Cl (pH 7.5)

150 mM NaCl

1.5 mM $MgCl_2$

0.34 M sucrose

10 % glycerol

1 mM DTT

0.1 % Triton X-100

Chromatin Extraction Buffer 2

3 mM EDTA

0.2 mM EGTA

1 mM DTT

LB Agar

1.5 % agar

1 % bactotryptone

0.5 % yeast extract

85 mM NaCl

LB Broth

1 % bactotryptone

0.5 % yeast extract

85 mM NaCl

2.2 Oligonucleotide sequences

2.2.1 gRNA sequences

guide RNA name	Sequence (5'->3')
gRNA_A	CCAGCAACGAAATCGGGAGA
gRNA_a	CGAATGACATCGGGCCGGAG
gRNA_B	TAGCCGCGTGGTCCGAGTCG
gRNA_b	TGACCCGAATGACATCGGGC

2.2.2 PCR primer sequences

Screening primers for *keap1*Δ

Primer name	Sequence (5'->3')
KEAP1 screening primer Forward	TGTGCTCTCTCCCCTCCAG
KEAP1 screening primer Reverse	CGGTGCATCCTGGTACTTGA
outside' primer Forward	CCAAGGTAAGGCAGGAATCTC
outside' primer Reverse	ATGATTCCCGCTTTGGACTTC
inside' primer 1 Forward	TGTGCTCTCTCCCCTCCAG
inside' primer 1 Reverse	CGGTGCATCCTGGTACTTGA
inside' primer 2 Forward	AGGTTGATCAGGTCGGGGAA
inside' primer 2 Reverse	TGAGCACTCGTCCATCCCTG
primer A Forward	AATTTTCCCTAGATCCTGCGGC
primer A Reverse	TTGGTTGTCGGTTGGGGAGC
primer B Forward	CCAAGGTAAGGCAGGAATCTC
primer B Reverse	TCACCATGACTAAGCAGAGCC
primer a Forward	GCTTTTGCATCTCACAGCTGC
primer b Reverse	ATGATTCCCGCTTTGGACTTC

Sequencing primers for *keap1*Δ

Primer name	Sequence (5'->3')
mid_KEAP1 seq 500_Forward	TCCGTGCCTGCAGTGACTTC
mid_KEAP1 seq 1000_Forward	CTTCCGACAGTCGCTCAGC
mid_KEAP1 seq 1500_Forward	TCACAGCAATGAACACCATCC

Cloning primers

Primer name	Sequence (5'->3')
KEAP1_cloning_F	GGGGACAAGTTTGTACAAAAAAGCAGGCTTCatgcagccagatcccaggcc
KEAP1_cloning_R	GGGGACCACTTTGTACAAGAAAGCTGGGTTCTAacaggtacagttctgctggtc
attB F KEAP1_KELCH-less	GGGGACAAGTTTGTACAAAAAAGCAGGCTTAATGCAGCCAGATCCCAGGcc
attB R KEAP1_KELCH-less	GGGGACCACTTTGTACAAGAAAGCTGGGTTTCACGTGGGCTTGTGCAGggtg
attB F KEAP1_BTB-less	GGGGACAAGTTTGTACAAAAAAGCAGGCTTAATGGACCCCAGCAATGCCatcg
attB R KEAP1_BTB-less	GGGGACCACTTTGTACAAGAAAGCTGGGTTTCAACAGGTACAGTTCTGCTGGTC
attB R KEAP1_Cysless	GGGGACCACTTTGTACAAGAAAGCTGGGTTCTAtcagctggtgctgttctgctggtca
attB R KEAP1	GGGGACCACTTTGTACAAGAAAGCTGGGTTCTAtcaacaggtacagttctgctgg

2.3 Methods

2.3.1 Cell culture

Both U2OS cells and RPE-1 cells were cultured in Dulbecco's Modified Eagle's Medium (DMEM) with high glucose and supplemented with 10 % fetal bovine serum (FBS), 2 % L-glutamine and 1 % penicillin/streptomycin. Confluency between 10-80 % was maintained throughout the culture with passages every 2-3 days. We used Eurofins cell line authentication service to confirm cell line identities by STR profiling.

To obtain protein depletion using siRNA transfection, cells were plated in a 6-well plate at a density of $3x10^5$ in an antibiotic-free culture medium. The following day,

cells were transfected with the specified siRNA concentration (50-75 nM) using Dharmafect-1 (Dharmacon). The transfection was repeated the following day and 24 hours later, antibiotic-free medium was replenished and cells were allowed to recover for 2 days before any experiments were performed. Pools of four siRNA sequences (Dharmacon) were used to deplete each targeted protein, and they were either siGENOME (KEAP1) or ON-TARGET plus (CUL3, BRCA1).

2.3.2 Generation of KEAP1 domain mutants

Amino acid residues 1-179 were removed to create the KEAP1$^{\Delta BTB}$ mutant and residues 315-624 were removed for the KEAP1$^{\Delta KELCH}$ mutant. This was achieved by amplifying only a partial sequence of KEAP1 cDNA, designing PCR primers that omit the terminal domain sequences. Each of the truncated cDNA sequences was then cloned into a lentiviral vector p580 and tagged on the N-terminus with FLAG-tag and HA-tag using the Gateway system. The S3H4 mutant was generated by synthesizing the cDNA with the help of Source BioScience and cloning it into a lentiviral system like described for the KEAP1$^{\Delta BTB}$ and KEAP1$^{\Delta KELCH}$ mutants. The 11Cys-less mutant cDNA was synthesized with the help of Source BioScience, cloned into a lentiviral vector p580 and tagged on the N-terminus with FLAG-tag and HA-tag using the Gateway system. The presence of the 11-Cys-less cDNA sequence in the final construct was confirmed by sequencing.

2.3.3 Production of lentivirus and lentiviral infection

293T cells were plated in antibiotic-free medium in a 10 cm dish at a density of $4x10^6$ and transfected 24 hours later with a lentiviral expression plasmid p580 and four plasmids encoding the *tat* gene, the *gag-pol* genes, the VSV-g envelope gene and the *rev* gene of the HIV-1 based system (the plasmids were a kind gift of Ross Chapman). The following morning, the transfection medium was removed, cells were washed with PBS and supplemented with complete culture medium. The medium containing the virus was collected 48 and 72 hours after the transfection, and filtered through a sterile 0.45 μm syringe filter (Fisher Scientific).

The viral titres were assessed by infecting wild-type RPE-1 cells seeded at low density with serial dilutions of the virus and selecting them with 2 μg/ml puromycin for 10 days, after which the cells were fixed and number of surviving colonies was counted. RPE-1 cells were seeded at a $1x10^6$ density in a 10 cm diameter dish. The following morning cells were infected using antibiotic-free medium, polybrene (Sigma-Aldrich) and a volume of virus-containing medium calculated based on the titre. After 8 hours of infection, the medium was removed, cells were washed with PBS and incubated overnight in fresh medium, before a 10-day-long selection regime with 2 μg/ml puromycin. Expression of the constructs was confirmed by Western blotting.

2.3.4 DNA extraction and PCR

To extract genomic DNA, cells were suspended in DNA extraction buffer and incubated at 65°C for 30 minutes, and after that at 95°C for 2 minutes. The PCRBIO Taq polymerase (PCR Biosystems) was used in screening PCRs, whereas the PCRBIO HiFi polymerase (PCR Biosystems) were used for subsequent cloning or sequencing of the PCR product.

2.3.5 Protein extract preparation

Whole-cell protein extracts were obtained by washing cells with PBS, pelleting them, resuspending in SDS loading buffer and boiling for 10 minutes.

Chromatin extracts were obtained by washing cells with ice-cold PBS, pelleting and incubating with chromatin extraction buffer 1 for 10 minutes on ice. Cells were then centrifuged at 3500 rcf, washed and incubated on ice with chromatin extraction buffer 2 for 30 minutes. After centrifuging at 17,000 rcf, the supernatant was discarded, and the pellet was resuspended in SDS loading buffer and boiled for 10 minutes.

2.3.6 Western blotting

Protein samples were analysed using SDS-polyacrylamide gel electrophoresis (SDS-PAGE). In-house prepared single percentage polyacrylamide gels were subjected to 160 V. Protein band sizes were assessed relating to a prestained protein ladder (PageRuler Plus, Fermentas). Transfer of proteins to a PVDF membrane (0.45 μm

pores, Millipore) pretreated with methanol was conducted in cold SDS-PAGE transfer buffer at 100 V for 90 minutes. The membranes were blocked in 5 % milk in TBS-T for 1 hour at room temperature, then incubated with primary antibody overnight at 4°C. Membranes were washed three times with TBS-T and incubated with secondary antibody for 1 hour. After three TBS-T washes, the membranes were incubated with Immobilon Western HRP substrate (Millipore) and imaged using Oddysey Fc Imager (LI-COR Biosciences). Images were analysed using Image Studio™ Lite software.

Primary antibodies used in described experiments:

Antibody	**Species**	**Source**	**Catalogue number**	**Working dilution**
CUL3	rabbit, polyclonal	Bethyl	A301-108A	1:1000
NRF2	mouse, monoclonal	Santa Cruz	Sc-365949	1:500
KEAP1*	mouse, monoclonal	Proteintech	60027-1-Ig	1:1000
KEAP1	rabbit, polyclonal	Abcam	ab139729	1:1000
PARP1	mouse, monoclonal	Biorad	MCA1522G	1:1000
PARP2	mouse, monoclonal	Enzo	ALX-809-639-L001	1:50
XRCC1	rabbit, monoclonal	Abcam	ab134056	1:1000

APEX-1	mouse, monoclonal	Abcam	ab194	1:2000
γH2AX	rabbit, monoclonal	Abcam	ab11174	1:2000
Rad51	rabbit, polyclonal	A gift from F. Esashi	7946	1:1000
HA	rabbit, monoclonal	Cell Signaling Technology	37245	1:1000
H3	rabbit, monoclonal	Abcam	ab176842	1:2000
Poly(ADP-ribose)	protein linked to rabbit Fc domain	Millipore	MABE1031	1:2000
Actin	mouse, monoclonal	Santa Cruz	sc-47778	1:2000

*The immunogen for the monoclonal anti-KEAP1 antibody #60027-1-Ig is the KEAP1 fusion protein Ag0779, encompassing the 325-624 amino acid residues encoded by *KEAP1.*

Secondary antibodies used in described experiments:

Antibody	**Species**	**Source**	**Working dilution**
anti-mouse HRP	rabbit	DAKO	1:10000
anti-rabbit HRP	swine	DAKO	1:10000

2.3.7 Clonogenic survival assay

Cells were trypsinised, counted and plated in a 6-well plate at a density of 400 cells per well to adhere overnight. The following day, cells were treated with DNA damaging agents or inhibitors, after which they were washed twice with PBS and supplemented with fresh medium. In case of MMS (Sigma-Aldrich) treatment, cells were exposed to the drug for 1 hour. For the sensitivity assays in *keap1*Δ5F and *keap1*Δ8C cells, MMS treatment was repeated on day 1, day 3 and day 5 after plating. Olaparib (Cambridge Bioscience) treatment was conducted for 24 hours with a range of concentrations. For combined olaparib and MMS treatment, cells were pre-treated with 10 μM olaparib for 1 hour before MMS addition and then incubated with olaparib for further 24 hours after the MMS exposure. In case of combined lucanthone (Selleckchem) and MMS treatment, cells were pre-treated with 4 μM lucanthone for 2 hours before 1-hour-long MMS treatment and incubated with lucanthone for further 24 hours. For O6-benzylguanine (O6-BG, Santa Cruz Biotechnology) combined with MMS treatment, cells were incubated with 10 μM O6-BG for 1 hour prior to MMS treatment, after which O6-BG was added to the fresh medium and left for the whole duration of the culture. All of the combined treatments with MMS and one of the above inhibitors were repeated three times within 48-hour-long intervals in experiments focusing on *keap1*Δ5F and *keap1*Δ8C cells. In experiments involving Rad51 inhibition, cells were incubated with a range of B02 (Sigma) concentrations for 48 hours.

Following 10-12 days of culture, cells were washed with PBS and fixed with cold (-20°C) methanol for 20 minutes at -20°C. Methanol was then removed and cells were incubated for 20 minutes at room temperature with 0.5 % crystal violet (Sigma Aldrich). After washing with water and drying, colonies larger than 50 cells were counted in each well and survival rate for various drug concentrations was calculated relative to the untreated condition.

2.3.8 Statistical analysis

Two-tailed Student's t-test and 2-way ANOVA were used to determine statistical significance.

3. Characterisation of KEAP1 as a novel MMS-tolerance factor

3.1 Introduction

3.1.1 Resolving base damage

Base lesions are the most frequent type of DNA damage and can result from various chemical modifications, such as oxidation, deamination, alkylation and hydrolysis (Bauer et al., 2015). Although less common than the other modifications, alkylation is the most mutagenic (Drabløs et al., 2004). Cells have developed numerous strategies for resolving base damage and can employ different pathways depending on the nature of the lesion. Alkylation resulting in O^6-methylguanine and O^4-methylthymine can be removed by MGMT through direct reversal repair (Mishina et al., 2008). Some alkyl modifications to the bases, as well as AP-sites, can be bypassed by polymerase kappa in translesion synthesis to enable continued replication (Stern et al., 2019). Base excision repair is the main pathway through which base damage of various nature is resolved and it involves multiple players (Krokan and Bjoras, 2013). MMS is a model methylating agent which largely gives rise to base damage recognised by BER, although it also induces base modifications that can be resolved by direct repair or replication-coupled repair (Chatterjee and Walker, 2017).

Despite our extensive knowledge of the major base damage repair pathways, much remains to be uncovered. One of the questions to be answered is how a specific base damage repair pathway is chosen. There are likely yet unidentified players involved which navigate the resolution of the lesion and steer it through one of the redundant pathways. For example, it is unclear what factors determine whether the DNA at the lesion is cleaved by a lyase or an endonuclease, and subsequently whether the base damage is resolved through the short patch or the long patch BER (Bauer et al., 2015). Although several distinct base damage repair pathways have been characterised, they do not function in isolation from one another. Interactions between the components of different pathways, known as pathway crosstalk, are crucial for the coordination of DNA damage repair (Limpose et al., 2017). These interactions are often dependent on and regulated by post-translational modifications (Limpose et al., 2017). While a number of base damage repair proteins have been shown to undergo post-translational modifications, such as the sumoylation of the G:T-mismatch glycosylase TDG, the biological significance of these modifications is often unknown (Limpose et al., 2017). Elucidating the complexity of the pathway crosstalk would provide us with a better understanding of how the repair of different types of base damage is regulated. Additionally, unknown alternative pathways might contribute to the base damage repair.

3.1.2 PARP1 and PARP2 act redundantly in BER but not in SSBR

The redundant nature of the PARP1 and PARP2 relationship was first implied by the observation that mice lacking *Parp1* and *Parp2* do not survive embryonic development (Menissier de Murcia, 2003). Moreover, the roles of PARP1 and PARP2 in recruiting XRCC1 to single-strand breaks have a certain degree of overlap (Hanzlikova et al., 2018). In line with the previous findings, recent work from our group has demonstrated that PARP1 and PARP2 have two related but independent roles in response to MMS-induced DNA damage - not only do PARP1 and PARP2 act redundantly in promoting strand ligation in BER, but they also stabilise replication forks at BER intermediates (Ronson et al., 2018). Interestingly, although PARP1 and PARP2 are redundant in resolving SSBs stemming from BER intermediates after MMS treatment, this redundancy was not observed in repair of SSBs of a different origin, that were induced directly by hydrogen peroxide (Ronson et al., 2018). This discrepancy in PARPs dynamic between resolution of two seemingly similar DNA lesions, hinted at an additional role of PARP1 and PARP2 that contributes to the repair of MMS-induced damage (Ronson et al., 2018). Research from our group has shown that PARP1 and PARP2 act redundantly stabilising Rad51 at stalled replication forks and preventing DSB formation as a result of collision with SSBs intermediates of BER (Ronson et al., 2018).

Taken together, these observations point to potential redundant roles of PARP1 and PARP2 in base damage tolerance pathways throughout the cell cycle. This, in turn,

raises the possibility that additional pathway or factors remain to be identified that promote tolerance to DNA base damage. The advent of genome-wide genetic screens using CRISPR/Cas9 provides an ideal mechanism to address this important question.

3.2 Aims

Research from our group has recently demonstrated that PARP1 and PARP2 act redundantly in BER, allowing cells to withstand the toxicity of the DNA alkylating agent methane methylsulfonate (MMS) (Ronson et al., 2018). We were interested to uncover novel players that might be involved in the BER pathway that could potentially interact with either PARP1 or PARP2 to resolve base damage. We employed genome-wide CRISPR-Cas9 dropout screen to look for genes conveying MMS tolerance. Among the top ten hits were several proteins already known to resolve base damage through direct reversal repair, translesion synthesis or base excision repair. However, we also identified a potential new role of KEAP1 in repair of MMS-induced damage. The aim of this chapter is to validate the hits of the CRISPR-Cas9 screen and verify KEAP1 as a novel MMS-tolerance factor.

3.3 Characterisation of novel genes required for tolerance to MMS

3.3.1 CRISPR genome-wide screen for genes whose absence sensitises cells to MMS

We set out to identify novel proteins that might play a role in base damage repair. With the help from the Target Discovery Institute at the University of Oxford, we conducted a pooled genome-wide CRISPR-Cas9 knock-out screen paired with MMS treatment (Figure 3.1 – Ronson and Jones, unpublished data).

Using single-guide RNAs (sgRNAs) to direct the Cas9 nuclease to a specific genomic sequence complementary to the 5' terminus of the sgRNA, CRISPR-Cas9 system enables precise genome editing in mammalian cells (Li et al., 2014; Ran et al., 2013). The double-strand break created at a specific site by Cas9 is then repaired by non-homologous end-joining (NHEJ), which introduces insertions and deletions (Ran et al., 2013). This often leads to a frameshift mutation and results in a gene knockout. The CRISPR-Cas9 technology can be used to knock out one or several genes, but has also been adapted as CRISPR-Cas9 lentiviral libraries, which together with high-throughput sequencing enables positive and negative selection genome-wide knockout screens (Li et al., 2014).

U2OS cells were transduced with a virus created using the Toronto KnockOut gRNA library v3 (TKOv3), which expresses Cas9 and 70,948 guides targeting 18,053 protein-coding genes (Hart et al., 2017). Following the transduction, cells were selected with 2 μg/ml puromycin for seven days to allow for incorporation of the lentiviral construct into the genome of the cell, which results in a stable expression of the sgRNAs. U2OS cells were then treated with 0.6 mM MMS for 1 hour to introduce base damage. After three days of recovery, samples were collected and processed using high-throughput DNA sequencing. MAGeCK pipeline was used to determine if there is a statistically significant decrease in abundance of each sgRNA in treated samples relative to control, quantified by a depletion score (Li et al., 2014). All 18,053 genes were ranked according to this metric, with the lowest scores in this drop-out screen corresponding to genes that are most likely to play a role in repair of MMS-induced damage (Figure 3.1).

Among the top ten hits were proteins known to be involved in base damage repair. The top hit was MGMT which removes the alkyl group from O^6-alkylguanine and O^4-alkylthymine in a sacrificial manner through direct reversal repair (Drabløs et al., 2004; Mishina et al., 2008). The translesion synthesis DNA polymerase kappa, which allows replication to bypass damage in the minor groove of DNA, including abasic sites, was identified as the third hit (Stern et al., 2019). Among the top ten hits were also proteins functioning in base excision repair, such as the AP-endonuclease APEX1 which cleaves the phosphodiester DNA backbone, generating a single-nucleotide gap; PARP1 which recognises the SSB and recruits other DNA repair factors to the lesion; the scaffold protein XRCC1 stabilising the DNA at the site of lesion; DNA

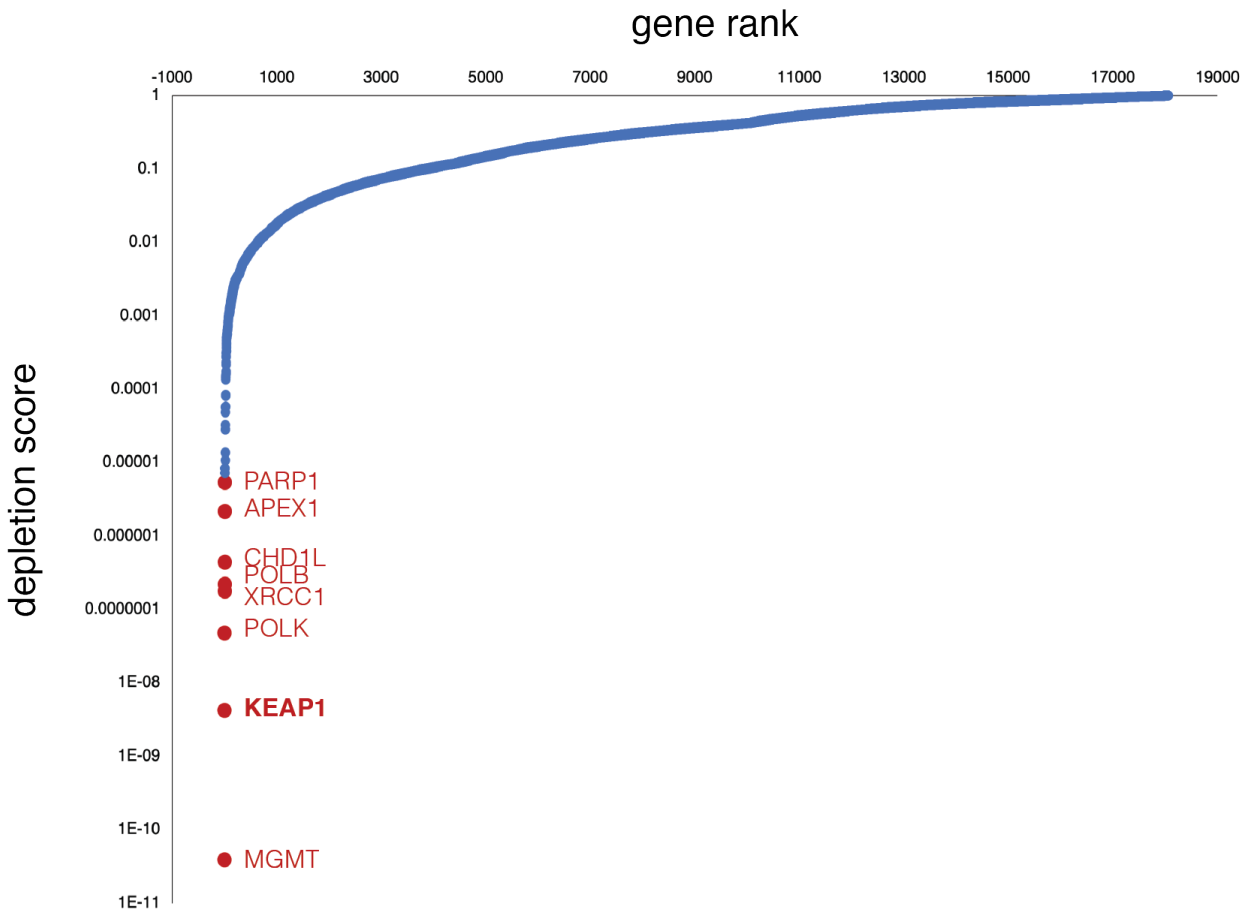

Figure 3.1 Genome-wide CRISPR-Cas9 loss-of-function screen identified genes whose inactivation could confer MMS sensitivity. U2OS cells were transduced with a TKOv3 human genome library and treated with MMS. Sequencing of the surviving cells and analysis yielded a list of genes whose absence resulted in dropout from the cell population. The second top hit is *KEAP1* (Ronson and Jones, unpublished data).

polymerase beta crucial for the gap-filling DNA synthesis; and the chromatin-remodelling DNA helicase ALC1 which makes the lesions accessible for the DNA damage repair machinery (Blessing et al., 2020; Kim and Wilson, 2012). The fact that these proteins are all involved in relevant DNA repair pathways serves as proof for the validity of the screen.

In addition to established SSBR proteins, as the second-ranking hit the screen also identified a novel gene, *KEAP1*, which is required for MMS tolerance (Figure 3.1). KEAP1 is a substrate adaptor for CUL3-RING ubiquitin E3 ligase, which plays an important role in oxidative stress response by regulating the proteasomal degradation of NRF2 (Kobayashi et al., 2004). KEAP1 uses a sophisticated cysteine sensor mechanism to detect various types of NRF2 inducers. KEAP1 has also been reported to block DNA repair by homologous recombination in the G1 phase by ubiquitylating PALB2 and preventing BRCA1 interaction (Suzuki et al., 2019; Orthwein et al., 2015). However, it has not been implicated in base damage repair. Given that KEAP1 was the second top hit of the screen and that it plays a role in homologous repair, we hypothesised that the protein might be involved in BER or an alternative base damage repair pathway.

3.3.2 KEAP1 depletion is not sufficient to reconstitute the MMS sensitivity observed in the CRISPR screen

In order to validate the findings of the CRISPR-Cas9 knockout screen, we set out to deplete KEAP1 in U2OS cells using siRNA. To establish conditions to deplete the expression of KEAP1 using siRNA, we selected two commercially available antibodies

against human KEAP1 (Abcam and Proteintech), which allowed us to detect KEAP1 by Western blotting (Figure 3.2). Accordingly, whole cell extract samples were collected at different time points after the siRNA transfection and analysed by Western blotting. KEAP1 has been reported to migrate as two protein bands in polyacrylamide gels (~76 kDa and 70 kDa). These represent the full-length KEAP1 isoform and its shorter isoform, most likely resulting from a post-translational proteolytic removal of a ~8 kDa polypeptide from the N-terminus (Qiu et al., 2018). Only one of the tested antibodies (Proteintech) recognised the two isoforms of KEAP1 (Figure 3.2 A). The expression of the two KEAP1 isoforms, as observed via Western blotting, was also lower in the samples transfected with siKEAP1 as compared to non-targeting siRNA 24 hours and 72 hours after the second transfection. However, 48 hours after transfection, expression of KEAP1 in the siKEAP1-trasfected cells increased to levels similar to those seen in control. Three different siRNA concentrations were tested and all of them were sufficient for KEAP1 knockdown (Figure 3.2A, top and bottom KEAP1 panels). Although there were considerable issues with the consistency of actin signal imaging, this experiment enabled us to assess the specificity of the tested antibodies and to define the conditions required for a successful KEAP1 depletion. Having established the conditions to deplete KEAP1, we wished to assess whether this sensitises cells to MMS. To achieve this, U2OS cells were transfected with siRNA targeting KEAP1 and treated with MMS for one hour, then cell viability was assessed in a colony survival assay. As previously described, *parp1*Δ cells are sensitive to MMS-induced damage (Ronson et al., 2018). However, no increase in MMS sensitivity was observed in KEAP1-depleted cells compared to control (Figure 3.3C). As demonstrated by

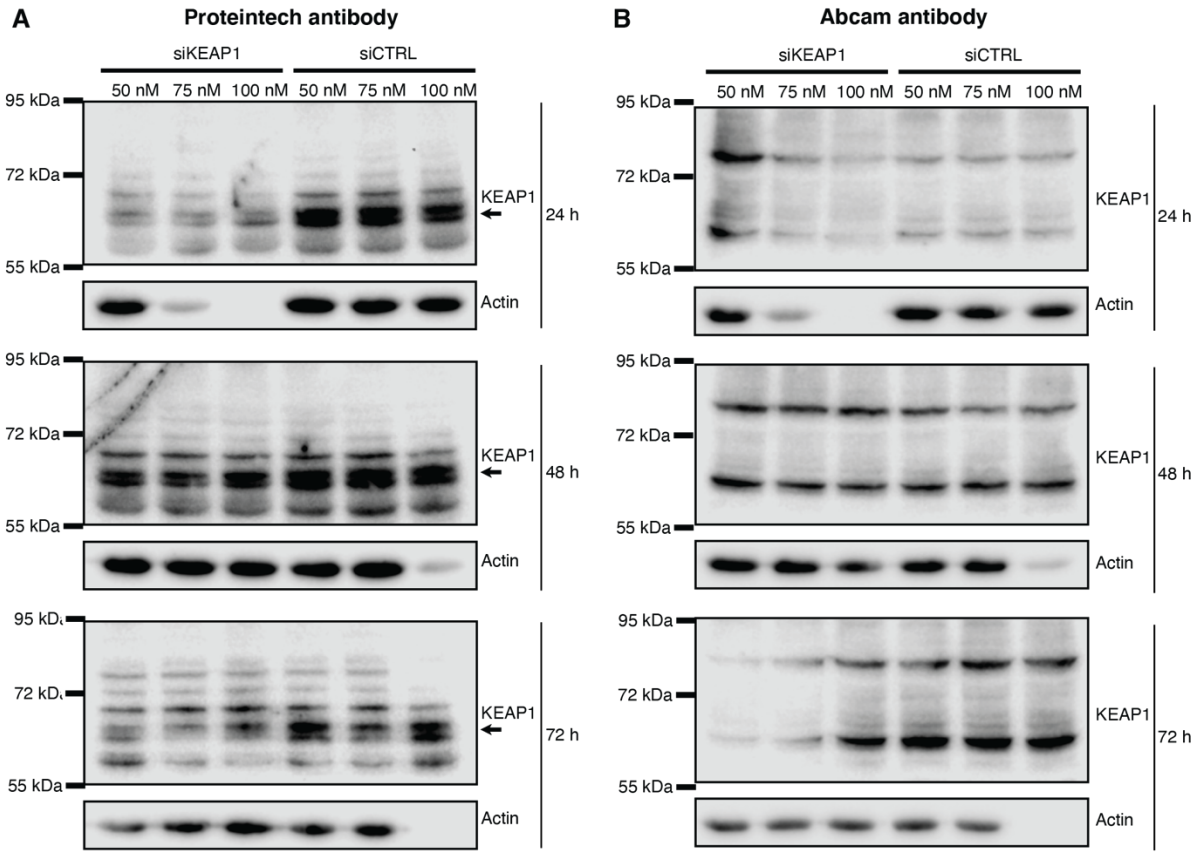

Figure 3.2 Optimisation of KEAP1 depletion and testing of KEAP1 antibodies. U2OS cells were transfected with different concentrations of siRNA (50 nM, 75 nM, 100 nM), either non-targeting (siCTRL) or targeting KEAP1 (siKEAP1). Transfection was repeated twice with a 24 hour incubation period. Whole cell extract samples were collected at 24, 48 and 72 hours after the second transfection and the efficiency of KEAP1 depletion was analysed by Western blotting. AT the same time, two commercial antibodies against KEAP1 were tested: **A.** Proteintech antibody and **B.** Abcam antibody.

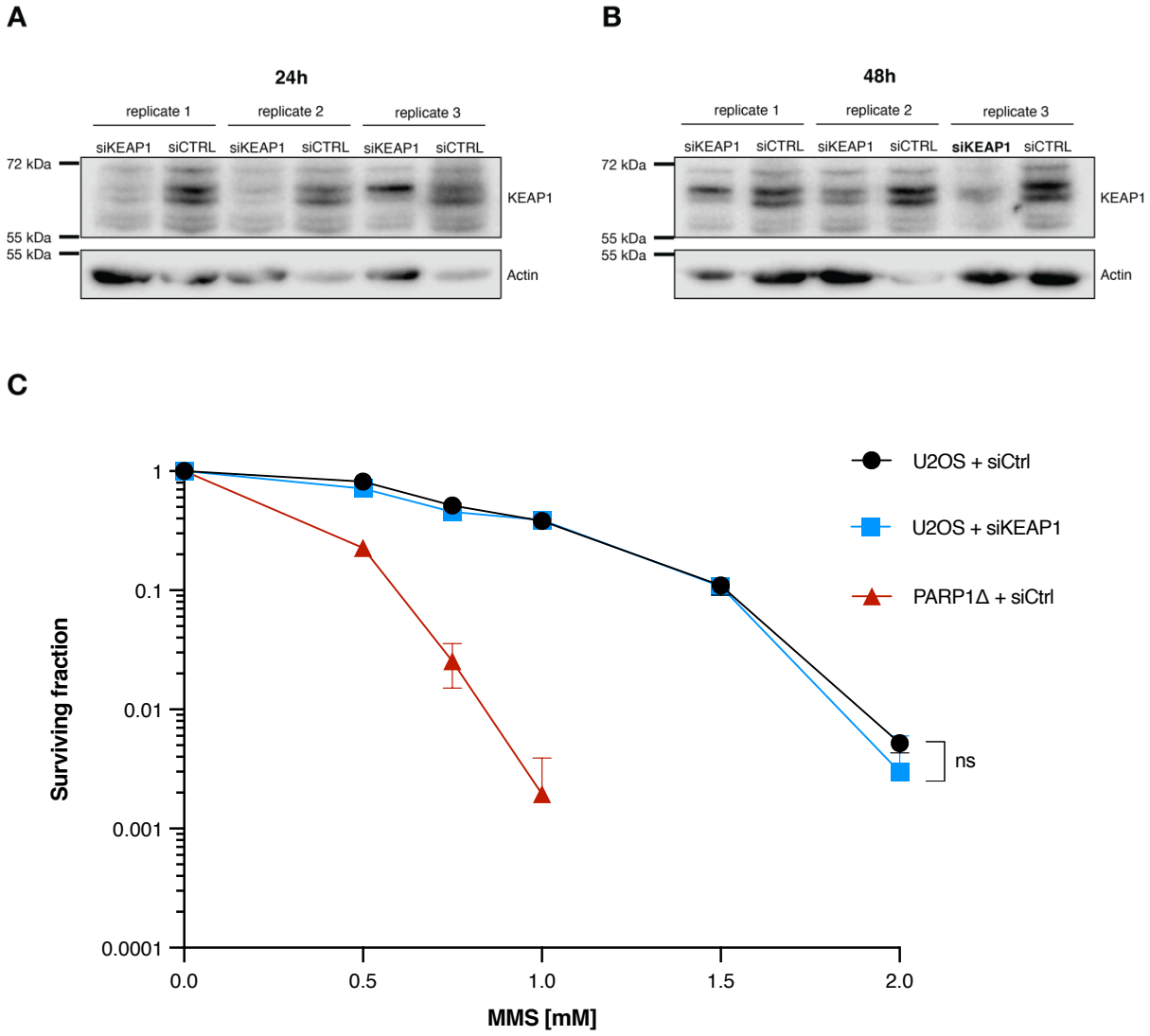

Figure 3.3 Depletion of KEAP1 is insufficient to sensitise cells to MMS. U2OS cells were transfected with 75 nM siRNA, either non-targeting (siCTRL) or targeting KEAP1 (siKEAP1). Transfection was repeated twice with a 24 hour incubation period. **A.** 24 hours after the second transfection, cells were seeded at low density with fresh medium and a whole cell extract sample was collected for analysis by Western blotting. **B.** Another whole cell extract sample for Western blotting was collected at 48 hours after the second transfection. **C.** 48 hours after the second transfection, cells were treated for 1 hour with MMS, washed twice with PBS, allowed to recover in fresh medium and cultured for 10-12 days to be assessed in a clonogenic survival assay. When surviving fraction equals 0, data points are not shown on the graph. Error bars indicate the standard error of three experimental replicates. Statistical significance tested with two-way ANOVA.

Western blotting, the KEAP1 depletion was not consistent across the three replicates. Moreover, we observe a relatively fast recovery of KEAP1 expression (48 hours after siRNA transfection), which might explain the lack of sensitivity to MMS in the colony survival assay (Figure 3.3 B). The presence of KEAP1, even when the expression levels are lower than in wild-type cells, seems to be sufficient to facilitate the repair of the DNA damage introduced by the alkylating agent MMS.

3.3.3 Generation of cell lines with disrupted KEAP1

3.3.3.1 Designing the KEAP1 knockout strategy and screening

In order to confirm whether KEAP1 plays a role in resolving damages to the DNA induced by MMS, we proceeded to test this hypothesis using KEAP1 deficient cells. Therefore, we employed CRISPR-Cas9 genome editing technology to disrupt *KEAP1* in U2OS and RPE-1 cells. KEAP1 is encoded by a 19,622 bp DNA sequence consisting of six exons and five introns (Figure 3.4, www.ncbi.nlm.nih.gov). Out of ten reported splicing variants of *KEAP1,* two give rise to the same full-length, 624-amino-acid-long KEAP1 isoform (www.uniprot.org). An alternatively spliced transcript variant missing the fourth and the fifth exons results in the expression of a 444-amino-acid-long KEAP1 isoform, which has been reported in the highly-metastatic human hepatoma cells and at low levels in several other cell lines (Kopacz et al., 2020; Qiu et al., 2018). Six other potential isoform sequences have been computationally mapped, although none of them have been reported to occur naturally (www.uniprot.org).

Initially, in collaboration with Joey Riepsaame from the Genome Engineering Oxford, we designed a strategy aiming at removing a splicing donor or acceptor site, as well as part of an early exon shared by all known isoforms. By not only removing a part of the first protein-coding exon, but also disrupting splicing, this approach would ensure that the protein would not be expressed in a truncated form, for example as a result of exon skipping (Mou et al., 2017).

Two sets of RNA guides (gRNAs) targeting either the intron or the exon boundaries of exon 2 were cloned into the pX459 vector. Vector pX459 contains two expression cassettes, one for a human codon-optimized Cas9 and one for the single gRNA, as well as ampicillin and puromycin resistance cassettes allowing for selection of bacteria and mammalian cell lines, respectively (Ran et al., 2013). U2OS cells were then transfected with one of the plasmid pairs and subsequently selected with puromycin for 24 hours, which should allow for enrichment of transfected cells in the population, while preventing the plasmid from being incorporated into the genome due to selection pressure. After recovering for 48 hours, cells were plated into 96-well plates using single cell FACS sorting to generate clonal lines. When the U2OS cells reached confluence, the clones were screened for mutations by PCR and Western blotting (data not shown). Surprisingly, we were not able to identify a single knockout cell line, despite having tested almost 400 clones. This could possibly be the result of low incision efficiency of the chosen gRNAs.

To address the possible issue of cutting efficiency, we modified our strategy to introduce the Cas9 cuts at the two extremities of the *KEAP1* gene and remove

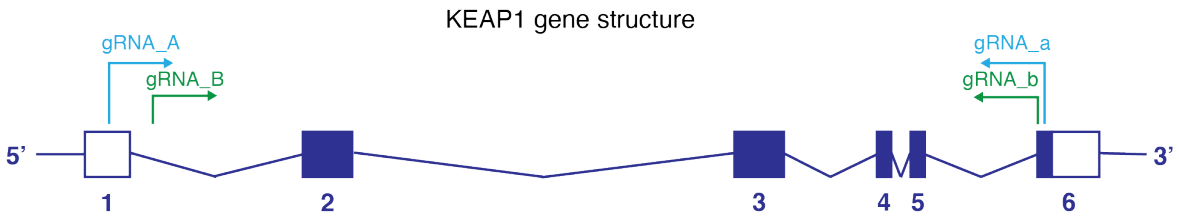

Figure 3.4 Designing the CRISPR-Cas9 knockout strategy. Gene structure of *KEAP1*. Rectangles symbolise exons, connecting lines symbolise introns. Coding sequence is marked as blue-filled rectangles. RNA guides were used in a combination of two pairs, each pair marked with a different colour.

almost the entire protein coding sequence (Figure 3.4). We designed two new pairs of gRNAs using the Desktop Genetics CRISPR Design Software DESKGEN (www.deskgen.com). The gRNAs were scored by the software and selected for the highest target specificity and lowest possibility of off-target activity genome-wide. We selected two pairs of RNA guides (pair gRNA_Aa and pair gRNA_Bb) (Figure 3.4) and cloned them into the pX459 vector as described earlier. Next, to test the hypothesis that *KEAP1* might be essential in U2OS, we transfected U2OS cells and RPE-1 cells in parallel with the two different pairs of guides, selected cells with puromycin for 24 hours and plated them as single cell clones in a 96-well plate using a FACS cell sorter. After the cells reached confluency, they were passaged. The remainder of the cells were transferred to a fresh 96-well plate and DNA extraction was performed in the plate, followed by a PCR screening for loss of *KEAP1* (Figure 3.5).

In the initial screen for gene disruption event, two PCR reactions were performed in parallel on DNA extracted from each sample. KEAP1 screening targeted the region of *KEAP1* that would be missing in a CRISPR/Cas9 edited cell. As a control for DNA extraction quality, another PCR reaction was performed in parallel, using primers targeting a region within *C16orf4* and previously tested in our laboratory under the same conditions (Figure 3.5). Based on the lack of PCR product, we were able to identify three clones of RPE-1 cells (5H, 5F, 8C) as potential candidates for a successful KEAP1 deletion (Figure 3.5). Interestingly, out of 392 U2OS cells plated after transfection and puromycin selection, only three survived and they still

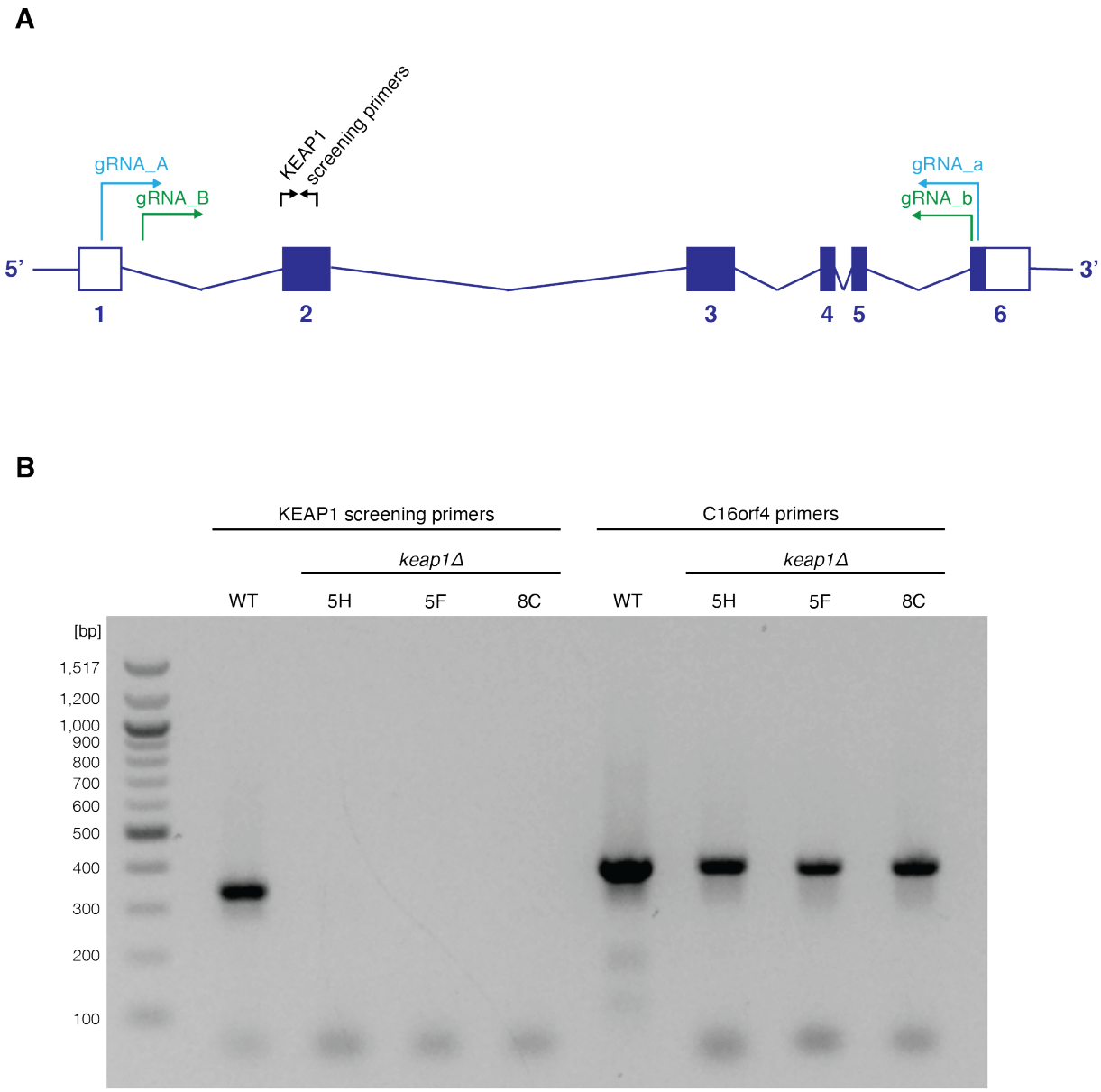

Figure 3.5 Screening for KEAP1 knockouts. PCR with primers targeting a region within the *KEAP1* gene was performed as an initial screen. Pictured are the three clones for which the PCR resulted in no product. As a positive control, PCR with primers targeting another gene was performed on the same matrix DNA.

expressed KEAP1, as tested by Western blotting (data not shown). All the figures describing generation of the knockout cell lines feature only RPE-1 cells. To verify whether the candidate clonal cell lines are true knockouts, the cell lines were expanded and DNA was extracted from a larger number of cells, using a more elaborate DNA extraction protocol which yields product of higher quality. Next, each of the clones was tested in PCR reactions using several different primer pairs (Figure 3.6 A, Figure 3.7 A). As predicted, the 'outside' primer pair gave rise to no product in the wild-type DNA, which was caused by the sequence between the primers being too long (nearly 18 kbp) to be amplified in a PCR reaction (Figure 3.6 B). PCR reaction using the same 'outside' primers resulted in DNA products for clones *keap1*Δ*5F* and *keap1*Δ*8C*, confirming that they lost the edited region of *KEAP1*. When using 'inside' primers, the opposite was true – the PCR reaction yielded no product in the *keap1*Δ*5F* and *keap1*Δ*8C* clones that were missing the targeted sequence, but did result in DNA amplification in the wild-type sample. Interestingly, *keap1*Δ*5H* exhibited a wild-type-like profile in both instances, suggesting it retained at least a large part of the gene.

To further verify the knockouts, we performed PCR reactions with primer pair A, B or a/b, flanking the respective individual Cas9 cut sites (Figure 3.7 A). In case of the edited *KEAP1* fragment being removed, one primer of each pair would not be able to anneal and start the DNA synthesis, which would result in no PCR product. This prediction was true for clones *keap1*Δ*5F* and *keap1*Δ*8C* (Figure 3.7 B). In clone *keap1*Δ*5H* however, the PCR reaction at both Cas9 cut sites resulted in DNA product which differed in size from that observed in the wild-type sample. Together with the

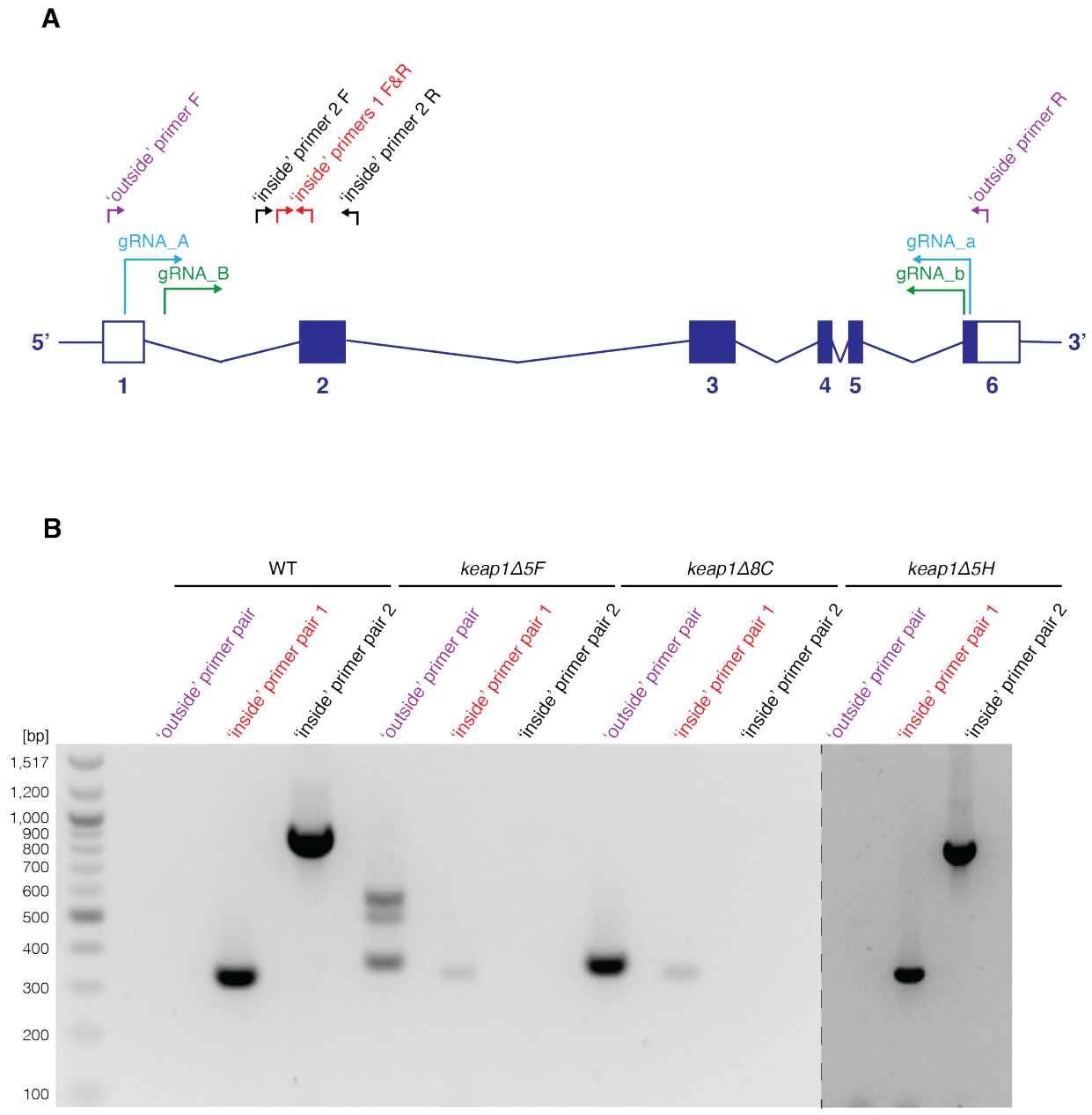

Figure 3.6 Verification of loss of *KEAP1* gene. A. PCR was performed using primers either targeting the portion of the *KEAP1* gene removed by CRISPR-Cas9, or flanking the region to be removed by CRISPR-Cas9, as shown in the schematic. F – forward; R – reverse. **B.** PCR products of different sizes were separated on an agarose gel and imaged. The dashed line indicates where images originating from two different agarose gels were joined.

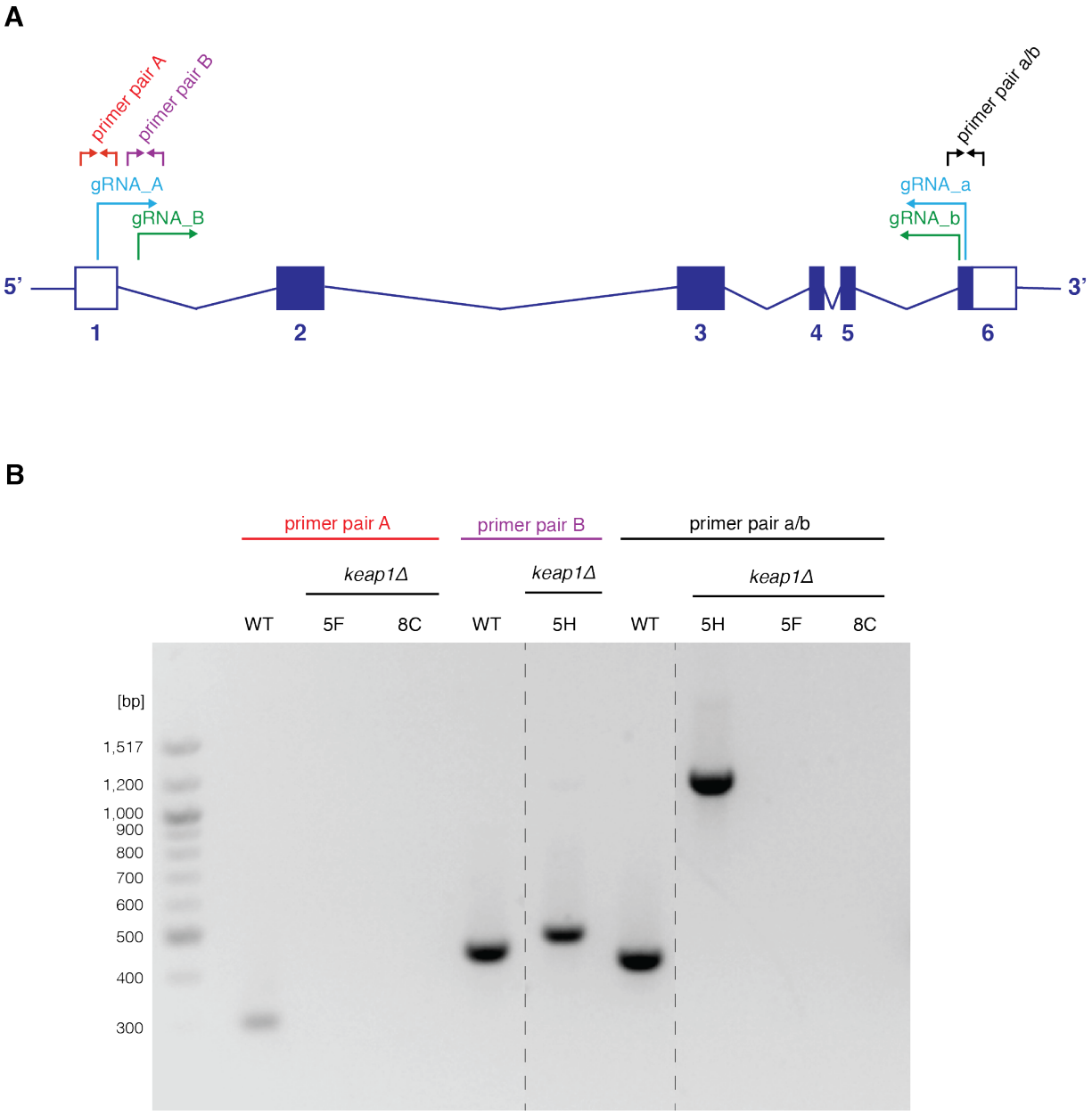

Figure 3.7 Verification of loss of *KEAP1* gene. A. PCR was performed using primers flanking the predicted Cas9 cut sites, as shown in the schematic. **B.** PCR products of different sizes were separated on an agarose gel and imaged. The presented image is a single agarose gel. The dashed lines indicate where the image was cropped and lanes with additional samples were removed for clarity.

fact that the 'inside' primers gave rise to a wild-type-like product (Figure 3.6), this suggests that while clone *keap1*Δ*5H* retained most of the *KEAP1* sequence, there are indels present at the sites targeted by Cas9. If the indels at the 5' terminus lead to a frameshift mutation, this would prevent the protein expression and result in a knockout.

In order to confirm the loss of *KEAP1* in clones *keap1*Δ*5F* and *keap1*Δ*8C,* and to understand the nature of indels in clone *keap1*Δ*5H,* Sanger sequencing was performed on the PCR products described above (Figure 3.8). In line with the PCR observations, sequencing data revealed that clones *keap1*Δ*5F* and *keap1*Δ*8C* lost nearly the entire protein-coding sequence of *KEAP1*, with small indels present at the cut sites targeted by Cas9 (Figure 3.8 A, refer to schematic in Figure 3.4). Interestingly, a 219 bp fragment from the wild-type *KEAP1* sequence was inserted in the opposite orientation in one of the *keap1*Δ*5F* alleles (
Figure 3.8 A). In clone *keap1*Δ*5H* the targeted gene sequence was retained, however there are indels present at both Cas9 cleavage sites (
Figure 3.8 B). At the 5' terminus, a 191 bp insertion and a 154 bp deletion were identified upstream of the cleavage site, which results is a frameshift mutation and, due to its location upstream of the coding sequence, prevents KEAP1 protein expression. At the 3' terminus of *KEAP1*, a 771 bp insertion and a 1 bp deletion are present downstream of the cleavage site. Moreover, Western blotting confirmed that the three described *keap1*Δ clones are true knockouts and do not express the KEAP1 protein (Figure 3.9).

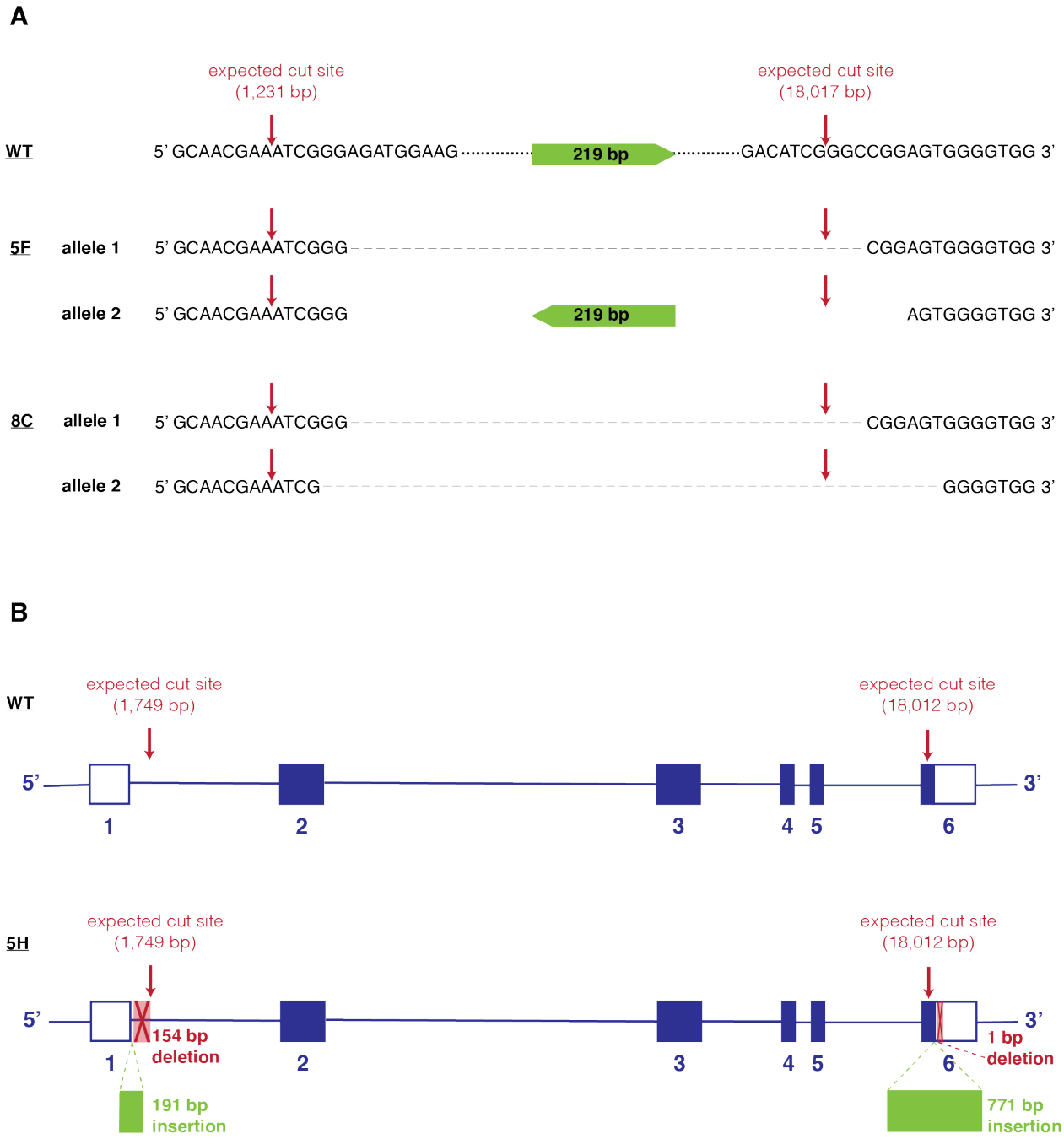

Figure 3.8 Verification of *keap1*Δ cell lines through sequencing. Sanger sequencing was performed on PCR products described earlier. **A.** Sequencing confirmed that a large portion (around 17.8 kbp) of *KEAP1* gene was deleted from the genome of clones *keap1*Δ*5F* and *keap1*Δ*8C.* Predicted Cas9 cut sites are marked with red arrows; dotted line symbolises the wild-type sequence not detailed in the schematic; the dashed line symbolises the deleted wild-type sequence; green box marks a 219 bp fragment of wild-type sequence inserted into one of *keap1*Δ*5F* alleles. **B.** Sequencing revealed that clone *keap1*Δ*5H* retained most of the wild-type sequence. However, there are insertions (green) and deletions (red) present at the Cas9 cut sites which cause a frameshift mutation. Clone *keap1*Δ*5H* does not display a different sequence that could be attributed to another allele, which suggests the sequence modification on both alleles is identical.

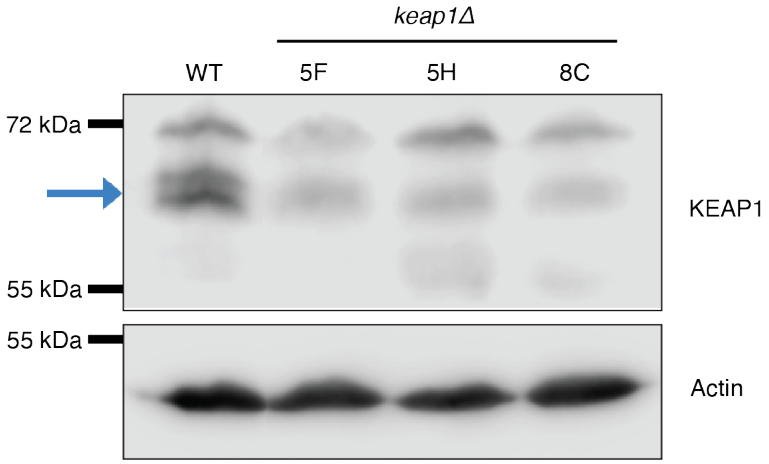

Figure 3.9 Verification of the *keap1*Δ cell lines on protein level. Whole cell extracts obtained from the three *keap1*Δ cell lines were tested for KEAP1 presence using Western blotting. The Proteintech anti-KEAP1 antibody (60027-1-Ig) was used to detect KEAP1 here and in all subsequent Western blotting data. The blue arrow indicated the double band of KEAP1.

3.3.3.2 Functional validation of keap1Δ cell lines – NRF2 stabilization

Perhaps the best understood role of KEAP1 is as the negative regulator of cellular levels of the antioxidant transcription factor NRF2 (Yamamoto et al., 1999). Under homeostatic conditions, KEAP1 acts as a substrate adaptor for the CUL3-based E3 ubiquitin ligase that ubiquitinates NRF2 and targets it for proteasomal degradation (Hayes at al., 2014). KEAP1 is inactivated by electrophilic NRF2 inducers modifying its highly reactive cysteine residues that prevent its interaction with NRF2 (Dinkova-Kostova et al. 2017). The disruption of the KEAP1-NRF2 interaction prevents NRF2 from being ubiquitinated and targeted for proteasomal degradation, leading to its accumulation in the cytoplasm (Dayalan Naidu et al., 2020). Having escaped degradation, NRF2 translocates to the nucleus, forms a heterodimer with a small musculoaponeurotic fibrosarcoma (sMAF) protein and binds to promoters containing antioxidant response elements (ARE), regulating the expression of over 250 genes (Dodson et al., 2019; Baird et al., 2020; Dayalan Naidu et al., 2020).

Depletion of KEAP1 using siRNA stabilises cellular NRF2 and causes its robust nuclear accumulation (Ashino et al., 2016). To validate *keap1*Δ cell lines, we tested whether they display elevated cellular levels of NRF2. Whole cell extracts and chromatin-enriched nuclear fractions were prepared from wild-type and *keap1*Δ cell lines and analysed for NRF2 levels using Western blotting. Both cellular and chromatin-bound NRF2 levels in all three *keap1*Δ cell lines were elevated (Figure 3.10), which results from a cellular shortage of KEAP1. Although it cannot be ruled out that a

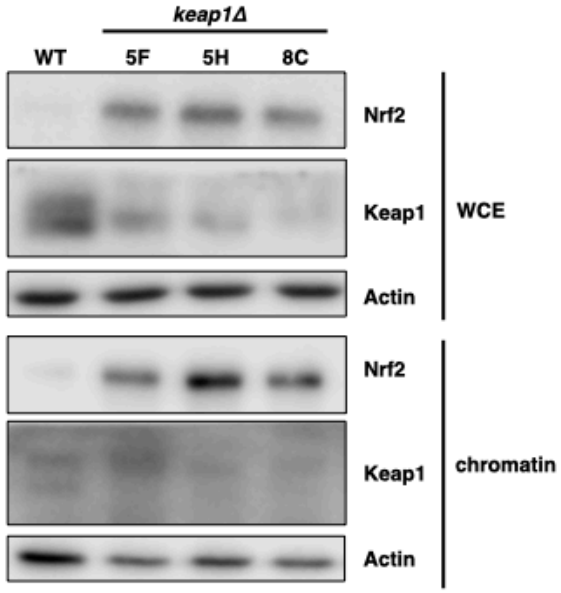

Figure 3.10 Loss of KEAP1 stabilises cellular levels of NRF2. Whole cell extracts and chromatin-enriched fraction samples were prepared from wild type RPE-1 cells and three *keap1*Δ cell lines. The samples were analysed by Western blotting with indicated antibodies.

heterozygous *KEAP1* knockout could also lead to elevated NRF2 levels due to haploinsufficiency, this data together with the sequencing results described in the previous section provide validation of the created *keap1*Δ clones.

3.3.3.3 RPE-1 keap1Δ cell lines show variable sensitivity to MMS

Having established several *keap1*Δ cell lines, we next tested the output of the gene disruption on the ability of cells to tolerate MMS. In order to achieve this, the three RPE-1 *keap1*Δ cell lines were treated with a range of MMS concentrations for 1 hour and cell survival was analysed in a clonogenic sensitivity assay (Figure 3.11). Wild type RPE-1 cells and *parp1*Δ U2OS cells were included in the experiment as a negative and positive control, respectively.

All three *keap1*Δ cell lines exhibit statistically significant sensitivity to MMS treatment, although the severity of phenotype differed between the clones (Figure 3.11). While clones *keap1*Δ*5F* and *keap1*Δ*8C* showed a milder sensitivity profile, *keap1*Δ*5H* was more affected by MMS. It is unclear why *keap1*Δ*5H* is more sensitive to MMS than *keap1*Δ*5F* and *keap1*Δ*8C*, although one possibility is that an additional mutation might be responsible for the higher MMS sensitivity of *keap1*Δ*5H.* Nevertheless, our data clearly point to a requirement for KEAP1 in cell tolerance of DNA base damage induced by MMS.

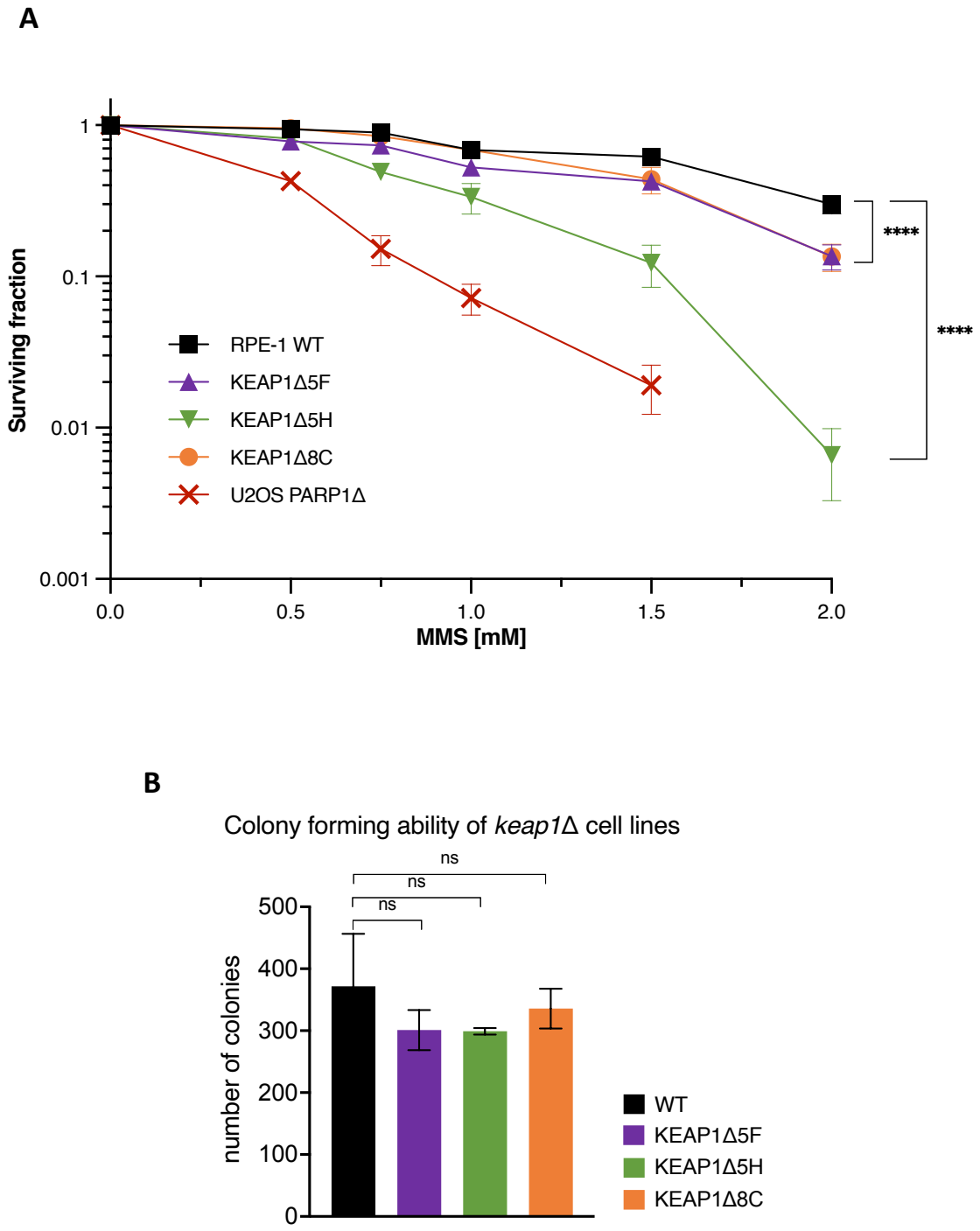

Figure 3.11 Loss of KEAP1 results in variable sensitivity to MMS. A. Wild type RPE-1 cells and three *keap1*Δ cell lines were seeded at low density and were treated for 1 hour with MMS on the next day, then washed twice with PBS, allowed to recover in fresh medium and cultured for 10-12 days to be assessed in a clonogenic survival assay. When surviving fraction equals 0, data points are not shown on the graph. Error bars indicate the standard error of three experimental replicates. Statistical significance was tested with two-way ANOVA. **B. Colony forming abilities vary slightly between the *keap1*Δ cell lines and the wild-type cells.** Number of colonies formed in the untreated condition was counted and the average for each cell line was plotted. Error bars indicate the standard error of three experimental replicates. Statistical significance was tested with Student's t-test.

Given the variability in phenotype achieved by knocking out *KEAP1,* we wished to confirm that the observed sensitivity to MMS is dependent on *KEAP1* gene by rescuing the phenotype by expression of recombinant KEAP1. KEAP1 cDNA sequence was cloned into a lentiviral vector and tagged on the N-terminus with FLAG-tag and HA-tag using the Gateway system (Figure 3.12 A). Each of the *keap1*Δ cell lines, as well as the wild-type parental cell line, were infected with either a lentiviral construct encoding a wild-type FLAG-HA-KEAP1 (+ KEAP1), or with an 'empty' construct (EV). A prolonged puromycin selection ensured that any cells that did not incorporate the construct into their genome were eliminated from the heterogenous cell population. Expression of the FLAG-HA-KEAP1 construct was then confirmed by Western blotting (Figure 3.12 B).

Next, we used the complemented cell lines and empty vector control cell lines to perform an MMS clonogenic sensitivity assay. As expected, expression of the wild-type KEAP1 rescued the phenotype of all three *keap1*Δ cell lines, but to various degrees (Figure 3.13, Figure 3.14). The milder phenotype profiles of *keap1*Δ*5F* and *keap1*Δ*8C* cell lines were fully rescued (Figure 3.14). However, the more severe phenotype of *keap1*Δ*5H* was only partially rescued by expression of recombinant KEAP1, further supporting the notion that an additional mutation, which contributes to MMS sensitivity, had occurred in this cell line (Figure 3.13). Nevertheless, the ability to reduce the sensitivity of clone *keap1*Δ*5H* to MMS by expression of KEAP1 confirms a requirement for this gene in MMS tolerance.

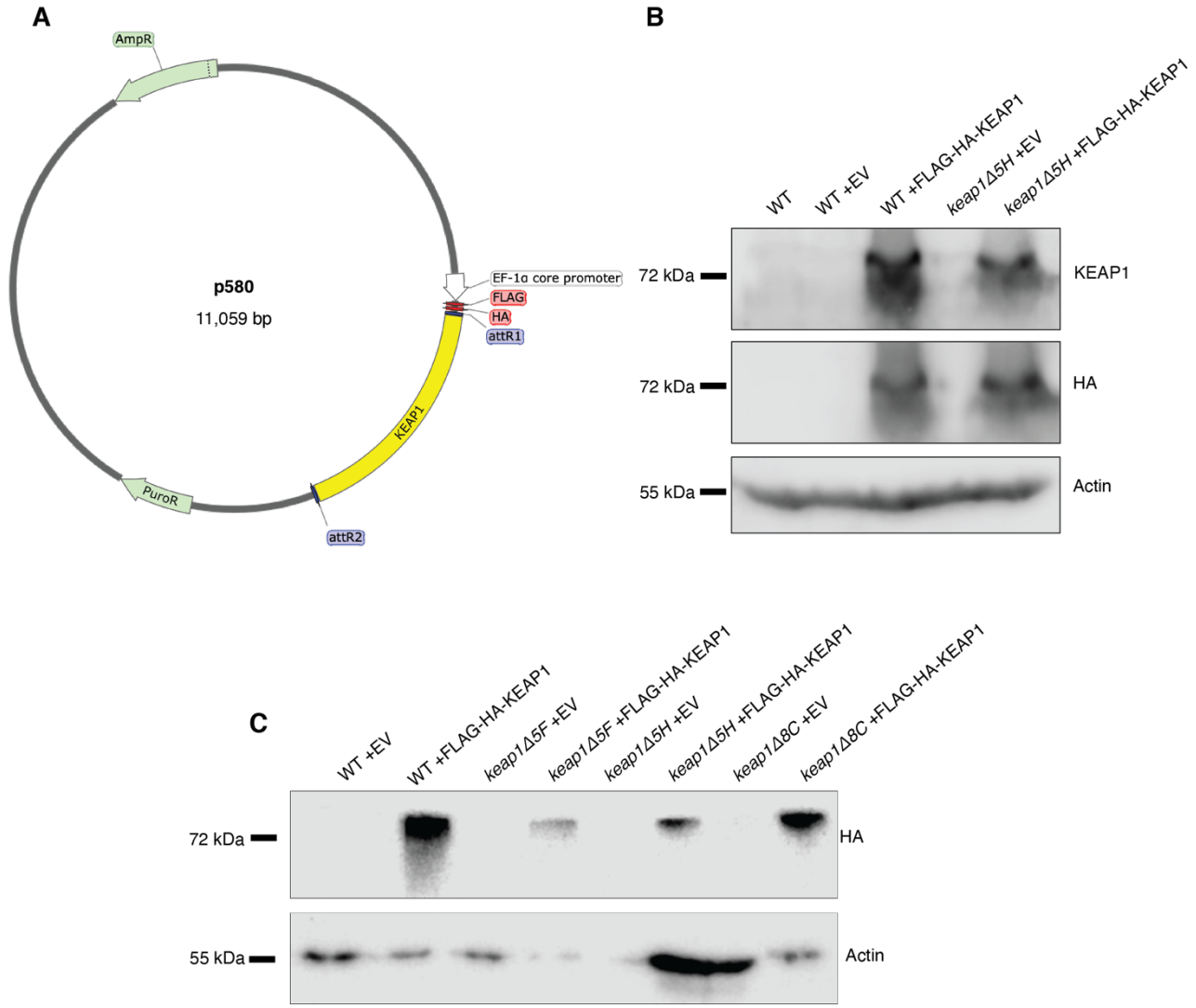

Figure 3.12 KEAP1 was re-expressed in *keap1*Δ cell lines. A. Wild-type KEAP1 cDNA was cloned into p580 vector and tagged with FLAG and HA tags on the N-terminus. **B, C.** Re-expression of exogenous FLAG-HA-KEAP1 in wild-type RPE-1 and in *keap1*Δ was confirmed by Western blotting.

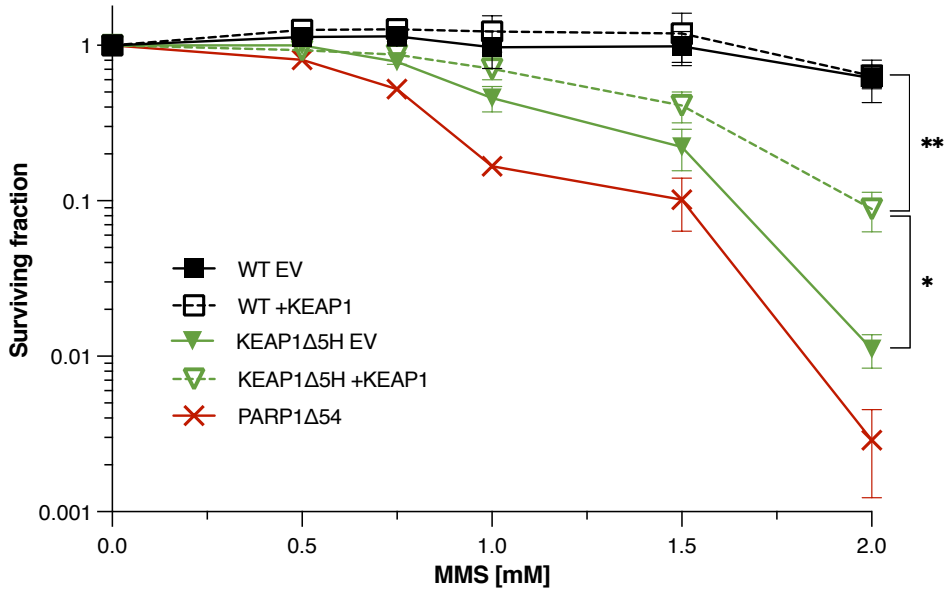

Figure 3.13 Re-expression of KEAP1 in *keap1Δ5H* partially rescues the mutant phenotype. Wild type RPE-1 cells and *keap1Δ5H* cells were transduced either with an empty vector or with vector expressing wild type KEAP1 and selected with puromycin. The established heterogenic cell lines were seeded at low density and treated for 1 hour with MMS on the next day, then washed twice with PBS, allowed to recover in fresh medium and cultured for 10-12 days to be assessed in a clonogenic survival assay. Error bars indicate the standard error of three experimental replicates. Statistical significance was tested with two-way ANOVA.

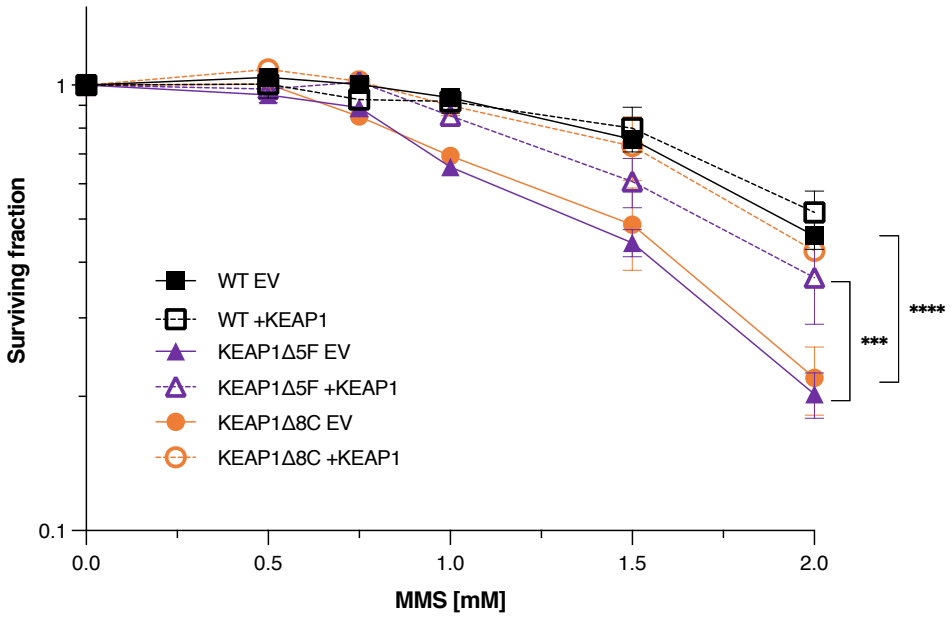

Figure 3.14 Re-expression of KEAP1 in *keap1Δ5F* and *keap1Δ8C* rescues the mutant phenotype. Wild type RPE-1 cells, *keap1Δ5F* and *keap1Δ8C* cells were transduced either with an empty vector or with vector expressing wild type KEAP1 and selected with puromycin. The established heterogenic cell lines were seeded at low density and treated for 1 hour with MMS on the next day, then washed twice with PBS, allowed to recover in fresh medium and cultured for 10-12 days to be assessed in a clonogenic survival assay. Error bars indicate the standard error of three experimental replicates. Statistical significance was tested with two-way ANOVA.

Although most studies report using one acute treatment to investigate MMS-induced damage, chronic low-dose treatment has been shown to result in a comparable cell sensitivity as measured by colony formation assay (Shiu et al., 2020). Moreover, a study in *Saccharomyces cerevisiae* described phenotypes for S-phase DNA damage checkpoint mutants that were only revealed by sublethal chronic MMS treatment (Murakami-Sekimata et al., 2010). The subtle, although significant sensitivity of *keap1*Δ cell lines to MMS prompted us to investigate whether an adjustment of the MMS treatment regime might exacerbate the observed phenotype. In particular, we wondered if repeated MMS treatments, resulting in accumulative base damage and increased mutational burden, would have a different effect on cells than one acute exposure.

Wild-type, *keap1⊿5F* and *keap1⊿8C* cells, either with re-expressed FLAG-HA-KEAP1 or with empty vector, were treated with a range of MMS concentrations. Cells were exposed to MMS three times at 0, 48 and 96 hours and each treatment lasted for 1 hour. Cell viability was assessed in a colony survival assay (Figure 3.15, Figure 3.16). The data shown in the two graphs originated from one dataset and is split in two figures for clarity. Repeated MMS doses increase the sensitivity of *keap1⊿5F* and *keap1⊿8C* cells, while allowing for this phenotype to be rescued by introduction of wild-type KEAP1 into the cell. This suggests that the role of KEAP1 in resolving base damage might be more prominent in the presence of severely accumulated mutations. Arguably, its novel role could be executed through base excision repair or an alternative base damage repair pathway.

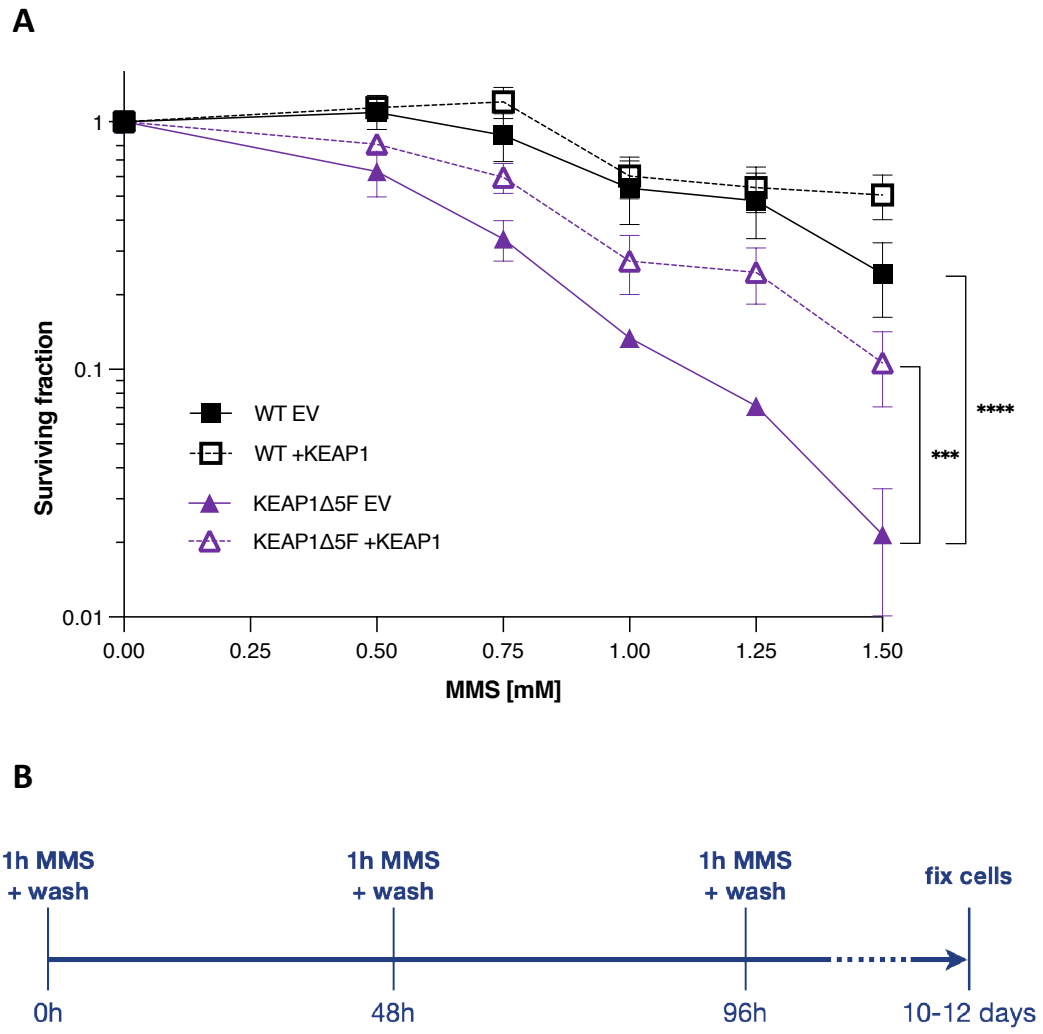

Figure 3.15 Exposure to chronic base damage exacerbates the phenotype observed in *keap1Δ5F*, while allowing its rescue by re-expression of KEAP1. Wild type RPE-1 cells and *keap1Δ5F* cells were transduced either with an empty vector or with vector expressing wild type KEAP1 and selected with puromycin. **A.** The established heterogenic cell lines were seeded at low density and treated for 1 hour with MMS on the next day, then washed twice with PBS and allowed to recover in fresh medium for 48 hours. The treatment was repeated two more times – 48 hours and 96 hours after the first treatment. The cells were cultured for a total of 10-12 days to be assessed in a clonogenic survival assay. Error bars indicate the standard error of three experimental replicates. Statistical significance was tested with two-way ANOVA. **B.** Schematic representation of the chronic MMS dosage strategy.

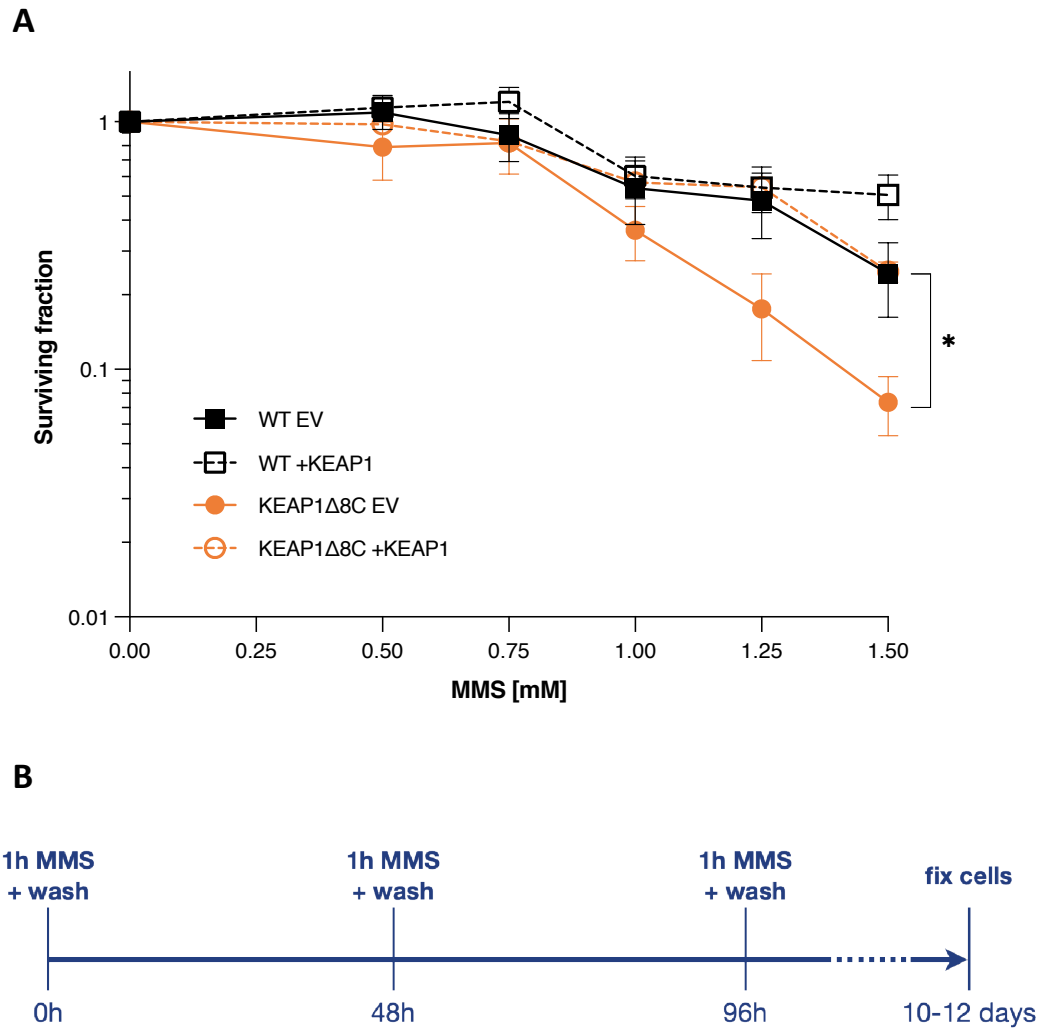

Figure 3.16 Exposure to chronic base damage exacerbates the phenotype observed in *keap1Δ8C*, while allowing its rescue by re-expression of KEAP1. Wild type RPE-1 cells and *keap1Δ8C* cells were transduced either with an empty vector or with vector expressing wild type KEAP1 and selected with puromycin. **A.** The established heterogenic cell lines were seeded at low density and treated for 1 hour with MMS on the next day, then washed twice with PBS and allowed to recover in fresh medium for 48 hours. The treatment was repeated two more times – 48 hours and 96 hours after the first treatment. The cells were cultured for a total of 10-12 days to be assessed in a clonogenic survival assay. Error bars indicate the standard error of three experimental replicates. Statistical significance was tested with two-way ANOVA. **B.** Schematic representation of the chronic MMS dosage strategy.

3.4 Discussion

In this chapter, we have described a genome-wide CRISPR-Cas9 knockout screen for genes that confer MMS tolerance. We were able to confirm the credibility of the screen by detecting, as high-ranking hits, several proteins known to be involved in tolerance to DNA base damage, including MGMT and components of the BER pathway (Figure 3.1). Most importantly, by identifying KEAP1 as the second-top hit in the screen, we uncovered a novel factor required for the cellular response to MMS-induced damage. Although it might be tempting to conclude that KEAP1 plays a role in BER, more research is needed to confirm that possibility and we will explore this in later chapters. KEAP1 could also act through another pathway which resolves base damage, such as direct reversal repair or replication-coupled repair (Cortez, 2019; Mishina et al., 2008). MMS produces a wide range of various types of damage, methylating not only DNA, but also RNA and protein (Kaufmann, 2015; Lee et al., 2007). It has been suggested that resistance to MMS could also rely on expression of proteins possessing the ability to degrade other proteins that were damaged by MMS-induced modifications (Burgis and Samson, 2007; Kaufmann, 2015). KEAP1 acts as a ubiquitin ligase in a complex with RBX1-CUL3, targeting its substrate proteins for degradation by 26S proteasome, so it would be possible for KEAP1 to play a similar role in MMS damage-induced response (Kobayashi et al., 2004). It is also possible that KEAP1 could be acting in some other pathway which resolves MMS-induced DNA damage.

We attempted to replicate the results of the screen by depleting KEAP1 in U2OS cells and testing the cell viability in response to MMS (Figure 3.2, Figure 3.3). Unfortunately, we were not able to confirm the findings of the CRISPR screen, as KEAP1-depleted cells did not display any greater sensitivity to MMS than wild-type cells. This could be explained by the difficulty of obtaining a true knockdown of KEAP1 in U2OS or maintaining the knockdown long enough for it to have an effect on colony survival assay (Figure 3.2). KEAP1 depletion seems to be ineffective especially at later time points (48 – 72 hours post-transfection), which coincides with MMS treatment. Incomplete KEAP1 depletion when encountering genotoxic stress could potentially still lead to sufficient response to MMS-induced damage, which would be observed as lack of sensitivity to the alkylating agent.

We successfully generated three independent RPE-1 *keap1*Δ cell lines and in all instances we were able to reconstitute the MMS sensitivity observed in the CRIPSR-Cas9 screen (Figure 3.11). This data serves as a validation of the screen and once again points to KEAP1 as a novel player in MMS-induced DNA damage response. Interestingly, there were differences in the severity of phenotype between the clones, with clones *keap1*Δ*5F* and *keap1*Δ8C being less sensitive than clone *keap1*Δ5H. However, this is not uncommon and one potential explanation could be clonal variation. Importantly, all of the *keap1*Δ cell lines had elevated cellular levels of NRF2, which is not directed for degradation in the absence of KEAP1 (Ashino et al., 2016). Moreover, the MMS sensitivity of *keap1*Δ5H was partially complemented, confirming that KEAP1 is required at least to some extent for MMS tolerance in this clone (Figure 3.13). The observed phenotype of increased MMS sensitivity of *keap1*Δ

cells was fully rescued by expression of FLAG-HA-KEAP1 in clones *keap1*Δ*5F* and *keap1*Δ8C (Figure 3.14). This data suggests a possible unknown mutation in clone *keap1*Δ5H that has an additive effect on MMS sensitivity. It would also explain why clone *keap1*Δ5H exhibits a stronger sensitivity to MMS treatment compared with the two other clones (Figure 3.11).

Although single, acute MMS treatment seems to be the gold standard in the field for investigating base damage (Fox and Fox, 1967; Lee et al., 2007; Ronson et al., 2018), some studies have reported encouraging results when opting for a chronic, lower dosage treatment (Murakami-Sekimata et al., 2010; Shiu et al., 2020). Differences in cell response to these two treatment regimens could reflect the differences in how cells process acute DNA damage versus accumulated, persistent mutations. These two situations could potentially activate different pathways or repair mechanisms. Interestingly, exposing *Saccharomyces cerevisiae* to chronic low doses of MMS revealed that mutations in S-phase checkpoint proteins result in increased reliance on translesion synthesis, while in the case of acute treatment the damage was resolved mostly through the BER pathway (Barbour et al., 2006; Murakami-Sekimata et al., 2010). Detangling the intricacies of the relationship between MMS dosage and cellular response could benefit us with a better understanding of the effect of environmental alkylating agents, such as those present in tobacco smoke (Drabløs et al., 2004). Moreover, since many important cancer drugs are alkylating agents, better comprehension of the repair processes they induce could improve the treatment available to patients and reduce the side effects (Middleton and Margison, 2003). In our observation, repeated MMS exposure increased the

sensitivity of clones *keap1*Δ5F and *keap1*Δ8C to the treatment, while allowing for a full phenotype rescue with expression of exogenous FLAG-HA-KEAP1 (Figure 3.15, Figure 3.16). This data suggests that repeated exposure to MMS increases the mutational burden and pressure on the DNA damage response system that KEAP1 acts through.

In this chapter, we identified and validated KEAP1 as a novel factor required for tolerance of MMS-induced DNA damage. In the following chapters we will explore its mechanism of action, pathway placement and relationship with PARPs in the context of MMS tolerance.

4. Understanding the KEAP1 mechanism of action in the context of MMS-induced damage

4.1 Introduction

4.1.1 KEAP1 interacts with CUL3 to form an E3 ubiquitin ligase complex

Cullin-RING ligases (CRLs) are a superfamily of highly conserved multimeric ubiquitin ligases (E3s) consisting of a scaffolding cullin protein, a catalytic subunit RING protein (RBX1 or RBX2), an adaptor and a substrate-recognising protein (Genschik et al., 2013; Sun et al., 2020). The subfamily of CRL3 contains Cullin-3 (CUL3), the RING protein RBX1 and a BTB domain protein which acts both as a substrate receptor and an adaptor (Pintard et al., 2003; Xu et al., 2003). One of the substrate adaptor proteins that form an E3 complex with CUL3-RBX1 is KEAP1 (Taguchi et al., 2011).

CUL3 is highly conserved and present in all eukaryotes. As part of CRL3 complex, CUL3 plays an important role in the regulation of various stress, developmental and cellular responses by facilitating ubiquitylation of substrate proteins, targeting them for proteasomal degradation (Genschik et al., 2013). Upon binding of the N-terminal domain of CUL3 to the BTB domain of the substrate adaptor KEAP1 and the formation of a E3 ubiquitin ligase complex with RBX1, the transcription factor NRF2

becomes ubiquitylated and is destined for proteasomal degradation (Cullinan et al., 2004; Dayalan Naidu and Dinkova-Kostova, 2020; Kobayashi et al., 2004). To date, all known cellular functions of KEAP1 are carried out as part of the CUL3-based ubiquitin ligase complex, suggesting this might also be true for any novel roles of KEAP1.

4.1.2 KEAP1 domains and their functions

KEAP1 functions as a substrate adaptor in the KEAP1-CUL3-RBX1 E3 ubiquitin ligase, recognising and positioning the substate to enable the transfer of ubiquitin onto the target protein (Dinkova-Kostova et al., 2017). Constituting an interface for protein-protein interactions, it contains binding sequences for its partners and targets. KEAP1 contains three functional domains: N-terminal BTB domain, intervening region (IVR) and C-terminal Kelch domain, which are described in detail in section 1.5 (Itoh et al., 1999). As all members of BTB-Kelch protein family, KEAP1 binds to CUL3 through its BTB domain, which is required for this interaction (Dayalan Naidu and Dinkova-Kostova, 2020; Furukawa and Xiong, 2005). A truncated KEAP1 lacking the BTB domain is unable to bind to CUL3, which prevents the assembly of the KEAP1-CUL3-RBX1 ligase and results in accumulation of NRF2 that is not targeted for degradation (Furukawa and Xiong, 2005; Kobayashi et al., 2004). Similarly, CUL3 binding can be abolished by introducing a triple alanine substitution mutations (V123A, I125A, G127A) in the third β-sheet and a double alanine substitution (M161A, G127A) in the fourth α-helix of KEAP1 (Furukawa and Xiong, 2005). These residues correspond with the regions of an adaptor protein SKP1 that directly interact with CUL1 and are thought to be the platform for KEAP1-CUL3 interaction

(Furukawa and Xiong, 2005). Importantly, the 3-box sequence at the N-terminal end of the IVR is also required for KEAP1 binding to CUL3 (Canning et al., 2013). In addition to mediating the CUL3 interaction, the BTB domain is also necessary for KEAP1 homodimerisation (Zipper and Mulcahy, 2002). Specifically, S104 within the BTB domain seems to play a crucial role, as its mutation to an alanine disrupts homodimerisation and leads to nuclear NRF2 accumulation (Dayalan Naidu and Dinkova-Kostova, 2020; Zipper and Mulcahy, 2002). The N-terminal Kelch domain is required for substrate binding and allows the KEAP1 homodimer to bind to ETGE and DLG motifs of NRF2 (Dinkova-Kostova et al., 2017). Binding to NRF2 through the Kelch domain is independent of other elements of the E3-ligase complex (Furukawa and Xiong, 2005). The Kelch domain is also necessary for the interaction of KEAP1 with PALB2 through its ETGE motif to suppress HR in G1 cells (Ma et al., 2012; Orthwein et al., 2015).

Although our knowledge about the functional significance of specific mutations within the KEAP1 domains has been advancing, there are still areas that need to be explored. For example, the regions responsible for KEAP1 homodimerisation and for binding CUL3 are partially overlapping, making it challenging to separate those functions. To date, the structures of the IVR domain or the complete KEAP1-CUL3-RBX1 complex have not been solved, leaving room for speculation about the exact spatial organisation and residue interactions within the complex. In the context of KEAP1-dependent MMS tolerance we observed, it would be interesting to understand which domains are crucial for this new role. Understanding the domain requirement in this context could clarify whether KEAP1 acts as an E3 ligase in

complex with CUL3 to confer MMS tolerance or if its ability to bind to a substrate through Kelch domain is necessary for this function.

4.1.3 The cysteine-based stress sensing system of KEAP1

The cysteine stress sensor system is central to the role of KEAP1 as NRF2 regulator (Dayalan Naidu and Dinkova-Kostova, 2020). It allows KEAP1 to recognise and respond to various NRF2 inducers through its highly reactive thiol groups, which can be modified by oxidants and electrophiles (Dinkova-Kostova et al., 2017). Among the 27 cysteines in the human KEAP1, there are differences in the reactivity and in the response to different types of inducers (Dayalan Naidu and Dinkova-Kostova, 2020). Observed redundancy in response to those inducers between certain cysteine residues, such as any combination of Cys226, Cys613 and Cys622/Cys624 in mouse KEAP1 forming a disulfide bond when exposed to H_2O_2, make it a challenge to untangle this sophisticated sensor network (Suzuki et al., 2019).

In a recent study, Suzuki and colleagues generated a mouse KEAP1 mutant lacking 11 cysteine residues, which made it unresponsive to most of NRF2 inducers, but still able to target NRF2 for ubiquitination and degradation (Suzuki et al., 2019). Importantly, in the generation of this mutant any cysteine substitutions that resulted in either an inability to bind CUL3 or that interfered with the ability to ubiquitylate NRF2 under basal conditions were identified and excluded (Suzuki et al., 2019). The resulting KEAP1$^{11Cys\text{-}less}$ mutant constitutes a promising model for testing whether a specific compound reacts with some of the most reactive cysteine residues of KEAP1

(Suzuki et al., 2019). We therefore hypothesise that the cysteine sensor might play an important part in the mechanism through which KEAP1 recognises and responds to MMS-induced damage. A reactive cysteine is also a characteristic of MGMT, the 'suicide' enzyme repairing alkylation base damage through direct reversal. MGMT removes the alkyl adduct from the modified oxygen molecule of O^6-meG or O^4-meT and transfers it to its Cys145 residue, becoming inactive (Gutierrez and O'Connor, 2021). It is tempting to speculate that the reactive cysteine residues of KEAP1 could accept alkyl groups from damaged bases in a similar mechanism.

4.2 Aims

Our data from the CRISPR-Cas9 screen point to KEAP1 as a novel factor in conferring tolerance to MMS-induced damage. We confirmed this finding by a series of clonogenic sensitivity assay analyses of KEAP1-deficient cells. In this chapter, we will aim to understand the mechanism responsible for the KEAP1-dependant tolerance of MMS-induced DNA damage.

Given the role of KEAP1 as the substrate adaptor in the E3 ubiquitin ligase complex it forms with CUL3 and RBX1, we hypothesise that KEAP1 might also act as a CUL3-based ubiquitin ligase to confer the MMS tolerance. Therefore, loss of CUL3 should lead to MMS-sensitivity, similar to KEAP1-deficiency. We will test the requirement for CUL3 for the repair of alkylation damage by siRNA-mediated CUL3 depletion and subsequent assessment of the effect this has on the cell sensitivity to MMS. Next, we will aim to understand the domain requirement of KEAP1 for its role in MMS-

induced damage repair, which might inform possible mechanism of its action. We will address this question by creation of domain mutants and testing their ability to confer MMS tolerance. KEAP1 is a cysteine-rich protein which recognises NRF2 inducers through its reactive cysteine residues. We hypothesise that these reactive residues might facilitate the recognition and possibly removal of alkyl groups from modified DNA bases, analogously to MGMT-mediated direct repair. We aim to assess this possibility by generating a KEAP1 mutant with 11 of its reactive cysteines inactivated, and examining its ability to rescue the MMS-sensitivity phenotype in *keap1*Δ cells.

4.3 KEAP1 interaction with CUL3 in the context of MMS sensitivity

The dependence of KEAP1 on binding CUL3 to form a functional E3 ligase prompted us to hypothesise that CUL3 depletion might sensitise cells to MMS in the same way that loss of KEAP1 did in the CRISPR-Cas9 screen (Chapter 3, Figure 3.1). To address this question, we set out to deplete CUL3 in U2OS cells and assess their viability in response to MMS treatment through a colony forming assay.

Initially, we optimised the conditions for CUL3 depletion using siRNA transfection in U2OS cells. Cells were transfected with three different concentrations of siCUL3 and whole cell extract samples were collected 24, 48 and 72 hours after the addition of

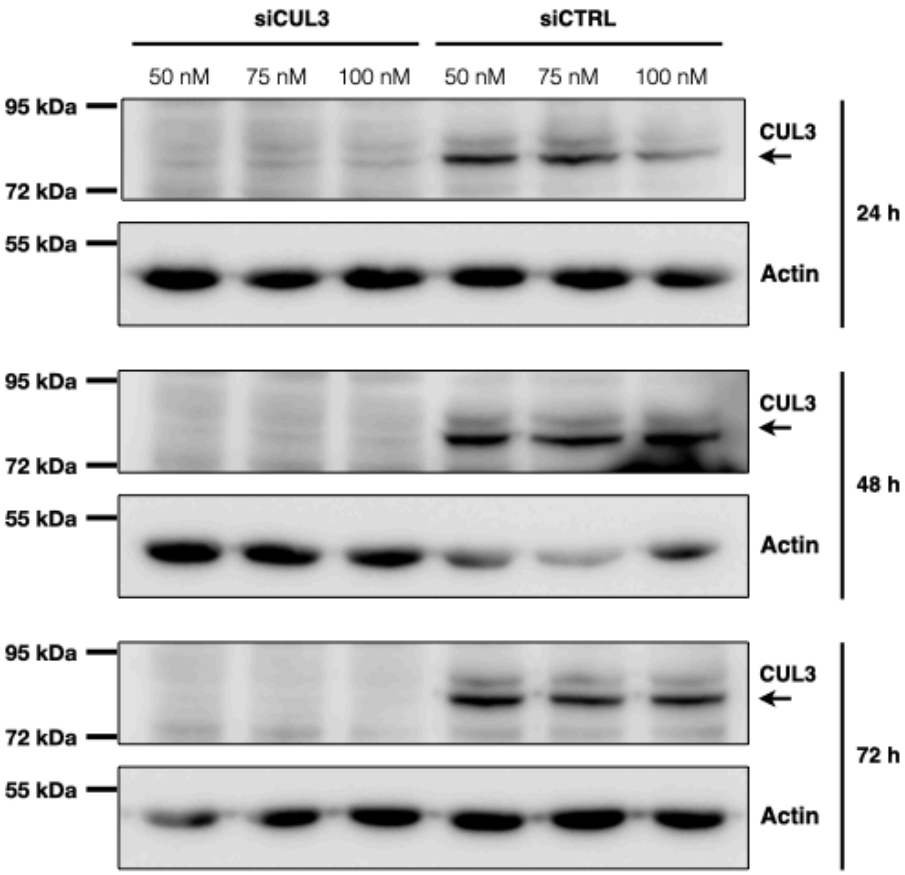

Figure 4.1 Optimisation of CUL3 depletion. U2OS cells were transfected with different concentrations (50 nM, 75 nM, 100 nM) of siRNA, either non-targeting (siCTRL) or targeting CUL3 (siCUL3). Transfection was repeated twice with a 24-hour-long incubation period. Whole cell extract samples for analysis by Western blotting were collected at 24 hours, 48 hours and 72 hours after the second transfection.

siRNA to the media. Depletion of CUL3 is stable and robust under all tested conditions, as shown by Western blotting (Figure 4.1).

Having established conditions to effectively deplete CUL3, U2OS cells transfected with 50 nM siCUL3 were seeded at low density and treated with MMS for 1 hour. After 10-12 days of culture, cell viability in response to MMS was assessed in a colony-forming assay (Figure 4.2). Compared to control, CUL3-depleted U2OS cells are more sensitive to MMS-induced DNA damage, suggesting that CUL3 is involved in the resolution of base damage. KEAP1 functions as part of an E3 complex with CUL3-RBX1, hence depletion of CUL3 would impede the formation of the complex and disrupt the KEAP1 function (Canning et al., 2015). This data, together with our previous results, suggests that KEAP1 and CUL3 might be acting together in repair of alkylation base damage. However, to verify this hypothesis, further experiments are required, including epistatic analysis of the relationship between KEAP1 and CUL3 in the context of MMS exposure.

The *keap1*Δ cell lines we created are based on RPE-1 cell line, hence we chose to replicate the experiment testing the effect of CUL3 depletion MMS sensitivity in this cell line. The same transfection and MMS treatment conditions were used as those previously applied to U2OS cells. After 10-12 days of culture, cell viability in response to MMS was assessed in a colony-forming assay. However, we did not observe increased sensitivity to MMS in siCUL3-transfected RPE-1 cells (Figure 4.3 A). This

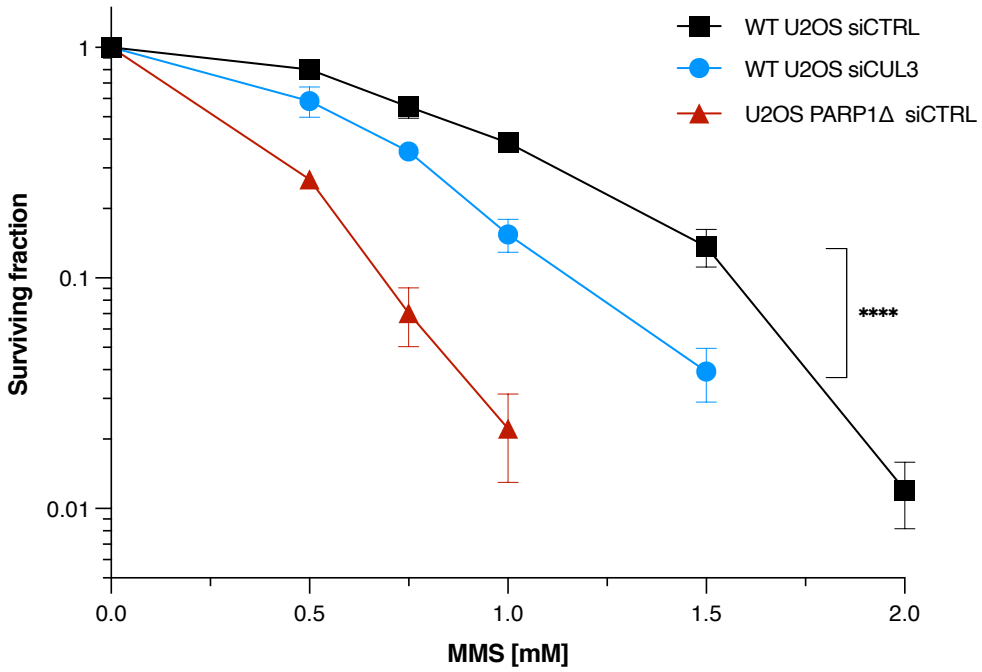

Figure 4.2 Depletion of CUL3 sensitises U2OS cells to MMS. U2OS cells were transfected with 50 nM siRNA, either non-targeting (siCTRL) or targeting CUL3 (siCUL3). Transfection was repeated twice with a 24 hour incubation period. 24 hours after the second transfection, cells were seeded at low density**.** The following day, they were treated for 1 hour with MMS, washed twice with PBS, allowed to recover in fresh medium and cultured for 10-12 days to be assessed in a clonogenic survival assay. When surviving fraction equals 0, data points are not shown on the graph. Error bars indicate the standard error of three experimental replicates. Statistical significance was tested with two-way ANOVA.

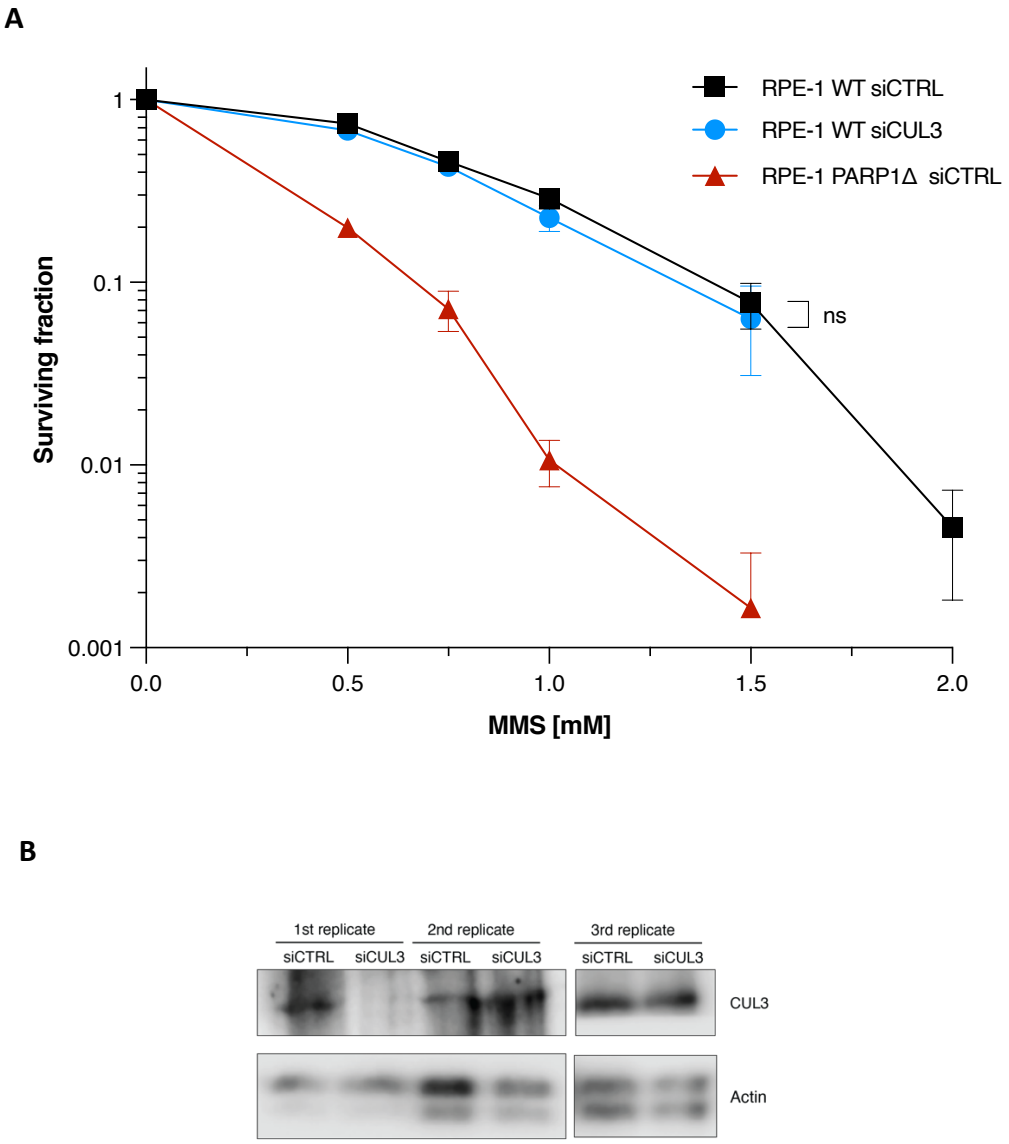

Figure 4.3 Depletion of CUL3 in RPE-1 cells is insufficient to sensitise cells to MMS. RPE-1 cells were transfected with 50 nM siRNA, either non-targeting (siCTRL) or targeting CUL3 (siCUL3). Transfection was repeated twice with a 24 hour incubation period. **A.** 24 hours after the second transfection, cells were seeded at low density**.** The following day, they were treated for 1 hour with MMS, washed twice with PBS, allowed to recover in fresh medium and cultured for 10-12 days to be assessed in a clonogenic survival assay. When surviving fraction equals 0, data points are not shown on the graph. Error bars indicate the standard error of three experimental replicates. Statistical significance was tested with two-way ANOVA. **B.** At the time of treatment, whole cell extract samples were collected and later analysed by Western blotting.

could be explained by the inefficacy of CUL3 depletion in that cell line, as shown by Western blotting (Figure 4.3 B).

4.4 Generation of KEAP1 mutants: a mutated cysteine stress sensor and three domain mutants

KEAP1 interacts with its substrates, such as NRF2, and with CUL3 through its binding domains. The cysteine sensor enables KEAP1 to recognise and respond to NRF2 inducers (Suzuki et al., 2019). We wished to further investigate the requirement for the KEAP1 domains and its cysteine sensor in response to MMS-induced base damage. To be able to explore the mechanism behind the KEAP1-dependent MMS tolerance, we generated constructs of mutant KEAP1 and expressed them in the *keap1*Δ5F and *keap1*Δ8C cell lines (Figure 4.4, Figure 4.5).

To address the question of domain requirement, we deleted the N-terminal BTB domain (1-179 amino acid residues) responsible for KEAP1 homodimerisation and binding to CUL3, and the Kelch domain (315-624 amino acid residues) responsible for substrate binding, creating KEAP1$^{\Delta BTB}$ and KEAP1$^{\Delta KELCH}$, respectively (Figure 4.4; Baird and Yamamoto, 2020; Furukawa and Xiong, 2005; Zipper and Mulcahy, 2002). Additionally, we targeted the amino acid residues within the BTB domain that are analogous to the residues in another BTB-domain protein, SKP1, directly interacting with CUL1 (Furukawa and Xiong, 2005). This 5 amino acid substitution (Val123Ala, Ile125Ala, Gly127Ala, Met161Ala, Tyr162Ala), reported under the name S3H4, has

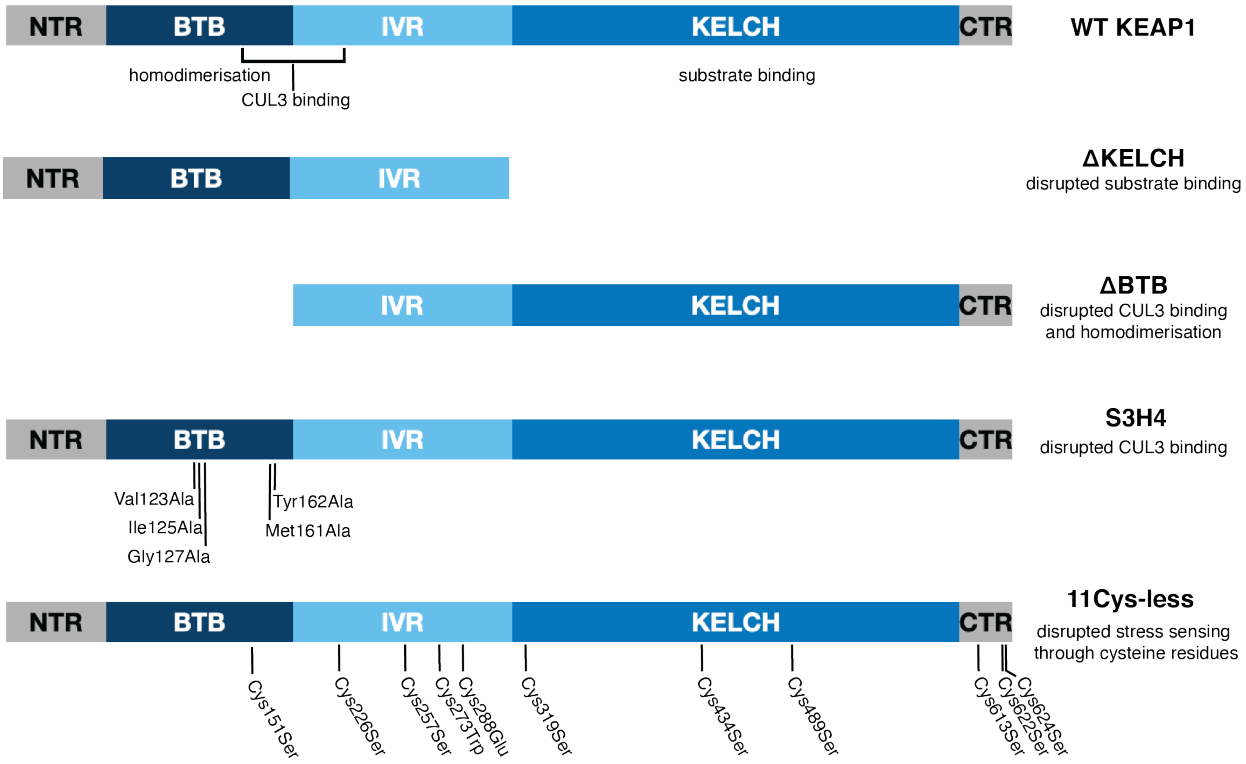

Figure 4.4 Schematic of KEAP1 mutants with truncation or amino acid substitution within the BTB and Kelch domain, and the KEAP1 11Cys-less mutant. Introduced amino acid substitutions have been marked. NTR – N-terminal region; BTB – Broad-Complex, Tramtrack and Bric a brac domain; IVR – intervening region; KELCH – Kelch domain; CTR – C-terminal region.**.** Schematic domain structure of wild-type KEAP1 compared with introduced mutations. NTR – N-terminal region; BTB – Broad-Complex, Tramtrack and Bric a brac domain; IVR – intervening region; KELCH – Kelch domain; CTR – C-terminal region.

been shown to disrupt the ability of KEAP1 to bind CUL3 (Figure 1.10; Furukawa and Xiong, 2005).

To test whether the cysteine sensor system of KEAP1 could play a role in the response to MMS-induced damage, we generated a human KEAP1 construct with 11 mutated cysteines, as has been previously tested in a mouse model (Figure 4.4; Suzuki et al., 2019). These 11 residue substitutions (Cys151Ser, Cys226Ser, Cys257Ser, Cys273Trp, Cys288Glu, Cys319Ser, Cys434Ser, Cys489Ser, Cys613Ser, Cys622Ser, Cys624Ser) prevent the recognition of and response to most known inducers of NRF2, while not impeding the ability of KEAP1 to ubiquitinate NRF2 and target it for degradation (Suzuki et al., 2019). Cys273 was substituted to tryptophan and Cys288 was substituted to glutamic acid to avoid the loss of ability to repress NRF2 accumulation induced by other substitutions at these residues (Saito et al., 2016; Suzuki et al., 2019).

Next, *keap1*Δ*5H* and *keap1*Δ8C cell lines were infected with the lentiviral constructs of mutant KEAP1: FLAG-HA-KEAP1$^{\Delta BTB}$ (+ΔBTB), FLAG-HA-KEAP1$^{\Delta KELCH}$ (+ΔKELCH), FLAG-HA-KEAP1^{S3H4} (+S3H4) or FLAG-HA-KEAP1$^{11Cys\text{-}less}$ (+11Cys-less). We chose these two cell lines to enable comparison between one that exhibits a higher sensitivity to MMS (*keap1*Δ5H) and one with a lower sensitivity (*keap1*Δ8C). Cells were selected with puromycin for a week to ensure the incorporation of the construct into the genome and resulting in a heterogenous population of cells expressing the KEAP1 mutant. Expression of all four mutant KEAP1 constructs was confirmed by Western

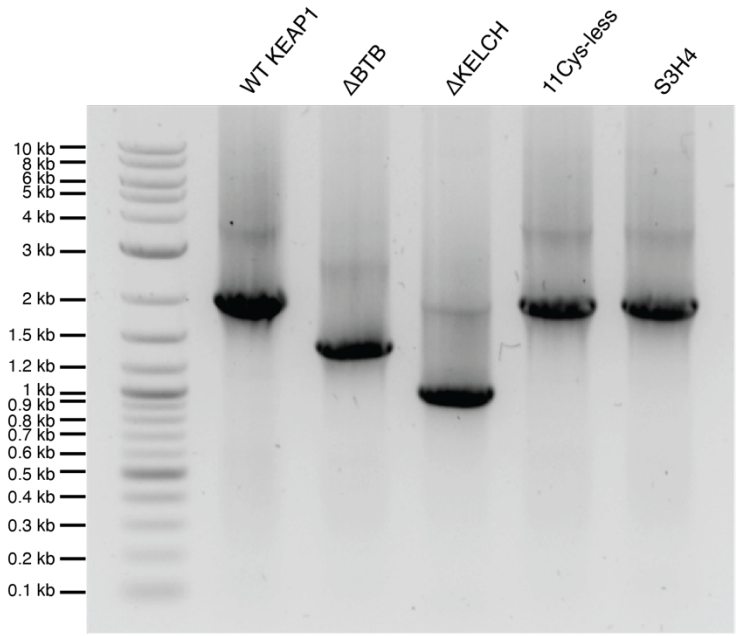

Figure 4.5 Agarose gel image of mutant KEAP1 cDNA sequences. KEAP1$^{\Delta BTB}$ and KEAP1$^{\Delta KELCH}$ mutants were obtained by PCR using primers that omit the domain being truncated. KEAP1^{S3H4} and KEAP1$^{11Cys\text{-}less}$ were synthesized with the help of Source BioScience and amplified by PCR. *attB* flanking sites compatible with the Gateway cloning system were introduced to all the mutant inserts at this stage.

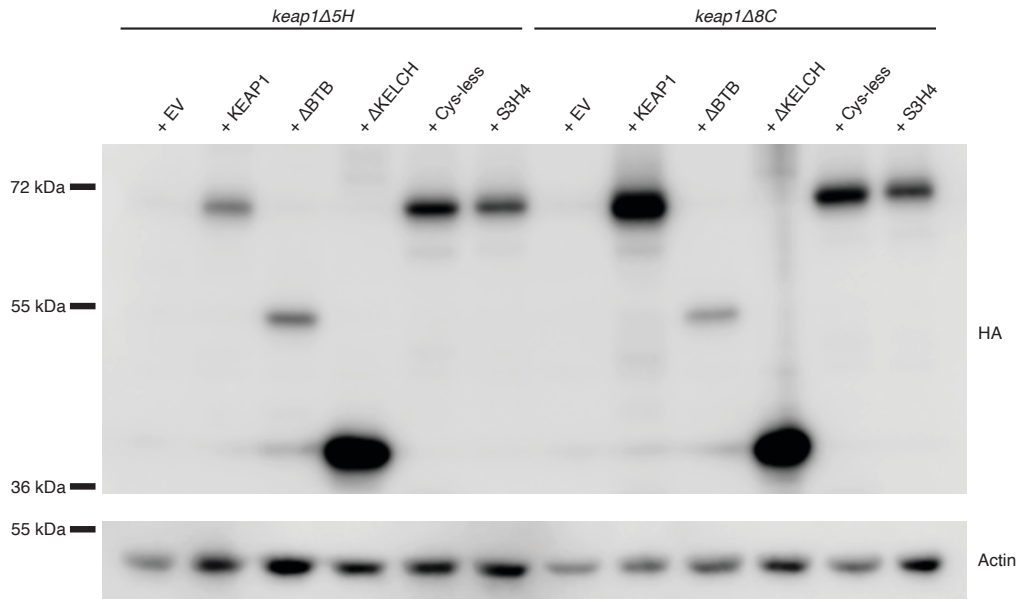

Figure 4.6 Domain mutants and amino acid substitution mutants of KEAP1 were re-expressed in *keap1*Δ cell lines. Re-expression of exogenous FLAG-HA-tagged KEAP1 mutants was confirmed by Western blotting.

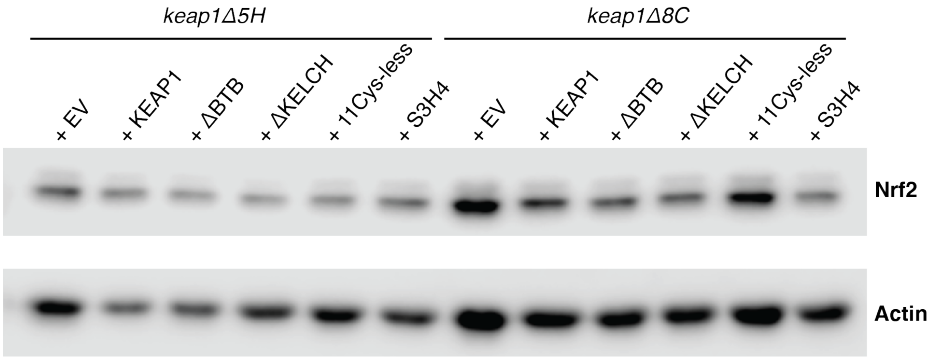

Figure 4.7 Influence of KEAP1 mutations on NRF2 accumulation tested by Western blotting. The expression levels of NRF2 in the KEAP1 domain mutants and in the 11Cys-less mutant were compared via Western blotting.

blotting (Figure 4.6). Interestingly, cell lines expressing mutants KEAP1$^{\Delta BTB}$, KEAP1$^{\Delta KELCH}$, KEAP1^{S3H4} and KEAP1$^{11Cys\text{-}less}$ display NRF2 expression levels similar to cell lines infected with wild-type KEAP1 and lower than in cells carrying an empty vector (Figure 4.7). In the presence of functional KEAP1, the cellular levels of NRF2 are lower than in KEAP1-deficient cells due to NRF2 being targeted for proteasomal degradation. On the other hand, genetic disruption of KEAP1 leads to NRF2 accumulation. This might suggest that the generated KEAP1 mutants retain some functionality of the wild-type protein in regards of NRF2 ubiquitylation. In the case of KEAP1$^{11Cys\text{-}less}$, retaining the ability to ubiquitylate NRF2 is an important indication that despite the mutations affecting recognition of NRF2 inducers, the protein remains functional, which allows the investigation of the effect of the cysteine sensor system alone. In *keap1*Δ5H, detectable levels of NRF2 suggest that the 11Cys-less mutant is capable of targeting NRF2 for proteasomal degradation. However, in *keap1*Δ8C expressing KEAP1$^{11Cys\text{-}less}$ the NRF2 level is increased compared to the cell line with re-expressed wild-type KEAP1, although lower than in *keap1*Δ8C (Figure 4.7). This might suggest that the *keap1*Δ8C cell line expressing the 11Cys-less mutant is not fully functional in regard to NRF2 degradation.

4.5 Role of KEAP1 domains in MMS-induced damage response

In order to understand the mechanism through which KEAP1 contributes to MMS tolerance in cells, it is crucial to investigate which of its domains are required for this

function. Considering that KEAP1 interacts with CUL3 as a substrate adaptor in the CRL3 complex and that our experiments in CUL3-depleted cells suggest CUL3 might play a role in KEAP1-dependent MMS tolerance, we decided to test whether the MMS-protective function of KEAP1 would be affected in the absence of the CUL3-binding BTB domain. However, the BTB domain is also responsible for KEAP1 homodimerisation. In order to untangle the effects of inhibiting the two functions of the domain, we resolved to also investigate the effect of a mutation of the five amino acids within the BTB domain suspected to constitute the CUL3 binding interface. We were also interested whether disruption of the substrate binding Kelch domain would impair the ability of KEAP1 to mitigate the effects of MMS toxicity. We earlier generated constructs of mutant KEAP1 and expressed them in the *keap1*Δ5F and *keap1*Δ8C cell lines, which will allow us to address these questions.

To this end, we performed clonogenic sensitivity assays on *keap1*Δ5H and *keap1*Δ8C cell lines expressing the three different KEAP1 mutants (Figure 4.8, Figure 4.9). Cells plated at low density were exposed to treatment with different MMS concentrations. Consistently with the drug treatment regime we employed in the previous chapter, *keap1*Δ5H was treated with MMS one time for 1 hour, while *keap1*Δ8C was treated with MMS three times every 48 hours, each time for 1 hour. Sensitivity to MMS was assessed by analysing the colony survival rates after 10-12 days of culture. The experiments were performed independently in *keap1*Δ5H and *keap1*Δ8C and show similar results. While exogenous expression of wild-type KEAP1

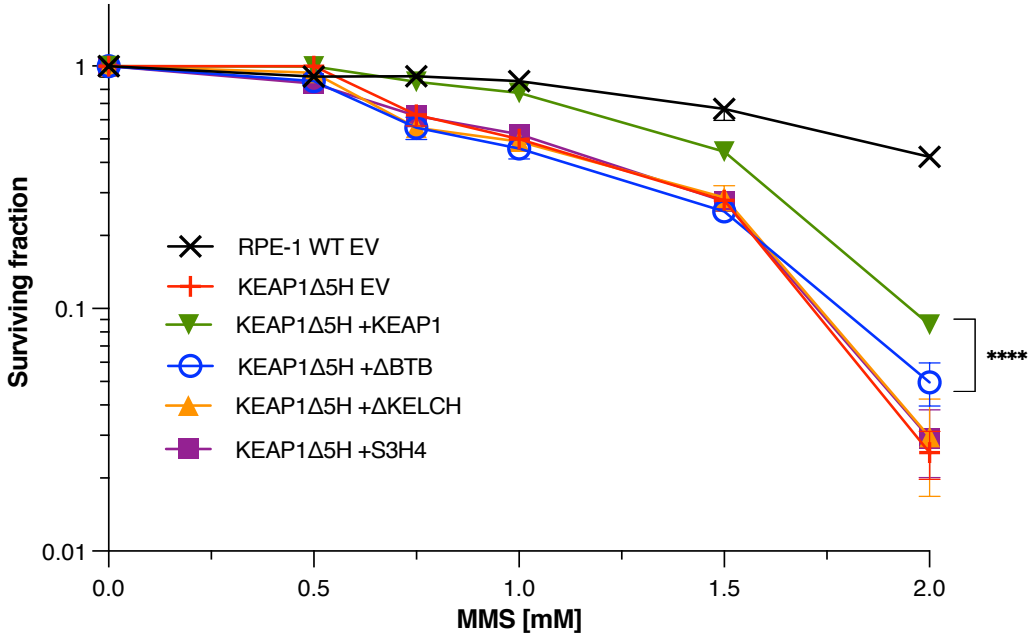

Figure 4.8 Disruptions of BTB or KELCH domain affect result in increased sensitivity to MMS observed in *keap1Δ5H* cell line. Cell line *keap1Δ5H* was transduced with KEAP1$^{\Delta BTB}$, KEAP1$^{\Delta KELCH}$ or KEAP1^{S3H4} mutants and selected with puromycin. The established heterogenic cell line was seeded at low density and treated for 1 hour with MMS on the next day, then washed twice with PBS, allowed to recover in fresh medium and cultured for 10-12 days to be assessed in a clonogenic survival assay. Wild-type RPE-1 and *keap1Δ5H* expressing an empty vector or with vector expressing wild type KEAP were used as controls. Error bars indicate the standard error of three experimental replicates. Statistical significance tested using two-way ANOVA.

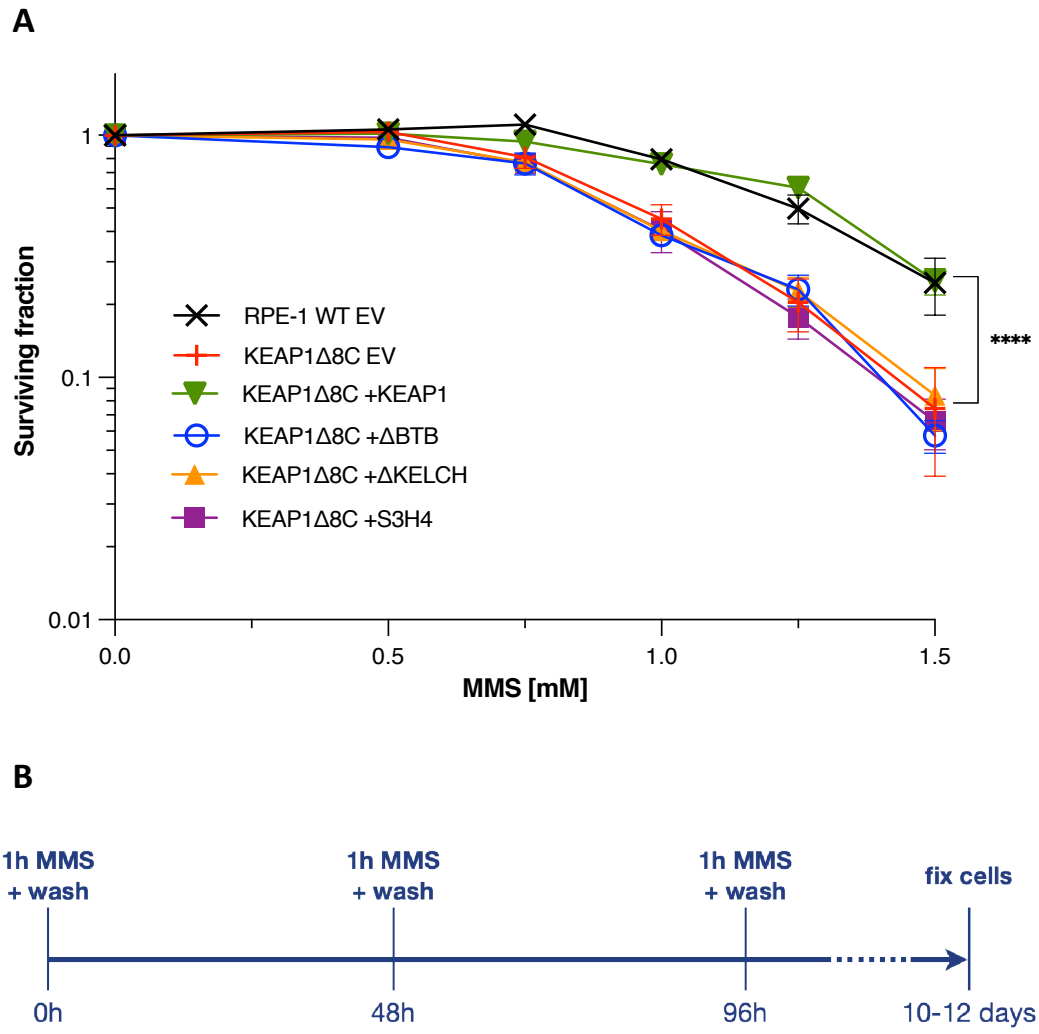

Figure 4.9 Disruptions of BTB or KELCH domain affect result in increased sensitivity to MMS observed in *keap1Δ8C* cell line. Cell line *keap1Δ8C* was transduced with KEAP1$^{\Delta BTB}$, KEAP1$^{\Delta KELCH}$ or KEAP1^{S3H4} mutants and selected with puromycin. **A.** The established heterogenic cell line was seeded at low density and treated for 1 hour with MMS on the next day, then washed twice with PBS and allowed to recover in fresh medium for 48 hours. The treatment was repeated two more times – 48 hours and 96 hours after the first treatment. The cells were cultured for a total of 10-12 days to be assessed in a clonogenic survival assay. Wild-type RPE-1 and *keap1Δ8C* expressing an empty vector or with vector expressing wild type KEAP were used as controls. Error bars indicate the standard error of three experimental replicates. Statistical significance tested using two-way ANOVA. **B.** Schematic representation of the chronic MMS dosage strategy.

rescues the MMS-sensitivity fully in *keap1*Δ8C and partially in *keap1*Δ5H, mutants KEAP1$^{\Delta BTB}$, KEAP1$^{\Delta KELCH}$ and KEAP1^{S3H4} fail to do so. Increased sensitivity to the drug in cells expressing KEAP1 with either truncated BTB domain or with mutations of suspected CUL3-binding region within the BTB domain demonstrates the necessity for functional BTB domain to enable the protective role of KEAP1 in presence of MMS-induced damage. This data suggests that, in the context of MMS tolerance, KEAP1 might function as part of the CRL3 complex. Moreover, these results indicate that Kelch domain is also required for KEAP1 to mitigate the impact of MMS toxicity on cells. As Kelch domain contains substrate binding motifs, the loss of function in KEAP1$^{\Delta KELCH}$ implies that KEAP1 executes its MMS-protective role by binding to a downstream protein, potentially a substrate for ubiquitylation.

4.6 Role of the cysteine sensor system of KEAP1 in MMS-induced DNA damage response

Given the ability of KEAP1 to sense various stress inducers through its cysteine residues, we hypothesised it is also possible that this sensor system might be at play in recognising MMS-induced damage (Dinkova-Kostova et al., 2002). Alkylating agents are highly electrophilic and able to modify cysteines forming irreversible covalent bonds, which positions MMS as a potential candidate for inducer of the cysteine sensor system (Dinkova-Kostova et al., 2002). We speculated that the recognition of MMS as a stressor by the reactive cysteines on KEAP1 could modulate its function. In this hypothetical model, KEAP1 would recognise MMS and respond to

it either by ubiquitylation of DDR proteins, acting as part of the CRL complex, or by signalling the damage in another CRL-independent manner.

In order to assess whether the substituted cysteine residues play a role in KEAP1-dependent MMS tolerance, clonogenic sensitivity assays were performed on *keap1*Δ5H and *keap1*Δ8C cell lines expressing the KEAP1$^{11Cys\text{-}less}$ mutant (Figure 4.10, Figure 4.11). Cells were plated at low density and treated with a range of MMS concentrations. Cell line *keap1*Δ5H was exposed to MMS one time for 1 hour, while *keap1*Δ8C was treated with MMS three times at 48-hour intervals, each time for 1 hour, consistent with experiments we described in the previous chapter. After 10-12 days of culture, cell viability was assessed by analysing the colony survival rates. The two experiments were performed independently in *keap1*Δ5H and *keap1*Δ8C. Interestingly, the KEAP1$^{11Cys\text{-}less}$ mutant rescued the phenotype in both cases, suggesting that the substituted 11 cysteine residues do not take part in KEAP1 response to MMS.

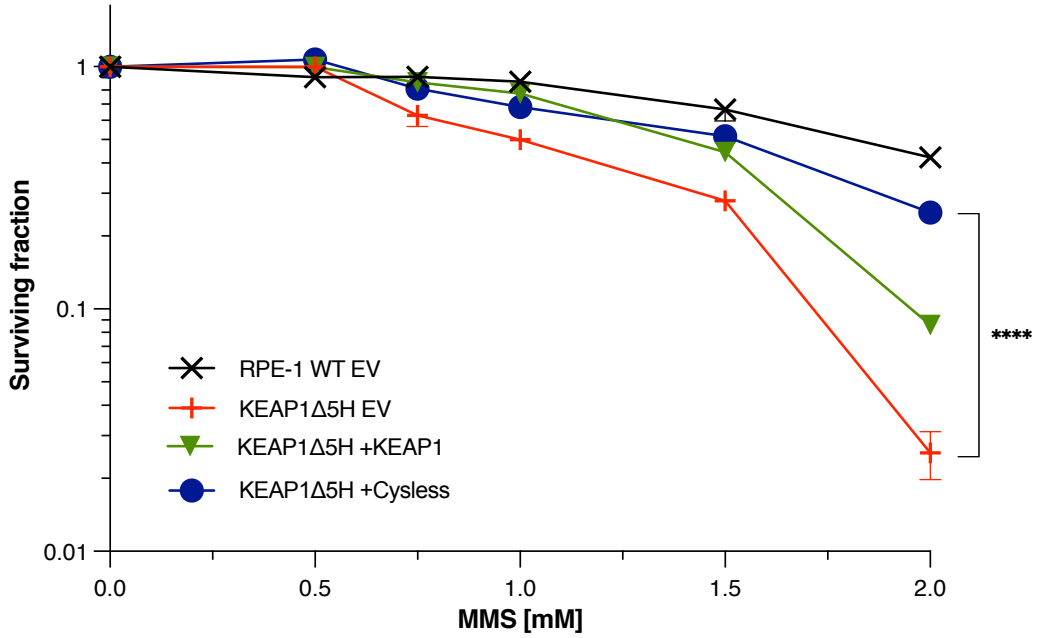

Figure 4.10 Mutation of 11 reactive cysteines in KEAP1 does not result in increased sensitivity of *keap1Δ5H* to MMS. Cell line *keap1Δ5H* was transduced with KEAP1$^{11Cys\text{-}less}$ mutant and selected with puromycin. The established heterogenic cell line was seeded at low density and treated for 1 hour with MMS on the next day, then washed twice with PBS, allowed to recover in fresh medium and cultured for 10-12 days to be assessed in a clonogenic survival assay. Wild-type RPE-1 and *keap1Δ5H* expressing an empty vector or with vector expressing wild type KEAP were used as controls. Error bars indicate the standard error of three experimental replicates. Statistical significance tested using two-way ANOVA.

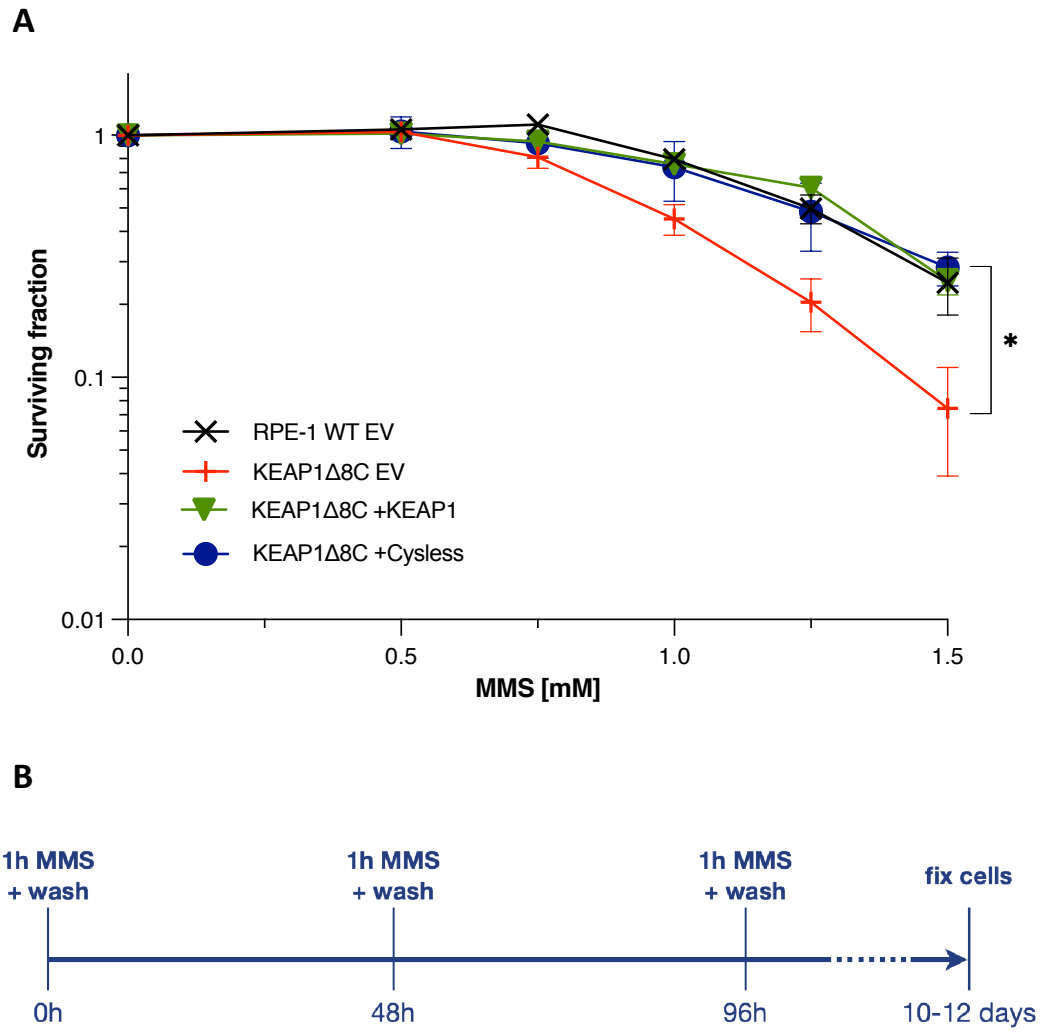

Figure 4.11 Mutation of 11 reactive cysteines in KEAP1 does not result in increased sensitivity of *keap1Δ8C* to MMS. Cell line *keap1Δ8C* was transduced with KEAP1$^{11Cys\text{-}less}$ mutant and selected with puromycin. The established heterogenic cell line was seeded at low density and treated for 1 hour with MMS on the next day, then washed twice with PBS and allowed to recover in fresh medium for 48 hours. The treatment was repeated two more times – 48 hours and 96 hours after the first treatment. The cells were cultured for a total of 10-12 days to be assessed in a clonogenic survival assay. Wild-type RPE-1 and *keap1Δ8C* expressing an empty vector or with vector expressing wild type KEAP were used as controls. Error bars indicate the standard error of three experimental replicates. Statistical significance tested using two-way ANOVA. **B.** Schematic representation of the chronic MMS dosage strategy.

4.7 Discussion

In this chapter, we explored the mechanism through which KEAP1 conveys tolerance to MMS. First, we investigated whether CUL3, a protein known to interact with KEAP1 as components of E3 ubiquitin ligase complex, is also involved in response to MMS-induced damage repair. Dependence of MMS tolerance on CUL3 would suggest that the role of KEAP1 in this context is carried our as KEAP1-CUL3-RBX1 ligase. Next, we explored the domain requirement for the function of KEAP1 in the context of MMS-induced damage repair by completely removing or introducing mutations within BTB and Kelch domains. Lastly, we tested the hypothesis that this novel function of KEAP1 might be dependent on its cysteine stress sensor. In this model, MMS would transfer an alkyl group onto one or more reactive cysteine residues and inactivate or modify the function of KEAP1.

Ubiquitylation is a post-translational modification which plays an important role in regulation of DNA damage repair pathways, for example, many of BER proteins are ubiquitylated (Carter and Parsons, 2018). However, often the ubiquitin ligase responsible for the modification of a specific repair factor, or even the functional impact of such PTM, remain unknown. Knowing that KEAP1 functions as a CUL3-based ubiquitin ligase, we wondered whether the KEAP1-dependent MMS tolerance might involve ubiquitylation and be also dependent on CUL3 (Cullinan et al., 2004). We therefore depleted CUL3 in U2OS cells and tested cell viability in response to MMS (Figure 4.1, Figure 4.2). As predicted based on its crucial interaction with KEAP1, CUL3 knockdown sensitised cells to MMS. Although we did not observe MMS

sensitivity in CUL3-depleted RPE-1 cells, taking into account the efficiency of the knockdown, this is not surprising (Figure 4.3). RPE-1 cells are often more difficult to transfect than for example U2OS, which can result in less efficient knockdown. This data would suggest that whichever pathway KEAP1 functions through in the context of MMS-induced damage repair, it might play its role as part of the E3 ubiquitin ligase complex with CUL3. Epistatic analysis of KEAP1 and CUL3 in the context of MMS treatment could test this hypothesis. However, we were not able to address this possibility due to the inefficient CUL3 depletion in our RPE-1-derived *keap1Δ* cell lines (data not shown). Given the current knowledge about the CUL3-RING ubiquitin ligase, we could hypothesise that KEAP1 could regulate MMS-induced DNA damage response by targeting proteins at the site of damage or certain transcription factors for degradation (Kobayashi et al., 2004). Alternatively, KEAP1 could suppress a protein-protein interaction through ubiquitylation, similarly as it does in the case of PALB2 and BRCA1 (Orthwein et al., 2015).

Next, we investigated the impact of disrupting different domains of KEAP1 on its ability to confer MMS tolerance. We have successfully expressed truncated domain mutants KEAP1$^{\Delta BTB}$ and KEAP1$^{\Delta KELCH}$, as well as an amino acid substitution mutant KEAP1^{S3H4}, in *keap1*Δ5H and *keap1*Δ8C cell lines. Colony survival assays once again confirmed that *keap1*Δ cell lines are sensitive to MMS and that this phenotype can be complemented by expression of wild-type KEAP1. In both tested cell lines, mutants KEAP1$^{\Delta BTB}$, KEAP1$^{\Delta KELCH}$ and KEAP1^{S3H4} were unable to complement the MMS sensitivity phenotype (Figure 4.8, Figure 4.9). These data point to both BTB and Kelch domain playing crucial parts in the mechanism through which KEAP1 is involved in

MMS-induced damage response. The BTB domain is necessary for both KEAP1 homodimerisation and its binding to CUL3 (Baird and Yamamoto, 2020). The incapability of the KEAP1$^{\Delta BTB}$ mutant to rescue the MMS-sensitivity phenotype supports the hypothesis that BTB domain is required for KEAP1 to confer MMS tolerance. However, separating the two functions of this domain is not trivial. In a study in murine KEAP1 a region critical for homodimerisation (amino acids 96-100) was substituted from the original HKVVL sequence to five alanines and co-expressed with a differentially tagged wild-type KEAP1 in *keap1*Δ 293T cells (Suzuki et al., 2011). The two co-expressed proteins failed to dimerise, similarly as observed in the case of deleting the entire BTB domain (Suzuki et al., 2011). Moreover, transgenic mice expressing solely the KEAP1^{mutHKVVL} were subject to juvenile mortality, as is the case for *Keap1-null* mice (Suzuki et al., 2011). Although this proves how crucial the KEAP1 dimerization is for its function *in vivo,* the study does not address whether binding to CUL3 has been affected. Other research focuses solely on the requirement for BTB domain to enable the interaction between KEAP1 and CUL3 (Furukawa and Xiong, 2005). The same study reported that KEAP1^{S3H4} with mutations introduced specifically at the predicted interaction sites with CUL3 makes the mutant KEAP1 unable to bind to this protein, however the effect on homodimerisation was not tested (Furukawa and Xiong, 2005). We have shown that KEAP1^{S3H4} mutation leads to a loss of function important for MMS tolerance (Figure 4.8, Figure 3.14). This could be solely the result of inability to bind CUL3, although we cannot exclude the possibility that homodimerization is also disrupted in the KEAP1^{S3H4} mutant. Perhaps this question could be further addressed in *keap1*Δ cells by expressing KEAP1 protein with C151W mutation, which significantly decreases CUL3 binding and leads to

consecutive NRF2 activation, and by testing the viability after MMS exposure (Eggler et al., 2009; Kobayashi et al., 2009). Structure analysis of the C151W mutant suggests that its BTB homodimerization interface is not disrupted, however no functional studies have tested that hypothesis (Cleasby et al., 2014).

While the structure of the CUL3-KEAP1-NRF2 complex has not been solved to date, the structures of BTB and Kelch domains have been determined and guide the current understanding of the structural basis of KEAP1 interactions with its targets, and specifically with NRF2 (Canning et al., 2013; Cleasby et al., 2014; Li et al., 2004). KEAP1 needs to form a homodimer and bind through the two Kelch domains to both ETGE and DLG motifs on NRF2 in order for NRF2 to be ubiquitylated and degraded by the proteosome (Horie et al., 2021). Disruption of CUL3 binding ultimately also results in the KEAP1 inability to target NRF2 for degradation (Furukawa and Xiong, 2005). Regardless of the exact dynamics of the CUL3-KEAP1 complex assembly and whether disrupting KEAP1 homodimerisation affects CUL3 biding and vice versa, our data from MMS sensitivity assays in KEAP1$^{\Delta BTB}$ and KEAP1^{S3H4} mutants indicates that KEAP1 is likely to act as part of the ubiquitin E3 ligase complex in the context of MMS-induced damage. This could be further confirmed by epistatic analysis of KEAP1 and CUL3 in response to MMS. As KEAP1 binds all of its known target proteins through its Kelch domain, we were interested whether deleting this domain has any impact on the MMS sensitivity (Kopacz et al., 2020; Li et al., 2004; Orthwein et al., 2015). KEAP1$^{\Delta KELCH}$ mutant does not complement the MMS sensitivity in RPE-1 *keap1*Δ cells, suggesting that also in this context KEAP1 regulates another key protein through interaction with Kelch domain. The Kelch domain binds to specific

ETGE and DLG interaction motifs on target proteins (Kopacz et al., 2020). Screening proteins for these conserved motifs and their variations could help identify the partner of KEAP1 in response to MMS.

MGMT repair methylated DNA bases directly by transferring the alkyl group onto its reactive cysteine residue (Gutierrez and O'Connor, 2021). Our data indicates that KEAP1 plays a role in alkylation damage repair and it is also known to possess a cysteine stress sensor, whose reactive cysteine residues can accept alkyl groups (Suzuki et al., 2019). We therefore hypothesised that the reactive cysteines of KEAP1 might remove alkyl groups from damaged bases in a manner similar to MGMT. To address the possible role of the cysteine sensor in resolving MMS-induced damage by KEAP1, we expressed KEAP1$^{11Cys\text{-}less}$ in *keap1*Δ cells and assessed their viability when exposed to MMS (Suzuki et al., 2019). Interestingly, this mutation did not affect the ability of KEAP1 to complement the MMS sensitivity phenotype (Figure 4.10, Figure 4.11). Given the electrophilic properties of MMS and the fact that other alkylating agents are known to modify the cysteines on KEAP1 and modulate its function, this result was unexpected (Dayalan Naidu and Dinkova-Kostova, 2020). However, there are important factors to consider that offer an explanation for this observation and do not exclude the possibility that the cysteine code plays a role in KEAP1 response to MMS.

Importantly, the substitutions we introduced in the KEAP1$^{11Cys\text{-}less}$ mutant we generated were based on research in murine model (Suzuki et al., 2019). While the mutated cysteines might be some of the most reactive in murine KEAP1, that may

not be true for the human protein (Suzuki et al., 2019). The reactivity of the cysteine residues differs significantly between the human and mouse KEAP1 (Sekhar et al., 2010). For example, N-iodoacetyl-N-biotinylhexylenedoamine (IAB) adducts murine KEAP1 at its highly reactive Cys273, but the reactivity of the same cysteine residue in human KEAP1 is decidedly lower in side-by-side comparison (Sekhar et al., 2010; Xiong Y, Liebler DC and Freeman M, unpublished results). In contrast, human KEAP1 readily forms adducts at Cys489 when exposed to dexamethasone (DEX), while this reagent does not adduct the same residue in murine KEAP1 (Dinkova-Kostova et al., 2002; Liebler et al., 2006; Sekhar et al., 2010). However, much remains unknown about the differences in cysteine reactivity between the two species in response to specific reagents.

It is then not unlikely that in the KEAP1$^{11Cys\text{-}less}$ mutant the key cysteines for sensing MMS-induced damage remain active and enable the mutant to react to this damage in an undisturbed manner. While it is possible that in the context of MMS KEAP1 acts through mechanisms independent from the cysteine sensor, to unequivocally exclude this possibility more research is needed. Systematic mutation of each of the 27 cysteine residues, alone and in combinations, could lead to generation of a more appropriate human equivalent of the in the murine KEAP1$^{11Cys\text{-}less}$ mutant, with all the crucial cysteines inactive while retaining its ability to target NRF2 for degradation under basal conditions. Such approach could contribute substantially to our current understanding of the KEAP1 cysteine code.

In this chapter we demonstrated that CUL3, a functional partner of KEAP1, is required for protection of U2OS cells from MMS-induced damage. We also created KEAP1 domain mutants in order to test whether they are required for MMS tolerance. We demonstrated that the BTB domain crucial for KEAP1 dimerization and its binding to CUL3 is necessary for the role KEAP1 plays in conferring tolerance to MMS-induced damage. Similarly, mutation of the predicted KEAP1 interface for interaction with CUL3 results in greater cellular sensitivity to MMS, supporting the notion that the interaction with CUL3 is required for KEAP1 function in this context. We showed that loss of the Kelch domain also increased the sensitivity of cells to MMS compared with wild-type KEAP1, suggesting the requirement for the interaction with the target protein for this newly described role of KEAP1. Interestingly, and contrary to our hypothesis, mutation of the 11 reactive cysteine residues in KEAP1 did not impair its function in response to MMS-induced DNA damage, suggesting the cysteine sensor is not required for this novel role of KEAP1. Taken together, these data suggest that the function of KEAP1 in the context of MMS tolerance might be executed through its interaction with CUL3 as part of the E3 ligase complex and also point to the importance of substrate binding capability. Our results imply that the cysteine sensor code might not play a part in the response to MMS-induced damage or the sensor for alkylation introduced by MMS might lie outside of the 11 cysteine residues tested in our approach. In the following chapters we will address the question of which pathway KEAP1 might act through in this role.

5. Identifying the pathway that KEAP1 regulates to combat MMS-induced damage

5.1 Introduction

5.1.1 KEAP1 and resolution of alkylation base damage – the missing puzzle pieces

Our results have demonstrated that KEAP1 plays an important role in the tolerance of MMS-induced DNA damage. We have shown that both the BTB and the Kelch domains are required for this novel function of KEAP1. Moreover, our data suggests that KEAP1 carries out its role in MMS-induced damage response as part of the CUL3-based ubiquitin ligase. What remains to be uncovered is the pathway through which KEAP1 might act in the context of MMS-induced damage resolution. Alkylation damage to DNA bases is largely resolved by two main pathways – direct repair or BER (Wyatt and Pittman, 2006). Although both of these pathways have been extensively studied and are well understood, areas for further research exist in both. It would be tempting to speculate that KEAP1 could be involved in either DR or BER, and perhaps play a role in some of the lesser understood aspects of these pathways.

Direct repair in human cells is performed by MGMT, a suicide enzyme which chemically reverses the DNA base adduct in a one-step reaction (Yu et al., 2020).

After transferring the alkyl group onto its reactive cysteine residues, MGMT becomes inactive and is targeted for ubiquitylation-dependent proteasomal degradation (Hwang et al., 2009). Given the repair itself is performed solely by the MGMT methyltransferase and no other proteins need to be recruited to the lesion to participate in this elegantly simple process, we have a substantial understanding of this repair mechanism. However, a recent study has reported the requirement for PARP-mediated PARylation of MGMT in resolution of TMZ-induced methylation DNA damage, which highlights the need to further research the regulation of MGMT (Wu et al., 2021). It is possible that more factors or perhaps other post-translational modifications are involved in this process.

Base excision repair pathway plays an important role in resolution of alkylation damage. In contrast to direct repair, BER involves a number of different proteins coordinating at the site of lesion. Although numerous studies, including from our group, have furthered our understanding of how BER is regulated at the enzymatic level, the complexity of the BER pathway still presents some unanswered questions and possible focus areas for future research. A number of proteins involved in BER undergo various post-translational modifications (PTMs) that can modify their functions, which contributes to the pathway regulation. Among other PTMs, ubiquitylation by E3 ubiquitin ligases plays a significant role in BER, regulating cellular protein levels, compartmental localisation or enzymatic activity (Carter and Parsons, 2018). Most of the BER proteins are known to be ubiquitylated, including DNA glycosylases UNG, SMUG and NEIL1, as well as the endonuclease APE1, the SSBs processor PARP1, the DNA polymerase β, XRCC1 and multiple other factors (Busso et

al., 2009; Carter and Parsons, 2018; Edmonds et al., 2017; Parsons et al., 2009; Schröfelbauer et al., 2005; Wang et al., 2008; Wei et al., 2013). The fact that E3 ubiquitin ligases contribute to controlling all stages of BER through modifying their targets, highlights the importance of understanding the intricacies of this mechanism of pathway regulation. Although several specific E3 ubiquitin ligases involved in BER have been identified, others remain to be uncovered. Moreover, some proteins, such as NEIL1, might be targeted by more than one E3 ligase (Edmonds et al., 2017). Evaluation of the relevance of ubiquitylation in the context of BER pathway regulation provides an interesting area for future research.

5.2 Aims

Our results have demonstrated that KEAP1 plays an important role in the tolerance of MMS-induced DNA damage. Previous findings, including some from our group, have highlighted the importance of PARP proteins participating in resolving DNA damage induced by MMS (Pommier et al., 2016; Ronson et al., 2018). The fact that both of these proteins respond to the same type of DNA lesions has prompted us to hypothesise that KEAP1 might be dependent on PARP1 in response to MMS-induced DNA lesions. To test this hypothesis, we first investigated the recruitment of KEAP1 to the site of damage. Next, we explore whether the observed chromatin enrichment of KEAP1 is regulated by PARP1. Lastly, we aim to identify the pathway that KEAP1 acts through in the context of resolving MMS-induced DNA damage. Using specific inhibitors, we probe the relationship of KEAP1 with protein factors

involved in known PARP1-dependent base damage repair pathways, looking for potential epistatic relationships.

5.3 KEAP1 is recruited to chromatin in response to MMS

5.3.1 KEAP1 is enriched in chromatin after MMS treatment

Following DNA damage, chromatin undergoes structural relaxation and proteins involved in the DNA damage repair are recruited to the site of lesion. We therefore hypothesised that if KEAP1 is involved in the repair of MMS-induced DNA damage, it would be recruited to the chromatin after exposure to MMS. To test this, we treated U2OS cells with 2 mM MMS for 1 hour and then allowed them to recover for 1-6 hours, as described previously by our group (Ronson et al., 2018). After the recovery, the cells were collected and either processed for whole cell extract or subjected to cell fractionation to isolate the chromatin-enriched fraction. These samples were then analysed via Western blotting for the KEAP1 protein signal levels. Indeed, we observed an enrichment of KEAP1 in the chromatin fraction after 2 hours of post-MMS recovery (Figure 5.1). This enrichment appears to be transient, which suggests KEAP1 might be recruited to chromatin to fulfil a specific function at the site of damage, after which it disassociates from the chromatin. This data supports our hypothesis and indicates that KEAP1 might be recruited to the site of MMS-induced DNA damage.

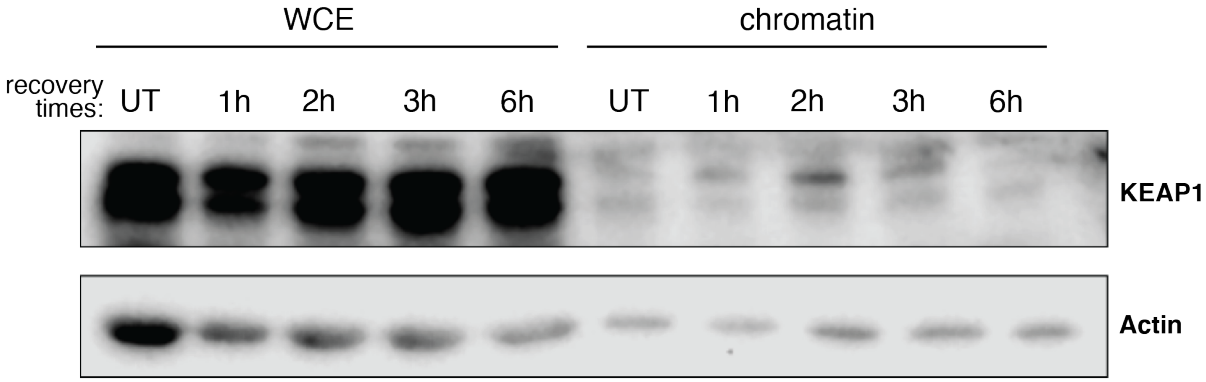

Figure 5.1 KEAP1 in enriched in the chromatin fraction of U2OS cells after 1 hour of MMS treatment with recovery. U2OS cells were treated with 2 mM MMS for 1 hour and then allowed to recover for 1-6 hours. Cell fractionation was then performed on collected cells. Whole-cell extracts (WCE) and chromatin-enriched fractions were then compared for KEAP1 signal via Western blotting. UT – untreated sample; 1h, 2h, 3h, 6h – number of hours of recovery after MMS removal.

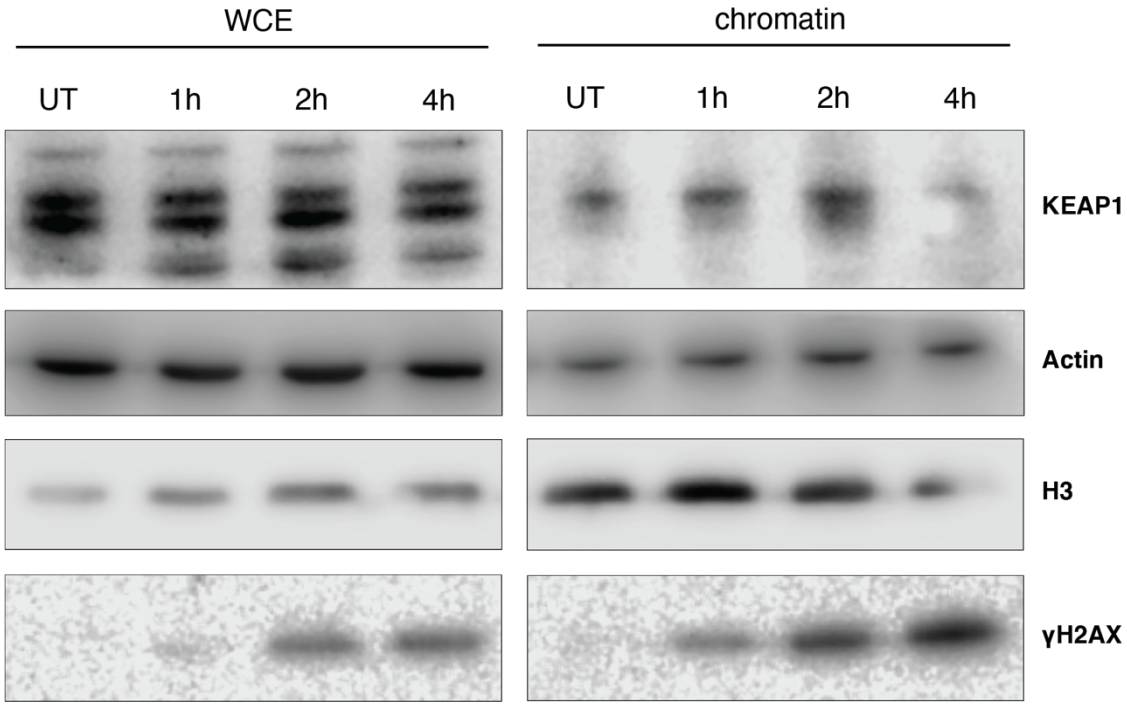

Figure 5.2 KEAP1 in enriched in the chromatin fraction of U2OS cells after MMS treatment. U2OS cells were treated with 2 mM MMS for 1-4 hours. Cell fractionation was then performed on collected cells. Whole-cell extracts (WCE) and chromatin-enriched fractions were then compared for KEAP1 signal via Western blotting. UT – untreated sample; 1h, 2h, 4h – duration of MMS treatment.

Next, we wished to explore whether this observation remains true when cells are subjected to MMS continuously, without recovery. We employed a slightly different MMS treatment regime and incubated U2OS cells with 2 mM MMS for longer times (1-4 hours) without allowing them to recover from the stress, as opposed to the 1-hour-long incubation with MMS and varied recovery times in the experiment discussed above. Cells were harvested immediately following the incubation and processed as described above. Western blot analysis of the samples reveals slight KEAP1 enrichment in the chromatin after just 1 hour of treatment, with the level of detectable KEAP1 in the chromatin peaking at 2 hours of treatment (Figure 5.2). Again, we observed that at later time points the presence of KEAP1 in the chromatin fraction is negligible, which might suggest its disassociation from the site of damage, presumably after having fulfilled its DNA damage-related function.

5.3.2 KEAP1 recruitment to chromatin is dependent on PARP1

As demonstrated by our results, KEAP1 plays a role in the repair of MMS-induced DNA damage, a process in which PARPs have been implicated (Pommier et al., 2016; Ronson et al., 2018). This prompted us to hypothesise that KEAP1 might be regulated by PARPs in the context of conveying MMS tolerance. To address this possibility, we tested the effect of PARP inhibitor olaparib on KEAP1 chromatin enrichment after MMS treatment. U2OS cells were incubated with 10 μM olaparib for 24 hours prior to MMS treatment for 1 hour. Cells were then allowed to recover for 1 hour in fresh media containing olaparib, after which they were harvested and processed for whole-cell extracts or cell fractionation to obtain the chromatin-enriched fraction.

Western blot imaging and analysis of the samples demonstrated that KEAP1 recruitment to chromatin after MMS exposure is hindered in the presence of olaparib (Figure 5.3). In contrast, in control sample a strong KEAP1 protein band was detected after MMS exposure. This data indicates that the recruitment of KEAP1 to chromatin following MMS treatment is PARP-dependent, suggesting KEAP1 might function through one of the PARP-dependent base damage repair pathways, such as BER or MGMT-mediated direct repair (Horton et al., 2014; Reynolds et al., 2015; Wu et al., 2021).

Olaparib has been reported to inhibit the activity of PARP1, PARP2 and PARP3 (Min and Im, 2020). However, it is estimated that at least 90 % of cellular PARylation activity in response to DNA damage is carried out by PARP1 (Kamaletdinova et al., 2019). We therefore chose to determine whether the response of KEAP1 to MMS-induced damage is regulated by PARP1, the most prominent member of the PARP protein family and known to be an important player in DDR (Ray Chaudhuri and Nussenzweig, 2017). To this end, an assay testing chromatin enrichment of KEAP1 was performed in MMS-treated wild-type and *parp1*Δ U2OS cells. Cells were treated with 2 mM MMS for 90 minutes and harvested for whole-cell and chromatin fraction extraction immediately after the treatment. Subsequent Western blotting analysis revealed inhibition of the MMS-induced KEAP1 recruitment to chromatin in *parp1*Δ cells, as opposed to wild-type cells, which exhibited pronounced KEAP1 enrichment (Figure 5.4). Together, these data demonstrate that the recruitment of KEAP1 to the DNA damage site following MMS exposure is dependent on PARP1. This in turn

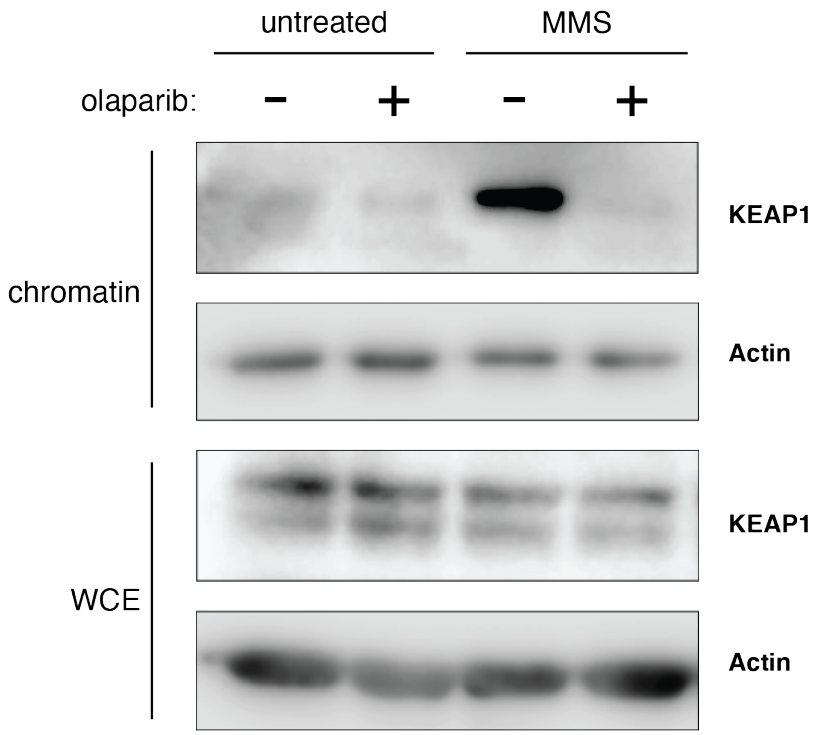

Figure 5.3 KEAP1 recruitment to chromatin is PARP-dependent. U2OS cells incubated with olaparib (or DMSO as negative control) were treated with 2 mM MMS for 1 hour, then left to recover without MMS for 1 hour and collected for cell fractionation. Whole-cell extracts (WCE) and chromatin-enriched samples were analysed by Western blotting for KEAP1 signal.

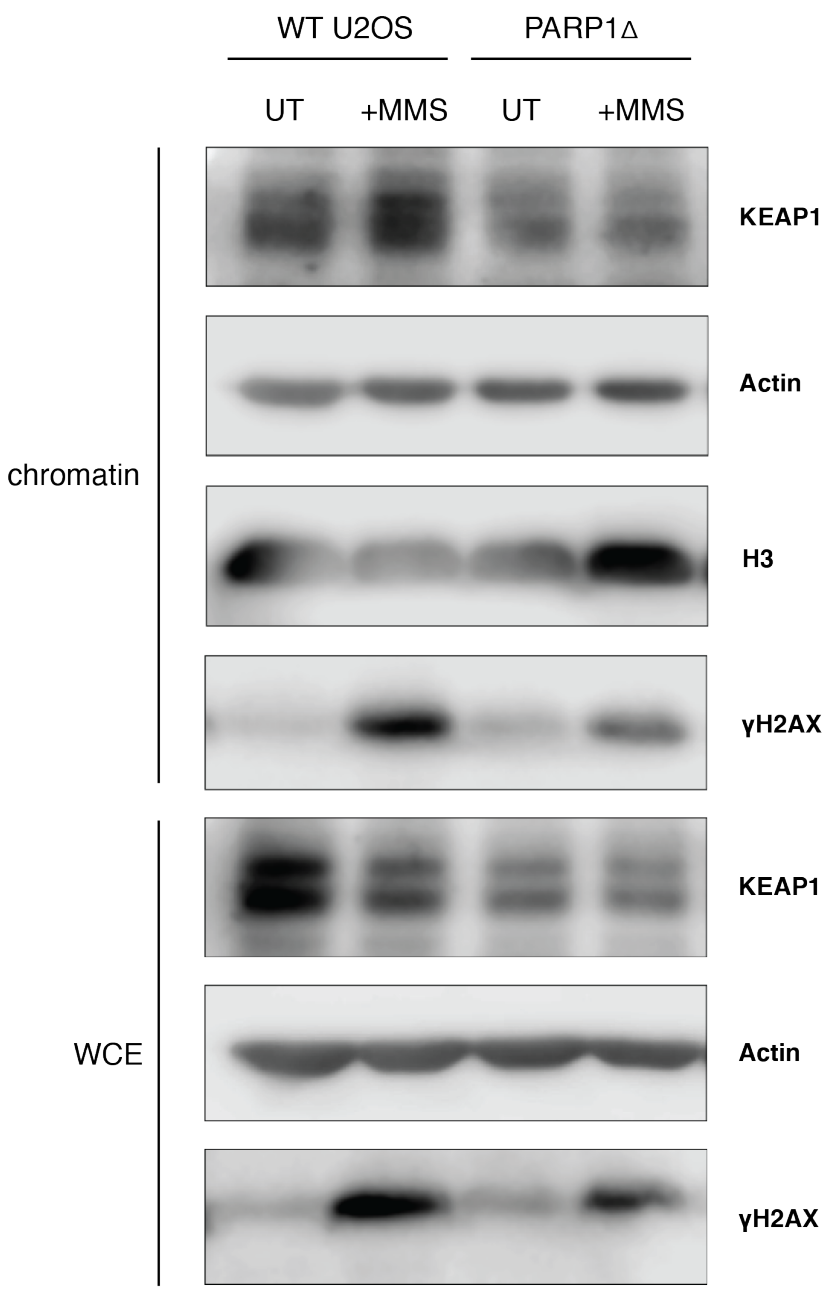

Figure 5.4 KEAP1 recruitment to chromatin is dependent on PARP1. Wild-type and *parp1Δ* U2OS cells were treated with 2 mM MMS for 90 minutes, then collected for cell fractionation. Whole-cell extracts (WCE) and chromatin-enriched samples were analysed by Western blotting for KEAP1 signal. UT – untreated sample.

suggests that in the context of MMS-induced damage, KEAP1 might act through a PARP1-dependent base damage repair pathway.

5.4 Loss of *KEAP1* is not epistatic with MGMT inhibition in the context of MMS sensitivity

Given the observed PARP-dependency of KEAP1 in the context of MMS-induced damage tolerance, we wished to establish whether it acts through a PARP-dependent base damage repair pathway, such as MGMT-mediated direct repair or BER (Horton et al., 2014; Reynolds et al., 2015; Wu et al., 2021).

Direct repair of base damage by MGMT is dependent on PARP (Wu et al., 2021). PARylation of MGMT is required for its binding to chromatin, facilitating the removal of O6-methylguanine (Wu et al., 2021). Therefore, we hypothesised that KEAP1 might be involved in MGMT-mediated direct repair. To explore this possibility, we set out to assess whether lack of KEAP1 and inhibition of MGMT are additive, or if the relationship was epistatic in terms of allowing cells to tolerate exposure to MMS. We used the MGMT activity inhibitor O6-benzylguanine (O6-BG) to block the resolution of alkylated base damage through direct repair. O6-benzylguanine works as a pseudosubstrate inhibitor for MGMT, transferring its benzyl group onto an active cysteine on MGMT (Dolan et al., 1990; Pegg et al., 1993). Previous studies indicate exposing cells to 10 μM O6-BG causes a >95 % inhibition of the MGMT DNA damage repair activity (Liang et al., 2020). Using this as a guide, we optimised the treatment regime, testing the effect of three different concentrations of O6-BG (5

μM, 10 μM, 15 μM) combined with 1-hour MMS treatment on wild-type RPE-1 cells cultured for colony survival assay (Figure 5.5).

While all tested O6-BG concentrations sensitised cells to MMS compared to control, the 10 μM O6-BG treatment was chosen for the subsequent experiments. This decision was based on the fact that while the optimisation was performed on wild-type cells and 10 μM O6-BG was sufficient to observe sensitisation to MMS, the KEAP1-deficient cell lines are less viable in colony forming assays compared to the wild-type. Therefore, we wished to avoid too strong of an effect of O6-BG treatment alone in *keap1*Δ, which could potentially make it difficult to analyse the data of combined O6-BG and MMS treatment in *keap1*Δ.

Next, *keap1*Δ5H and wild-type RPE-1 cells were seeded at low density and either pre-treated with 10 μM O6-BG prior to 1-hour exposure to a range of MMS concentrations, or simply treated with MMS without the MGMT inhibitor. After the MMS removal, cells were either cultured with O6-BG or without it, and survival ratio compared to wild-type was assessed through a colony forming assay (Figure 5.6). While MMS alone had a profound effect on the survival of *keap1*Δ5H cells, the combination with O6-BG treatment lowered the survival rate even further.

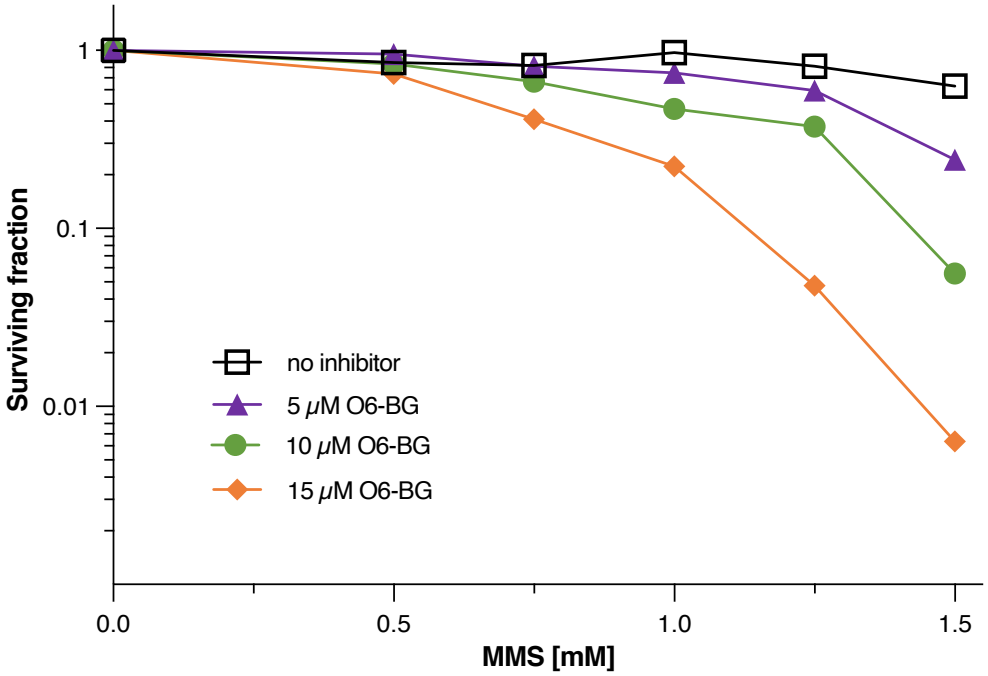

Figure 5.5 Optimisation of MGMT inhibition with O6-benzylguanine treatment. RPE-1 wild-type cells seeded at low density were incubated with three different O6-benzylguanine (O6-BG) concentrations and then treated for 1 hour with a range of MMS concentrations. After 12 days of culture, the cell viability was assessed based on the colony number. The data shown represents optimisation of conditions with n=1.

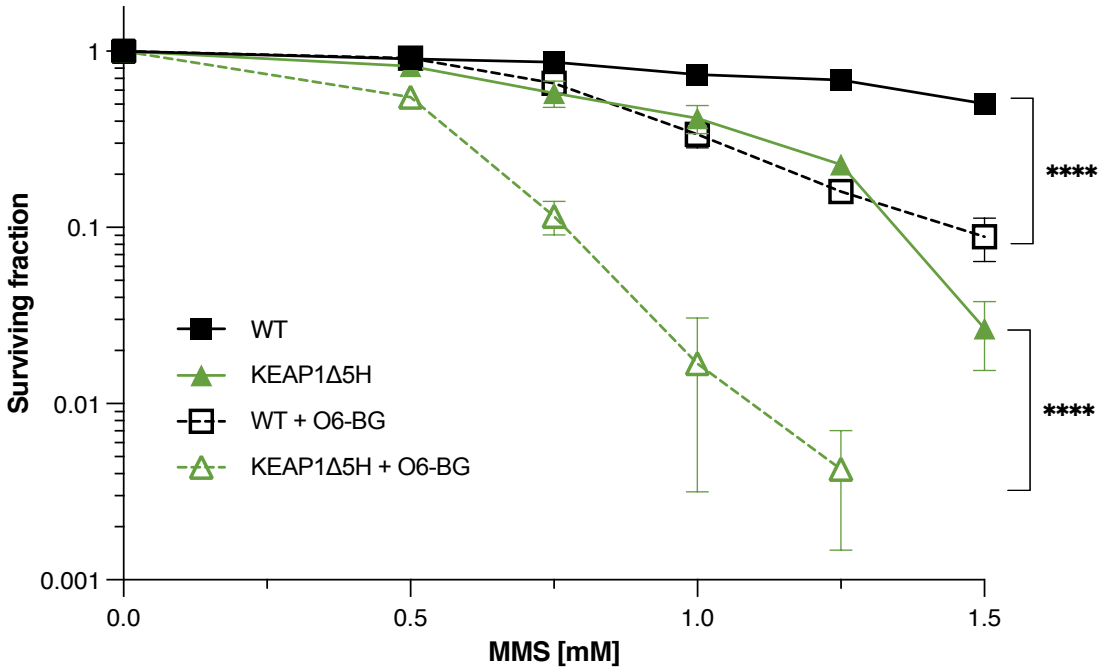

Figure 5.6 KEAP1 deletion is additive with MGMT inhibition in *keap1*Δ5H cell line. Wild-type RPE-1 and *keap1*Δ5H cells seeded at low density were pre-incubated with 10 μM O6-benzylguanine for 1 hour and treated for 1 hour with a range of MMS concentrations. After 12 days of culture with O6-BG in the medium, the cell viability was assessed based on the colony number; n=3. When surviving fraction equals 0, data points are not shown on the graph. Statistical significance was assessed by a 2-way ANOVA test.

(Figure 5.6). These results clearly demonstrate an additive effect of lack of *KEAP1* gene and inhibition of MGMT activity in the *keap1*Δ5H cells, indicating they are not epistatic.

In order to confirm this observation in *keap1*Δ5F and *keap1*Δ8C, the combined MMS and O6-BG treatment regimen was modified to create chronic DNA damage stress, as described in chapter 3. Cells were pre-treated with 10 μM O6-BG before being exposed to MMS for 1 hour. The MMS treatment was repeated three times, 48 hours apart, and O6-BG was present throughout the culture for colony survival assay. The control cells were treated repeatedly with MMS but with omission of O6-BG. Colony survival rate compared to the wild-type cells was assessed after 12 days of culture (Figure 5.7). Under the described conditions, both *keap1*Δ5F and *keap1*Δ8C were sensitive to MMS treatment without the inhibitor. Upon combining of MMS with inhibition of MGMT activity, the number of viable colonies decreased further (Figure 5.7).

These data suggest that the relationship between KEAP1 and MGMT is not epistatic. The effects of loss of function of KEAP1 and MGMT on cells exposed to alkylation damage by MMS are additive. This indicates the two proteins act through independent pathways responding to alkylation DNA damage and conferring tolerance to MMS.

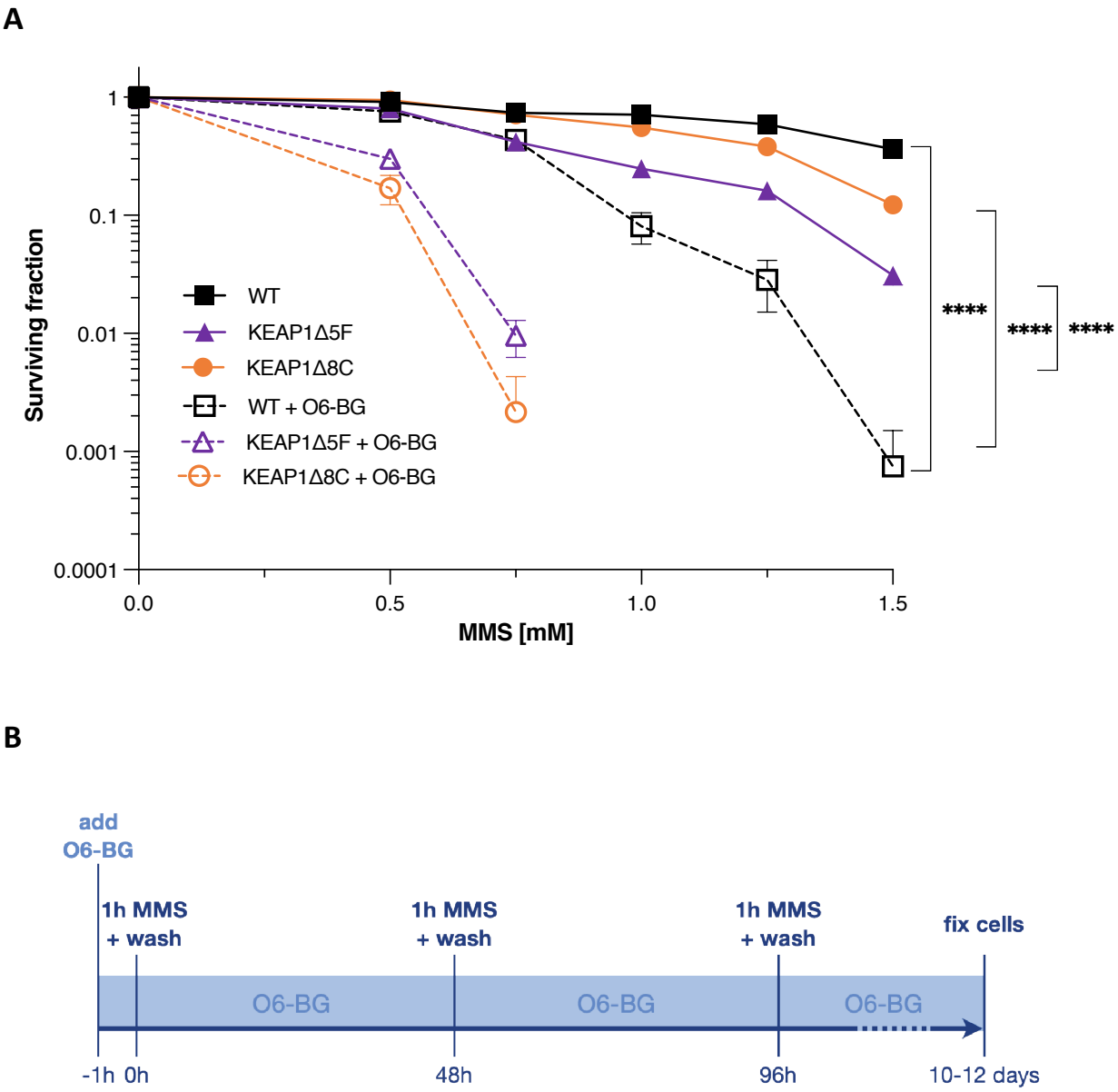

Figure 5.7 KEAP1 deletion is additive with MGMT inhibition in conditions of chronic DNA damage. **A.** Cell lines *keap1Δ*5F, *keap1Δ*8C and wild-type RPE-1 cells seeded at low density were pre-incubated with 10 μM O6-benzylguanine for 1 hour and treated for 1 hour with a range of MMS concentrations. The MMS treatment was repeated three times within 48-hour intervals. After 12 days of culture with O6-BG in the medium, the cell viability was assessed based on the colony number; n=3. When surviving fraction equals 0, data points are not shown on the graph. Statistical significance was assessed by a 2-way ANOVA test. **B.** Schematic representation of the chronic MMS dosage strategy combined with O6-BG treatment.

5.5 Loss of *KEAP1* is not epistatic with APE1 inhibition in the context of MMS sensitivity

Base excision repair is one of the main pathways of repairing alkylation damage to DNA (Ray Chaudhuri and Nussenzweig, 2017). Moreover, PARP1 together with PARP2 play a role in promoting resolution of DNA base damage through BER (Ronson et al., 2018). We hypothesized that considering its PARP-dependent chromatin recruitment upon alkylation damage, KEAP1 might be involved in BER.

We therefore sought to inhibit DNA damage repair through BER and test whether loss of KEAP1 would have an additive effect on cell survival following MMS exposure, or if *KEAP1* deletion and BER inhibition are epistatic. We chose APE1 as the inhibition target, as this is the primary endonuclease enzyme acting in the early stages of BER which recognises the apurinic/apyrimidinic (AP) sites and cleaves them to create 3'-OH ends necessary for DNA synthesis (Izumi and Mellon, 2021). To disrupt APE1, we exploited lucanthone (LUCA), a DNA intercalator that inhibits APE1 lyase activity through a direct protein binding and without affecting its redox activity (Luo and Kelley, 2004; Naidu et al., 2011). To test whether inhibition of BER with lucanthone would further sensitise *keap1*Δ cells to MMS, we adjusted the conditions described by Luo and Kelley, 2004, involving 2 hours of pre-treatment with lucanthone followed by a 1-hour treatment with MMS (Figure 5.8). The lucanthone treatment in the conditions following Luo and Kelly, 2004 did not have an effect on the cell

A

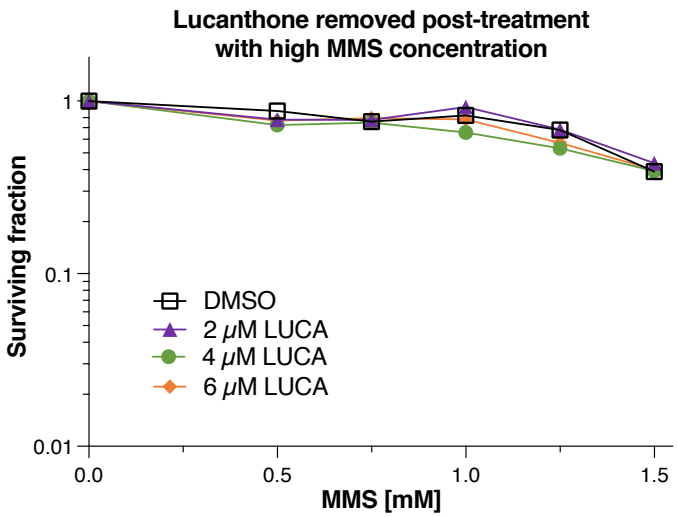
Lucanthone removed post-treatment
with high MMS concentration
Surviving fraction
1
0.1
0.01
0.0
0.5
1.0
1.5
MMS [mM]
DMSO
2 μM LUCA
4 μM LUCA
6 μM LUCA

B

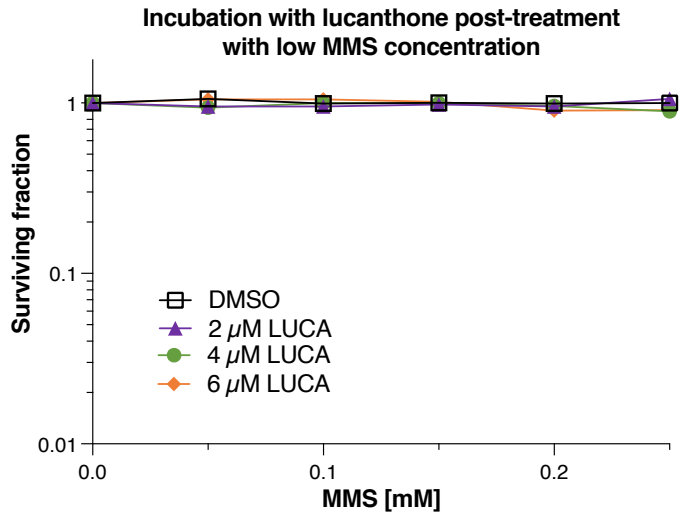
Incubation with lucanthone post-treatment
with low MMS concentration
Surviving fraction
1
0.1
0.01
0.0
0.1
0.2
MMS [mM]
DMSO
2 μM LUCA
4 μM LUCA
6 μM LUCA

C

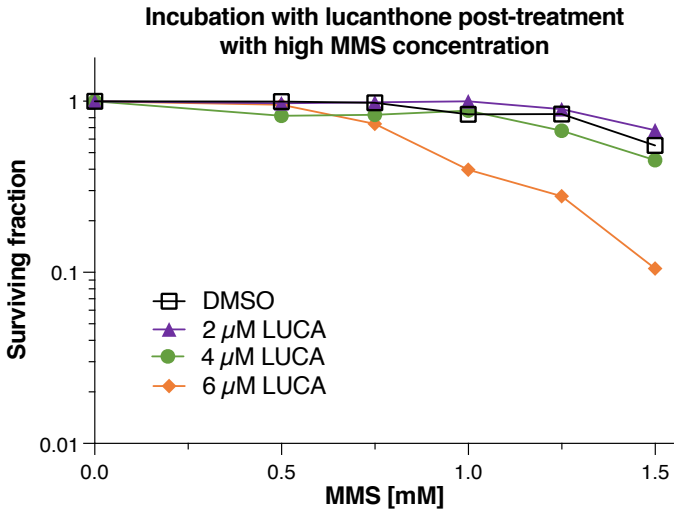
Incubation with lucanthone post-treatment
with high MMS concentration
Surviving fraction
1
0.1
0.01
0.0
0.5
1.0
1.5
MMS [mM]
DMSO
2 μM LUCA
4 μM LUCA
6 μM LUCA

Figure 5.8 Optimisation of BER inhibition with lucanthone. A - **Lucanthone removed post-treatment.** RPE-1 wild-type cells seeded at low density were incubated with three different lucanthone (LUCA) concentrations for 2 hours and then treated for 1 hour with a range of MMS concentrations. After the MMS treatment, the growth medium was changed to one not containing lucanthone. After 12 days of culture, the cell viability was assessed based on the colony number. The data shown represents optimisation of conditions with n=1. **B - Low MMS concentrations and incubation with lucanthone post-treatment.** RPE-1 wild-type cells seeded at low density were incubated with three different lucanthone (LUCA) concentrations for 2 hours and then treated for 1 hour with a range of low MMS concentrations. After the MMS treatment, the growth medium was refreshed and cells were incubated with lucanthone for another 24 hours. After 12 days of culture, the cell viability was assessed based on the colony number. The data shown represents optimisation of conditions with n=1. **C - High MMS concentrations and incubation with lucanthone post-treatment.** RPE-1 wild-type cells seeded at low density were incubated with three different lucanthone (LUCA) concentrations for 2 hours and then treated for 1 hour with a range of high MMS concentrations. After the MMS treatment, the growth medium was refreshed and cells were incubated with lucanthone for another 24 hours. After 12 days of culture, the cell viability was assessed based on the colony number. The data shown represents optimisation of conditions with n=1.

survival (Figure 5.8 A). We then lowered the concentration of MMS and added a 24-hour-long incubation with lucanthone post-MMS, which also did not impact the cell viability (Figure 5.8 B). Finally, we increased the range of MMS concentrations to the starting point and combined it with the 24 hours of post-MMS lucanthone treatment, which allowed us to observe the impact of both drugs on the cell viability (Figure 5.8 C).

To investigate whether the relationship between KEAP1 and APE1 is epistatic, wild-type and *keap1*Δ5H RPE-1 cells were plated at low density and treated with 4 μM lucanthone for 2 hours, after which they were exposed to MMS for 1 hour and incubated for another 24 hours with lucanthone to ensure a continuous APE1 inhibition. After 12 days of culture, the survival ratio was evaluated through colony forming assay. When exposed both to the APE1 inhibitor and MMS, the *keap1*Δ5H cells showed greater sensitivity than to the MMS treatment alone (Figure 5.9). The effects of *KEAP1* deletion and APE1 inhibition on *keap1*Δ5H sensitivity to MMS are additive and not epistatic, which suggests that KEAP1 does not act in BER.

To confirm this conclusion, we wished to replicate this observation in the two *keap1*Δ cell lines exhibiting a milder MMS sensitivity phenotype. We therefore adjusted the combined MMS and lucanthone treatment regimen to introduce conditions of chronic DNA damage stress, as described in the earlier chapters. Cell lines *keap1*Δ5F and *keap1*Δ8C were analysed via a colony survival assay, however the combined lucanthone and MMS treatment was repeated three times, with 48 hours of intervals between the drug administrations. Indeed, both *keap1*Δ5F and

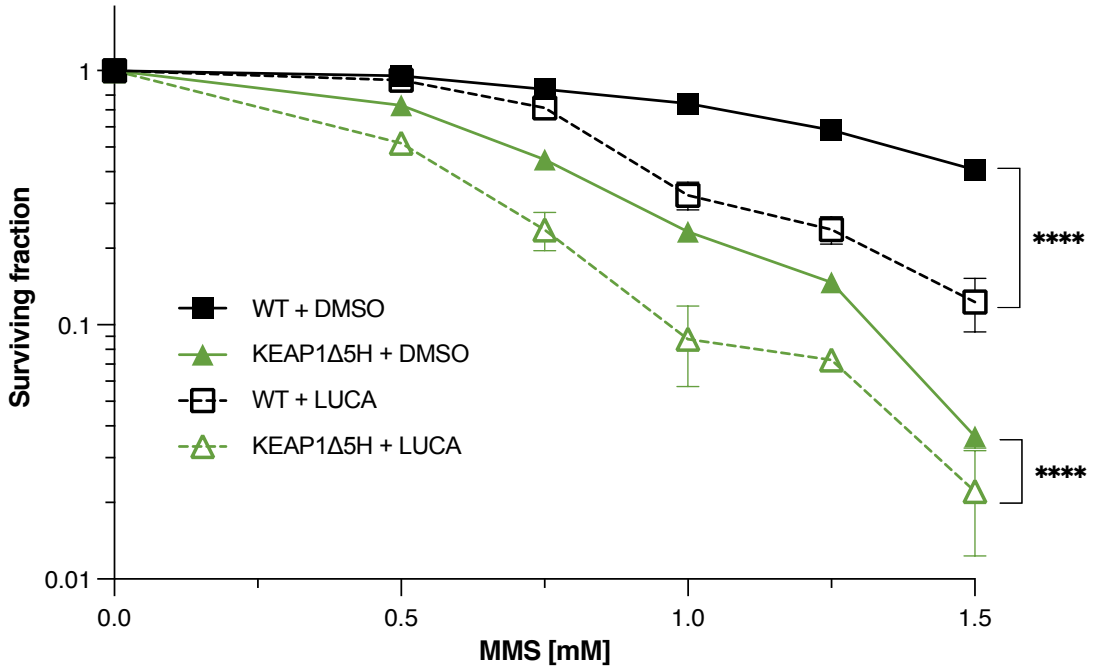

Figure 5.9 KEAP1 deletion is not epistatic with BER inhibition in *keap1*Δ5H. Wild-type RPE-1 and *keap1*Δ5H cells seeded at low density were incubated with 4 μM lucanthone for 2 hours and the treated for 1 hour with a range of MMS concentrations. After removing MMS from the medium, cells were incubated with lucanthone for further 24 hours. After 12 days of culture, the cell viability was assessed based on the colony number**;** n=3. Statistical significance was assessed by a 2-way ANOVA test.

A

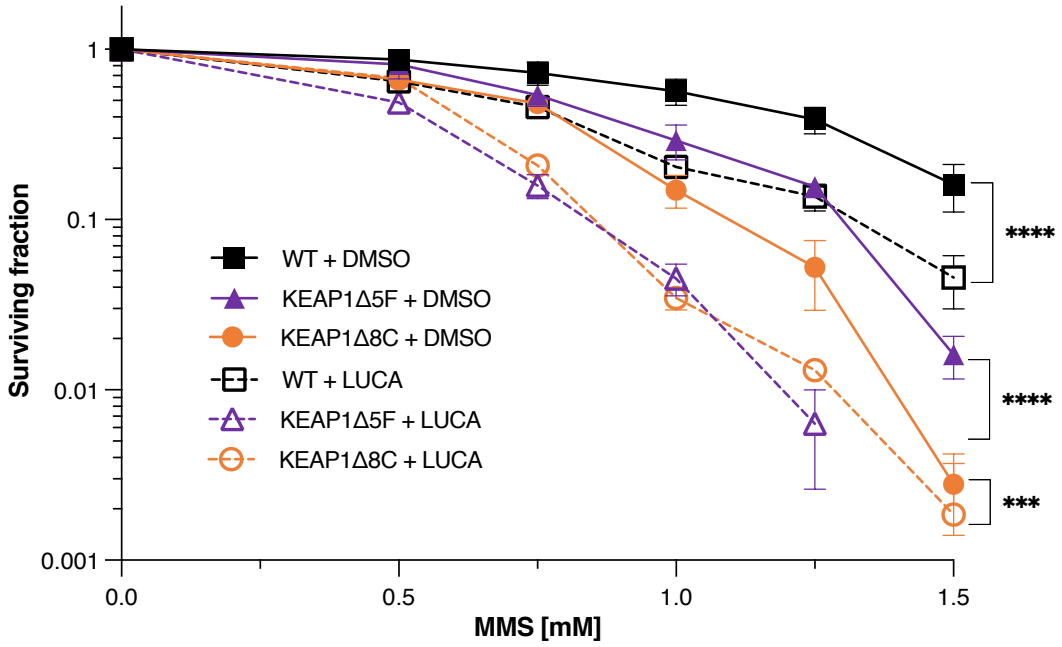

B

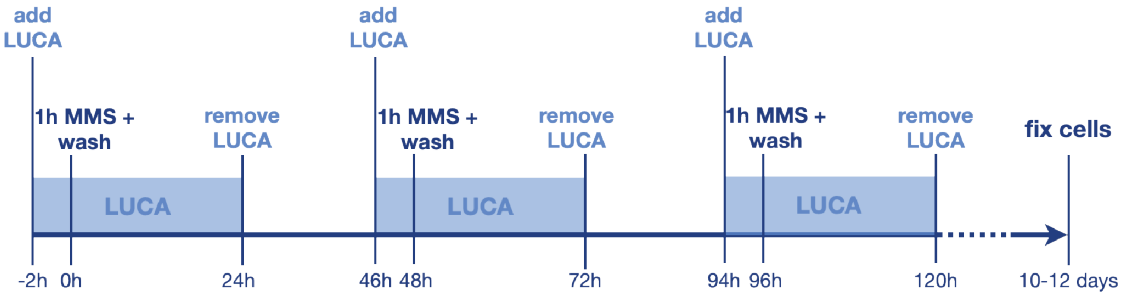

Figure 5.10 KEAP1 deletion is not epistatic with BER inhibition in conditions of chronic DNA damage. **A.** Cell lines *keap1Δ*5F, *keap1Δ*8C and wild-type RPE-1 cells seeded at low density were incubated with 4 μM lucanthone for 2 hours prior to a 1-hour treatment with a range of MMS concentrations. After removing MMS from the medium, cells were incubated with lucanthone for further 24 hours. The combined MMS and lucanthone treatment was repeated three times within 48 hour intervals. After 12 days of culture, the cell viability was assessed based on the colony number; n=3. When surviving fraction equals 0, data points are not shown on the graph. Statistical significance was assessed by a 2-way ANOVA test. **B.** Schematic representation of the chronic MMS dosage strategy combined with lucanthone (LUCA) treatment.

*keap1*Δ8C displayed sensitivity to the repeated MMS treatment alone (Figure 5.10). Addition of lucanthone combined with the MMS exposure amplified the sensitivity, which points to an additive effect of loss of KEAP1 and APE1. Taken together, these data indicate that KEAP1 and APE1 do not act through the same pathway in response to alkylation base damage. Instead, these factors seem to be involved in two independent processes resolving damage induced by MMS.

5.6 Discussion

Recruitment to the site of damage is a common characteristic of proteins involved in DNA damage recognition, signalling and repair. Having established KEAP1 plays a role in the resolution of MMS-induced damage, we wished to confirm its subcellular localisation in response to damage. Employing cell fractionation, we observed that KEAP1 localises to chromatin post-MMS exposure in U2OS cells (Figure 5.1, Figure 5.2). A pattern of a transient recruitment of KEAP1 to chromatin between two- and three-hours post-MMS exposure was identified. The transiency of KEAP1 chromatin enrichment is consistent with the dogma that repair factors need to disassociate from DNA after having fulfilled their role, which provides the downstream repair proteins with access to the lesion and enables the DNA repair to proceed smoothly.

Moreover, we have shown that the recruitment of KEAP1 to chromatin in response to MMS exposure is inhibited in the presence of olaparib, indicating PARP-dependency. KEAP1 enrichment in chromatin was also inhibited in cells lacking PARP1, confirming that it is in fact dependent on PARP1 and not an artefact of the

inhibitor activity. This PARP1-dependent chromatin recruitment of KEAP1 in the context of MMS is in line with the fact that PARP1 is involved in BER, one of the main pathways resolving alkylation base damage, and that it has been implicated in the regulation of direct repair of alkylation damage by MGMT. Upon binding to SSBs resulting from BER processing, PARP1 becomes activated and auto-PARylates itself, which facilitates the recruitment of XRCC1 to the lesion (El-Khamisy, 2003). Although, unlike XRCC1, KEAP1 lacks PAR-binding domains, there are other possible recruitment mechanisms that could be at play. We hypothesize that KEAP1 might be recruited to the lesion in a PARP-dependent manner by interacting with downstream repair proteins. We speculate that KEAP1 might be involved in regulation of base damage repair by ubiquitylation of DDR proteins at the site of damage. Although in human cells the overwhelming majority of poly(ADP-ribose) polymerase activity (85-90%) is carried out by PARP1, there is also evidence of redundancy between PARP1 and PARP2 in BER coordination, including in interaction with XRCC1 (Hoch and Polo, 2020; Ronson et al., 2018; Vasil'eva et al., 2021). Therefore, we cannot exclude the possibility that PARP2 is also involved in facilitating the accumulation of KEAP1 in chromatin following MMS exposure, and that it might also be partially redundant with PARP1 in that function. However, further research in *parp2*Δ and *parp1/2*Δ cells is needed to address this issue.

Next, we proceeded to assess which of the base damage repair pathways KEAP1 might participate in. As mentioned above, alkylation base damage is mainly resolved by BER, as well as by MGMT-mediated repair (Soll et al., 2017). PARP1 is known to be involved in BER and recently it has been reported that PARylation of MGMT by

PARP1 is required for repair of TMZ-induced methylation damage in glioblastoma (Masson et al., 1998; Wu et al., 2021). Having demonstrated that the recruitment of KEAP1 to chromatin in response to MMS-induced damage is dependent on PARP1, we hypothesised that KEAP1 might be involved in either BER or direct repair through MGMT. However, the epistatic analysis we performed with the use of pathway inhibitors suggests otherwise. Loss of KEAP1 and MGMT inhibition are not epistatic, indicating they work through different pathways. In the case of epistatic analysis of KEAP1 deletion and BER inhibition, we used an inhibitor targeting APE1, which is an enzyme responsible for one of the early stages of the pathway, preceding the assembly of the repair factors at the resulting SSB, including PARP1.

There are several possible interpretations for the lack of observed epistasis between APE1 inhibition and KEAP1 deletion. Firstly, it can be argued that KEAP1 might carry out its function in BER at an earlier step of the pathway. For example, it could regulate BER by ubiquitylating one of the DNA glycosylases. MPG, the human glycosylase required for removal of methylated bases, has been shown to interact with E3 ubiquitin ligases UHRF1 and UHRF3 (Carter and Parsons, 2018; Montaldo et al., 2019). However, there is no evidence to date that MPG is regulated by ubiquitylation. Additionally, both the timing of KEAP1 recruitment to chromatin and its dependence on PARP1 described in this chapter provide an argument against KEAP1 involvement in the initiating stage of BER.

Another scenario to consider is the participation of KEAP1 in base damage repair through an APE1-independent BER subpathway. NEIL1 and NEIL2 are DNA

glycosylase/AP lyases producing DNA incisions with 3' phosphate ends, which cannot be removed by APE1 and instead require PNKP activity (Fortini and Dogliotti, 2007; Wiederhold et al., 2004). While both NEIL1 and NEIL2 display a preference for oxidated bases regarding their DNA glycosylase activity, it has been suggested that the NEIL1/PNKP subpathway participates in the repair of AP sites produced by other DNA glycosylases, allowing to bypass the APE1 requirement for efficient BER (Wiederhold et al., 2004). It has been reported that PNKP-deficient cells are more sensitive to MMS, indicating the NEIL1/PNKP subpathway provides some redundancy with classical BER in resolution of alkylation base damage (S. Mitra and Kaina, 1993; Wiederhold et al., 2004). Furthermore, NEIL1 is known to bind PARP1 and stimulate its poly(ADP-ribosyl)ation activity (Hegde et al., 2012; Noren Hooten et al., 2012). KEAP1 could potentially interact with the NEIL1/PNKP subpathway downstream of PARP1. However, considering the increased MMS sensitivity of *keap1*Δ cells with undisturbed BER, as described in previous chapters, such a scenario seems rather unlikely. If KEAP1 did in fact participate in MMS-induced damage resolution through the NEIL1/PNKP subpathway, then in the context of repair of alkylation base damage in the presence of functional MPG the *keap1*Δ phenotype would be masked by redundancy with classical BER.

Furthermore, it is possible that KEAP1 might convey the MMS tolerance by participating in replication-coupled repair. These replication stress response mechanisms enable the replication fork to overcome the hindrance of unresolved lesions, including base damage. Importantly, PARP1 has been implicated in the regulation of one of these pathways, namely the fork reversal (Ray Chaudhuri et al.,

2012). PARP1 prevents the fork restart and stabilises the reversed replication forks (Berti et al., 2013). It is tempting to speculate that KEAP1 could participate in fork reversal regulation via an interaction downstream of PARP1. However, it has been recently reported that PARP1 activity at reversed replication fork is inhibited upon ubiquitylation by an E3 ubiquitin ligase MDM2, which promotes PARP1 degradation and replication fork progression (Giansanti et al., 2022). Although not completely excluding such scenario, this finding would argue against KEAP1 directly ubiquitylating PARP1 in the context of reversed fork in a manner similar to MDM2. While it is not uncommon for a protein to be targeted by more than one ubiquitin ligase, this study demonstrates that ubiquitylation of PARP1 at a perturbed replication fork counteracts the repair of the damage by fork reversal inhibition. PARP1 also interacts with PCNA, a critical factor in DNA replication and replication-associated processes (Boehm et al., 2016; Prosperi and Scovassi, 2013). PCNA mono- and polyubiquitylation plays a crucial role in determining between translesion synthesis (TLS) and template switching (TS) pathways (Kanao and Masutani, 2017). PCNA monoubiquitylation triggers TLS, while polyubiquitylation promotes repair through TS and fork reversal (Ashour and Mosammaparast, 2021b; Kannouche et al., 2004; Vujanovic et al., 2017). While the E3 ubiquitin ligases HLTF and SHPRH are responsible for PCNA polyubiquitylation in mammalian cells, polyubiquitylated PCNA is still present in *Hltf/Shprh* double-deficient mouse embryonic fibroblasts (Krijger et al., 2011; Seelinger and Otterlei, 2020). Thus, another E3 ligase must be involved in PCNA polyubiquitylation (Qiu et al., 2021). KEAP1 could hypothetically play that role in a PARP1-dependent manner. However, more research is necessary to evaluate the possible role of KEAP1 in replication-coupled repair.

Finally, KEAP1 could be contributing to the resolution of MMS-induced DNA damage through another, yet unknown pathway. Recent research has identified a novel alkylation-specific damage repair pathway relying on an E3 ubiquitin ligase (Brickner et al., 2017a). Ubiquitin signalling is sensed by the ASCC complex, which induces recruitment of alkylation repair enzymes ALKBH3 and ASCC3 (Brickner et al., 2017b). Given the well-established function of KEAP1 as a ubiquitin ligase substrate adaptor, it is tempting to hypothesise that KEAP1 could also regulate a novel alkylation damage repair pathway through ubiquitylation.

In this chapter, we demonstrated that KEAP1 is enriched in chromatin following MMS exposure. This is supporting the evidence for the role KEAP1 plays in MMS-induced DNA damage repair, which was presented in previous chapters. Moreover, we showed that the recruitment of KEAP1 to chromatin is dependent on PARP1, which is also known to be involved in response to MMS damage. Next, we probed whether in this context KEAP1 might act through one of the main pathways responsible for resolution of alkylation base damage, namely direct repair by MGMT or through BER. However, after having conducted epistatic analysis using pathway inhibitors, we propose that KEAP1 is likely involved in an alternative pathway resolving base damage.

6. KEAP1 relationship with PARP inhibitors and PARP trapping

6.1 Introduction

6.1.1 Synthetic lethal relationship between PARP inhibition and HR deficiency

KEAP1 is required for tolerance of MMS-induced damage (Chapter 3). Although identifying the pathway that KEAP1 functions in to carry out this novel role has proved challenging, our data demonstrates a critical requirement for PARP1 in the recruitment of KEAP1 to chromatin following MMS exposure. Loss of PARP1 or PARP inhibition are synthetic lethal with defective homologous recombination (HR) repair (Bryant et al., 2005; Farmer et al., 2005; Ronson et al., 2018). Although PARP inhibition was initially found to be synthetic lethal with BRCA1/2 deficiency, it has been demonstrated that this relationship extends to BRCAness, which describes mutations mimicking BRCA1/2 deficiency (Byrum et al., 2019). While the consensus on the exact mechanism responsible for the synthetic lethal interaction between PARP inhibition and BRCAness is yet to be reached, it is understood that the cytotoxicity results from functional loss of two partially redundant DNA damage repair pathways. Considering the PARP1-dependent chromatin enrichment of KEAP1, we hypothesise that loss of KEAP1, similar to PARP1 loss or inhibition, might be synthetic lethal with defective HR.

6.1.2 Synthetic lethality and PARP 'anti-trappers'

Counterintuitively, PARP inhibition is also synthetic lethal with the loss of certain PARP1-dependent factors. PARP inhibition by either olaparib or veliparib results in hypersensitivity in Polβ-deficient and in XRCC1-deficient cells (Horton et al., 2014). Both XRCC1 and Polβ function in BER pathway in a PARP1-dependent manner (Campalans et al., 2013; Sukhanova et al., 2010). Moreover, loss of the chromatin remodeler ALC1, whose activation relies on binding through its macrodomain to PARP1-synthetised PAR chains, is also synthetic lethal with PARP inhibition (Blessing et al., 2020; Ooi et al., 2021).

Synthetic lethality between two factors acting in the same pathway, as opposed to two different pathways as is the case for PARPi and BRCA1/2 deficiency, may seem contradictory. However, recent reports have demonstrated that PARP trapping plays an important role in those synthetic lethal relationships. Blessing *et al.* found that cells deficient in ALC1 display retention of PARP2, but not PARP1, at the DNA damage sites (Blessing et al., 2020). This effect was potentiated by the trapping properties of PARPi, and the PARP2 retention in chromatin in ALC1-deficient cells was reversed upon re-expression of wild-type ALC1, proving that ALC1 is necessary for the release of PARP2 from chromatin (Blessing et al., 2020). In line with the model of PARP trapping driving the synthetic lethal interaction between BRCA deficiency and PARPi, the anti-trapping function of ALC1 provides an explanation for the synthetic lethal interaction between ALC1-deficiency and defective HR (Hewitt et al., 2021). Another study published later that month reported that ALC1 is required

for the removal of inactive PARP1 from chromatin, demonstrating that ALC-deficient cells display increased levels of PARP1 trapping, which is enhanced in the presence of PARPi (Juhász et al., 2020). A different group has shown that XRCC1 prevents endogenous PARP1 trapping and SSB accumulation during BER (Demin et al., 2021). Interestingly, loss of XRCC1 results in PARP1 trapping after exposure to MMS with or without PARP inhibition, but no trapping was observed when treated with PARPi KU0058948 only (Demin et al., 2021). The newly described roles of ALC1 and XRCC1 as PARP 'anti-trappers' provide an explanation of the synthetic lethal interaction with trapping PARPi, such as olaparib (Murai et al., 2012; Rose et al., 2020). Taken together, these reports suggest an alternative scenario is possible, where the loss of PARP1-dependent KEAP1 would be synthetic lethal with PARP inhibition, and KEAP1 could function as a PARP1 'anti-trapper'.

6.2 Aims

KEAP1 is required for tolerance of MMS-induced damage and is recruited to chromatin in a PARP-dependent manner following MMS exposure. Given this PARP1-dependence and the known synthetic lethal relationship between PARP inhibition and HR, we hypothesise that loss of KEAP1 is also synthetic lethal with HR disruption. In this chapter we will investigate the effect of BRCA1 depletion and Rad51 inhibition on the survival of *keap1*Δ cells to test this hypothesis. Taking into account the synthetic lethality between PARPi and loss of PARP-dependent factors recently shown to function as PARP 'anti-trappers', we will also consider possible cytotoxic interaction between KEAP1-deficiency and PARPi. We hypothesise that alternatively,

KEAP1 could assist PARP1 removal from DNA damage sites. This will be addressed by examining the relationship between KEAP1 loss and PARP inhibition, as well as by analysis of poly(ADP-ribosyl)ation changes and PARP trapping in the chromatin of *keap1*Δ cells.

6.3 KEAP1 deletion is not synthetic lethal with HR

Considering PARP1 is required to recruit KEAP1 to sites of MMS-induced damage, we wanted to test whether the loss of KEAP1 is synthetic lethal with HR. Using siRNA, we depleted one of the critical HR factors, BRCA1, both in wild-type RPE-1, *keap1*Δ and *parp1*Δ cells. The cells were then seeded at low density, cultured for 10-12 days and analysed for the number of surviving colonies (Figure 6.1). Interestingly, we did not observe a negative effect of BRCA1 depletion on the survival rate of *keap1*Δ cells. It is worth noting, however, that the cell line we used as a positive control, *parp1*Δ54 (RPE-1-derived PARP1-deficient clonal cell line described by Ronson et al., 2018), showed only a mild sensitivity to BRCA1 depletion that is not statistically significant. Given the well documented synthetic lethal relationship between impaired HR and PARP1 loss or inhibition, we were expecting a more prominent synthetic killing effect on the *parp1*Δ cells (Fong et al., 2009; Ronson et al., 2018). Although we confirmed the BRCA1 depletion via Western blotting, this cell line behaviour makes the data difficult to interpret.

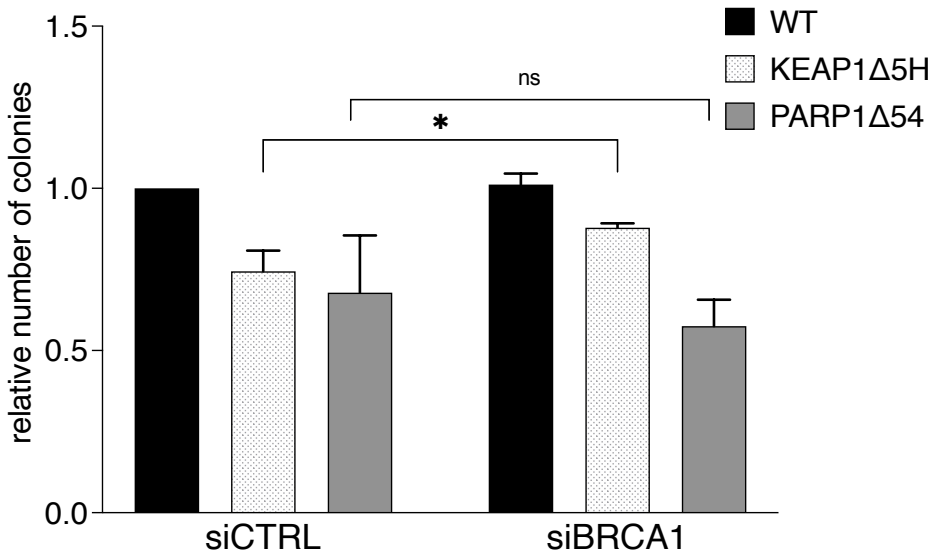

Figure 6.1 KEAP1 deletion is not synthetic lethal with BRCA1 depletion. RPE-1 cells were transfected with 50 nM siRNA, either non-targeting (siCTRL) or targeting BRCA1 (siBRCA1). Transfection was repeated twice with a 24 hour incubation period. 24 hours after the second transfection, cells were seeded at low density and cultured for 10-12 days to be assessed in a clonogenic survival assay. Values shown are average numbers of colonies relative to WT siCTRL, collected from three independent experiments.

To further explore the question of synthetic lethality between the loss of KEAP1 and impaired HR, we employed the Rad51 inhibitor B02. Rad51 is a crucial factor for HR, as it binds to single stranded DNA and participates in the formation of nucleofilament, promoting DNA strand exchange (Huang et al., 2012). The B02 inhibitor prevents Rad51 binding to DNA, disrupting HR, and has been shown to result in synthetic lethality when combined with PARP1 loss (Huang et al., 2012; Ronson et al., 2018). We inhibited Rad51 using a range of B02 concentrations in wild-type and *keap1*Δ RPE-1 cell lines and compared cell survival in a colony formation assay (Figure 6.2). Again, we did not observe lower viability in any of the KEAP1-deficient cell lines, which indicates there is no synthetic lethal relationship between KEAP1 loss and Rad51 inhibition. However, also in this experiment the control cell line *parp1*Δ54 did not behave as predicted and exhibited no sensitivity to Rad51 inhibition. While our group had previously successfully demonstrated synthetic lethal interaction between Rad51 inhibition and PARP1-deficiency, those experiments were performed using *parp1*Δ U2OS cell lines, which are not suitable as a control for the RPE-1-derived *keap1*Δ cells (Ronson et al., 2018). Although a reliable positive control is an issue that should be corrected in future experiments, we did not observe any synthetic lethal interaction between KEAP1 loss and HR disruption in repeated experiments.

6.4 KEAP1 deletion is synthetic lethal with PARP inhibition

Disruption of the PARP1-dependent chromatin remodeller ALC1 has recently been shown to cause cells to become hypersensitive to PARP inhibitors

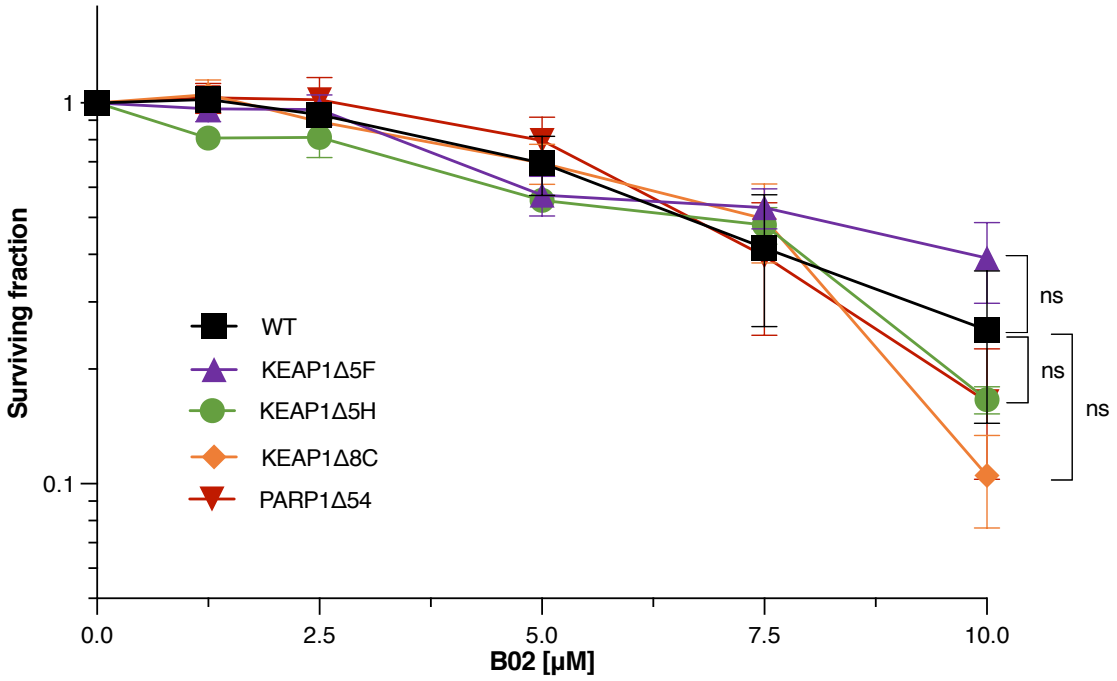

Figure 6.2 KEAP1 deletion is not synthetic lethal with Rad51 inhibition. RPE-1 cells were seeded at low density were incubated with B02 for 48 hours. After 12 days of culture, the cell viability was assessed based on the colony number; n=3. Statistical significance was tested with two-way ANOVA.

(Blessing et al., 2020). XRCC1 deficiency also results in hypersensitivity to PARP inhibition (Horton et al., 2014). Given that we observed the dependence of KEAP1 on PARP1 in the recruitment to chromatin, we hypothesised that disruption of KEAP1, similarly to ALC1 and XRCC1, might be synthetic lethal with PARP inhibition. To test this hypothesis, we assessed the cytotoxicity of KEAP1 gene disruption and olaparib treatment. Wild-type RPE-1 and *keap1*Δ cell lines were treated with various concentrations of olaparib for 24 hours and cell survival was assessed through a colony formation assay (Figure 6.3). As a positive control for synthetic lethality, RPE-1 wild-type cells were depleted of BRCA2 using siRNA and then treated with olaparib along with the other cell lines. Interestingly, two of the KEAP1-deficient cell lines, *keap1*Δ5H and *keap1*Δ8C, were sensitive to olaparib, suggesting a synthetic lethal interaction between KEAP1 deficiency and PARP inhibition. Variability in olaparib sensitivity between the *keap1*Δ cell lines, including a weaker phenotype for clone *keap1*Δ5F, could be possibly attributed to clonal variation, and it is not uncommon to observe some phenotypic differences between CRISPR-Cas9 knockout clones.

To confirm the observed synthetic lethal interaction between KEAP1 deficiency and PARP inhibition, clonogenic survival assays were repeated using 5H and 8C *keap1*Δ cell lines with re-expressed wild-type KEAP1. Wild-type RPE-1, *keap1*Δ5H and *keap1*Δ8C cells, carrying either an empty vector of expressing wild-type KEAP1, were treated with increasing olaparib concentrations and assessed for cell viability through a colony forming assay (Figure 6.4). Both *keap1*Δ5H and *keap1*Δ8C transduced with an empty vector display olaparib sensitivity comparable with or more severe than BRCA2-deficient cells. However, the olaparib sensitivity phenotype

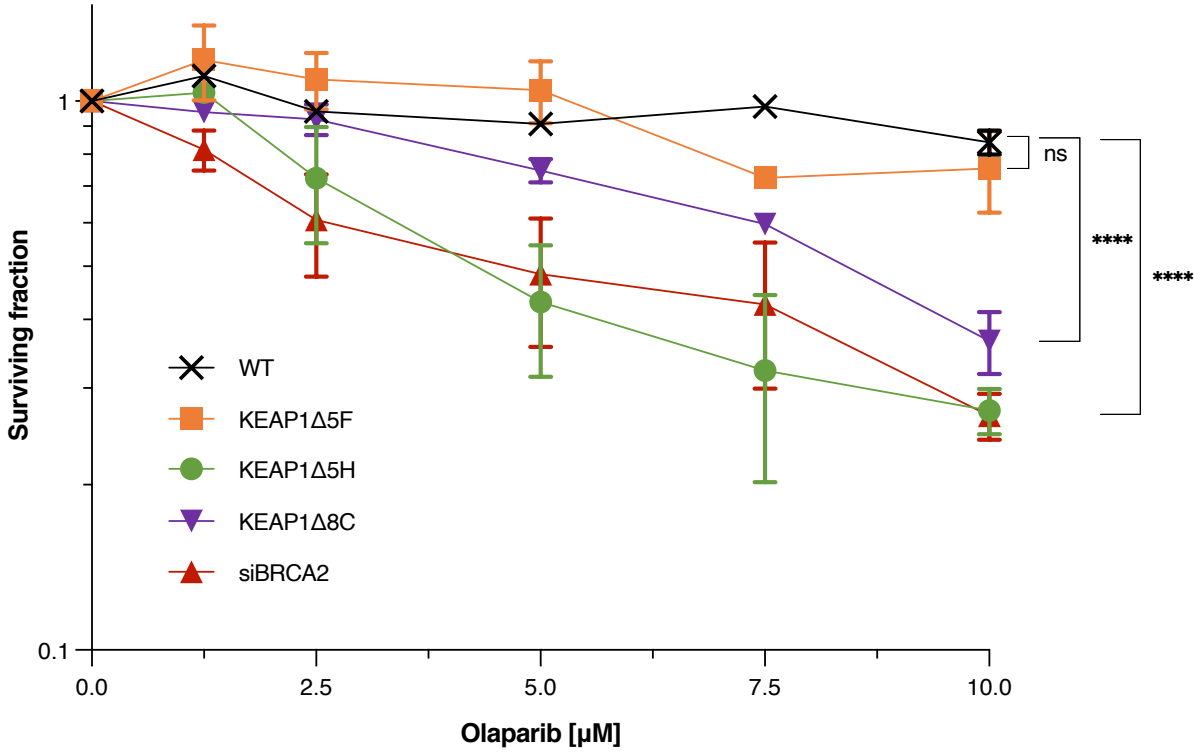

Figure 6.3 Loss of KEAP1 is synthetic lethal with PARP inhibition. Cell lines *keap1Δ*5F, *keap1Δ*5H, *keap1Δ*8C, wild-type RPE-1 cells and BRCA2 knockdown RPE-1 cells were seeded at low density were incubated with olaparib for 24 hours. After 12 days of culture, the cell viability was assessed based on the colony number; n=3. Statistical significance tested via two-way ANOVA.

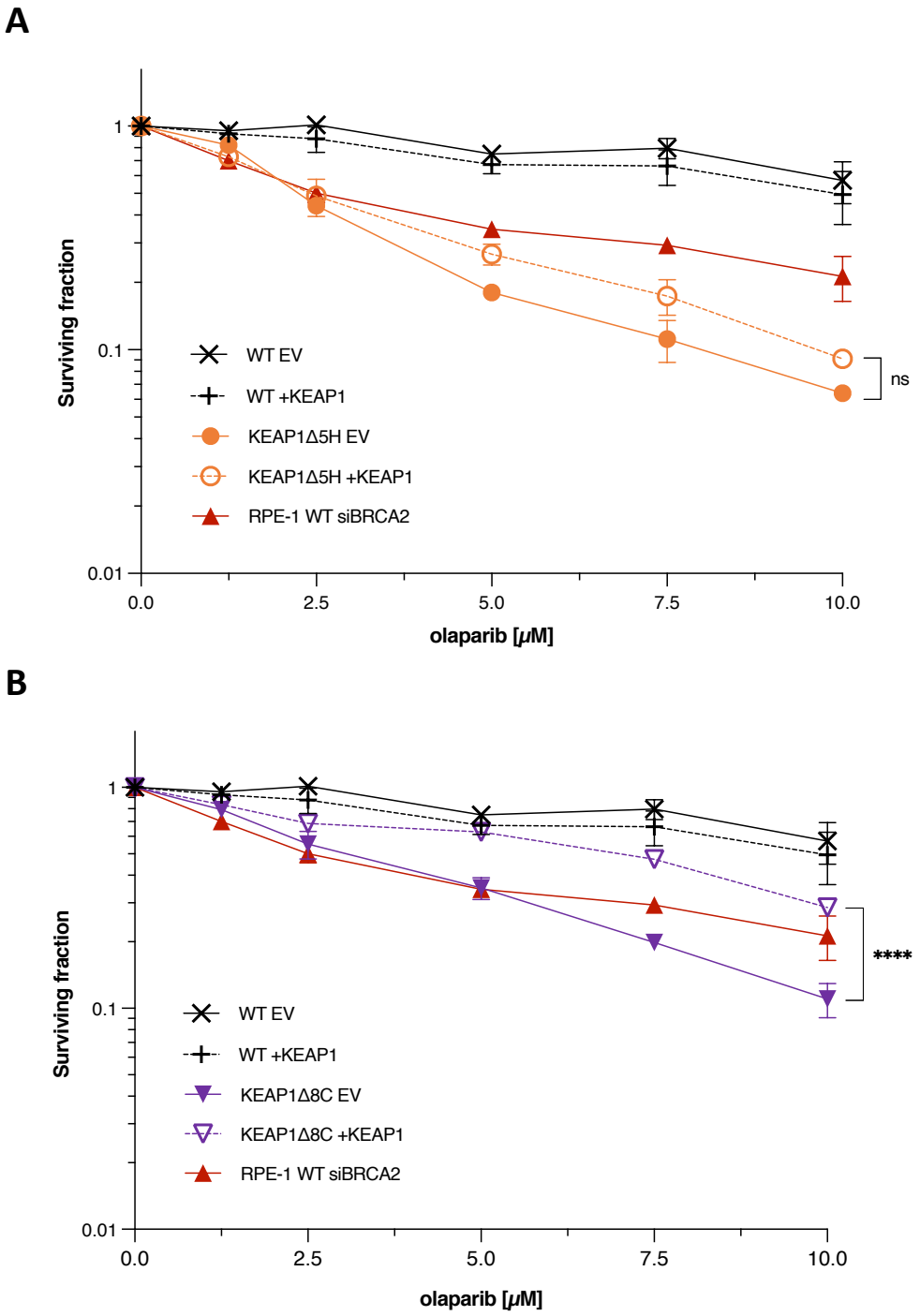

Figure 6.4 Sensitivity to PARP inhibition is complemented upon re-expression of KEAP1 in *keap1Δ8C* but not in *keap1Δ5H.* Cell lines *keap1Δ*5H, *keap1Δ*8C and wild-type RPE-1 cells, transduceded either with an empty vector (EV) or with a vector encoding HA-Flag-KEAP1 (+KEAP1), were seeded at low density were incubated with olaparib for 24 hours. BRCA2 knockdown RPE-1 cells were used as a positive control and treated in the same way. After 12 days of culture, the cell viability was assessed based on the colony number. Datasets were split for clarity and the graphs illustrate the olaparib effect on **A.** *keap1Δ*5H cells **B.** *keap1Δ*8C cells; n=3. Statistical significance tested via two-way ANOVA.

is complemented upon re-expression of KEAP1 in *keap1*Δ8C, but not in *keap1*Δ5H. It is worth noting that the *keap1*Δ5H cell line also exhibits a more severe MMS sensitivity compared to *keap1*Δ8C and *keap1*Δ5F, and unlike the other *keap1*Δ cell lines, the MMS sensitivity phenotype is only partially complemented in the *keap1*Δ5H clone. This again suggests that the *keap1*Δ cell line might carry an additional mutation that exacerbates its sensitivity to DNA damage beyond the effect of KEAP1 loss. However, the hypersensitivity to PARP inhibition observed in both 5H and 8C clones of *keap1*Δ cell lines, together with complementation of this phenotype in the 8C clone in the presence of wild-type KEAP1, suggest a possible synthetic lethality between KEAP1 deficiency and PARP inhibition.

6.5 KEAP1 domain requirement for PARPi tolerance

Having established that loss of KEAP1 and PARP inhibition are synthetic lethal and that re-expression of wild-type KEAP1 complemented this phenotype in *keap1*Δ8C cells, we set out to determine which of the KEAP1 domains is required to convey olaparib tolerance. To address this question, we performed clonogenic survival assays to assess the olaparib sensitivity of *keap1*Δ8C cells either lacking KEAP1, or with re-expressed wild-type KEAP1 or mutant KEAP1 proteins (Figure 6.5). The mutant KEAP1 constructs included the domain mutants KEAP1$^{\Delta BTB}$, KEAP1$^{\Delta KELCH}$ and KEAP1^{S3H4}, as well as the mutant of highly reactive cysteines, KEAP1$^{11Cys\text{-}less}$, which were described in detail in Chapter 4. In line with the previous result, loss of KEAP1 was synthetic lethal with PARP inhibition, while re-expression of wild-type KEAP1 rescued that phenotype. Consistent with what we observed in the case of MMS-

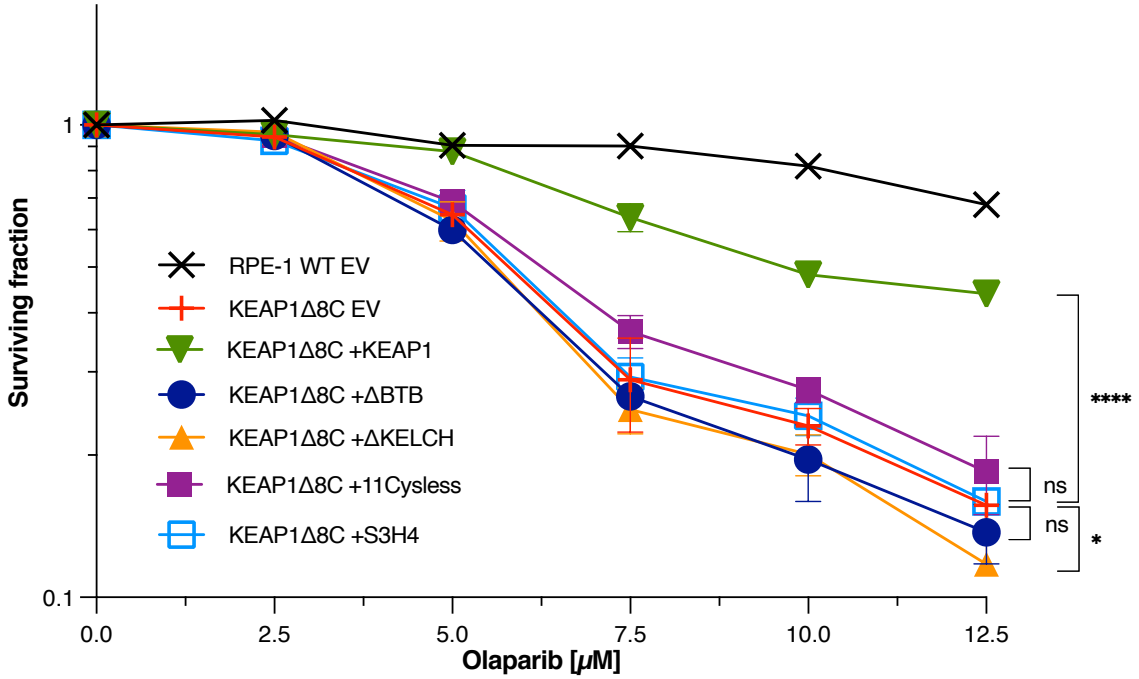

Figure 6.5 All domains of KEAP1 are required to complement olaparib sensitivity. Cell lines *keap1Δ8C* expressing either mutant proteins KEAP1$^{\Delta BTB}$, KEAP1$^{\Delta KELCH}$, KEAP1^{S3H4} and KEAP1$^{11Cys\text{-}less}$ or wild-type KEAP1, or expressing an empty vector, were seeded at low density and incubated with olaparib for 24 hours. After 12 days of culture, the cell viability was assessed based on the colony number; n=3. Statistical significance was tested with two-way ANOVA.

induced damage tolerance, each of the three mutations within KEAP1 domains results in the inability of the protein to complement the phenotype of olaparib sensitivity. This indicates the functional importance of both the BTB and the Kelch domains in PARP inhibition tolerance.

Interestingly, the reactive cysteines mutant KEAP1$^{11Cys\text{-}less}$ failed to rescue the olaparib sensitivity phenotype of the *keap1*Δ8C cell line (Figure 6.5). This data demonstrates the requirement for one or more of the mutated cysteine residues and suggests that the cysteine sensor mechanism of KEAP1 might play a role in conveying tolerance to PARP inhibition. Intriguingly, this observation is in contrast to the KEAP1$^{11Cys\text{-}less}$ mutant complementing the MMS sensitivity in *keap1*Δ8C and *keap1*Δ5H cells on par with the wild-type KEAP1 (Figure 4.10, Figure 4.11). Thus, it is likely that conveying tolerance to MMS-induced damage and to PARP inhibition are two novel, but separate, functions of KEAP1.

6.6 PARP trapping in *keap1*Δ cells

In addition to inhibiting the catalytic activity of PARPs, olaparib also traps PARP1 and PARP2 bound to the damaged DNA, which contributes to the inhibitor's toxicity (Murai et al., 2012). Given the trapping properties of olaparib, it is tempting to speculate that the PARP inhibition-induced toxicity observed upon loss of KEAP1 results from PARP accumulation at the site of DNA damage. Our results demonstrating PARP1-dependent recruitment of KEAP1 to chromatin, together with recent reports of ALC1 and XRCC1 acting as PARP anti-trappers, prompted us to

hypothesise that KEAP1 might contribute to resolution of MMS-induced damage by removing PARP from the site of DNA lesion (Blessing et al., 2020; Demin et al., 2021). To test this hypothesis, we examined the retention of PARPs in chromatin of KEAP1-deficient cells.

To explore the impact of KEAP1 loss on PARP trapping and activity, we first examined the changes to the poly(ADP-ribosyl)ation pattern in *keap1*Δ5H cells exposed to DNA damage by MMS. Cells were treated with 1.5 mM MMS for 1 hour and allowed 1-6 hours of recovery, then collected and processed for whole-cell extracts and cell fractionation. The protein samples of the whole-cell extract and the chromatin fraction were analysed for the intensity of the poly(ADP-ribosyl)ation signal by Western blotting (Figure 6.6). The level of poly(ADP-ribosyl)ation 0-3 hours after MMS exposure is higher both in the whole-cell extracts and in the chromatin fraction of *keap1*Δ5H cells compared to wild-type. This elevated level of poly(ADP-ribosyl)ation in KEAP1-deficient cells could result from hyperactivation of PARPs due to increased level of DNA damage. Alternatively, chromatin retention of activated PARPs might cause the observed increase in poly(ADP-ribosyl)ation.

Next, we examined the recruitment of PARP1 and PARP2 to chromatin in KEAP1-deficient cells. Wild-type RPE-1 and *keap1*Δ5H cells were treated with 1.5 mM MMS for 1 hour and allowed to recover for 1-6 hours, after which they were harvested and processed for cell fractionation. Whole cell extracts and the chromatin-enriched fractions were analysed for specific protein signals by Western blotting (Figure 6.7

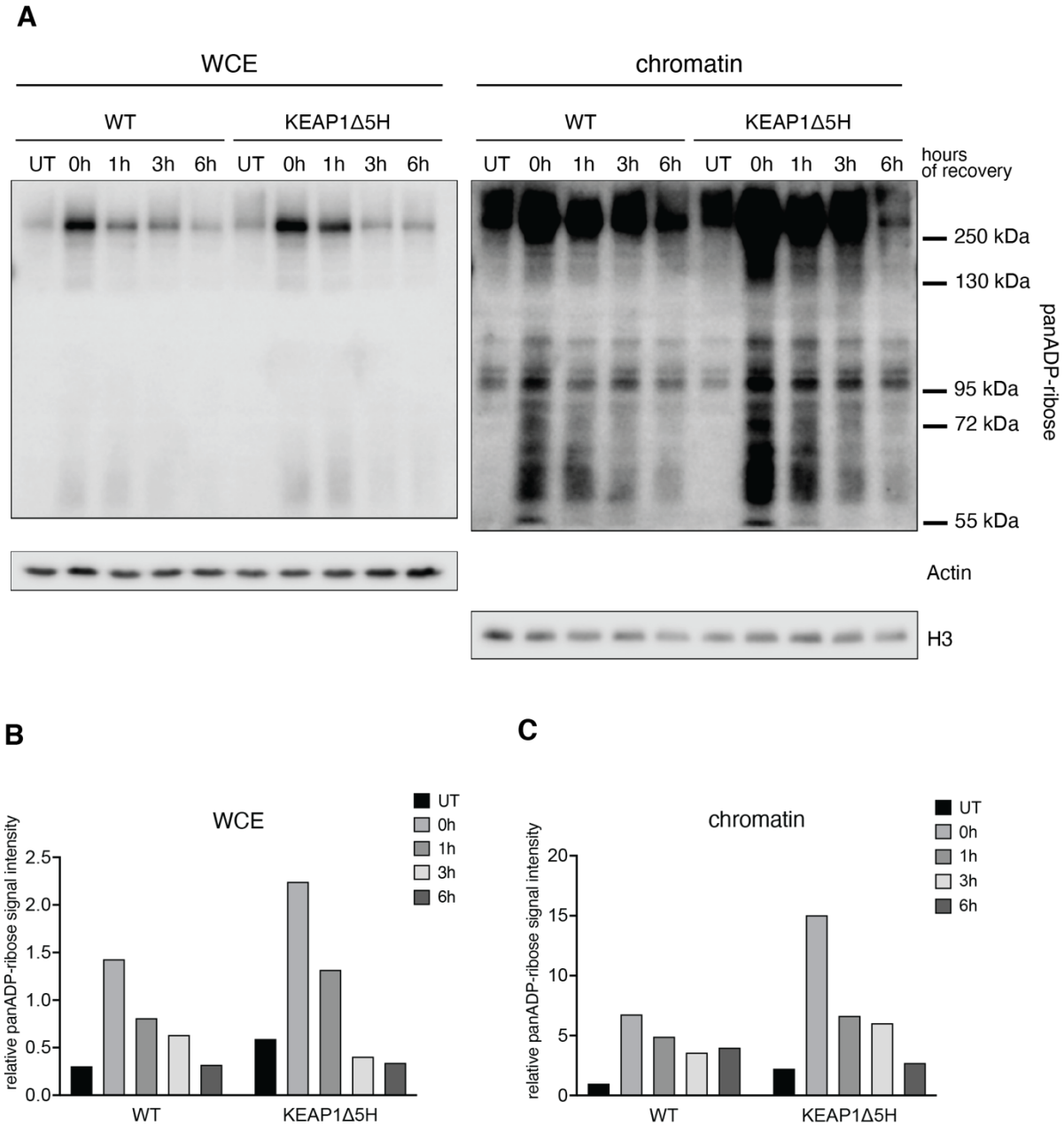

Figure 6.6 Loss of KEAP1 results in elevated levels of poly(ADP-ribosyl)ation in response to MMS exposure. Wild-type RPE-1 and *keap1Δ*5H cells were treated with 1.5 mM MMS for 1 hour, then harvested at different recovery time points and processed for cell fractionation. **A.** Level of poly(ADP-ribosyl)ation of proteins in the whole cell extracts (WCE) and in the chromatin-enriched fraction was assessed via Western blotting. The signal from anti-panADP-ribose antibody was quantified and shown as **B.** relative to the actin signal for WCE and **C.** relative to the H3 signal for the chromatin fraction; n=1.

A). Strikingly, while the chromatin-bound level of PARP1 in wild-type cells peaked at 1 hour post-treatment, in the KEAP1-deficient cells we observed chromatin retention of PARP1 into the sixth hour post-treatment. However, at lower levels, the chromatin retention of PARP2 was also observed in MMS-treated *keap1*Δ cells. Moreover, an accumulation of XRCC1 and increased levels of γH2AX can be observed in the chromatin fraction of the KEAP1-deficient cell line in response to MMS, indicating accumulating DNA damage. The signal intensities for chromatin-bound PARP1 and PARP2 from three independent experiments were measured using ImageStudioLite software and plotted as relative to the H3 signal intensity (Figure 6.7 B, C). This quantitative analysis confirmed the observed PARP1 and PARP2 retention in chromatin in KEAP1-deficient cells in response to MMS-induced damage.

One intriguing interpretation of the data in this chapter is that KEAP1 deficiency results in the retention of PARP1 and PARP2 in chromatin when exposed to DNA damage, an effect which can be exacerbated by the PARP-trapping quality of olaparib. Alternatively, the increased levels of poly(ADP-ribosyl)ation and increased recruitment of PARP1 and PARP2 to chromatin could be explained by the accumulation of DNA damage due to defective DNA damage repair in KEAP1-deficient cells.

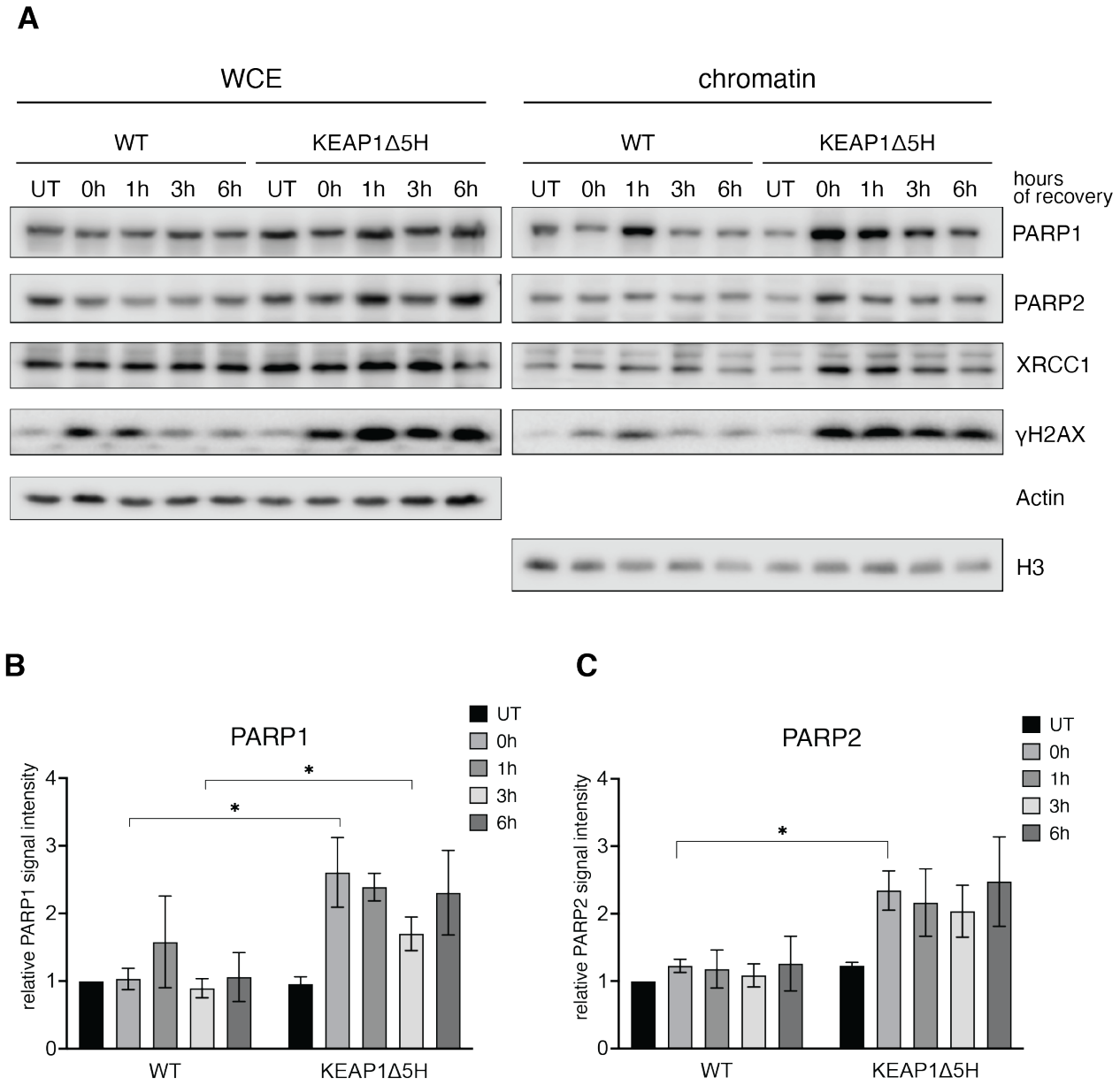

Figure 6.7 Loss of KEAP1 results in PARP retention in chromatin. Wild-type RPE-1 and *keap1Δ*5H cells were treated with 1.5 mM MMS for 1 hour, then harvested at different recovery time points and processed for cell fractionation. **A.** Protein expression levels in the whole cell extracts (WCE) and in the chromatin-enriched fraction were assessed via Western blotting. Signal intensity relative to H3 was measured across three independent experiments and plotted for chromatin-bound **B.** PARP1 and **C.** PARP2; n=3.

6.7 Discussion

In this chapter, we explored the relationships of KEAP1 with factors that are known to be synthetic lethal with PARP inhibition. Since it is known that PARP inhibition is synthetic lethal with several PARP-dependent factors, we also considered that loss of KEAP1 might lead to hypersensitivity when combined with PARPi. This was motivated by the PARP1-dependency of KEAP1 in recruitment to chromatin following MMS exposure that we demonstrated earlier.

First, we tested whether KEAP1-deficiency, analogously to PARP1 loss or inhibition, would result in hypersensitivity when combined with deficient HR. However, neither BRCA1 depletion nor inhibition of Rad51 led to increased sensitivity of *keap1*Δ cells. These results indicate there is no synthetic lethal interaction between KEAP1 loss and HR deficiency. Of note, this would be in support of our data from Chapter 5, where we demonstrated that KEAP1 does not act through the canonical BER pathway. However, these conclusions should be approached with caution due to the abnormal behaviour of the RPE-1-derived *parp1*Δ54 control cell line, which exhibited mild to none synthetic lethal effect with HR disruption. While our group has demonstrated synthetic lethal interaction with Rad51 inhibition in PARP1-deficient U2OS-derived cell lines, similar experiments were not performed using the *parp1*Δ54 cell line outside of the work described in this thesis (Ronson et al., 2018). The *parp1*Δ54 cell line was confirmed to be truly PARP1-deficient through sequencing and Western blotting, and similarly to the U2OS-derived cell line it exhibits increased MMS sensitivity and elevated Rad51 foci in response to MMS in XRCC1-depleted

background (Ronson et al., 2018). It is possible that an off-target Cas9 activity resulted in a mutation or chromosomal rearrangement which affects the cell line phenotype in the context of B02 inhibition. An alternative positive control for synthetic lethality between PARP1-deficiency and HR disruption for future experiments could be inhibition of PARP1 in wild-type RPE-1 cells by olaparib, combined with HR disruption.

Having concluded that loss of KEAP1 is not synthetic lethal with HR deficiency, we addressed the possibility that it might be instead synthetic lethal with PARP inhibition. Indeed, the *keap1*Δ5H and *keap1*Δ8C cell lines are sensitive to olaparib. This cytotoxic effect was reverted upon re-expression of wild-type KEAP1 in the 8C but not in the 5H *keap1*Δ cell line. Although the lack of phenotype complementation in the *keap1*Δ5H clone suggests a certain amount of caution in drawing conclusions, the rescue of clone 8C is statistically significant. This data advocates for a synthetic lethal interaction between KEAP1 deficiency and PARP inhibition. Given the fact that KEAP1 recruitment to chromatin is dependent on PARP1, this relationship might seem counterintuitive. However, it would be in line with deficiencies of other PARP-dependent DNA damage repair factors, such as XRCC1 and ALC1, being synthetic lethal with PARP inhibition (Blessing et al., 2020; Horton et al., 2014). Both ALC1 and XRCC1 have recently been described as PARP 'anti-trappers' (Blessing et al., 2020; Demin et al., 2021). It is therefore tempting to speculate that after being recruited to chromatin in a PARP1-dependent manner, KEAP1 might similarly play a role in removing bound PARPs from DNA damage sites. In accordance with this model, PARPi would exacerbate PARP trapping which cannot be removed in the absence of

KEAP1, and therefore lead to hypersensitivity. However, a previous study reported a different effect of PARP inhibition on KEAP1-deificient cells (Orthwein et al., 2015). In contrast to our data, Orthwein *et al.* observed resistance to olaparib upon deletion of KEAP1 in 293T cells (Orthwein et al., 2015). This discrepancy could be a result of genetic differences between cell lines. Unfortunately, the cell line used in the 2015 study by Orthwein *et al.* was unavailable upon request as it had been lost, therefore we were not able to use it to test our findings.

We have found that both the BTB and the Kelch domains are required for KEAP1 to protect against the cytotoxic effect of PARP inhibition. This is in agreement with our previous observation of the requirement for both of these domains in conferring MMS tolerance. While the BTB domain of KEAP1 is required for homodimerisation and to enable binding to CUL3, the Kelch domain is necessary for binding to the substrates (Baird and Yamamoto, 2020; Tian et al., 2018). This would therefore indicate that in the context of preventing the cytotoxic effect of PARPi, similarly as in the context of MMS tolerance, KEAP1 might be acting as an E3-ubiquitin ligase complex.

In contrast to our data in the context of MMS-induced damage, the KEAP1$^{11\text{Cys-less}}$ mutant failed to complement the phenotype of hypersensitivity to PARPi in KEAP1-deficient cells. This indicates that the cysteine stress sensor is required for the protective function of KEAP1 against PARPi. We could speculate that the small molecule PARP inhibitor, olaparib, might be an inducer recognised by the cysteine sensor. Following the model of NRF2 inducers, this would then trigger inactivation of

KEAP1 and prevent ubiquitylation of its substrate. However, it is unclear why inhibiting ubiquitylation of the KEAP1 substrate in the context of PARP inhibition would be protective, while KEAP1 loss leading to permanent ubiquitylation evasion by the substrate would result in synthetic lethality.

Given the hypersensitivity to PARPi observed in the *keap1*Δ cells, we next explored the hypothesis that KEAP1 might be a PARP 'anti-trapper'. We set out by assessing the changes in poly(ADP-ribosyl)ation between wild-type and *keap1*Δ cells. Interestingly, gene disruption of KEAP1 increased the level of poly(ADP-ribosyl)ation in the chromatin-enriched fraction post-MMS treatment. Similar observation was made in the case of ALC-1 deficient cells treated with hydrogen peroxide (Blessing et al., 2020).

Lastly, we compared the chromatin-bound levels of PARP1 and PARP2 in wild-type and KEAP1-deficient cells exposed to MMS. We observed chromatin retention of both PARP1 and PARP2 in the absence of KEAP1. MMS treatment resulted in increased accumulation of XRCC1 and yH2AX in the chromatin fraction of *keap1*Δ cells, similarly as observed in ALC1-deficient cells in response to damage (Blessing et al., 2020). The enrichment of PARP1 and PARP2 in chromatin in the absence of KEAP1 resembles reports from research on ALC1-deficiency and XRCC1-deficiency in the context of PARP-trapping (Blessing et al., 2020; Demin et al., 2021; Juhász et al., 2020).

Although it is tempting to speculate that KEAP1 could function as a PARP 'anti-trapper', further research is required to test this hypothesis. It is possible that the observed PARP1 and PARP2 chromatin enrichment in KEAP1-deficient cells is not caused by an increase in PARP trapping. Instead, it could be the result of DNA damage accumulation due to impaired repair of alkylation base damage in KEAP1-deficient cells. Live-cell imaging of fluorescently tagged PARP1 and PARP2 following laser microirradiation of *keap1*Δ cells could reveal the kinetic dynamic of the recruitment of PARPs to DNA lesions. Immunofluorescence staining of PARP1 and PARP2 in *keap1*Δ cells at different time points following exposure to MMS could also determine whether KEAP1 deficiency induces PARP1/2 retention in chromatin. DNA SSBs detection using alkaline comet assay could quantify the damage resulting from impaired base damage repair in KEAP1-deficient cells. The synthetic lethal interaction we uncovered between PARPi and KEAP1 deficiency could have potential implications on cancer therapy. *KEAP1* mutations leading to loss of function have been identified in various types of cancer, including endometrial cancer, hepatocellular carcinoma, head and neck cancer, and more, with the highest prevalence of *KEAP1* mutations in non-small cell lung cancer (Chen et al., 2020). PARPi treatment could have potential benefits for targeted therapy of cancer cells harbouring *KEAP1* mutations.

Taken together, the increased poly(ADP-ribosyl)ation and chromatin retention of activated PARP1 and PARP2 in *keap1*Δ cells induced by MMS indicate that KEAP1 plays a role in removing PARP1 and PARP2 from DNA damage sites. The synthetic lethality of PARP inhibition and KEAP1 deficiency supports a model in which KEAP1 is

required for the release of DNA-bound PARPs. Our results suggest that KEAP1 might confer its protective role against PARP trapping as part of the E3 ubiquitin ligase complex. We could therefore imagine a model in which KEAP1 assists in releasing PARPs from DNA damage sites either through direct ubiquitylation of PARPs or by modifying the activity of some downstream factors that in turn remove PARPs trapped on DNA.

7. General discussion

The work presented in this thesis identified and characterised a novel factor involved in the repair of DNA base damage. Specifically, to identify potential candidate proteins, we performed a genome-wide CRISP-Cas9 dropout screen for genes required for MMS tolerance. Among the ten top hits were factors already known to be involved in BER and SSBR, lending validity to the screen. Importantly, however, the second-ranking gene was *KEAP1,* which encodes a protein that acts as part of an E3 ubiquitin ligase complex and had not been previously implicated in repair of MMS-induced DNA damage.

To confirm that KEAP1 conveys MMS tolerance, we generated RPE-1 *keap1*Δ cell lines and performed a series of assays to characterise the role of KEAP1 in base damage repair. In agreement with the screen results, the *keap1*Δ cells are sensitive to MMS treatment as measured by a colony survival assay and that phenotype was complemented by re-expression of wild-type KEAP1. This confirms the validity of the screen and demonstrates that KEAP1 plays a role in response to MMS-induced DNA damage. Interestingly, two out of the three generated *keap1*Δ cell lines were only mildly sensitive to a single dose of MMS but exhibit a more dramatic sensitivity when exposed repeatedly to lower MMS concentrations. Literature reports of studies in *Saccharomyces cerevisiae* with defective S-phase checkpoint proteins indicate that acute MMS exposure might trigger damage preferentially resolved through BER, while damage induced by chronic low doses of MMS relies more on translesion

synthesis (Barbour et al., 2006; Murakami-Sekimata et al., 2010). This would suggest that KEAP1 might participate in resolution of persistent DNA damage resulting from chronic, low-level exposure to the alkylating agent, and could act through a pathway other than BER. The increased mutational pressure caused by repeated MMS exposure bears resemblance to chronic exposure to environmental alkylating agents or certain cancer treatments, which signals a potential clinical significance to understanding the role of KEAP1 in this context.

We next investigated the mechanism through which KEAP1 conveys resistance to MMS. Ubiquitylation plays an important role in DNA damage response and modulation of the repair pathways. Protein ubiquitylation is known to facilitate the recruitment of repair factors to chromatin, as well as determine the choice between alternative repair pathways, as in the case of monoubiquitylated PCNA promoting the error-prone TLS, in contrast to polyubiquitylated PCNA driving repair through template switching (Cohn and D'Andrea, 2008). Numerous BER proteins are ubiquitylated, although much remains to be uncovered about the E3 ubiquitin ligases involved in the regulation of this pathway (Carter and Parsons, 2018). Interestingly, it was also proposed that factors driving the degradation of proteins damaged by alkylation could confer resistance to MMS (Burgis and Samson, 2007; Kaufmann, 2015). Given the well-defined role of KEAP1 as part of the ubiquitin ligase complex that can target other proteins for proteasomal degradation, we considered the possibility that it might function as part of the same complex in the context of DNA base damage repair. Depletion of CUL3 sensitises U2OS cells to MMS treatment. Because CUL3 is required for the assembly of the E3 ligase complex with

KEAP1 and RBX1, this suggests that KEAP1 might act as a ubiquitin ligase in the context of MMS tolerance (Canning et al., 2015). Epistatic analysis of the relationship between KEAP1 and CUL3 would be required to test this possibility. However, CUL3-depleted RPE-1 cells display no MMS sensitivity, which puts that conclusion into question. It is important to note, though, that the inconsistency in the MMS sensitivity phenotype following CUL3-depletion could be due to the intrinsic differences between cancer and non-cancer cell lines. CUL3 also did not score high in the CRISPR-Cas9 screen for genes that relay MMS tolerance, which further casts doubt on the requirement for assembly of the KEAP1-CUL3-RBX1 complex for effective base damage repair. Based on these results, the role of CUL3 in conveying MMS tolerance as part of the ubiquitin complex with KEAP1 remains unclear and could be further investigated by disrupting *CUL3* in the wild-type and in *keap1*Δ background and comparing the MMS sensitivity.

We also assessed the domain requirement for the role KEAP1 plays in DNA base damage repair. We found that both the BTB and the Kelch domains are required for KEAP1 to confer MMS tolerance, as disruptions of either of these domains resulted in the inability to complement the MMS sensitivity phenotype caused by KEAP1 deficiency. The BTB domain is required for the homodimerisation of KEAP1 and for the binding of CUL3, while the Kelch domain is necessary to bind the ETGE and DLG motifs on the known KEAP1 substrates (Baird and Yamamoto, 2020; Horie et al., 2021). Our data indicates that these functions are crucial for the role of KEAP1 response to MMS-induced DNA damage. Both of these domains are required for KEAP1 to perform as part of the E3 ubiquitin ligase complex, providing another

argument for the ubiquitin ligase substrate adaptor role of KEAP1 to be vital for conveying MMS tolerance (Furukawa and Xiong, 2005; Itoh et al., 1999; Page et al., 2014). This is further supported by our observation that the KEAP1^{S3H4} mutant, where we substituted the amino acids at the predicted CUL3-binding site within the BTB domain, was also unable to rescue the MMS sensitivity phenotype in *keap1*Δ cells (Furukawa and Xiong, 2005). Moreover, the KEAP1-CUL3-RBX1 ubiquitin ligase complex was reported to suppress the DNA repair through HR in G1 cells by ubiquitylation of PALB2, which prevents its interaction with BRCA1 (Orthwein et al., 2015). Recent research from Nima Mosammaparast's laboratory identified a previously unknown ubiquitin-dependent repair pathway specific to alkylation damage (Brickner et al., 2017b). In this pathway, K63-linked polyubiquitylation signal produced by RNF113A E3 ligase is recognised by ASCC2 and drives the assembly of the ASCC complex at the damage site, which then recruits alkylation repair enzymes ALKBH3 and ASCC3 to the lesion (Brickner et al., 2017b). These findings demonstrating the existence of alkylation damage repair-specific pathway that is dependent on ubiquitin, prompt us to consider the possibility that a similar repair mechanism might be regulated by the KEAP1 E3 ubiquitin ligase complex. Although KEAP1 induced primarily the K48-linked polyubiquitylation which targets substrate for proteasomal degradation, it is also capable of producing the K63-linked polyubiquitin chains, that regulate proteasome-independent pathways (Ohtake et al., 2018; Reichard et al., 2016). Therefore, we propose that KEAP1 might be involved in the regulation of DNA base damage repair either by recruiting repair factors to the lesion by producing ubiquitin signal, or by modulating functions or protein levels of repair factors through ubiquitylation. However, further research is needed to

determine this hypothesis and the potential participation of CUL3 and RBX1 in the KEAP1-dependent alkylation damage repair. Investigation of KEAP1 foci formation following MMS-induced DNA damage and their co-localisation with polyubiquitin signal and CUL3/RBX1 could offer some more insight. Immunoprecipitation or pulldown of KEAP1 after MMS exposure and mass spectrometry analysis could help identify potential interactions required for the repair of alkylation damage.

Using its reactive cysteine sensor, KEAP1 can recognise specific small-molecule inducers (Suzuki et al., 2019). We hypothesised that the cysteine sensor might also play a role in recognition of MMS damage by KEAP1. However, re-expression of the KEAP1$^{11Cys\text{-}less}$ mutant with substitutions within the highly reactive cysteines fully restored the MMS-tolerance in KEAP1-deficient cells. This indicates that the mutated residues are not required for the role of KEAP1 in alkylation base damage repair. On the other hand, out of the 27 cysteines within KEAP1, we only mutated 11 highly reactive residues, which does not exhaust all the possibilities for MMS recognition by the remaining cysteines. Moreover, there are known redundancies between the residues within the cysteine stress sensor system of KEAP1, and likely more to be uncovered (Sekhar et al., 2010). Additionally, there are significant differences in reactivity of corresponding cysteine residues between human and murine KEAP1 (Sekhar et al., 2010). We introduced into human KEAP1 the same cysteine mutations that have been shown to affect the cysteine sensor in murine KEAP1, which could have a different effect on the reactivity of the sensor system depending on the species (Suzuki et al., 2019). Moreover, the KEAP1$^{11Cys\text{-}less}$ mutant in the original study was selected to sense H_2O_2 and its ability to recognise cysteine alkylation by

methylating agents, or MMS in particular, was not assessed (Suzuki et al., 2019). Although the KEAP1$^{11Cys\text{-}less}$ mutant rescued the MMS sensitivity phenotype similarly to wild-type KEAP1, it does not exclude the possibility that the cysteine sensor system is involved in recognition of methylation damage and enabling DNA damage repair.

Following MMS exposure, KEAP1 becomes enriched in the chromatin fraction, indicating recruitment to the sites of damage. We also found this recruitment to be PARP1-dependent, which prompted us to hypothesize that KEAP1 might function through one of the PARP1-dependent base damage repair pathways. However, no PAR-binding domains that could facilitate PARP1-driven recruitment have been identified in KEAP1. Instead, KEAP1 contains the Kelch domain which binds the ETGE/DLG motifs on target proteins (Tong et al., 2006). Therefore, it is tempting to speculate that through these motifs, KEAP1 could bind factors acting downstream of PARP1 in the repair pathway and be recruited to the site of damage as a result of this interaction.

The two main pathways that resolve the majority of alkylation base damage are BER and direct repair by MGMT, and both of these pathways depend on PARP1 (Carter and Parsons, 2016; Mishina et al., 2008; Soll et al., 2017). The role of PARP1 in recruiting XRCC1 to SSBs that arise from BER processing has been well established, and recently it has been reported that the repair of TMZ-induced damage in glioblastoma requires PARylation of MGMT by PARP1 (Masson et al., 1998; Wu et al., 2021). Surprisingly, our data indicate that KEAP1 deficiency is not epistatic with the

inhibition of either MGMT or the crucial BER enzyme APE1, and therefore it most likely does not function within either of these two pathways (Fishel and Kelley, 2007). Although it cannot be ruled out that KEAP1 acts through an APE1-independent NEIL1/PNKP-driven subpathway, we argue that functional classical BER would mask any defect in the redundant subpathway and likely no MMS sensitivity would be observed in the *keap1*Δ cells (Sankar Mitra and Kaina, 1993; Wiederhold et al., 2004). We therefore hypothesise that KEAP1 might be involved in one of the replication-coupled repair mechanisms. Considering that PARP1 is required to stabilise the reversed replication fork and prevents untimely fork restart, a PARP1-dependent role of KEAP1 in regulation of fork reversal would be possible (Berti et al., 2013). The requirement for BTB and Kelch domains to convey MMS tolerance demonstrated earlier, as well as the MMS sensitivity observed in CUL3-depleted U2OS cells, suggest KEAP1 would likely function in this context as an E3 ubiquitin ligase. Ubiquitylation by MDM2 has been reported to regulate the role of PARP1 at the reversed replication fork, leading to proteasomal degradation of PARP1 and promoting fork progression (Giansanti et al., 2022). We could hypothesise that KEAP1 could possibly contribute to that regulation of reversed replication forks, perhaps acting redundantly with MDM2. What seems to be a more appealing possibility is the probable involvement of KEAP1 in the determination between two other mechanisms of replication-coupled repair, namely translesion synthesis and template switching. Mono- and polyubiquitylation of PCNA is a crucial factor in this decision-making process and while two E3 ubiquitin ligases responsible for PCNA polyubiquitylation have been identified, there is an indication that an additional ubiquitin ligase might be involved (Kanao and Masutani, 2017; Krijger et al., 2011;

Qiu et al., 2021; Seelinger and Otterlei, 2020). Moreover, PCNA interacts directly with PARP1 (Prosperi and Scovassi, 2013). Therefore, it could be hypothesised that KEAP1 polyubiquitylates PCNA after being recruited to the lesion in a PARP1-dependent manner, promoting repair through template switching. However, further research is needed to verify these hypotheses.

We also established that there is no synthetic lethal interaction between KEAP1 deficiency and defective HR, despite the PARP1-dependancy of KEAP1. Surprisingly, a synthetic lethal interaction between KEAP1 deficiency and PARP inhibition was identified. We were able to reverse the cytotoxic effect of this interaction by reintroduction of wild-type KEAP1, indicating that in addition to its role in conveying MMS tolerance as demonstrated earlier, KEAP1 is also a cytoprotective factor against PARPi. However, this is in contrast to reported KEAP1 deletion in 293T cells resulting in resistance to olaparib treatment (Orthwein et al., 2015). On the other hand, our data also indicates that both the BTB and the Kelch domains are necessary for PARPi tolerance, suggesting that the PARPi-protective role of KEAP1 might depend on its ability to form a functional ubiquitin ligase complex. Interestingly, substitutions of the highly reactive cysteines in KEAP1$^{11Cys\text{-}less}$ mutant prevented complementation of the PARPi sensitivity phenotype in KEAP1-deficient cells. This demonstrates that, in contrast to its role in MMS tolerance, the cysteine-based stress sensor system of KEAP1 is required for resistance to PARPi. The complementation of MMS sensitivity phenotype by KEAP1$^{11Cys\text{-}less}$ also proves that this mutant is functional and can form the ubiquitin ligase complex with CUL3. It is tempting to speculate that the highly reactive cysteines of KEAP1 could recognise

olaparib similarly to numerous already identified inducers (Baird and Yamamoto, 2020).

Synthetic lethal interaction between a deficiency in a PARP-dependent factor and PARPi might seem counterintuitive, however, it is not unprecedented. Recent reports portray XRCC1 and ALC1, both PARP1-dependent SSBR factors, as PARP 'anti-trappers', required for release of PARPs from DNA lesions (Blessing et al., 2020; Demin et al., 2021; Juhász et al., 2020). Both ALC1 and XRCC1 deficiencies are also synthetic lethal with PARP inhibition (Blessing et al., 2020; Horton et al., 2014). These similarities with KEAP1 prompted us to hypothesise that counteracting PARP trapping by KEAP1 might be the mechanism that drives synthetic lethality of PARPi in KEAP1-deficient cells. As predicted, we observed chromatin retention of PARP1 and PARP2 in *keap1*Δ cells following MMS treatment. The level of poly(ADP-ribosyl)ation, as well as XRCC1 and yH2AX, was also increased in the chromatin fraction of KEAP1-deificient cells after MMS exposure. This is in line with the observations of ALC1-deficient cells undergoing MMS treatment, supporting the hypothesis of KEAP1 as a PARP anti-trapper (Blessing et al., 2020). However, the enrichment of PARP in the chromatin and increased poly(ADP-ribosyl)ation could alternatively be interpreted as increased DNA damage resulting from introducing alkylation base damage in the absence of KEAP1 leading to defective repair, but not necessarily evidence of PARP trapping. To distinguish between these two situations, further experiments would be required. Live-cell imaging of laser microirradiation-induced PARP trapping in *keap1*Δ cells or immunofluorescence staining of endogenous PARPs following MMS-induced damage in KEAP1-deficient cells could provide us with a better

understanding of the kinetics of PARP retention and release from sites of damage in the absence of KEAP1.

Concurrently with the completion of the experimental work presented in this thesis, another group reported synthetic lethal relationship between PARPi and KEAP1 deficiency and the mechanism driving the lethality, allowing us to revise the interpretation of our data presented above in light of the new information. In their work, Marzio et al. identify EMSY (EMSY transcriptional repressor, BRCA2 interacting) as a novel ubiquitylation substrate for KEAP1 (Marzio et al., 2022). In the absence of KEAP1, EMSY escapes proteasomal degradation and its accumulation inhibits BRCA2 activity, inducing a BRCAness phenotype (Marzio et al., 2022). The EMSY-induced inhibition of HR repair provides an explanation for the lack of synthetic lethal relationship between defective HR and KEAP deficiency in our experiments. More importantly, the BRCAness phenotype of the KEAP1-deficient leads to synthetic lethal interaction with PARPi, in line with our observations from colony survival assays (Marzio et al., 2022). Our data demonstrating the requirement for both BTB and Kelch domain to confer PARPi tolerance are in agreement with the degradation of EMSY by the KEAP1 ubiquitin ligase. The study by Marzio et al. does not disprove our results indicating the requirement for the cysteine sensor of KEAP1 for its PARPi-protective role. However, the uncovered mechanism driving the synthetic lethal relationship between KEAP1 deficiency and PARPi does not support our initial interpretation of this data. We previously hypothesised that KEAP1 might recognise small molecule PARPi through its cysteine sensor and, similarly as upon binding the NRF2 inducers, lose the ability to ubiquitylate its substrate, upregulating

cellular levels of a hypothetical PARPi-protective factor. When confronted with the mentioned study, this hypothesis seems unlikely, given that it is the effective proteasomal degradation of EMSY that reverses the PARPi sensitivity (Marzio et al., 2022). We also suggested that PARP1/2 trapping in chromatin in the absence of KEAP1 might contribute to the synthetic lethal interaction. This could be further addressed by comparing the kinetics of PARP1/2 chromatin retention between *keap1*Δ, *EMSY*Δ, *keap1*/*EMSY*Δ and wild-type cells.

In summary, this thesis uncovered at least two novel roles of KEAP1. Firstly, we identify KEAP1 as a novel factor involved in the DNA base damage repair. We propose that KEAP1 might convey the tolerance to alkylation damage as part of the KEAP1-CUL3-RBX1 ubiquitin ligase complex. The presented data indicates that KEAP1 is recruited to DNA lesions in a PARP-dependent manner. We hypothesise that upon recruitment, KEAP1 polyubiquitylates other repair proteins, either modifying their function or regulating their cellular levels by targeting them from proteasomal degradation (Figure 7.1). KEAP1 is not involved in regulation of BER or direct repair through MGMT, but we propose it might play a role in replication-coupled repair. Further research into the exact mechanism behind KEAP1 function in base damage repair can help understand the regulation network of DNA damage repair pathways. Ubiquitylation is a common post-translational modification and its impact on DNA damage repair cannot be underestimated. Secondly, we uncovered a new synthetic lethal relationship between PARP inhibition and KEAP1 deficiency. While we did not identify the mechanism behind this interaction, a study published concurrently with the experimental work presented in this thesis being finalised, described that loss of

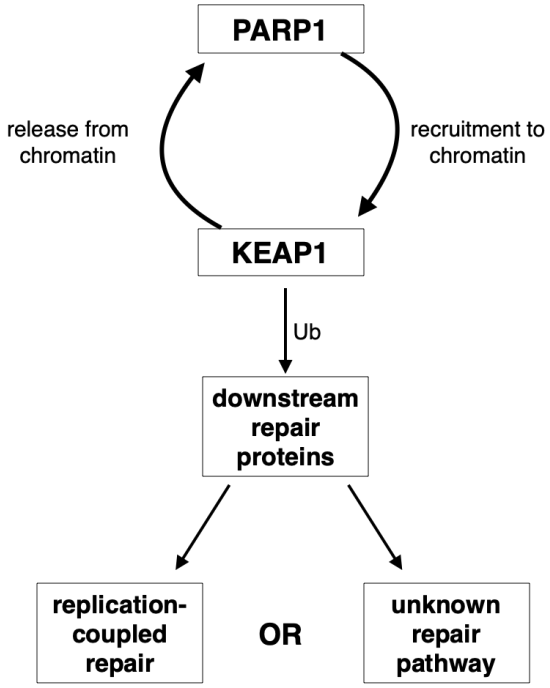

Figure 7.1 Proposed model of KEAP1 functions in response to alkylation base damage. KEAP1 is recruited to the site of DNA lesion in a PARP1-dependent manner. It likely modifies other repair proteins by ubiquitylation, either regulating their cellular levels or modifying their function in the repair of base damage, likely through replication-coupled repair or other unknown pathway. KEAP1 might play a role in the release of PARP1/2 from chromatin upon alkylation damage.

the KEAP1 ubiquitin ligase drives accumulation of its substrate EMSY, resulting in inhibition of the HR repair and sensitisation of cells to PARPi (Marzio et al., 2022). We therefore conclude that the synthetic lethal interaction between the KEAP1 deficiency and PARPi is driven by the BRCAness phenotype induced by the accumulation of undegraded EMSY (Marzio et al., 2022). Thirdly, we propose KEAP1 deficiency enhances PARP trapping at the DNA lesions, resulting in genomic instability and cell death. Our data suggest KEAP1 enables the release of PARP1 and PARP2 from the sites of damage, and that this anti-trapping role of KEAP1 depends on its ability to form the ubiquitin ligase complex and on the cysteine sensor system. It is unclear whether the PARP anti-trapping activity of KEAP1 could be involved in the same mechanism that is responsible for the tolerance of alkylation damage, or if these are in fact two separate functions of KEAP1 in DNA damage repair. Similarly, PARP trapping in KEAP1-deficient cells could potentiate the effect of the synthetic lethal interaction resulting from EMSY accumulation.

Importantly, the novel synthetic lethal interaction between KEAP1 deficiency and PARPi presents a new potential opportunity for expanding the use of PARP inhibitors in clinic. Orthotopically transplanted KEAP1-deficient lung tumour exhibited PARPi-sensitivity and correlated with increased survival in mice, offering a promising outlook on future research aiming to employ this synthetic lethal relationship in clinic (Marzio et al., 2022). Developing a therapeutical strategy targeting the KEAP1-deficient NSCLCs could have an important positive impact on the patients suffering from cancers with high prevalence of KEAP1 mutations.

8. Bibliography

AACR Project GENIE Consortium, 2017. AACR Project GENIE: Powering Precision Medicine through an International Consortium. Cancer Discov 7, 818–831. https://doi.org/10.1158/2159-8290.CD-17-0151

Abida, W., Patnaik, A., Campbell, D., Shapiro, J., Bryce, A.H., McDermott, R., Sautois, B., Vogelzang, N.J., Bambury, R.M., Voog, E., Zhang, J., Piulats, J.M., Ryan, C.J., Merseburger, A.S., Daugaard, G., Heidenreich, A., Fizazi, K., Higano, C.S., Krieger, L.E., Sternberg, C.N., Watkins, S.P., Despain, D., Simmons, A.D., Loehr, A., Dowson, M., Golsorkhi, T., Chowdhury, S., TRITON2 investigators, 2020. Rucaparib in Men With Metastatic Castration-Resistant Prostate Cancer Harboring a BRCA1 or BRCA2 Gene Alteration. J Clin Oncol 38, 3763–3772. https://doi.org/10.1200/JCO.20.01035

Adamowicz, M., Hailstone, R., Demin, A.A., Komulainen, E., Hanzlikova, H., Brazina, J., Gautam, A., Wells, S.E., Caldecott, K.W., 2021. XRCC1 protects transcription from toxic PARP1 activity during DNA base excision repair. Nat Cell Biol 23, 1287–1298. https://doi.org/10.1038/s41556-021-00792-w

Adamson, B., Smogorzewska, A., Sigoillot, F.D., King, R.W., Elledge, S.J., 2012. A genome-wide homologous recombination screen identifies the RNA-binding protein RBMX as a component of the DNA-damage response. Nat Cell Biol 14, 318–328. https://doi.org/10.1038/ncb2426

Ahel, D., Hořejší, Z., Wiechens, N., Polo, S.E., Garcia-Wilson, E., Ahel, I., Flynn, H., Skehel, M., West, S.C., Jackson, S.P., Owen-Hughes, T., Boulton, S.J., 2009. Poly(ADP-ribose)-dependent regulation of DNA repair by the chromatin remodelling enzyme ALC1. Science 325, 1240–1243. https://doi.org/10.1126/science.1177321

Akbari, M., Visnes, T., Krokan, H.E., Otterlei, M., 2008. Mitochondrial base excision repair of uracil and AP sites takes place by single-nucleotide insertion and long-patch DNA synthesis. DNA Repair (Amst) 7, 605–616. https://doi.org/10.1016/j.dnarep.2008.01.002

Almeida, K.H., Sobol, R.W., 2007. A unified view of base excision repair: lesion-dependent protein complexes regulated by post-translational modification. DNA Repair (Amst) 6, 695–711. https://doi.org/10.1016/j.dnarep.2007.01.009

Amé, J.-C., Rolli, V., Schreiber, V., Niedergang, C., Apiou, F., Decker, P., Muller, S., Höger, T., Murcia, J.M., Murcia, G. de, 1999. PARP-2, A Novel Mammalian DNA Damage-dependent Poly(ADP-ribose) Polymerase *. Journal of Biological Chemistry 274, 17860–17868. https://doi.org/10.1074/jbc.274.25.17860

Andronikou, C., Rottenberg, S., 2021. Studying PAR-Dependent Chromatin Remodeling to Tackle PARPi Resistance. Trends in Molecular Medicine 27, 630–642. https://doi.org/10.1016/j.molmed.2021.04.010

Ashino, T., Yamamoto, M., Numazawa, S., 2016. Nrf2/Keap1 system regulates vascular smooth muscle cell apoptosis for vascular homeostasis: role in neointimal formation after vascular injury. Scientific Reports 6. https://doi.org/10.1038/srep26291

Ashour, M.E., Mosammaparast, N., 2021a. Mechanisms of damage tolerance and repair during DNA replication. Nucleic Acids Research 49, 3033–3047. https://doi.org/10.1093/nar/gkab101

Ashour, M.E., Mosammaparast, N., 2021b. Mechanisms of damage tolerance and repair during DNA replication. Nucleic Acids Research 49, 3033–3047. https://doi.org/10.1093/nar/gkab101
Bainbridge, L.J., Teague, R., Doherty, A.J., 2021. Repriming DNA synthesis: an intrinsic restart pathway that maintains efficient genome replication. Nucleic Acids Research 49, 4831–4847. https://doi.org/10.1093/nar/gkab176
Baird, L., Yamamoto, M., 2020. The Molecular Mechanisms Regulating the KEAP1-NRF2 Pathway. Molecular and Cellular Biology 40. https://doi.org/10.1128/MCB.00099-20
Barbour, L., Ball, L.G., Zhang, K., Xiao, W., 2006. DNA Damage Checkpoints Are Involved in Postreplication Repair. Genetics 174, 1789–1800. https://doi.org/10.1534/genetics.106.056283
Bardwell, V.J., Treisman, R., 1994. The POZ domain: a conserved protein-protein interaction motif. Genes Dev. 8, 1664–1677. https://doi.org/10.1101/gad.8.14.1664
Bauer, N.C., Corbett, A.H., Doetsch, P.W., 2015. The current state of eukaryotic DNA base damage and repair. Nucleic Acids Res gkv1136. https://doi.org/10.1093/nar/gkv1136
Beck, C., Robert, I., Reina-San-Martin, B., Schreiber, V., Dantzer, F., 2014. Poly(ADP-ribose) polymerases in double-strand break repair: Focus on PARP1, PARP2 and PARP3. Experimental Cell Research, DNA DAMAGE AND REPAIR 329, 18–25. https://doi.org/10.1016/j.yexcr.2014.07.003
Begley, T.J., Samson, L.D., 2003. AlkB mystery solved: oxidative demethylation of N1-methyladenine and N3-methylcytosine adducts by a direct reversal mechanism. Trends Biochem Sci 28, 2–5. https://doi.org/10.1016/s0968-0004(02)00010-5
Berti, M., Ray Chaudhuri, A., Thangavel, S., Gomathinayagam, S., Kenig, S., Vujanovic, M., Odreman, F., Glatter, T., Graziano, S., Mendoza-Maldonado, R., Marino, F., Lucic, B., Biasin, V., Gstaiger, M., Aebersold, R., Sidorova, J.M., Monnat, R.J., Lopes, M., Vindigni, A., 2013. Human RECQ1 promotes restart of replication forks reversed by DNA topoisomerase I inhibition. Nat Struct Mol Biol 20, 347–354. https://doi.org/10.1038/nsmb.2501
Berti, M., Vindigni, A., 2016. Replication stress: getting back on track. Nature Structural & Molecular Biology 23, 103–109. https://doi.org/10.1038/nsmb.3163
Blessing, C., Mandemaker, I.K., Gonzalez-Leal, C., Preisser, J., Schomburg, A., Ladurner, A.G., 2020. The Oncogenic Helicase ALC1 Regulates PARP Inhibitor Potency by Trapping PARP2 at DNA Breaks. Molecular Cell 80, 862-875.e6. https://doi.org/10.1016/j.molcel.2020.10.009
Boehm, E.M., Gildenberg, M.S., Washington, M.T., 2016. The many roles of PCNA in eukaryotic DNA replication. Enzymes 39, 231–254. https://doi.org/10.1016/bs.enz.2016.03.003
Bonfiglio, J.J., Fontana, P., Zhang, Q., Colby, T., Gibbs-Seymour, I., Atanassov, I., Bartlett, E., Zaja, R., Ahel, I., Matic, I., 2017. Serine ADP-Ribosylation Depends on HPF1. Mol Cell 65, 932-940.e6. https://doi.org/10.1016/j.molcel.2017.01.003
Brickner, J.R., Soll, J.M., Lombardi, P.M., Vågbø, C.B., Mudge, M.C., Oyeniran, C., Rabe, R., Jackson, J., Sullender, M.E., Blazosky, E., Byrum, A.K., Zhao, Y., Corbett, M.A., Gécz, J., Field, M., Vindigni, A., Slupphaug, G., Wolberger, C., Mosammaparast, N., 2017a. A ubiquitin-dependent signalling axis specific for ALKBH-mediated DNA dealkylation repair. Nature 551, 389–393. https://doi.org/10.1038/nature24484
Brickner, J.R., Soll, J.M., Lombardi, P.M., Vågbø, C.B., Mudge, M.C., Oyeniran, C., Rabe, R., Jackson, J., Sullender, M.E., Blazosky, E., Byrum, A.K., Zhao, Y., Corbett, M.A., Gécz,

J., Field, M., Vindigni, A., Slupphaug, G., Wolberger, C., Mosammaparast, N., 2017b. A ubiquitin-dependent signalling axis specific for ALKBH-mediated DNA dealkylation repair. Nature 551, 389–393. https://doi.org/10.1038/nature24484
Brickner, J.R., Townley, B.A., Mosammaparast, N., 2019. Intersections between transcription-coupled repair and alkylation damage reversal. DNA Repair 81, 102663. https://doi.org/10.1016/j.dnarep.2019.102663
Bridges, C.B., 1922. The Origin of Variations in Sexual and Sex-Limited Characters. The American Naturalist 56, 51–63. https://doi.org/10.1086/279847
Brown, J.S., Jackson, S.P., 2015. Ubiquitylation, neddylation and the DNA damage response. Open Biol 5. https://doi.org/10.1098/rsob.150018
Bryant, H.E., Petermann, E., Schultz, N., Jemth, A.-S., Loseva, O., Issaeva, N., Johansson, F., Fernandez, S., McGlynn, P., Helleday, T., 2009. PARP is activated at stalled forks to mediate Mre11-dependent replication restart and recombination. EMBO J. 28, 2601–2615. https://doi.org/10.1038/emboj.2009.206
Bryant, H.E., Schultz, N., Thomas, H.D., Parker, K.M., Flower, D., Lopez, E., Kyle, S., Meuth, M., Curtin, N.J., Helleday, T., 2005. Specific killing of BRCA2-deficient tumours with inhibitors of poly(ADP-ribose) polymerase. Nature 434, 913–917. https://doi.org/10.1038/nature03443
Burgis, N.E., Samson, L.D., 2007. The Protein Degradation Response of Saccharomyces cerevisiae to Classical DNA-Damaging Agents. Chem. Res. Toxicol. 20, 1843–1853. https://doi.org/10.1021/tx700126e
Busso, C.S., Iwakuma, T., Izumi, T., 2009. Ubiquitination of mammalian AP endonuclease (APE1) regulated by the p53–MDM2 signaling pathway. Oncogene 28, 1616–1625. https://doi.org/10.1038/onc.2009.5
Byrum, A.K., Vindigni, A., Mosammaparast, N., 2019. Defining and Modulating 'BRCAness.' Trends in Cell Biology 29, 740–751. https://doi.org/10.1016/j.tcb.2019.06.005
Caldecott, K.W., 2008. Single-strand break repair and genetic disease. Nature Reviews Genetics 9, 619–631. https://doi.org/10.1038/nrg2380
Caldecott, K.W., Aoufouchi, S., Johnson, P., Shall, S., 1996. XRCC1 polypeptide interacts with DNA polymerase beta and possibly poly (ADP-ribose) polymerase, and DNA ligase III is a novel molecular "nick-sensor" in vitro. Nucleic Acids Res 24, 4387–4394.
Campalans, A., Kortulewski, T., Amouroux, R., Menoni, H., Vermeulen, W., Radicella, J.P., 2013. Distinct spatiotemporal patterns and PARP dependence of XRCC1 recruitment to single-strand break and base excision repair. Nucleic Acids Res 41, 3115–3129. https://doi.org/10.1093/nar/gkt025
Canning, P., Cooper, C.D.O., Krojer, T., Murray, J.W., Pike, A.C.W., Chaikuad, A., Keates, T., Thangaratnarajah, C., Hojzan, V., Marsden, B.D., Gileadi, O., Knapp, S., von Delft, F., Bullock, A.N., 2013. Structural Basis for Cul3 Protein Assembly with the BTB-Kelch Family of E3 Ubiquitin Ligases. Journal of Biological Chemistry 288, 7803–7814. https://doi.org/10.1074/jbc.M112.437996
Canning, P., Sorrell, F.J., Bullock, A.N., 2015. Structural basis of Keap1 interactions with Nrf2. Free Radic Biol Med 88, 101–107. https://doi.org/10.1016/j.freeradbiomed.2015.05.034
Cantoni, G.L., 1953. S-Adenosylmethionine; a new intermediate formed enzymatically from L-methionine and adenosinetriphosphate. J Biol Chem 204, 403–416.
Carter, R.J., Parsons, J.L., 2018. Regulation of the Base Excision Repair Pathway by Ubiquitination, in: Boutou, E., Stürzbecher, H.-W. (Eds.), Ubiquitination Governing

DNA Repair - Implications in Health and Disease. InTech. https://doi.org/10.5772/intechopen.70733
Carter, R.J., Parsons, J.L., 2016. Base Excision Repair, a Pathway Regulated by Posttranslational Modifications. Molecular and Cellular Biology 36, 1426–1437. https://doi.org/10.1128/MCB.00030-16
Chaharbakhshi, E., Jemc, J.C., 2016. Broad-complex, tramtrack, and bric-à-brac (BTB) proteins: Critical regulators of development: C HAHARBAKHSHI AND J EMC. genesis 54, 505–518. https://doi.org/10.1002/dvg.22964
Chambon, P., Weill, J.D., Mandel, P., 1963. Nicotinamide mononucleotide activation of a new DNA-dependent polyadenylic acid synthesizing nuclear enzyme. Biochemical and Biophysical Research Communications 11, 39–43. https://doi.org/10.1016/0006-291X(63)90024-X
Chatterjee, N., Walker, G.C., 2017. Mechanisms of DNA damage, repair and mutagenesis. Environ Mol Mutagen 58, 235–263. https://doi.org/10.1002/em.22087
Chen, X., Su, C., Ren, S., Zhou, C., Jiang, T., 2020. Pan-cancer analysis of KEAP1 mutations as biomarkers for immunotherapy outcomes. Annals of Translational Medicine 8, 141–141. https://doi.org/10.21037/atm.2019.11.52
Choo, Y.Y., Hagen, T., 2012. Mechanism of Cullin3 E3 Ubiquitin Ligase Dimerization. PLoS ONE 7, e41350. https://doi.org/10.1371/journal.pone.0041350
Ciccarone, F., Zampieri, M., Caiafa, P., 2017. PARP1 orchestrates epigenetic events setting up chromatin domains. Seminars in Cell & Developmental Biology 63, 123–134. https://doi.org/10.1016/j.semcdb.2016.11.010
Cleasby, A., Yon, J., Day, P.J., Richardson, C., Tickle, I.J., Williams, P.A., Callahan, J.F., Carr, R., Concha, N., Kerns, J.K., Qi, H., Sweitzer, T., Ward, P., Davies, T.G., 2014. Structure of the BTB Domain of Keap1 and Its Interaction with the Triterpenoid Antagonist CDDO. PLoS ONE 9, e98896. https://doi.org/10.1371/journal.pone.0098896
Cohn, M.A., D'Andrea, A.D., 2008. Chromatin Recruitment of DNA Repair Proteins: Lessons from the Fanconi Anemia and Double-Strand Break Repair Pathways. Molecular Cell 32, 306–312. https://doi.org/10.1016/j.molcel.2008.10.009
Cong, K., Kousholt, A.N., Peng, M., Panzarino, N.J., Lee, W.T.C., Nayak, S., Krais, J., Calvo, J., Bere, M., Rothenberg, E., Johnson, N., Jonkers, J., Cantor, S.B., 2019. PARPi synthetic lethality derives from replication-associated single-stranded DNA gaps. https://doi.org/10.1101/781989
Cong, K., Peng, M., Kousholt, A.N., Lee, W.T.C., Lee, S., Nayak, S., Krais, J., VanderVere-Carozza, P.S., Pawelczak, K.S., Calvo, J., Panzarino, N.J., Turchi, J.J., Johnson, N., Jonkers, J., Rothenberg, E., Cantor, S.B., 2021. Replication gaps are a key determinant of PARP inhibitor synthetic lethality with BRCA deficiency. Molecular Cell 81, 3128-3144.e7. https://doi.org/10.1016/j.molcel.2021.06.011
Coquelle, N., Havali-Shahriari, Z., Bernstein, N., Green, R., Glover, J.N.M., 2011. Structural basis for the phosphatase activity of polynucleotide kinase/phosphatase on single- and double-stranded DNA substrates. Proceedings of the National Academy of Sciences 108, 21022–21027. https://doi.org/10.1073/pnas.1112036108
Cordeiro de Lima, V.C., Corassa, M., Saldanha, E., Freitas, H., Arrieta, O., Raez, L., Samtani, S., Ramos, M., Rojas, C., Burotto, M., Chamorro, D.F., Recondo, G., Ruiz-Patiño, A., Más, L., Zatarain-Barrón, L., Mejía, S., Nicolas Minata, J., Martín, C., Bautista Blaquier, J., Motta Guerrero, R., Aliaga-Macha, C., Carracedo, C., Ordóñez- Reyes, C., Garcia-Robledo, J.E., Corrales, L., Sotelo, C., Ricaurte, L., Santoyo, N., Cuello, M.,

Jaller, E., Rodríguez, J., Archila, P., Bermudez, M., Gamez, T., Russo, A., Viola, L., Malapelle, U., de Miguel Perez, D., Rolfo, C., Rosell, R., Cardona, A.F., 2022. STK11 and KEAP1 mutations in non-small cell lung cancer patients: Descriptive analysis and prognostic value among Hispanics (STRIKE registry-CLICaP). Lung Cancer 170, 114–121. https://doi.org/10.1016/j.lungcan.2022.06.010

Cortez, D., 2019. Replication-Coupled DNA Repair. Molecular Cell 74, 866–876. https://doi.org/10.1016/j.molcel.2019.04.027

Cortez, D., 2015. Preventing Replication Fork Collapse to Maintain Genome Integrity. DNA Repair (Amst) 32, 149–157. https://doi.org/10.1016/j.dnarep.2015.04.026

Craggs, T.D., Hutton, R.D., Brenlla, A., White, M.F., Penedo, J.C., 2014. Single-molecule characterization of Fen1 and Fen1/PCNA complexes acting on flap substrates. Nucleic Acids Res 42, 1857–1872. https://doi.org/10.1093/nar/gkt1116

Crone, T.M., Pegg, A.E., 1993. A single amino acid change in human O6-alkylguanine-DNA alkyltransferase decreasing sensitivity to inactivation by O6-benzylguanine. Cancer Res 53, 4750–4753.

Cullinan, S.B., Gordan, J.D., Jin, J., Harper, J.W., Diehl, J.A., 2004. The Keap1-BTB Protein Is an Adaptor That Bridges Nrf2 to a Cul3-Based E3 Ligase: Oxidative Stress Sensing by a Cul3-Keap1 Ligase. Mol Cell Biol 24, 8477–8486. https://doi.org/10.1128/MCB.24.19.8477-8486.2004

Dayalan Naidu, S., Dinkova-Kostova, A.T., 2020. KEAP1, a cysteine-based sensor and a drug target for the prevention and treatment of chronic disease. Open Biology 10, 200105. https://doi.org/10.1098/rsob.200105

de Murcia, J.M., Niedergang, C., Trucco, C., Ricoul, M., Dutrillaux, B., Mark, M., Oliver, F.J., Masson, M., Dierich, A., LeMeur, M., Walztinger, C., Chambon, P., de Murcia, G., 1997. Requirement of poly(ADP-ribose) polymerase in recovery from DNA damage in mice and in cells. Proc. Natl. Acad. Sci. U.S.A. 94, 7303–7307. https://doi.org/10.1073/pnas.94.14.7303

Demin, A.A., Hirota, K., Tsuda, M., Adamowicz, M., Hailstone, R., Brazina, J., Gittens, W., Kalasova, I., Shao, Z., Zha, S., Sasanuma, H., Hanzlikova, H., Takeda, S., Caldecott, K.W., 2021. XRCC1 prevents toxic PARP1 trapping during DNA base excision repair. Molecular Cell 81, 3018-3030.e5. https://doi.org/10.1016/j.molcel.2021.05.009

Densham, R.M., Morris, J.R., 2019. Moving Mountains—The BRCA1 Promotion of DNA Resection. Front. Mol. Biosci. 6, 79. https://doi.org/10.3389/fmolb.2019.00079

Dhanoa, B.S., Cogliati, T., Satish, A.G., Bruford, E.A., Friedman, J.S., 2013. Update on the Kelch-like (KLHL) gene family. Hum Genomics 7, 13. https://doi.org/10.1186/1479-7364-7-13

Di Federico, A., De Giglio, A., Parisi, C., Gelsomino, F., 2021. STK11/LKB1 and KEAP1 mutations in non-small cell lung cancer: Prognostic rather than predictive? Eur J Cancer 157, 108–113. https://doi.org/10.1016/j.ejca.2021.08.011

Dianov, G.L., Hübscher, U., 2013. Mammalian base excision repair: the forgotten archangel. Nucleic Acids Res 41, 3483–3490. https://doi.org/10.1093/nar/gkt076

Dinkova-Kostova, A.T., Holtzclaw, W.D., Cole, R.N., Itoh, K., Wakabayashi, N., Katoh, Y., Yamamoto, M., Talalay, P., 2002. Direct evidence that sulfhydryl groups of Keap1 are the sensors regulating induction of phase 2 enzymes that protect against carcinogens and oxidants. Proc. Natl. Acad. Sci. U.S.A. 99, 11908–11913. https://doi.org/10.1073/pnas.172398899

Dinkova-Kostova, A.T., Kostov, R.V., Canning, P., 2017. Keap1, the cysteine-based mammalian intracellular sensor for electrophiles and oxidants. Archives of Biochemistry and Biophysics 617, 84–93. https://doi.org/10.1016/j.abb.2016.08.005

Dolan, M.E., Moschel, R.C., Pegg, A.E., 1990. Depletion of mammalian O6-alkylguanine-DNA alkyltransferase activity by O6-benzylguanine provides a means to evaluate the role of this protein in protection against carcinogenic and therapeutic alkylating agents. Proc Natl Acad Sci U S A 87, 5368–5372. https://doi.org/10.1073/pnas.87.14.5368

Drabløs, F., Feyzi, E., Aas, P.A., Vaagbø, C.B., Kavli, B., Bratlie, M.S., Peña-Diaz, J., Otterlei, M., Slupphaug, G., Krokan, H.E., 2004. Alkylation damage in DNA and RNA—repair mechanisms and medical significance. DNA Repair 3, 1389–1407. https://doi.org/10.1016/j.dnarep.2004.05.004

Drew, Y., 2015. The development of PARP inhibitors in ovarian cancer: from bench to bedside. Br J Cancer 113, S3–S9. https://doi.org/10.1038/bjc.2015.394

Edmonds, M.J., Carter, R.J., Nickson, C.M., Williams, S.C., Parsons, J.L., 2017. Ubiquitylation-dependent regulation of NEIL1 by Mule and TRIM26 is required for the cellular DNA damage response. Nucleic Acids Research 45, 726–738. https://doi.org/10.1093/nar/gkw959

Eggler, A.L., Liu, G., Pezzuto, J.M., van Breemen, R.B., Mesecar, A.D., 2005. Modifying specific cysteines of the electrophile-sensing human Keap1 protein is insufficient to disrupt binding to the Nrf2 domain Neh2. Proc. Natl. Acad. Sci. U.S.A. 102, 10070–10075. https://doi.org/10.1073/pnas.0502402102

Eggler, A.L., Small, E., Hannink, M., Mesecar, A.D., 2009. Cul3-mediated Nrf2 ubiquitination and ARE activation are dependent on the partial molar volume at position 151 of Keap1. Biochem J 422, 10.1042/BJ20090471. https://doi.org/10.1042/BJ20090471

El-Khamisy, S.F., 2003. A requirement for PARP-1 for the assembly or stability of XRCC1 nuclear foci at sites of oxidative DNA damage. Nucleic Acids Research 31, 5526–5533. https://doi.org/10.1093/nar/gkg761

Ensminger, M., Iloff, L., Ebel, C., Nikolova, T., Kaina, B., Löbrich, M., 2014. DNA breaks and chromosomal aberrations arise when replication meets base excision repair. Journal of Cell Biology 206, 29–43. https://doi.org/10.1083/jcb.201312078

Falnes, P.Ø., 2004. Repair of 3-methylthymine and 1-methylguanine lesions by bacterial and human AlkB proteins. Nucleic Acids Res 32, 6260–6267. https://doi.org/10.1093/nar/gkh964

Farmer, H., McCabe, N., Lord, C.J., Tutt, A.N.J., Johnson, D.A., Richardson, T.B., Santarosa, M., Dillon, K.J., Hickson, I., Knights, C., Martin, N.M.B., Jackson, S.P., Smith, G.C.M., Ashworth, A., 2005. Targeting the DNA repair defect in BRCA mutant cells as a therapeutic strategy. Nature 434, 917–921. https://doi.org/10.1038/nature03445

Fishel, M.L., Kelley, M.R., 2007. The DNA base excision repair protein Ape1/Ref-1 as a therapeutic and chemopreventive target. Molecular Aspects of Medicine 28, 375–395. https://doi.org/10.1016/j.mam.2007.04.005

Fok, J.H.L., Ramos-Montoya, A., Vazquez-Chantada, M., Wijnhoven, P.W.G., Follia, V., James, N., Farrington, P.M., Karmokar, A., Willis, S.E., Cairns, J., Nikkilä, J., Beattie, D., Lamont, G.M., Finlay, M.R.V., Wilson, J., Smith, A., O'Connor, L.O., Ling, S., Fawell, S.E., O'Connor, M.J., Hollingsworth, S.J., Dean, E., Goldberg, F.W., Davies, B.R., Cadogan, E.B., 2019. AZD7648 is a potent and selective DNA-PK inhibitor that enhances radiation, chemotherapy and olaparib activity. Nat Commun 10, 5065. https://doi.org/10.1038/s41467-019-12836-9

Fong, P.C., Boss, D.S., Yap, T.A., Tutt, A., Wu, P., Mergui-Roelvink, M., Mortimer, P., Swaisland, H., Lau, A., O'Connor, M.J., Ashworth, A., Carmichael, J., Kaye, S.B., Schellens, J.H.M., de Bono, J.S., 2009. Inhibition of Poly(ADP-Ribose) Polymerase in Tumors from BRCA Mutation Carriers. N Engl J Med 361, 123–134. https://doi.org/10.1056/NEJMoa0900212

Fontana, P., Bonfiglio, J.J., Palazzo, L., Bartlett, E., Matic, I., Ahel, I., 2017. Serine ADP-ribosylation reversal by the hydrolase ARH3. eLife 6, e28533. https://doi.org/10.7554/eLife.28533

Fortini, P., Dogliotti, E., 2007. Base damage and single-strand break repair: Mechanisms and functional significance of short- and long-patch repair subpathways. DNA Repair 6, 398–409. https://doi.org/10.1016/j.dnarep.2006.10.008

Fox, M., Fox, B.W., n.d. Effect of Methyl Methaiiesulfonate on the Growth of P388 Lymphoma Cells in Vitro and on Their Rate of Progress through the Cell Cycle 27, 9.

Fu, D., Calvo, J.A., Samson, L.D., 2012. Balancing repair and tolerance of DNA damage caused by alkylating agents. Nat Rev Cancer 12, 104–120. https://doi.org/10.1038/nrc3185

Furukawa, M., Xiong, Y., 2005. BTB Protein Keap1 Targets Antioxidant Transcription Factor Nrf2 for Ubiquitination by the Cullin 3-Roc1 Ligase. Mol Cell Biol 25, 162–171. https://doi.org/10.1128/MCB.25.1.162-171.2005

Genschik, P., Sumara, I., Lechner, E., 2013. The emerging family of CULLIN3-RING ubiquitin ligases (CRL3s): cellular functions and disease implications. EMBO J 32, 2307–2320. https://doi.org/10.1038/emboj.2013.173

Giansanti, C., Manzini, V., Dickmanns, Antje, Dickmanns, Achim, Palumbieri, M.D., Sanchi, A., Kienle, S.M., Rieth, S., Scheffner, M., Lopes, M., Dobbelstein, M., 2022. MDM2 binds and ubiquitinates PARP1 to enhance DNA replication fork progression. Cell Reports 39, 110879. https://doi.org/10.1016/j.celrep.2022.110879

Gibbs-Seymour, I., Fontana, P., Rack, J.G.M., Ahel, I., 2016. HPF1/C4orf27 Is a PARP-1-Interacting Protein that Regulates PARP-1 ADP-Ribosylation Activity. Molecular Cell 62, 432–442. https://doi.org/10.1016/j.molcel.2016.03.008

González-Martín, A., Pothuri, B., Vergote, I., DePont Christensen, R., Graybill, W., Mirza, M.R., McCormick, C., Lorusso, D., Hoskins, P., Freyer, G., Baumann, K., Jardon, K., Redondo, A., Moore, R.G., Vulsteke, C., O'Cearbhaill, R.E., Lund, B., Backes, F., Barretina-Ginesta, P., Haggerty, A.F., Rubio-Pérez, M.J., Shahin, M.S., Mangili, G., Bradley, W.H., Bruchim, I., Sun, K., Malinowska, I.A., Li, Y., Gupta, D., Monk, B.J., 2019. Niraparib in Patients with Newly Diagnosed Advanced Ovarian Cancer. New England Journal of Medicine 381, 2391–2402. https://doi.org/10.1056/NEJMoa1910962

Gottipati, P., Vischioni, B., Schultz, N., Solomons, J., Bryant, H.E., Djureinovic, T., Issaeva, N., Sleeth, K., Sharma, R.A., Helleday, T., 2010. Poly(ADP-Ribose) Polymerase Is Hyperactivated in Homologous Recombination–Defective Cells. Cancer Research 70, 5389–5398. https://doi.org/10.1158/0008-5472.CAN-09-4716

Gunn, A.R., Banos-Pinero, B., Paschke, P., Sanchez-Pulido, L., Ariza, A., Day, J., Emrich, M., Leys, D., Ponting, C.P., Ahel, I., Lakin, N.D., 2016. The role of ADP-ribosylation in regulating DNA interstrand crosslink repair. Journal of Cell Science 129, 3845–3858. https://doi.org/10.1242/jcs.193375

Gutierrez, R., O'Connor, T.R., 2021. DNA direct reversal repair and alkylating agent drug resistance. CDR. https://doi.org/10.20517/cdr.2020.113

Hanzlikova, H., Gittens, W., Krejcikova, K., Zeng, Z., Caldecott, K.W., 2017. Overlapping roles for PARP1 and PARP2 in the recruitment of endogenous XRCC1 and PNKP into oxidized chromatin. Nucleic Acids Res 45, 2546–2557. https://doi.org/10.1093/nar/gkw1246

Hanzlikova, H., Kalasova, I., Demin, A.A., Pennicott, L.E., Cihlarova, Z., Caldecott, K.W., 2018. The Importance of Poly(ADP-Ribose) Polymerase as a Sensor of Unligated Okazaki Fragments during DNA Replication. Molecular Cell 71, 319-331.e3. https://doi.org/10.1016/j.molcel.2018.06.004

Hart, T., Tong, A.H.Y., Chan, K., Van Leeuwen, J., Seetharaman, A., Aregger, M., Chandrashekhar, M., Hustedt, N., Seth, S., Noonan, A., Habsid, A., Sizova, O., Nedyalkova, L., Climie, R., Tworzyanski, L., Lawson, K., Sartori, M.A., Alibeh, S., Tieu, D., Masud, S., Mero, P., Weiss, A., Brown, K.R., Usaj, M., Billmann, M., Rahman, M., Costanzo, M., Myers, C.L., Andrews, B.J., Boone, C., Durocher, D., Moffat, J., 2017. Evaluation and Design of Genome-Wide CRISPR/SpCas9 Knockout Screens. G3 Genes|Genomes|Genetics 7, 2719–2727. https://doi.org/10.1534/g3.117.041277

Hegde, M., Hegde, P., Arijit, D., Boldogh, I., Mitra, S., 2012. Human DNA Glycosylase NEIL1's Interactions with Downstream Repair Proteins Is Critical for Efficient Repair of Oxidized DNA Base Damage and Enhanced Cell Survival. Biomolecules 2, 564–578. https://doi.org/10.3390/biom2040564

Hegi, M.E., Diserens, A.-C., Gorlia, T., Hamou, M.-F., de Tribolet, N., Weller, M., Kros, J.M., Hainfellner, J.A., Mason, W., Mariani, L., Bromberg, J.E.C., Hau, P., Mirimanoff, R.O., Cairncross, J.G., Janzer, R.C., Stupp, R., 2005. MGMT gene silencing and benefit from temozolomide in glioblastoma. N Engl J Med 352, 997–1003. https://doi.org/10.1056/NEJMoa043331

Hewitt, G., Borel, V., Segura-Bayona, S., Takaki, T., Ruis, P., Bellelli, R., Lehmann, L.C., Sommerova, L., Vancevska, A., Tomas-Loba, A., Zhu, K., Cooper, C., Fugger, K., Patel, H., Goldstone, R., Schneider-Luftman, D., Herbert, E., Stamp, G., Brough, R., Pettitt, S., Lord, C.J., West, S.C., Ahel, I., Ahel, D., Chapman, J.R., Deindl, S., Boulton, S.J., 2021. Defective ALC1 nucleosome remodeling confers PARPi sensitization and synthetic lethality with HRD. Molecular Cell 81, 767-783.e11. https://doi.org/10.1016/j.molcel.2020.12.006

Hoch, N.C., Polo, L.M., 2020. ADP-ribosylation: from molecular mechanisms to human disease. Genet. Mol. Biol. 43, e20190075. https://doi.org/10.1590/1678-4685-gmb-2019-0075

Hong, F., Sekhar, K.R., Freeman, M.L., Liebler, D.C., 2005. Specific Patterns of Electrophile Adduction Trigger Keap1 Ubiquitination and Nrf2 Activation. Journal of Biological Chemistry 280, 31768–31775. https://doi.org/10.1074/jbc.M503346200

Hopkins, T.A., Ainsworth, W.B., Ellis, P.A., Donawho, C.K., DiGiammarino, E.L., Panchal, S.C., Abraham, V.C., Algire, M.A., Shi, Y., Olson, A.M., Johnson, E.F., Wilsbacher, J.L., Maag, D., 2019. PARP1 Trapping by PARP Inhibitors Drives Cytotoxicity in Both Cancer Cells and Healthy Bone Marrow. Molecular Cancer Research 17, 409–419. https://doi.org/10.1158/1541-7786.MCR-18-0138

Horie, Y., Suzuki, T., Inoue, J., Iso, T., Wells, G., Moore, T.W., Mizushima, T., Dinkova-Kostova, A.T., Kasai, T., Kamei, T., Koshiba, S., Yamamoto, M., 2021. Molecular basis for the disruption of Keap1–Nrf2 interaction via Hinge & Latch mechanism. Commun Biol 4, 576. https://doi.org/10.1038/s42003-021-02100-6

Horton, J.K., Stefanick, D.F., Prasad, R., Gassman, N.R., Kedar, P.S., Wilson, S.H., 2014. Base Excision Repair Defects Invoke Hypersensitivity to PARP Inhibition. Molecular Cancer Research 12, 1128–1139. https://doi.org/10.1158/1541-7786.MCR-13-0502

Hottiger, M.O., Hassa, P.O., Lüscher, B., Schüler, H., Koch-Nolte, F., 2010. Toward a unified nomenclature for mammalian ADP-ribosyltransferases. Trends in Biochemical Sciences 35, 208–219. https://doi.org/10.1016/j.tibs.2009.12.003

Huang, F., Mazina, O.M., Zentner, I.J., Cocklin, S., Mazin, A.V., 2012. Inhibition of Homologous Recombination in Human Cells by Targeting RAD51 Recombinase. J. Med. Chem. 55, 3011–3020. https://doi.org/10.1021/jm201173g

Hübner, M.R., Eckersley-Maslin, M.A., Spector, D.L., 2013. Chromatin organization and transcriptional regulation. Current Opinion in Genetics & Development 23, 89–95. https://doi.org/10.1016/j.gde.2012.11.006

Hwang, C.-S., Shemorry, A., Varshavsky, A., 2009. Two proteolytic pathways regulate DNA repair by cotargeting the Mgt1 alkylguanine transferase. Proc Natl Acad Sci U S A 106, 2142–2147. https://doi.org/10.1073/pnas.0812316106

Isogai, S., Kanno, S.-I., Ariyoshi, M., Tochio, H., Ito, Y., Yasui, A., Shirakawa, M., 2010. Solution structure of a zinc-finger domain that binds to poly-ADP-ribose. Genes Cells 15, 101–110. https://doi.org/10.1111/j.1365-2443.2009.01369.x

Itoh, K., Wakabayashi, N., Katoh, Y., Ishii, T., Igarashi, K., Engel, J.D., Yamamoto, M., 1999. Keap1 represses nuclear activation of antioxidant responsive elements by Nrf2 through binding to the amino-terminal Neh2 domain. Genes Dev 13, 76–86.

Izumi, T., Mellon, I., 2021. Base excision repair and nucleotide excision repair, in: Genome Stability. Elsevier, pp. 293–322. https://doi.org/10.1016/B978-0-323-85679-9.00017-9

Ji, A.X., Privé, G.G., 2013. Crystal Structure of KLHL3 in Complex with Cullin3. PLoS ONE 8, e60445. https://doi.org/10.1371/journal.pone.0060445

Johansson, M., 1999. A Human Poly(ADP-ribose) Polymerase Gene Family (ADPRTL): cDNA Cloning of Two Novel Poly(ADP-ribose) Polymerase Homologues. Genomics 57, 442–445. https://doi.org/10.1006/geno.1999.5799

Juhász, S., Smith, R., Schauer, T., Spekhardt, D., Mamar, H., Zentout, S., Chapuis, C., Huet, S., Timinszky, G., 2020. The chromatin remodeler ALC1 underlies resistance to PARP inhibitor treatment. Sci. Adv. 6, eabb8626. https://doi.org/10.1126/sciadv.abb8626

Jumper, J., Evans, R., Pritzel, A., Green, T., Figurnov, M., Ronneberger, O., Tunyasuvunakool, K., Bates, R., Žídek, A., Potapenko, A., Bridgland, A., Meyer, C., Kohl, S.A.A., Ballard, A.J., Cowie, A., Romera-Paredes, B., Nikolov, S., Jain, R., Adler, J., Back, T., Petersen, S., Reiman, D., Clancy, E., Zielinski, M., Steinegger, M., Pacholska, M., Berghammer, T., Bodenstein, S., Silver, D., Vinyals, O., Senior, A.W., Kavukcuoglu, K., Kohli, P., Hassabis, D., 2021. Highly accurate protein structure prediction with AlphaFold. Nature 596, 583–589. https://doi.org/10.1038/s41586-021-03819-2

Kaelin, W.G., 2005. The Concept of Synthetic Lethality in the Context of Anticancer Therapy. Nat Rev Cancer 5, 689–698. https://doi.org/10.1038/nrc1691

Kamaletdinova, T., Fanaei-Kahrani, Z., Wang, Z.-Q., 2019. The Enigmatic Function of PARP1: From PARylation Activity to PAR Readers. Cells 8, 1625. https://doi.org/10.3390/cells8121625

Kanao, R., Masutani, C., 2017. Regulation of DNA damage tolerance in mammalian cells by post-translational modifications of PCNA. Mutation Research/Fundamental and

Molecular Mechanisms of Mutagenesis 803–805, 82–88. https://doi.org/10.1016/j.mrfmmm.2017.06.004
Kannouche, P.L., Wing, J., Lehmann, A.R., 2004. Interaction of Human DNA Polymerase η with Monoubiquitinated PCNA: A Possible Mechanism for the Polymerase Switch in Response to DNA Damage. Molecular Cell 14, 491–500. https://doi.org/10.1016/S1097-2765(04)00259-X
Kassab, M.A., Yu, L.L., Yu, X., 2020. Targeting dePARylation for cancer therapy. Cell Biosci 10, 7. https://doi.org/10.1186/s13578-020-0375-y
Kaufman, B., Shapira-Frommer, R., Schmutzler, R.K., Audeh, M.W., Friedlander, M., Balmaña, J., Mitchell, G., Fried, G., Stemmer, S.M., Hubert, A., Rosengarten, O., Steiner, M., Loman, N., Bowen, K., Fielding, A., Domchek, S.M., 2015. Olaparib Monotherapy in Patients With Advanced Cancer and a Germline BRCA1/2 Mutation. J Clin Oncol 33, 244–250. https://doi.org/10.1200/JCO.2014.56.2728
Kaufmann, W.K., 2015. Systems Biology of the DNA Damage Response, in: Systems Biology in Toxicology and Environmental Health. Elsevier, pp. 207–224. https://doi.org/10.1016/B978-0-12-801564-3.00009-2
Kim, Y.-J., Wilson, D.M., 2012. Overview of Base Excision Repair Biochemistry. Curr Mol Pharmacol 5, 3–13.
Kindler, H.L., Hammel, P., Reni, M., Van Cutsem, E., Macarulla, T., Hall, M.J., Park, J.O., Hochhauser, D., Arnold, D., Oh, D.-Y., Reinacher-Schick, A., Tortora, G., Algül, H., O'Reilly, E.M., Bordia, S., McGuinness, D., Cui, K., Locker, G.Y., Golan, T., 2022. Overall Survival Results From the POLO Trial: A Phase III Study of Active Maintenance Olaparib Versus Placebo for Germline BRCA-Mutated Metastatic Pancreatic Cancer. J Clin Oncol 40, 3929–3939. https://doi.org/10.1200/JCO.21.01604
Kobayashi, A., Kang, M.-I., Okawa, H., Ohtsuji, M., Zenke, Y., Chiba, T., Igarashi, K., Yamamoto, M., 2004. Oxidative Stress Sensor Keap1 Functions as an Adaptor for Cul3-Based E3 Ligase To Regulate Proteasomal Degradation of Nrf2. Molecular and Cellular Biology 24, 7130–7139. https://doi.org/10.1128/MCB.24.16.7130-7139.2004
Kobayashi, M., Li, L., Iwamoto, N., Nakajima-Takagi, Y., Kaneko, H., Nakayama, Y., Eguchi, M., Wada, Y., Kumagai, Y., Yamamoto, M., 2009. The Antioxidant Defense System Keap1-Nrf2 Comprises a Multiple Sensing Mechanism for Responding to a Wide Range of Chemical Compounds. Mol Cell Biol 29, 493–502. https://doi.org/10.1128/MCB.01080-08
Kondo, N., Takahashi, A., Ono, K., Ohnishi, T., 2010. DNA Damage Induced by Alkylating Agents and Repair Pathways. Journal of Nucleic Acids 2010, 1–7. https://doi.org/10.4061/2010/543531
Kopacz, A., Kloska, D., Forman, H.J., Jozkowicz, A., Grochot-Przeczek, A., 2020. Beyond repression of Nrf2: An update on Keap1. Free Radical Biology and Medicine 157, 63–74. https://doi.org/10.1016/j.freeradbiomed.2020.03.023
Kopacz, A., Klóska, D., Proniewski, B., Cysewski, D., Personnic, N., Piechota-Polańczyk, A., Kaczara, P., Zakrzewska, A., Forman, H.J., Dulak, J., Józkowicz, A., Grochot-Przęczek, A., 2019. Keap1 controls protein S-nitrosation and apoptosis-senescence switch in endothelial cells. Redox Biol 28, 101304. https://doi.org/10.1016/j.redox.2019.101304
Krietsch, J., Rouleau, M., Pic, É., Ethier, C., Dawson, T.M., Dawson, V.L., Masson, J.-Y., Poirier, G.G., Gagné, J.-P., 2013. Reprogramming cellular events by poly(ADP-ribose)-

binding proteins. Molecular Aspects of Medicine 34, 1066–1087. https://doi.org/10.1016/j.mam.2012.12.005
Krijger, P.H.L., Lee, K.-Y., Wit, N., van den Berka, P.C.M., Wu, X., Roest, H.P., Maas, A., Ding, H., Hoeijmakers, J.H.J., Myung, K., Jacobs, H., 2011. HLTF and SHPRH are not essential for PCNA polyubiquitination, survival and somatic hypermutation: Existence of an alternative E3 ligase. DNA Repair (Amst) 10, 438–444. https://doi.org/10.1016/j.dnarep.2010.12.008
Krokan, H.E., Bjoras, M., 2013. Base Excision Repair. Cold Spring Harbor Perspectives in Biology 5, a012583–a012583. https://doi.org/10.1101/cshperspect.a012583
Kwak, M.-K., Itoh, K., Yamamoto, M., Kensler, T.W., 2002. Enhanced Expression of the Transcription Factor Nrf2 by Cancer Chemopreventive Agents: Role of Antioxidant Response Element-Like Sequences in the *nrf2* Promoter. Mol Cell Biol 22, 2883–2892. https://doi.org/10.1128/MCB.22.9.2883-2892.2002
L., S., R., T., 2013. Direct Repair in Mammalian Cells, in: Chen, C. (Ed.), New Research Directions in DNA Repair. InTech. https://doi.org/10.5772/54449
Langelier, M.-F., Planck, J.L., Roy, S., Pascal, J.M., 2012. Structural Basis for DNA Damage-Dependent Poly(ADP-ribosyl)ation by Human PARP-1. Science 336, 728–732. https://doi.org/10.1126/science.1216338
Langelier, M.-F., Riccio, A.A., Pascal, J.M., 2014. PARP-2 and PARP-3 are selectively activated by 5′ phosphorylated DNA breaks through an allosteric regulatory mechanism shared with PARP-1. Nucleic Acids Research 42, 7762–7775. https://doi.org/10.1093/nar/gku474
Lankinen, M.H., Vilpo, L.M., Vilpo, J.A., 1996. UV- and gamma-irradiation-induced DNA single-strand breaks and their repair in human blood granulocytes and lymphocytes. Mutat Res 352, 31–38. https://doi.org/10.1016/0027-5107(95)00172-7
Ledermann, J.A., Oza, A.M., Lorusso, D., Aghajanian, C., Oaknin, A., Dean, A., Colombo, N., Weberpals, J.I., Clamp, A.R., Scambia, G., Leary, A., Holloway, R.W., Gancedo, M.A., Fong, P.C., Goh, J.C., O'Malley, D.M., Armstrong, D.K., Banerjee, S., García-Donas, J., Swisher, E.M., Cameron, T., Maloney, L., Goble, S., Coleman, R.L., 2020. Rucaparib for patients with platinum-sensitive, recurrent ovarian carcinoma (ARIEL3): post-progression outcomes and updated safety results from a randomised, placebo-controlled, phase 3 trial. Lancet Oncol 21, 710–722. https://doi.org/10.1016/S1470-2045(20)30061-9
Lee, M.-Y., Kim, M.-A., Kim, H.-J., Bae, Y.-S., Park, J.-I., Kwak, J.-Y., Chung, J.H., Yun, J., 2007. Alkylating agent methyl methanesulfonate (MMS) induces a wave of global protein hyperacetylation: Implications in cancer cell death. Biochemical and Biophysical Research Communications 360, 483–489. https://doi.org/10.1016/j.bbrc.2007.06.084
Lehmann, L.C., Hewitt, G., Aibara, S., Leitner, A., Marklund, E., Maslen, S.L., Maturi, V., Chen, Y., van der Spoel, D., Skehel, J.M., Moustakas, A., Boulton, S.J., Deindl, S., 2017. Mechanistic Insights into Autoinhibition of the Oncogenic Chromatin Remodeler ALC1. Mol Cell 68, 847-859.e7. https://doi.org/10.1016/j.molcel.2017.10.017
Lepiniec, L., Babiychuk, E., Kushnir, S., Van Montagu, M., Inzé, D., 1995. Characterization of an Arabidopsis thaliana cDNA homologue to animal poly(ADP-ribose) polymerase. FEBS LETTERS 364, 103–108.
Li, H., Liu, Y., Xiao, Y., Wilson, C.N., Bai, H.J., Jones, M.D., Wang, S., DeVore, J.E., Maier, E.Y., Durant, S.T., Boufraqech, M., Weyemi, U., 2023. CRISPR metabolic screen identifies

ATM and KEAP1 as targetable genetic vulnerabilities in solid tumors. Proc. Natl. Acad. Sci. U.S.A. 120, e2212072120. https://doi.org/10.1073/pnas.2212072120
Li, M., Yu, X., 2015. The role of poly(ADP-ribosyl)ation in DNA damage response and cancer chemotherapy. Oncogene 34, 3349–3356. https://doi.org/10.1038/onc.2014.295
Li, W., Xu, H., Xiao, T., Cong, L., Love, M.I., Zhang, F., Irizarry, R.A., Liu, J.S., Brown, M., Liu, X.S., 2014. MAGeCK enables robust identification of essential genes from genome-scale CRISPR/Cas9 knockout screens 12.
Li, X., Zhang, D., Hannink, M., Beamer, L.J., 2004. Crystal Structure of the Kelch Domain of Human Keap1. Journal of Biological Chemistry 279, 54750–54758. https://doi.org/10.1074/jbc.M410073200
Liang, S., Ezerskyte, M., Wang, J., Pelechano, V., Dreij, K., 2020. Transcriptional mutagenesis dramatically alters genome-wide p53 transactivation landscape. Sci Rep 10, 13513. https://doi.org/10.1038/s41598-020-70412-4
Liebler, D.C., Hong, F., Sekhar, K.R., Freeman, M.L., 2006. Chapter 3 Site-Specific Modification of the Electrophile Sensor Protein Keap1 and Activation of Nrf2-Dependent Gene Expression, in: Advances in Molecular Toxicology. Elsevier, pp. 65–83. https://doi.org/10.1016/S1872-0854(06)01003-4
Limpose, K., Corbett, A.H., Doetsch, P.W., 2017. BERing the burden of damage: Pathway crosstalk and posttranslational modification of base excision repair proteins regulate DNA damage management. DNA Repair (Amst) 56, 51–64. https://doi.org/10.1016/j.dnarep.2017.06.007
Litton, J.K., Rugo, H.S., Ettl, J., Hurvitz, S.A., Gonçalves, A., Lee, K.-H., Fehrenbacher, L., Yerushalmi, R., Mina, L.A., Martin, M., Roché, H., Im, Y.-H., Quek, R.G.W., Markova, D., Tudor, I.C., Hannah, A.L., Eiermann, W., Blum, J.L., 2018. Talazoparib in Patients with Advanced Breast Cancer and a Germline BRCA Mutation. New England Journal of Medicine 379, 753–763. https://doi.org/10.1056/NEJMoa1802905
Liu, C., Vyas, A., Kassab, M.A., Singh, A.K., Yu, X., 2017. The role of poly ADP-ribosylation in the first wave of DNA damage response. Nucleic Acids Research 45, 8129–8141. https://doi.org/10.1093/nar/gkx565
Lo, S.-C., Li, X., Henzl, M.T., Beamer, L.J., Hannink, M., 2006. Structure of the Keap1:Nrf2 interface provides mechanistic insight into Nrf2 signaling. EMBO J 25, 3605–3617. https://doi.org/10.1038/sj.emboj.7601243
Lundin, C., 2005. Methyl methanesulfonate (MMS) produces heat-labile DNA damage but no detectable in vivo DNA double-strand breaks. Nucleic Acids Research 33, 3799–3811. https://doi.org/10.1093/nar/gki681
Luo, M., Kelley, M.R., 2004. Inhibition of the Human Apurinic/Apyrimidinic Endonuclease (Ape1) Repair Activity and Sensitization of Breast Cancer Cells to DNA Alkylating Agents with Lucanthone. ANTICANCER RESEARCH 8.
Ma, J., Cai, H., Wu, T., Sobhian, B., Huo, Y., Alcivar, A., Mehta, M., Cheung, K.L., Ganesan, S., Kong, A.-N.T., Zhang, D.D., Xia, B., 2012. PALB2 Interacts with KEAP1 To Promote NRF2 Nuclear Accumulation and Function. Mol Cell Biol 32, 1506–1517. https://doi.org/10.1128/MCB.06271-11
Marzio, A., Kurz, E., Sahni, J.M., Di Feo, G., Puccini, J., Jiang, S., Hirsch, C.A., Arbini, A.A., Wu, W.L., Pass, H.I., Bar-Sagi, D., Papagiannakopoulos, T., Pagano, M., 2022. EMSY inhibits homologous recombination repair and the interferon response, promoting lung cancer immune evasion. Cell 185, 169-183.e19. https://doi.org/10.1016/j.cell.2021.12.005

Masson, M., Niedergang, C., Schreiber, V., Muller, S., Menissier-de Murcia, J., de Murcia, G., 1998. XRCC1 Is Specifically Associated with Poly(ADP-Ribose) Polymerase and Negatively Regulates Its Activity following DNA Damage. Mol Cell Biol 18, 3563–3571. https://doi.org/10.1128/MCB.18.6.3563

Mateo, J., Porta, N., Bianchini, D., McGovern, U., Elliott, T., Jones, R., Syndikus, I., Ralph, C., Jain, S., Varughese, M., Parikh, O., Crabb, S., Robinson, A., McLaren, D., Birtle, A., Tanguay, J., Miranda, S., Figueiredo, I., Seed, G., Bertan, C., Flohr, P., Ebbs, B., Rescigno, P., Fowler, G., Ferreira, A., Riisnaes, R., Pereira, R., Curcean, A., Chandler, R., Clarke, M., Gurel, B., Crespo, M., Nava Rodrigues, D., Sandhu, S., Espinasse, A., Chatfield, P., Tunariu, N., Yuan, W., Hall, E., Carreira, S., de Bono, J.S., 2020. Olaparib in patients with metastatic castration-resistant prostate cancer with DNA repair gene aberrations (TOPARP-B): a multicentre, open-label, randomised, phase 2 trial. Lancet Oncol 21, 162–174. https://doi.org/10.1016/S1470-2045(19)30684-9

Maya-Mendoza, A., Moudry, P., Merchut-Maya, J.M., Lee, M., Strauss, R., Bartek, J., 2018. High speed of fork progression induces DNA replication stress and genomic instability. Nature 559, 279–284. https://doi.org/10.1038/s41586-018-0261-5

McMahon, M., Itoh, K., Yamamoto, M., Hayes, J.D., 2003. Keap1-dependent Proteasomal Degradation of Transcription Factor Nrf2 Contributes to the Negative Regulation of Antioxidant Response Element-driven Gene Expression. Journal of Biological Chemistry 278, 21592–21600. https://doi.org/10.1074/jbc.M300931200

McMahon, M., Lamont, D.J., Beattie, K.A., Hayes, J.D., 2010. Keap1 perceives stress via three sensors for the endogenous signaling molecules nitric oxide, zinc, and alkenals. Proc. Natl. Acad. Sci. U.S.A. 107, 18838–18843. https://doi.org/10.1073/pnas.1007387107

McMahon, M., Thomas, N., Itoh, K., Yamamoto, M., Hayes, J.D., 2006. Dimerization of Substrate Adaptors Can Facilitate Cullin-mediated Ubiquitylation of Proteins by a "Tethering" Mechanism. Journal of Biological Chemistry 281, 24756–24768. https://doi.org/10.1074/jbc.M601119200

McNeill, D.R., Whitaker, A.M., Stark, W.J., Illuzzi, J.L., McKinnon, P.J., Freudenthal, B.D., Wilson, D.M., III, 2020. Functions of the major abasic endonuclease (APE1) in cell viability and genotoxin resistance. Mutagenesis 35, 27–38. https://doi.org/10.1093/mutage/gez046

Mehrotra, P.V., Ahel, D., Ryan, D.P., Weston, R., Wiechens, N., Kraehenbuehl, R., Owen-Hughes, T., Ahel, I., 2011. DNA Repair Factor APLF Is a Histone Chaperone. Molecular Cell 41, 46–55. https://doi.org/10.1016/j.molcel.2010.12.008

Menissier de Murcia, J., 2003. Functional interaction between PARP-1 and PARP-2 in chromosome stability and embryonic development in mouse. The EMBO Journal 22, 2255–2263. https://doi.org/10.1093/emboj/cdg206

Messner, S., Hottiger, M.O., 2011. Histone ADP-ribosylation in DNA repair, replication and transcription. Trends in Cell Biology 21, 534–542. https://doi.org/10.1016/j.tcb.2011.06.001

Middleton, M.R., Margison, G.P., 2003. Improvement of chemotherapy efficacy by inactivation of a DNA-repair pathway. The Lancet Oncology 4, 37–44. https://doi.org/10.1016/S1470-2045(03)00959-8

Min, A., Im, S.-A., 2020. PARP Inhibitors as Therapeutics: Beyond Modulation of PARylation. Cancers (Basel) 12, 394. https://doi.org/10.3390/cancers12020394

Miseta, A., Csutora, P., 2000. Relationship Between the Occurrence of Cysteine in Proteins and the Complexity of Organisms. Molecular Biology and Evolution 17, 1232–1239. https://doi.org/10.1093/oxfordjournals.molbev.a026406
Mishina, Y., Duguid, E.M., He, C., 2008. Direct Reversal of DNA Alkylation Damage 39.
Mitra, S., 2007. MGMT: A personal perspective. DNA Repair 6, 1064–1070. https://doi.org/10.1016/j.dnarep.2007.03.007
Mitra, S., Kaina, B., 1993. Regulation of repair of alkylation damage in mammalian genomes. Prog Nucleic Acid Res Mol Biol 44, 109–142. https://doi.org/10.1016/s0079-6603(08)60218-4
Mitra, Sankar, Kaina, B., 1993. Regulation of Repair of Alkylation Damage in Mammalian Genomes, in: Cohn, W.E., Moldave, K. (Eds.), Progress in Nucleic Acid Research and Molecular Biology. Academic Press, pp. 109–142. https://doi.org/10.1016/S0079-6603(08)60218-4
Montaldo, N.P., Bordin, D.L., Brambilla, A., Rösinger, M., Fordyce Martin, S.L., Bjørås, K.Ø., Bradamante, S., Aas, P.A., Furrer, A., Olsen, L.C., Kunath, N., Otterlei, M., Sætrom, P., Bjørås, M., Samson, L.D., van Loon, B., 2019. Alkyladenine DNA glycosylase associates with transcription elongation to coordinate DNA repair with gene expression. Nat Commun 10, 5460. https://doi.org/10.1038/s41467-019-13394-w
Mou, H., Smith, J.L., Peng, L., Yin, H., Moore, J., Zhang, X.-O., Song, C.-Q., Sheel, A., Wu, Q., Ozata, D.M., Li, Y., Anderson, D.G., Emerson, C.P., Sontheimer, E.J., Moore, M.J., Weng, Z., Xue, W., 2017. CRISPR/Cas9-mediated genome editing induces exon skipping by alternative splicing or exon deletion. Genome Biol 18, 108. https://doi.org/10.1186/s13059-017-1237-8
Mourón, S., Rodriguez-Acebes, S., Martínez-Jiménez, M.I., García-Gómez, S., Chocrón, S., Blanco, L., Méndez, J., 2013. Repriming of DNA synthesis at stalled replication forks by human PrimPol. Nat Struct Mol Biol 20, 1383–1389. https://doi.org/10.1038/nsmb.2719
Murai, J., Huang, S.N., Das, B.B., Renaud, A., Zhang, Y., Doroshow, J.H., Ji, J., Takeda, S., Pommier, Y., 2012. Trapping of PARP1 and PARP2 by Clinical PARP Inhibitors. Cancer Research 72, 5588–5599. https://doi.org/10.1158/0008-5472.CAN-12-2753
Murakami-Sekimata, A., Huang, D., Piening, B.D., Bangur, C., Paulovich, A.G., 2010. The Saccharomyces cerevisiae RAD9, RAD17 and RAD24 genes are required for suppression of mutagenic post-replicative repair during chronic DNA damage. DNA Repair 9, 824–834. https://doi.org/10.1016/j.dnarep.2010.04.007
Naidu, M.D., Agarwal, R., Pena, L.A., Cunha, L., Mezei, M., Shen, M., Wilson, D.M., Liu, Y., Sanchez, Z., Chaudhary, P., Wilson, S.H., Waring, M.J., 2011. Lucanthone and Its Derivative Hycanthone Inhibit Apurinic Endonuclease-1 (APE1) by Direct Protein Binding. PLoS ONE 6, e23679. https://doi.org/10.1371/journal.pone.0023679
Nazarkina, Z.K., Khodyreva, S.N., Marsin, S., Lavrik, O.I., Radicella, J.P., 2007. XRCC1 interactions with base excision repair DNA intermediates. DNA Repair (Amst) 6, 254–264. https://doi.org/10.1016/j.dnarep.2006.10.002
Nijman, S.M.B., 2011. Synthetic lethality: General principles, utility and detection using genetic screens in human cells. FEBS Letters 585, 1–6. https://doi.org/10.1016/j.febslet.2010.11.024
Nikolova, T., Ensminger, M., Löbrich, M., Kaina, B., 2010. Homologous recombination protects mammalian cells from replication-associated DNA double-strand breaks

arising in response to methyl methanesulfonate. DNA Repair 9, 1050–1063. https://doi.org/10.1016/j.dnarep.2010.07.005
Noren Hooten, N., Fitzpatrick, M., Kompaniez, K., Jacob, K.D., Moore, B.R., Nagle, J., Barnes, J., Lohani, A., Evans, M.K., 2012. Coordination of DNA repair by NEIL1 and PARP-1: a possible link to aging. Aging 4, 674–685. https://doi.org/10.18632/aging.100492
Ogura, T., Tong, K.I., Mio, K., Maruyama, Y., Kurokawa, H., Sato, C., Yamamoto, M., 2010. Keap1 is a forked-stem dimer structure with two large spheres enclosing the intervening, double glycine repeat, and C-terminal domains. Proc. Natl. Acad. Sci. U.S.A. 107, 2842–2847. https://doi.org/10.1073/pnas.0914036107
Ohtake, F., Tsuchiya, H., Saeki, Y., Tanaka, K., 2018. K63 ubiquitylation triggers proteasomal degradation by seeding branched ubiquitin chains. Proceedings of the National Academy of Sciences 115, E1401–E1408. https://doi.org/10.1073/pnas.1716673115
Ooi, S.-K., Sato, S., Tomomori-Sato, C., Zhang, Y., Wen, Z., Banks, C.A.S., Washburn, M.P., Unruh, J.R., Florens, L., Conaway, R.C., Conaway, J.W., 2021. Multiple roles for PARP1 in ALC1-dependent nucleosome remodeling. Proceedings of the National Academy of Sciences 118, e2107277118. https://doi.org/10.1073/pnas.2107277118
Orthwein, A., Noordermeer, S.M., Wilson, M.D., Landry, S., Enchev, R.I., Sherker, A., Munro, M., Pinder, J., Salsman, J., Dellaire, G., Xia, B., Peter, M., Durocher, D., 2015. A mechanism for the suppression of homologous recombination in G1 cells. Nature 528, 422–426. https://doi.org/10.1038/nature16142
Padmanabhan, B., Tong, K.I., Ohta, T., Nakamura, Y., Scharlock, M., Ohtsuji, M., Kang, M.-I., Kobayashi, A., Yokoyama, S., Yamamoto, M., 2006. Structural Basis for Defects of Keap1 Activity Provoked by Its Point Mutations in Lung Cancer. Molecular Cell 21, 689–700. https://doi.org/10.1016/j.molcel.2006.01.013
Page, A., Volchkova, V.A., Reid, S.P., Mateo, M., Bagnaud-Baule, A., Nemirov, K., Shurtleff, A.C., Lawrence, P., Reynard, O., Ottmann, M., Lotteau, V., Biswal, S.S., Thimmulappa, R.K., Bavari, S., Volchkov, V.E., 2014. Marburgvirus Hijacks Nrf2-Dependent Pathway by Targeting Nrf2-Negative Regulator Keap1. Cell Reports 6, 1026–1036. https://doi.org/10.1016/j.celrep.2014.02.027
Palazzo, L., Leidecker, O., Prokhorova, E., Dauben, H., Matic, I., Ahel, I., 2018. Serine is the major residue for ADP-ribosylation upon DNA damage. eLife 7, e34334. https://doi.org/10.7554/eLife.34334
Park, C.-K., Kim, J.E., Kim, J.Y., Song, S.W., Kim, J.W., Choi, S.H., Kim, T.M., Lee, S.-H., Kim, I.H., Park, S.-H., 2012. The Changes in MGMT Promoter Methylation Status in Initial and Recurrent Glioblastomas. Transl Oncol 5, 393–397.
Parsons, J.L., Tait, P.S., Finch, D., Dianova, I.I., Edelmann, M.J., Khoronenkova, S.V., Kessler, B.M., Sharma, R.A., McKenna, W.G., Dianov, G.L., 2009. Ubiquitin ligase ARF-BP1/Mule modulates base excision repair. The EMBO Journal 28, 3207–3215. https://doi.org/10.1038/emboj.2009.243
Pascucci, B., Maga, G., Hübscher, U., Bjoras, M., Seeberg, E., Hickson, I.D., Villani, G., Giordano, C., Cellai, L., Dogliotti, E., 2002. Reconstitution of the base excision repair pathway for 7,8-dihydro-8-oxoguanine with purified human proteins. Nucleic Acids Res 30, 2124–2130.
Patel, A.G., Sarkaria, J.N., Kaufmann, S.H., 2011. Nonhomologous end joining drives poly(ADP-ribose) polymerase (PARP) inhibitor lethality in homologous recombination-deficient cells. Proc. Natl. Acad. Sci. U.S.A. 108, 3406–3411. https://doi.org/10.1073/pnas.1013715108

Pegg, A.E., Boosalis, M., Samson, L., Moschel, R.C., Byers, T.L., Swenn, K., Dolan, M.E., 1993. Mechanism of inactivation of human O6-alkylguanine-DNA alkyltransferase by O6-benzylguanine. Biochemistry 32, 11998–12006. https://doi.org/10.1021/bi00096a009

Pierce, N.W., Kleiger, G., Shan, S., Deshaies, R.J., 2009. Detection of sequential polyubiquitylation on a millisecond timescale. Nature 462, 615–619. https://doi.org/10.1038/nature08595

Pintard, L., Willis, J.H., Willems, A., Johnson, J.-L.F., Srayko, M., Kurz, T., Glaser, S., Mains, P.E., Tyers, M., Bowerman, B., Peter, M., 2003. The BTB protein MEL-26 is a substrate-specific adaptor of the CUL-3 ubiquitin-ligase. Nature 425, 311–316. https://doi.org/10.1038/nature01959

Pogozelski, W.K., Tullius, T.D., 1998. Oxidative Strand Scission of Nucleic Acids: Routes Initiated by Hydrogen Abstraction from the Sugar Moiety. Chem. Rev. 98, 1089–1108. https://doi.org/10.1021/cr960437i

Polo, L.M., Xu, Y., Hornyak, P., Garces, F., Zeng, Z., Hailstone, R., Matthews, S.J., Caldecott, K.W., Oliver, A.W., Pearl, L.H., 2019. Efficient Single-Strand Break Repair Requires Binding to Both Poly(ADP-Ribose) and DNA by the Central BRCT Domain of XRCC1. Cell Rep 26, 573-581.e5. https://doi.org/10.1016/j.celrep.2018.12.082

Pommier, Y., OConnor, M.J., de Bono, J., 2016. Laying a trap to kill cancer cells: PARP inhibitors and their mechanisms of action. Science Translational Medicine 8, 362ps17-362ps17. https://doi.org/10.1126/scitranslmed.aaf9246

Preiss, J., Schlaeger, R., Hilz, H., 1971. Specific inhibition of poly adpribose polymerase by thymidine and nicotinamide in HeLa cells. FEBS Letters 19, 244–246. https://doi.org/10.1016/0014-5793(71)80524-0

Prosperi, E., Scovassi, I.A., 2013. Dynamic Interaction between PARP-1, PCNA and p21waf1/cip1, Madame Curie Bioscience Database [Internet]. Landes Bioscience.

Qiu, L., Wang, M., Zhu, Y., Xiang, Y., Zhang, Y., 2018. A Naturally-Occurring Dominant-Negative Inhibitor of Keap1 Competitively against Its Negative Regulation of Nrf2. Int J Mol Sci 19. https://doi.org/10.3390/ijms19082150

Qiu, S., Jiang, G., Cao, L., Huang, J., 2021. Replication Fork Reversal and Protection. Frontiers in Cell and Developmental Biology 9.

Quinet, A., Vindigni, A., 2018. Superfast DNA replication causes damage in cancer cells. Nature 559, 186–187. https://doi.org/10.1038/d41586-018-05501-6

Quinn, J., Jiang, S., Carter, J., Reardon, D., Desjardins, A., Vredenburgh, J., Rich, J., Gururangan, S., Friedman, A., Bigner, D., Sampson, J., Mclendon, R., Herndon, J., Threatt, S., Friedman, H., 2009. Phase II Trial of Gliadel plus O-6-Benzylguanine in Adults with Recurrent Glioblastoma Multiforme. Clinical cancer research : an official journal of the American Association for Cancer Research 15, 1064–8. https://doi.org/10.1158/1078-0432.CCR-08-2130

Quinn, J.A., Desjardins, A., Weingart, J., Brem, H., Dolan, M.E., Delaney, S.M., Vredenburgh, J., Rich, J., Friedman, A.H., Reardon, D.A., Sampson, J.H., Pegg, A.E., Moschel, R.C., Birch, R., McLendon, R.E., Provenzale, J.M., Gururangan, S., Dancey, J.E., Maxwell, J., Tourt-Uhlig, S., Herndon, J.E., Bigner, D.D., Friedman, H.S., 2005. Phase I Trial of Temozolomide Plus O6-Benzylguanine for Patients With Recurrent or Progressive Malignant Glioma. JCO 23, 7178–7187. https://doi.org/10.1200/JCO.2005.06.502

Rack, J.G.M., Liu, Q., Zorzini, V., Voorneveld, J., Ariza, A., Honarmand Ebrahimi, K., Reber, J.M., Krassnig, S.C., Ahel, D., van der Marel, G.A., Mangerich, A., McCullagh, J.S.O.,

Filippov, D.V., Ahel, I., 2021. Mechanistic insights into the three steps of poly(ADP-ribosylation) reversal. Nat Commun 12, 4581. https://doi.org/10.1038/s41467-021-24723-3

Rack, J.G.M., Palazzo, L., Ahel, I., 2020. (ADP-ribosyl)hydrolases: structure, function, and biology. Genes Dev. 34, 263–284. https://doi.org/10.1101/gad.334631.119

Ran, F.A., Hsu, P.D., Wright, J., Agarwala, V., Scott, D.A., Zhang, F., 2013. Genome engineering using the CRISPR-Cas9 system. Nat Protoc 8, 2281–2308. https://doi.org/10.1038/nprot.2013.143

Ranson, M., Middleton, M.R., Bridgewater, J., Lee, S.M., Dawson, M., Jowle, D., Halbert, G., Waller, S., McGrath, H., Gumbrell, L., McElhinney, R.S., Donnelly, D., McMurry, T.B.H., Margison, G.P., 2006. Lomeguatrib, a Potent Inhibitor of O6-Alkylguanine-DNA-Alkyltransferase: Phase I Safety, Pharmacodynamic, and Pharmacokinetic Trial and Evaluation in Combination with Temozolomide in Patients with Advanced Solid Tumors. Clinical Cancer Research 12, 1577–1584. https://doi.org/10.1158/1078-0432.CCR-05-2198

Ray Chaudhuri, A., Hashimoto, Y., Herrador, R., Neelsen, K.J., Fachinetti, D., Bermejo, R., Cocito, A., Costanzo, V., Lopes, M., 2012. Topoisomerase I poisoning results in PARP-mediated replication fork reversal. Nat Struct Mol Biol 19, 417–423. https://doi.org/10.1038/nsmb.2258

Ray Chaudhuri, A., Nussenzweig, A., 2017. The multifaceted roles of PARP1 in DNA repair and chromatin remodelling. Nature Reviews Molecular Cell Biology 18, 610–621. https://doi.org/10.1038/nrm.2017.53

Reddy, S.P., 2008. The Antioxidant Response Element and Oxidative Stress Modifiers in Airway Diseases. Curr Mol Med 8, 376–383.

Reichard, E.L., Chirico, G.G., Dewey, W.J., Nassif, N.D., Bard, K.E., Millas, N.E., Kraut, D.A., 2016. Substrate Ubiquitination Controls the Unfolding Ability of the Proteasome *. Journal of Biological Chemistry 291, 18547–18561. https://doi.org/10.1074/jbc.M116.720151

Reynolds, P., Cooper, S., Lomax, M., O'Neill, P., 2015. Disruption of PARP1 function inhibits base excision repair of a sub-set of DNA lesions. Nucleic Acids Research 43, 4028–4038. https://doi.org/10.1093/nar/gkv250

Rivera, A.L., Pelloski, C.E., Gilbert, M.R., Colman, H., De La Cruz, C., Sulman, E.P., Bekele, B.N., Aldape, K.D., 2010. MGMT promoter methylation is predictive of response to radiotherapy and prognostic in the absence of adjuvant alkylating chemotherapy for glioblastoma. Neuro Oncol 12, 116–121. https://doi.org/10.1093/neuonc/nop020

Ronson, G.E., Piberger, A.L., Higgs, M.R., Olsen, A.L., Stewart, G.S., McHugh, P.J., Petermann, E., Lakin, N.D., 2018. PARP1 and PARP2 stabilise replication forks at base excision repair intermediates through Fbh1-dependent Rad51 regulation. Nature Communications 9. https://doi.org/10.1038/s41467-018-03159-2

Rose, M., Burgess, J.T., O'Byrne, K., Richard, D.J., Bolderson, E., 2020. PARP Inhibitors: Clinical Relevance, Mechanisms of Action and Tumor Resistance. Front. Cell Dev. Biol. 8, 564601. https://doi.org/10.3389/fcell.2020.564601

Rudolph, J., Roberts, G., Luger, K., 2021a. Histone Parylation factor 1 contributes to the inhibition of PARP1 by cancer drugs. Nat Commun 12, 736. https://doi.org/10.1038/s41467-021-20998-8

Rudolph, J., Roberts, G., Muthurajan, U.M., Luger, K., 2021b. HPF1 and nucleosomes mediate a dramatic switch in activity of PARP1 from polymerase to hydrolase. eLife 10, e65773. https://doi.org/10.7554/eLife.65773

Saito, R., Suzuki, T., Hiramoto, K., Asami, S., Naganuma, E., Suda, H., Iso, T., Yamamoto, H., Morita, M., Baird, L., Furusawa, Y., Negishi, T., Ichinose, M., Yamamoto, M., 2016. Characterizations of Three Major Cysteine Sensors of Keap1 in Stress Response. Mol Cell Biol 36, 271–284. https://doi.org/10.1128/MCB.00868-15

Sale, J.E., Lehmann, A.R., Woodgate, R., 2012. Y-family DNA polymerases and their role in tolerance of cellular DNA damage. Nat Rev Mol Cell Biol 13, 141–152. https://doi.org/10.1038/nrm3289

Schoenfeld, A.R., Apgar, S., Dolios, G., Wang, R., Aaronson, S.A., 2004. BRCA2 Is Ubiquitinated In Vivo and Interacts with USP11, a Deubiquitinating Enzyme That Exhibits Prosurvival Function in the Cellular Response to DNA Damage. Mol Cell Biol 24, 7444–7455. https://doi.org/10.1128/MCB.24.17.7444-7455.2004

Schröfelbauer, B., Yu, Q., Zeitlin, S.G., Landau, N.R., 2005. Human Immunodeficiency Virus Type 1 Vpr Induces the Degradation of the UNG and SMUG Uracil-DNA Glycosylases. Journal of Virology 79, 10978–10987. https://doi.org/10.1128/JVI.79.17.10978-10987.2005

Scully, R., Panday, A., Elango, R., Willis, N.A., 2019. DNA double-strand break repair-pathway choice in somatic mammalian cells. Nature Reviews Molecular Cell Biology. https://doi.org/10.1038/s41580-019-0152-0

Seelinger, M., Otterlei, M., 2020. Helicase-Like Transcription Factor HLTF and E3 Ubiquitin Ligase SHPRH Confer DNA Damage Tolerance through Direct Interactions with Proliferating Cell Nuclear Antigen (PCNA). Int J Mol Sci 21, 693. https://doi.org/10.3390/ijms21030693

Sekhar, K.R., Rachakonda, G., Freeman, M.L., 2010. Cysteine-based regulation of the CUL3 adaptor protein Keap1. Toxicology and Applied Pharmacology 244, 21–26. https://doi.org/10.1016/j.taap.2009.06.016

Shen, Y., Rehman, F.L., Feng, Y., Boshuizen, J., Bajrami, I., Elliott, R., Wang, B., Lord, C.J., Post, L.E., Ashworth, A., 2013. BMN 673, a Novel and Highly Potent PARP1/2 Inhibitor for the Treatment of Human Cancers with DNA Repair Deficiency. Clinical Cancer Research 19, 5003–5015. https://doi.org/10.1158/1078-0432.CCR-13-1391

Shibata, T., Ohta, T., Tong, K.I., Kokubu, A., Odogawa, R., Tsuta, K., Asamura, H., Yamamoto, M., Hirohashi, S., 2008. Cancer related mutations in NRF2 impair its recognition by Keap1-Cul3 E3 ligase and promote malignancy. Proceedings of the National Academy of Sciences 105, 13568–13573. https://doi.org/10.1073/pnas.0806268105

Shieh, W.M., Amé, J.-C., Wilson, M.V., Wang, Z.-Q., Koh, D.W., Jacobson, M.K., Jacobson, E.L., 1998. Poly(ADP-ribose) Polymerase Null Mouse Cells Synthesize ADP-ribose Polymers *. Journal of Biological Chemistry 273, 30069–30072. https://doi.org/10.1074/jbc.273.46.30069

Shiu, J.-L., Wu, C.-K., Chang, S.-B., Sun, Y.-J., Chen, Y.-J., Lai, C.-C., Chiu, W.-T., Chang, W.-T., Myung, K., Su, W.-P., Liaw, H., 2020. The HLTF–PARP1 interaction in the progression and stability of damaged replication forks caused by methyl methanesulfonate. Oncogenesis 9, 104. https://doi.org/10.1038/s41389-020-00289-5

Slade, D., Dunstan, M.S., Barkauskaite, E., Weston, R., Lafite, P., Dixon, N., Ahel, M., Leys, D., Ahel, I., 2011. The structure and catalytic mechanism of a poly(ADP-ribose) glycohydrolase. Nature 477, 616–620. https://doi.org/10.1038/nature10404

Soll, J.M., Sobol, R.W., Mosammaparast, N., 2017. Regulation of DNA Alkylation Damage Repair: Lessons and Therapeutic Opportunities. Trends in Biochemical Sciences 42, 206–218. https://doi.org/10.1016/j.tibs.2016.10.001

Srivenugopal, K.S., Yuan, X.H., Friedman, H.S., Ali-Osman, F., 1996. Ubiquitination-dependent proteolysis of O6-methylguanine-DNA methyltransferase in human and murine tumor cells following inactivation with O6-benzylguanine or 1,3-bis(2-chloroethyl)-1-nitrosourea. Biochemistry 35, 1328–1334. https://doi.org/10.1021/bi9518205

Stern, H.R., Sefcikova, J., Chaparro, V.E., Beuning, P.J., 2019. Mammalian DNA Polymerase Kappa Activity and Specificity. Molecules 24, 2805. https://doi.org/10.3390/molecules24152805

Sukhanova, M., Khodyreva, S., Lavrik, O., 2010. Poly(ADP-ribose) polymerase 1 regulates activity of DNA polymerase beta in long patch base excision repair. Mutat Res 685, 80–89. https://doi.org/10.1016/j.mrfmmm.2009.08.009

Sultanov, D., Gerasimova, N., Kudryashova, K., Maluchenko, N., Kotova, E., Langelier, M.-F., Pascal, J., Kirpichnikov, M., Feofanov, A., Studitsky, V., 2017. Unfolding of core nucleosomes by PARP-1 revealed by spFRET microscopy. AIMS Genet 4, 21–31. https://doi.org/10.3934/genet.2017.1.21

Sun, Y., Wei, W., Jin, J., 2020. Cullin-RING Ligases and Protein Neddylation: Biology and Therapeutics, Advances in Experimental Medicine and Biology. Springer Singapore, Singapore. https://doi.org/10.1007/978-981-15-1025-0

Suskiewicz, M.J., Zobel, F., Ogden, T.E.H., Fontana, P., Ariza, A., Yang, J.-C., Zhu, K., Bracken, L., Hawthorne, W.J., Ahel, D., Neuhaus, D., Ahel, I., 2020. HPF1 completes the PARP active site for DNA damage-induced ADP-ribosylation. Nature 579, 598–602. https://doi.org/10.1038/s41586-020-2013-6

Suzuki, T., Maher, J., Yamamoto, M., 2011. Select Heterozygous *Keap1* Mutations Have a Dominant-Negative Effect on Wild-Type Keap1 *In Vivo*. Cancer Research 71, 1700–1709. https://doi.org/10.1158/0008-5472.CAN-10-2939

Suzuki, T., Muramatsu, A., Saito, R., Iso, T., Shibata, T., Kuwata, K., Kawaguchi, S., Iwawaki, T., Adachi, S., Suda, H., Morita, M., Uchida, K., Baird, L., Yamamoto, M., 2019. Molecular Mechanism of Cellular Oxidative Stress Sensing by Keap1. Cell Reports 28, 746-758.e4. https://doi.org/10.1016/j.celrep.2019.06.047

Taguchi, K., Fujikawa, N., Komatsu, M., Ishii, T., Unno, M., Akaike, T., Motohashi, H., Yamamoto, M., 2012. Keap1 degradation by autophagy for the maintenance of redox homeostasis. Proc. Natl. Acad. Sci. U.S.A. 109, 13561–13566. https://doi.org/10.1073/pnas.1121572109

Taguchi, K., Motohashi, H., Yamamoto, M., 2011. Molecular mechanisms of the Keap1–Nrf2 pathway in stress response and cancer evolution. Genes to Cells 16, 123–140. https://doi.org/10.1111/j.1365-2443.2010.01473.x

Talalay, P., De Long, M.J., Prochaska, H.J., 1988. Identification of a common chemical signal regulating the induction of enzymes that protect against chemical carcinogenesis. Proc Natl Acad Sci U S A 85, 8261–8265.

Teloni, F., Altmeyer, M., 2016. Readers of poly(ADP-ribose): designed to be fit for purpose. Nucleic Acids Res 44, 993–1006. https://doi.org/10.1093/nar/gkv1383

Terada, M., Fujiki, H., Marks, P.A., Sugimura, T., 1979. Induction of erythroid differentiation of murine erythroleukemia cells by nicotinamide and related compounds. [WWW Document]. https://doi.org/10.1073/pnas.76.12.6411

Tian, W., Vega, M.R. de la, Schmidlin, C.J., Ooi, A., Zhang, D.D., 2018. Kelch-like ECH-associated protein 1 (KEAP1) differentially regulates nuclear factor erythroid-2–related factors 1 and 2 (NRF1 and NRF2). J. Biol. Chem. 293, 2029–2040. https://doi.org/10.1074/jbc.RA117.000428

Tong, K.I., Katoh, Y., Kusunoki, H., Itoh, K., Tanaka, T., Yamamoto, M., 2006. Keap1 Recruits Neh2 through Binding to ETGE and DLG Motifs: Characterization of the Two-Site Molecular Recognition Model. Mol Cell Biol 26, 2887–2900. https://doi.org/10.1128/MCB.26.8.2887-2900.2006

Tong, K.I., Padmanabhan, B., Kobayashi, A., Shang, C., Hirotsu, Y., Yokoyama, S., Yamamoto, M., 2007. Different Electrostatic Potentials Define ETGE and DLG Motifs as Hinge and Latch in Oxidative Stress Response. Mol Cell Biol 27, 7511–7521. https://doi.org/10.1128/MCB.00753-07

Topatana, W., Juengpanich, S., Li, S., Cao, J., Hu, J., Lee, J., Suliyanto, K., Ma, D., Zhang, B., Chen, M., Cai, X., 2020. Advances in synthetic lethality for cancer therapy: cellular mechanism and clinical translation. J Hematol Oncol 13, 118. https://doi.org/10.1186/s13045-020-00956-5

Tutt, A.N.J., Garber, J.E., Kaufman, B., Viale, G., Fumagalli, D., Rastogi, P., Gelber, R.D., de Azambuja, E., Fielding, A., Balmaña, J., Domchek, S.M., Gelmon, K.A., Hollingsworth, S.J., Korde, L.A., Linderholm, B., Bandos, H., Senkus, E., Suga, J.M., Shao, Z., Pippas, A.W., Nowecki, Z., Huzarski, T., Ganz, P.A., Lucas, P.C., Baker, N., Loibl, S., McConnell, R., Piccart, M., Schmutzler, R., Steger, G.G., Costantino, J.P., Arahmani, A., Wolmark, N., McFadden, E., Karantza, V., Lakhani, S.R., Yothers, G., Campbell, C., Geyer, C.E., OlympiA Clinical Trial Steering Committee and Investigators, 2021. Adjuvant Olaparib for Patients with BRCA1- or BRCA2-Mutated Breast Cancer. N Engl J Med 384, 2394–2405. https://doi.org/10.1056/NEJMoa2105215

van Beek, L., McClay, É., Patel, S., Schimpl, M., Spagnolo, L., Maia de Oliveira, T., 2021. PARP Power: A Structural Perspective on PARP1, PARP2, and PARP3 in DNA Damage Repair and Nucleosome Remodelling. Int J Mol Sci 22, 5112. https://doi.org/10.3390/ijms22105112

Varadi, M., Anyango, S., Deshpande, M., Nair, S., Natassia, C., Yordanova, G., Yuan, D., Stroe, O., Wood, G., Laydon, A., Žídek, A., Green, T., Tunyasuvunakool, K., Petersen, S., Jumper, J., Clancy, E., Green, R., Vora, A., Lutfi, M., Figurnov, M., Cowie, A., Hobbs, N., Kohli, P., Kleywegt, G., Birney, E., Hassabis, D., Velankar, S., 2022. AlphaFold Protein Structure Database: massively expanding the structural coverage of protein-sequence space with high-accuracy models. Nucleic Acids Research 50, D439–D444. https://doi.org/10.1093/nar/gkab1061

Vasil'eva, I., Moor, N., Anarbaev, R., Kutuzov, M., Lavrik, O., 2021. Functional Roles of PARP2 in Assembling Protein–Protein Complexes Involved in Base Excision DNA Repair. IJMS 22, 4679. https://doi.org/10.3390/ijms22094679

Velichkova, M., Guttman, J., Warren, C., Eng, L., Kline, K., Vogl, A.W., Hasson, T., 2002. A human homologue ofDrosophila kelch associates with myosin-VIIa in specialized adhesion junctions. Cell Motil. Cytoskeleton 51, 147–164. https://doi.org/10.1002/cm.10025

Verbeek, B., Southgate, T.D., Gilham, D.E., Margison, G.P., 2008. O6-Methylguanine-DNA methyltransferase inactivation and chemotherapy. Br Med Bull 85, 17–33. https://doi.org/10.1093/bmb/ldm036

Vodenicharov, M.D., Sallmann, F.R., Satoh, M.S., Poirier, G.G., 2000. Base excision repair is efficient in cells lacking poly(ADP-ribose) polymerase 1. Nucleic Acids Res 28, 3887–3896.

Vujanovic, M., Krietsch, J., Raso, M.C., Terraneo, N., Zellweger, R., Schmid, J.A., Taglialatela, A., Huang, J.-W., Holland, C.L., Zwicky, K., Herrador, R., Jacobs, H., Cortez, D., Ciccia, A., Penengo, L., Lopes, M., 2017. Replication Fork Slowing and Reversal upon DNA Damage Require PCNA Polyubiquitination and ZRANB3 DNA Translocase Activity. Molecular Cell 67, 882-890.e5. https://doi.org/10.1016/j.molcel.2017.08.010

Wang, T., Simbulan-Rosenthal, C.M., Smulson, M.E., Chock, P.B., Yang, D.C.H., 2008. Polyubiquitylation of PARP-1 through ubiquitin K48 is modulated by activated DNA, NAD+, and dipeptides. Journal of Cellular Biochemistry 104, 318–328. https://doi.org/10.1002/jcb.21624

Wang, Z., Michaud, G.A., Cheng, Z., Zhang, Y., Hinds, T.R., Fan, E., Cong, F., Xu, W., 2012. Recognition of the iso-ADP-ribose moiety in poly(ADP-ribose) by WWE domains suggests a general mechanism for poly(ADP-ribosyl)ation-dependent ubiquitination. Genes Dev 26, 235–240. https://doi.org/10.1101/gad.182618.111

Wei, H., Yu, X., 2016. Functions of PARylation in DNA Damage Repair Pathways. Genomics, Proteomics & Bioinformatics 14, 131–139. https://doi.org/10.1016/j.gpb.2016.05.001

Wei, L., Nakajima, S., Hsieh, C.-L., Kanno, S., Masutani, M., Levine, A.S., Yasui, A., Lan, L., 2013. Damage response of XRCC1 at sites of DNA single strand breaks is regulated by phosphorylation and ubiquitylation after degradation of poly(ADP-ribose). Journal of Cell Science 126, 4414–4423. https://doi.org/10.1242/jcs.128272

Weinstein, J.N., Collisson, E.A., Mills, G.B., Shaw, K.M., Ozenberger, B.A., Ellrott, K., Shmulevich, I., Sander, C., Stuart, J.M., 2013. The Cancer Genome Atlas Pan-Cancer Analysis Project. Nat Genet 45, 1113–1120. https://doi.org/10.1038/ng.2764

Westbye, M.P., Feyzi, E., Aas, P.A., Vågbø, C.B., Talstad, V.A., Kavli, B., Hagen, L., Sundheim, O., Akbari, M., Liabakk, N.-B., Slupphaug, G., Otterlei, M., Krokan, H.E., 2008. Human AlkB Homolog 1 Is a Mitochondrial Protein That Demethylates 3-Methylcytosine in DNA and RNA. J Biol Chem 283, 25046–25056. https://doi.org/10.1074/jbc.M803776200

Wiederhold, L., Leppard, J.B., Kedar, P., Karimi-Busheri, F., Rasouli-Nia, A., Weinfeld, M., Tomkinson, A.E., Izumi, T., Prasad, R., Wilson, S.H., Mitra, S., Hazra, T.K., 2004. AP Endonuclease-Independent DNA Base Excision Repair in Human Cells. Molecular Cell 15, 209–220. https://doi.org/10.1016/j.molcel.2004.06.003

Wijdeven, R.H., Pang, B., van der Zanden, S.Y., Qiao, X., Blomen, V., Hoogstraat, M., Lips, E.H., Janssen, L., Wessels, L., Brummelkamp, T.R., Neefjes, J., 2015. Genome-Wide Identification and Characterization of Novel Factors Conferring Resistance to Topoisomerase II Poisons in Cancer. Cancer Research 75, 4176–4187. https://doi.org/10.1158/0008-5472.CAN-15-0380

Wu, S., Li, X., Gao, F., de Groot, J.F., Koul, D., Yung, W.K.A., 2021. PARP-mediated PARylation of MGMT is critical to promote repair of temozolomide-induced O6-methylguanine DNA damage in glioblastoma. Neuro-Oncology 23, 920–931. https://doi.org/10.1093/neuonc/noab003

Wyatt, M.D., Pittman, D.L., 2006. Methylating Agents and DNA Repair Responses: Methylated Bases and Sources of Strand Breaks. Chem. Res. Toxicol. 19, 1580–1594. https://doi.org/10.1021/tx060164e

Xu, L., Wei, Y., Reboul, J., Vaglio, P., Shin, T.-H., Vidal, M., Elledge, S.J., Harper, J.W., 2003. BTB proteins are substrate-specific adaptors in an SCF-like modular ubiquitin ligase containing CUL-3. Nature 425, 316–321. https://doi.org/10.1038/nature01985

Yamamoto, M., Kensler, T.W., Motohashi, H., 2018. The KEAP1-NRF2 System: a Thiol-Based Sensor-Effector Apparatus for Maintaining Redox Homeostasis. Physiological Reviews 98, 1169–1203. https://doi.org/10.1152/physrev.00023.2017

Yang, C.-G., Yi, C., Duguid, E.M., Sullivan, C.T., Jian, X., Rice, P.A., He, C., 2008. Crystal structures of DNA/RNA repair enzymes AlkB and ABH2 bound to dsDNA. Nature 452, 961–965. https://doi.org/10.1038/nature06889

Yi, M., Dong, B., Qin, S., Chu, Q., Wu, K., Luo, S., 2019. Advances and perspectives of PARP inhibitors. Exp Hematol Oncol 8, 29. https://doi.org/10.1186/s40164-019-0154-9

Yu, W., Zhang, L., Wei, Q., Shao, A., 2020. O6-Methylguanine-DNA Methyltransferase (MGMT): Challenges and New Opportunities in Glioma Chemotherapy. Front. Oncol. 9, 1547. https://doi.org/10.3389/fonc.2019.01547

Zandarashvili, L., Langelier, M.-F., Velagapudi, U.K., Hancock, M.A., Steffen, J.D., Billur, R., Hannan, Z.M., Wicks, A.J., Krastev, D.B., Pettitt, S.J., Lord, C.J., Talele, T.T., Pascal, J.M., Black, B.E., 2020. Structural basis for allosteric PARP-1 retention on DNA breaks. Science 368, eaax6367. https://doi.org/10.1126/science.aax6367

Zarkovic, G., Belousova, E.A., Talhaoui, I., Saint-Pierre, C., Kutuzov, M.M., Matkarimov, B.T., Biard, D., Gasparutto, D., Lavrik, O.I., Ishchenko, A.A., 2018. Characterization of DNA ADP-ribosyltransferase activities of PARP2 and PARP3: new insights into DNA ADP-ribosylation. Nucleic Acids Research 46, 2417–2431. https://doi.org/10.1093/nar/gkx1318

Zhang, F., Ma, J., Wu, J., Ye, L., Cai, H., Xia, B., Yu, X., 2009. PALB2 Links BRCA1 and BRCA2 in the DNA-Damage Response. Curr Biol 19, 524–529. https://doi.org/10.1016/j.cub.2009.02.018

Zhou, Y., Feng, X., Koh, D.W., 2010. Enhanced DNA Accessibility and Increased DNA Damage Induced by the Absence of Poly(ADP-ribose) Hydrolysis. Biochemistry 49, 7360–7366. https://doi.org/10.1021/bi100979j

Zipper, L.M., Mulcahy, R.T., 2002. The Keap1 BTB/POZ Dimerization Function Is Required to Sequester Nrf2 in Cytoplasm. Journal of Biological Chemistry 277, 36544–36552. https://doi.org/10.1074/jbc.M206530200